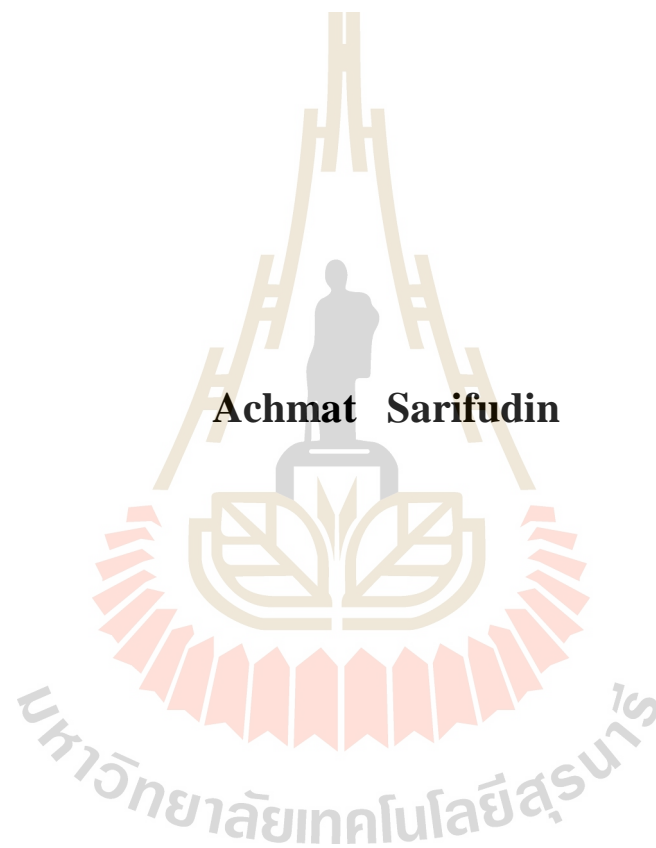# HYDRATION RELATED PROPERTIES OF ETHANOL-TREATED STARCH AND ITS APPLICATIONS

Achmat Sarifudin

A Thesis Submitted in Partial Fulfillment of the Requirements for the

Degree of Doctor of Philosophy in Food Technology

Suranaree University of Technology

Academic Year 2018

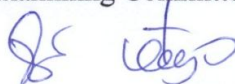# คุณสมบัติด้านการดูดซับน้ำและการประยุกต์ใช้ของสตาร์ชที่ดัดแปรด้วยเอทานอล

นายอาหมัด ซาริฟูดิน

HYDRATION RELATED PROPERTIES OF ETHANOL-TREATED
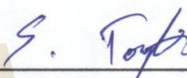
STARCH AND ITS APPLICATIONS

Suranaree University of Technology has approved this thesis submitted in partial fulfillment of the requirements for the Degree of Doctor of Philosophy.

Thesis Examining Committee

_____
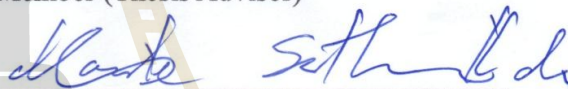
(Assoc. Prof. Dr. Jirawat Yongsawatdigul)

Chairperson

_____

(Asst. Prof. Dr. Sunanta Tongta)

Member (Thesis Advisor)

_____

(Assoc. Prof. Dr. Manote Sutheerawattananonda)

Member

_____

(Prof. Dr. Chaiyot Tangsathitkulchai)

Member

_____

(Asst. Prof. Dr. Supagorn Rugmai)

Member

_____

(Prof. Dr. Santi Maensiri)

Vice Rector for Academic Affairs

and Internationalization

_____

(Prof. Dr. Neung Teaumroong)

Dean of Institute of Agricultural Technology

อาหมัด ซาริฟูดิน : คุณสมบัติด้านการดูดซับน้ำและการประยุกต์ใช้ของสตาร์ชที่ดัดแปร
ด้วยเอทานอล (HYDRATION RELATED PROPERTIES OF ETHANOL-TREATED
STARCH AND ITS APPLICATIONS) อาจารย์ที่ปรึกษา: ผู้ช่วยศาสตราจารย์ ดร.สุนันทา
ทองทา, 227 หน้า.

งานวิจัยนี้ออกแบบมาเพื่อศึกษาคุณสมบัติด้านการดูดซับน้ำ และการนำไปใช้ประโยชน์
ของสตาร์ชดัดแปรด้วยเอทานอล (ETS) ในส่วนแรกศึกษาการปรับเปลี่ยนโครงสร้างในระหว่างการ
ทำให้เป็น ETS ของสตาร์ชข้าวโพด (ETMS) และมันฝรั่ง (ETPS) ด้วยเทคนิค in-situ WAXS และ
SAXS ร่วมกับ light microscope พบว่า ETMS แสดง V-type crystalline structure ตั้งแต่ที่อุณหภูมิ
86 องศาเซลเซียส ซึ่งผลจากการวิเคราะห์ paracrystalline แสดงให้เห็นว่า เมื่อให้ความร้อนไปที่
อุณหภูมิ 70 และ 80 องศาเซลเซียสแก่ ETMS และ ETPS ทำให้การจัดเรียงส่วนผลึก (crystalline
lamellae) มีความสมบูรณ์มากขึ้น แม้ว่าจะไม่พบลักษณะ Maltese cross ซึ่งแบบจำลองของการ
ปรับเปลี่ยนโครงสร้างใช้อธิบายการปรับเปลี่ยนโครงสร้างระดับ crystalline ระดับ lamellae และ
ระดับ granular ระหว่างการให้ความร้อนของ ETS ได้

ส่วนที่สองเป็นการศึกษาความสัมพันธ์ระหว่างคุณสมบัติในการดูดซับน้ำ คุณสมบัติ
ทางด้านรูพรุนและโครงสร้างของ ETS พบว่า ETS จากสตาร์ชข้าวโพด และมันฝรั่งมีรูที่มีลักษณะ
ไม่แข็ง (non-rigid) และเป็นร่อง (slit-shaped) สำหรับเม็ดสตาร์ช ETS จากสตาร์ชข้าวโพด และมัน
ฝรั่งนั้นน้ำสามารถเข้าไปในเม็ดสตาร์ชได้จากรอยแยก ส่วนอสัญฐานดูดซับน้ำ ละลายโครงสร้าง V-
type crystalline และเม็ดสตาร์ช EST สามารถอุ้มน้ำไว้ได้ สำหรับ ETS ที่ไม่อยู่ในรูปของเม็ดสตาร์ช
(non-granular ETS) จากสตาร์ชมันสำปะหลังและข้าว ส่วนอสัญฐาน และ V-type crystalline ดูดซับ
น้ำ และกักเก็บน้ำไว้ด้วยโครงข่ายสามมิติของเจลสตาร์ชเมื่อจับกับน้ำ

ส่วนที่สามและสี่เป็นการศึกษาผลของการดูดซับน้ำต่อคุณสมบัติเชิงโครงสร้างของ ETS
ซึ่ง ETMS และ ETPS ผ่านการก็บในสภาวะที่มีความชื้นสัมพัทธ์ 3 ระดับ (11, 57 และ 100%) เป็น
เวลา 6 วัน พบว่าที่ความชื้น 11% สามารถคงโครงสร้าง คุณสมบัติทางสัณฐานวิทยา และความสามารถ
ในการดูดซับน้ำ (WAC) ไว้ได้ เมื่อความชื้นสัมพัทธ์เพิ่มขึ้น ทำให้เกิดการเคลื่อนที่ของสตาร์ช ซึ่ง
ส่งผลให้โครงสร้าง และคุณสมบัติทางสัณฐานวิทยาเปลี่ยนไป และยังส่งผลให้ WAC ลดลงอีกด้วย
เมื่อ ETS อยู่ในสภาวะที่มีน้ำปริมาณมาก โครงสร้าง V-crystal ของ ETS จะถูกทำลาย ทำให้เกิดเป็น
โครงสร้างของอสัญฐาน ที่โครงสร้างระดับ lamellae ETS ที่ดูดซับน้ำไว้จะมีโครงสร้างแบบแผ่น
(sheet-like structure)

ส่วนสุดท้ายเป็นการศึกษาการเตรียมเม็ดยาจาก ETS เพื่อใช้กักเก็บ lauric acid (LA) และ ascorbic acid (AA) สำหรับขนส่งสาร โดยศึกษา 2 วิธี ซึ่งประกอบด้วยการผสมแบบแห้ง (dry mixing) และการละลายในตัวทำละลาย (solvent solubilization) โดย ETS เตรียมได้จากสตาร์ชแป้ง มันสำปะหลัง (C) ที่อุณหภูมิ 3 ระดับ คือ 80, 90 และ 100°C (C-80, C-90 และ C-100) ผลการ วิเคราะห์โครงสร้างแสดงให้เห็นว่า ไม่มีปฏิสัมพันธ์ระหว่างสารออกฤทธิ์ และส่วนประกอบสตาร์ช ของ ETS ลักษณะทางสัญฐานวิทยาของ ETS ที่ C-80 ยังแสดงลักษณะเม็ดสตาร์ช ในขณะที่ C-90 และ C-100 ไม่แสดงโครงสร้างของเม็ดสตาร์ช เมื่อแช่เม็ดยาของ C-80 พบว่ามีการกระจายตัวทันที และปลดปล่อยสารที่ถูกกักเก็บออกมาอย่างรวดเร็ว ส่วนผลในด้านพฤติกรรมการดูดซับน้ำและ คุณสมบัติด้านการปลดปล่อยชี้ให้เห็นว่าเม็ดยาของ C-90 และ C-100 เหมาะสำหรับการปลดปล่อย อย่างต่อเนื่อง ซึ่ง LA และ AA มีกลไกการปลดปล่อยที่แตกต่างกัน

สาขาวิชาเทคโนโลยีอาหาร ลายมือชื่อนักศึกษา_____

ปีการศึกษา 2561 ลายมือชื่ออาจารย์ที่ปรึกษา_____

ACHMAT SARIFUDIN : HYDRATION RELATED PROPERTIES OF
ETHANOL-TREATED STARCH AND ITS APPLICATIONS. THESIS
ADVISOR : ASST. PROF. SUNANTA TONGTA, Ph.D. 227 PP.

HYDRATION RELATED PROPERTIES/ETHANOL-TREATED
STARCH/STRUCTURAL TRANSFORMATIONS/PORE
CHARACTERIZATIONS/TABLET/CONTROLLED RELEASE

This research was designed to comprehensively study the hydration related properties of ethanol-treated starch (ETS) and its application. In the first part of study, the structural transformations of maize and potato starches (ETMS and ETPS) during ETS conversion was investigated using in-situ WAXS and SAXS techniques. The result indicated that the V-type crystalline structure of ETMS initially appeared at 86 °C. The result of paracrystalline analysis suggested that upon heating the crystalline lamellae of ETS realigned toward the most perfect register at 80°C and 70°C for ETMS and ETPS, respectively.

In the second part of study, the relationship between water absorption capacity and the pore characteristics and structural properties of ETS were assayed. The results indicated that ETS from maize and potato starches contains pores with the characteristics of non-rigid and slit-shaped pores. For granular ETS from maize and potato starches, water penetrates the granule through fissures, hydrates the amorphous regions, melts the V-type crystalline structure, and is held within the ETS granules upon water absorption. For non-granular ETS from cassava and rice starches, water hydrates the amorphous and V-type crystalline structures, and it is entrapped within

the three-dimensional network of starch components entanglement upon contact with water.

The third and fourth parts of the study were intended to study the effect of limited and excessive hydration on the properties of ETS, ETMS and ETPS were exposed in three relative humidity levels (11, 57, and 100%) for 6 days. Results indicated that increasing the humidity exposure induced the starch components movement which changed the structure and morphological properties and also decreased the WAC. When ETS was exposed to excess water, the V-crystal structure of ETS was destroyed resulting in an amorphous structure. At the lamellae level, hydrated ETS formed a sheet-like structure.

The last part of the study was aimed to evaluate tablets of ETS from cassava starch for encapsulation matrix of lauric acid (LA) and ascorbic acid (AA). Two encapsulation methods including dry mixing (D) and ethanol solubilization (S) methods were studied. The structural analysis result indicated that no interaction between the active compounds and the starch components of ETS. Morphological data showed that enriched ETS of C-80 exhibited granular form, while that of C-90 and C-100 displayed non-granular structure. Upon soaking, tablets of C-80 dispersed immediately and released the encapsulated compounds rapidly. The result of hydration behavior and release properties analysis suggested that tablets of C-90 and C-100 were suitable for sustained release in which LA and AA were released by different mechanisms.

School of Food Technology   Student's Signature_____

Academic Year 2018   Advisor's Signature_____

ACKNOWLEDGEMENTS

Sciences, Khon Kaen University for analysis of tablet's physical-mechanical strength properties.

I would like to acknowledge my research institute, Recearch Center for Appropriate Technology, Indonesian Institute of Sciences (P2TTG-LIPI) which has given me permission and opportunity to pursue the PhD program. I also acknowledge all colleagues in the Ajarn ST lab for providing a pleasant working atmosphere during my work in the lab, helping me in many different ways throughout my research, and being good friends who will live in my heart forever. I would to express my gratitude to Suranaree University of Technology for giving me scholarship to pursue the PhD degree under the project of SUT Scholarship for ASEAN countries year of 2015.

Finally, I am thankful to all Indonesian students in SUT for warm friendship, my loving parents and siblings, my father and mother in law in Indonesia for their encouragement, motivation and also for directing me in the right path. Without them, I would never accomplish this journey. Last but not least, my love and heart-felt gratitude go to my beloved wife, Enny Sholichah and two handsome boys, M. Hilmi Hakim and M. Ilham Syarif for their consistent support, understanding, patience, and love throughout my studies. Because of them and their support, I was able to successfully complete this journey. Thanks again and I love you all so much.

Achmat Sarifudin

CONTENTS

CONTENTS (Continued)

CONTENTS (Continued)

CONTENTS (Continued)

CONTENTS (Continued)

CONTENTS (Continued)

CONTENTS (Continued)

CONTENTS (Continued)

CONTENTS (Continued)

LIST OF TABLES

LIST OF FIGURES

LIST OF FIGURES (Continued)

LIST OF FIGURES (Continued)

LIST OF FIGURES (Continued)

LIST OF FIGURES (Continued)

LIST OF FIGURES (Continued)

LIST OF FIGURES (Continued)

Figure   **Page**

LIST OF ABBREVIATIONS

AA   =   Ascorbic acid

BET surface area   =   Bruenner, Emmet, Teller (BET) surface area

BJH method   =   Barrett, Joyner and Halenda (BJH) method

CWSS   =   Cold water swelling starch

DP   =   Degree of polymerization

DSC   =   Differential scanning calorimeter

ESEM   =   Environmental scanning electron microscope

ETMS   =   Ethanol-treated maize starch

ETPS   =   Ethanol-treated potato starch

ETS   =   Ethanol-treated starch

FESEM   =   Field emission scanning electron microscope

GCWSS   =   Granular cold water swelling starch

IUPAC   =   International union of pure and applied chemistry

LA   =   Lauric acid

LM   =   Light microscope

LIST OF ABBREVIATIONS (Continued)

SAXS	=	Small angle X-ray scattering
SLRI	=	Synchrotron light research institute
WAC	=	Water adsorption capacity
WAXD	=	Wide angle X-ray diffraction
WAXS	=	Wide angle X-ray scattering

CHAPTER I

INTRODUCTION

1.1 Introduction

Starch is staple ingredient for food and non-food industries. However, native starch shows many inherent lack of characteristics to be used directly in the industries. Starch modification is required to fulfill raw material or product specifications. Modified starch for thickening, gelling or encapsulating agents has different specifications (Chiu and Solarek, 2009). Likewise, modified starch for non-food applications such as for paper industry, warp sizing textiles and glass fibre sizing industries, have certain standards to be followed (Xie, Liu, and Cui, 2005).

Starch modification is mainly purposed to alter the starch structure; hence, the physical properties of starch are altered (Kaur, Ariffin, Bhat, and Karim, 2012; Tharanathan, 2005). Three basic starch modification methods are commonly practiced, including physical, chemical and enzymatic approaches. Pre-gelatinization (Pitchon, O'Rourke, and Joseph, 1981), annealing (Jacobs, Mischenko, Koch, Eerlingen, Delcour, and Reynaers, 1998; Kiseleva, Genkina, Tester, Wasserman, Popov, and Yuryev, 2004; Waduge, Hoover, Vasanthan, Gao, and Li, 2006), heat moisture (Hoover and Manuel, 1996; Stute, 1992) and extrusion (Colonna and Mercier, 1989) treatments are classical examples of starch modification by physical means. Four fundamental chemical reactions have been explored to modify starch including hydrolysis (Pratiwi, Faridah, and Lioe, 2018; Wang and Copeland, 2015)

, oxidations (Wurzburg, 1986), substitutions (Grundschober and Prey, 1963) and crosslinking (Rutenberg and Solarek, 1984; Yu, Wang, and Ma, 2005). Starch modification by enzymatic methods involves several classes of enzymes such as hydrolase (Chan, Braun, French, and Robyt, 1984; Karim, Sufha, and Zaidul, 2008) and transferase (Oh, Choi, Lee, Kim, and Moon, 2008). Moreover, combination of the modification treatments makes possible to tailor-made the modified starch to satisfy certain application. Each method exhibits its own advantage and disadvantage. Among them, physical and enzymatic methods are considered to be the safest ones since they do not involve any harmful chemicals; therefore, the products are classified in food grade class (Park, Park, Lee, Yoo, and Kim, 2008).

One of the most popular starch modification product obtained by physical means is cold water swelling starch (CWSS). CWSS was developed in tandem with pre-gelatinized starch to overcome the low solubility of native starch (Eastman and Moore, 1984). These products are often called as instant starches since they adsorb cold water and swell promptly, giving appearance and texture of a cooked-like starch. Therefore, they are commonly used for ready-to-be-consumed product (Eastman, et al., 1984). CWSS is superior to pre-gelatinized starch in terms of its textural and appearance properties (Light, 1990).

Methods to prepare CWSS include (a) annihilation the internal part of starch granule by a special design spray dryer (Pitchon, et al., 1981), (b) heating starch with ethanol (ETS) (Dries, Gomand, Goderis, and Delcour, 2014; Eastman, et al., 1984; Zhang, Dhital, Haque, and Gidley, 2012b) or polyhydric alcohols (Rajagopalan and Seib, 1991) and (c) mixing starch slurry with starch gelatinization inducer (sodium hydroxide) and anti-swelling agent (ethanol) in certain proportions (Chen and Jane,

1994a; Jane and Seib, 1991; Singh and Singh, 2003). Each processes exhibits their own advantages and disadvantages in terms of the level of process greenness, the production cost, and the production simplicity. Heating ETS can be considered as the simplest and safest method to prepare CWSS. The method only requires ethanol which can be removed from the product during the product drying (Dries, et al., 2014; Zhang, et al., 2012b).

The V-type crystalline structure is the main structural characteristic of CWSS (Chen, et al., 1994a; Dries, et al., 2014; Jane, Craig, Seib, and Hoseney, 1986a; Jane, et al., 1991; Zhang, et al., 2012b). Investigation has been conducted to explore the V-crystalline formation during CWSS conversion. Dries, et al. (2014) attempted to observe the exothermic peak of V-type crystal formation by differential scanning calorimetry (DSC) method, but it was not successful. In another investigation, Dries, Gomand, Delcour, and Goderis (2016) reported that the formation of a V-type crystalline structure during ETS conversion was affected by the degree of polymerization (DP) of amylose of the parental starch. For ETS prepared from starch with low DP amylose such as maize and rice, the formation of a V-type crystal was started when the native crystal structure was melted at 95°C. Furthermore, for ETS prepared from starch with a high DP amylose (potato), the V-type crystalline structure was formed during holding at 95°C and progressed further during subsequent cooling. However, since they did not monitor the actual sample temperature throughout the conversion process, their results needed further verification. In terms of designing a highly efficient process, investigation of processing parameters during ETS conversion, i.e., time and temperature for the V-type crystalline formation would be beneficial.

CWSS is prominent for its capability to adsorb cold water and swell immediately, forming a soft gel product. This property has attracted starch researchers to investigate the structure of CWSS. Jane, Craig, Seib, and Hoseney (1986b) noticed that the Maltese cross characteristic of native starch disappeared, indicating that the destruction of starch lamellae structure occurred. Observation at the atomic structural level of CWSS by wide-angle X-ray diffraction (WAXD) technique showed that the characteristic peaks of V-type crystalline structure emerged while the peaks of native starch structure vanished (Chen and Jane, 1994b; Dries, et al., 2016; Dries, et al., 2014; Jane, et al., 1986b; Kaur, Fazilah, and Karim, 2011; Rajagopalan and Seib, 1992b; Zhang, et al., 2012b). After the V-type crystalline structure was formed, ethanol removal did not affect the X-ray scattering pattern of the V-type crystalline structure (Dries, et al., 2014; Le Bail, Bizot, Pontoire, and Buleon, 1995; Whittam, Orford, Ring, Clark, Parker, Cairns, and Miles, 1989). Drying process removes ethanol from the amylose helix, leaving an empty cavity. Moreover, Dries, et al. (2014) suggested that ethanol removal is not mandatory to obtain CWSS with cold water swelling properties since the ethanol is freely exchangeable with water. The V-type crystalline structure of amylose-ethanol complex is known to be soluble in cold water (French and Murphy, 1977).

Jane, et al. (1986a) developed a model to explain the structural transformations of native starch (A-type) to become CWSS. Nonetheless, their model was oversimplified since it described the transformations as a single step process occurs at the crystalline structural level, while related phenomena at the higher structural levels, i.e. lamellae and granular, were not considered. A model that covers

the transformations of starch at different structural levels during CWSS conversion is not yet available.

Hydration characteristic of starch is influenced by the starch porosity and structural properties. Some native starch, such as maize and rice starch, inherently shows higher porosity than the other starch (Juszczak, Fortuna, and Wodnicka, 2002; Zhang, Cui, Liu, Gong, Huang, and Han, 2012a). Moreover, treatments (i.e. drying, gelatinization, enzyme hydrolysis) also increase the porosity of native starch . Porous starch is a modified starch that exhibits high porosity. It is usually prepared by enzymatic hydrolysis treatments with amylase and amyloglucosidase (Sujka and Jamroz, 2007, 2009; Wang, Lv, Jiang, Niu, Pang, and Jiang, 2016). Porous starch possesses a considerably high specific surface area to volume ratio which due to tremendous amount of pores or hollows dispersed from the surface extending to the center of starch granule (Sujka, et al., 2007, 2009). Porous starch has ability to adsorb higher amount of solvents than its native counterpart. Therefore, it is widely applied in a variety of fields, including food, cosmetics, topical lotions, washing detergents and agricultural products (Wang, Yuan, and Yue, 2015; Zeller, Saleeb, and Ludescher, 1998).

Many studies have confirmed the capability of CWSS to adsorb high amount of water at low temperature (Chen, et al., 1994a; Dries, et al., 2014; Jane, et al., 1986a; Jane, et al., 1991; Rajagopalan, et al., 1991; Rajagopalan and Seib, 1992a; Rajagopalan, et al., 1992b; Singh, et al., 2003). CWSS can adsorb water up to 12 times than its weight (Majzoobi, Kaveh, Blanchard, and Farahnaky, 2015) but porous starch can only maximally adsorb water up to 3 times than its weight (Wang, et al.,

2016). This can be an advantage of using CWSS over porous starch in terms of their adsorption capacity.

In terms of adsorption science, material with high adsorption capability can be an indication that it has high porosity. The porosity may originate from surface pores or internal granule spaces (Lowell, Shields, Thomas, and Thommes, 2010; Rouquerol, Rouquerol, and Sing, 1999; Sing, Everett, Haul, Moscou, Pierotti, Rouquerol, and Siemieniewska, 2008). Pores of porous starch are classified in macropore region because their pore diameter predominantly is about 1 μm (Sujka, et al., 2009; Sujka and Jamroz, 2010). Moreover, porous rice starch exhibited the highest surface area (1.66 m^2/g) meanwhile the lowest one was porous potato starch (0.4 m^2/g) (Sujka, et al., 2010). Therefore, based on the pore characterization, porous rice starch is highly potential to be used for carrying agent (Juszczak, et al., 2002; Sujka, et al., 2010). Even though CWSS has higher water adsorption capacity than porous starch but the pore characteristics of CWSS has not been reported. Thus, the pore characteristics of CWSS are necessary to be studied, to understand the reasons behind its high water adsorption capability and also to choose its suitability for specific applications.

From chemistry point of view, the capability of CWSS to adsorb cold water and swell promptly is closely related to the hydration property of starch. Starch hydration is defined as a process to combine hydroxyl groups in starch structure with water molecules either by physical interactions or chemical bonds. Wynne-Jones and Blanshard (1986) gave broader sense of hydration as changes in the state of water. In starch processing, hydration of starch is fundamental process to be carried out to accomplish fully gelatinized starch upon gelatinization process (Lemke,

Burghammer, Flot, Rössle, and Riekel, 2004). This process takes place on different length scale of starch granule. At the crystalline structural level, hydration proceeds when water molecules are incorporated into crystal lattice sites (Imberty and Perez, 1988). At lamellar level, hydration converts nematic to smectic phase of amylopectin cluster of native starch as observed by Small angle X-ray scattering method (Waigh, Gidley, Komanshek, and Donald, 2000). Consequently, hydration of native starch raises a characteristic peak of SAXS pattern which is believed originating from alternating layer of hydrated crystalline and amorphous lamella of a thickness of 9 nm (Jenkins, Cameron, and Donald, 1993; Suzuki, Chiba, and Yarno, 1997).

Study on hydration of CWSS was initiated by Jane, et al. (1986a). They reported that when CWSS from corn starch was exposed to 100% relative humidity for 13 days, the A-type crystalline structure reappeared. Furthermore, when it was stored at low humidity, the cold water swelling capability of CWSS was still preserved but the peaks of V-type crystalline structure lost its sharpness. However, a comprehensive study to understand the effect of hydration levels, i.e. limited and excessive hydration, on the properties of CWSS is still required.

CWSS has been used to encapsulate active ingredients (Chen and Jane, 1995; Dries, Gomand, Pycarelle, Smet, Goderis, and Delcour, 2017). They reported that the encapsulated product properties by CWSS were influenced by the encapsulation method. Chen, et al. (1995) used water as a medium during encapsulating atrazine by CWSS. They reported that chemical interactions between atrazine and starch components did not occur; instead, B-type diffraction appeared as an indication of starch gel retrogradation. Dries, et al. (2017) used multiple encapsulation stages

involving water-ethanol mixture to encapsulate ascorbyl palmitate using CWSS. The method was applied to retain the V-type crystalline structure in the final product. Development of more practical encapsulation method by using ETS as encapsulation matrix that applicable for industrial scale is still required.

Tablet is one of medicinal products commonly used for drug delivery system. Tablets can be defined as a solid unit dosage form of medicaments. Tablet might be prepared with or without suitable excipients and prepared by either molding or by compression (Wise, 2000). Tablet provides some advantageous over other medicinal products due to simplicity in production, relatively low cost production, suitability to entrap labile drugs, ease to consume and store, and relatively consistent during dissolution (Adeleye, Femi-Oyewo, and Odeniyi, 2014; Adeoye and Alebiowu, 2014; Lawal, Odeniyi, and Itiola, 2015). Tablet may contain many type of excipients such as diluents agents, binders or granulating agents, glidants (flow aids), lubricants, dis-integrants, sweeteners or flavour enhancer and pigments. Modified starch has been explored for tablets excipient for several decades (Hatairat, Wolfgang, Sujin, and Saiyavit, 2003; Lawal, et al., 2015; Odeniyi and Ayorinde, 2014; Pachuau, Dutta, Devi, Deka, and Hauzel, 2018).

Boonwatcharapan, Srisuk, Palladino, Sutthiparinyanont, and Chitropas (2016) has investigated alcohol-alkaline-treated rice starch as a tablet disintegrant. They reported that the modified rice starch exhibited higher water solubility and swelling capacity compared to that of native rice starch. They also suggested that the modified rice starch was a good disintegrant for direct-compressed tablet formulations, especially in the presence of water insoluble fillers. However, investigation of CWSS

or ETS for medicinal tablets excipients for different type of active ingredients, namely hydrophilic and hydrophobic compounds, and also release mechanisms of the active ingredients have not yet been conducted.

1.2   Research objectives

The main objective of this research was to comprehensively study the hydration related properties of ETS and its application. Furthermore, to achieve the goal of the research, this research is divided into four parts in which each part has specific objectives as follow:

1.2.1 To study the structural transformations of native starch during ETS conversion using in-situ WAXS and SAXS techniques combined with light microscope method.

1.2.2 To investigate the relationship between the water absorption capacity and the pore characteristic and structural properties of ETS.

1.2.3 To study the alterations of structural, morphological properties and water adsorption capacity of ETS upon limited and excessive hydrations.

1.2.4 The last objective of the study was to evaluate tablet prepared from ETS as encapsulation matrix of lauric acid and ascorbic acid in relation to its hydration and release properties.

1.3   Research hypotheses

The main hypothesis of the study was the hydration related properties of ETS are dependent on the parental starch and degree of conversion. Furthermore, in order to study the hydration related properties of ETS and its application systematically, the

main hypothesis was divided into four sub hypothesis, in which they were specified and studied independently as follows:

    a. The transformations at three starch organizational level including atomic, lamellae, granular structural levels occur during ETS conversion.

    b. The pore characteristic and structural properties of ETS influences its water absorption capacity.

    c. The level of hydration, i.e. limited and excessive hydration, alters the properties of ETS at different extent.

    d. Tablet made from ETS is suitable for encapsulation matrix of sustained release system.

1.4 Scope of the study

This research was intended to study the hydration related properties of ETS and explored the application of ETS for encapsulation matrix. Therefore, the study covered several parts including: (a) Investigation on the transformation of starch at crystalline, lamellae and granular levels during ETS conversion. Two starch sources (maize and potato) representing different starch polymorphs, namely A-and B-type starches were selected. (b) Factors influencing the water absorption capacity of ETS including pore characteristics, and structural were investigated. For this study, the ETS was prepared from four starch varieties (maize, potato, rice and cassava) and three conversion temperature levels (80, 90, and 100°C). (c) Impact of limited and excessive hydration on the properties of ETS was studied. To study the effect of limited hydration, maize and potato ETS prepared were exposed to environments with different humidity (11%, 57%, and 100%) for 6 days. Excessive hydration experiment

was carried out by soaking ETS with excess water for 2 h. (d) The scope of the last part of study covered investigation of hydration and release properties of ETS tablet used for encapsulating matrix of lauric acid and ascorbic acid. Encapsulation was carried out by dry mixing and ethanol solubilization methods.

1.5   Expected results

It was expected that results of this study will give comprehensive knowledge on the hydration related properties of ETS and its application. The results of the study of structural transformations at different organizational levels of starch during ETS conversion will provide a fundamental knowledge on the formation of structures responsible for the hydration related properties of ETS. The result of pore characterization and structure properties of ETS and their relation to the water absorption capacity of ETS will provide a basis to choose the suitability of ETS for specific applications related to its high water absorption property. The result of investigation on the alterations of structure and hydration related properties of ETS before and after limited and excessive hydration will provide important information on how to handle the ETS on post-production and during transportation process. Lastly, the result of comprehensive study on the application of ETS for encapsulating matrix in the form of tablet might be implemented for sustained release system of nutraceutical or pharmaceutical ingredients.

1.6   References

Adeleye, O.A., Femi-Oyewo, M.N., and Odeniyi, M.A. (2014). The effect of processing variables on the mechanical and release properties of tramadol

matrix tablets incorporating cissus populnea gum as controlled release excipient. **Polimery w Medycynie** 44(4): 209-220.

Adeoye, O., and Alebiowu, G. (2014). Flow, packing and compaction properties of novel coprocessed multifunctional directly compressible excipients prepared from tapioca starch and mannitol. **Pharmaceutical Development and Technology** 19(8): 901-910.

Boonwatcharapan, Y., Srisuk, P., Palladino, P., Sutthiparinyanont, S., and Chitropas, P. (2016). Preparation and evaluation of alcohol-alkaline-treated rice starch as a tablet disintegrant. **Tropical Journal of Pharmaceutical Research** 15(2): 221-229.

Chan, Y.C., Braun, P.J., French, D., and Robyt, J.F. (1984). Porcine pancreatic .alpha.-amylase hydrolysis of hydroxyethylated amylose and specificity of subsite binding. **Biochemistry** 23(24): 5795-5800.

Chen, J., and Jane, J. (1994a). Preparation of granular cold-water-soluble starches by alcoholic-alkaline treatment. **Cereal chemistry** 7(6): 618-622.

Chen, J., and Jane, J. (1994b). Properties of granular cold-water-soluble starches prepared by alcoholic-alkaline treatments. **Cereal chemistry** 71(6): 623-626.

Chen, J., and Jane, J. (1995). Effectiveness of granular cold-water-soluble starch as a controlled release matrix. **Cereal chemistry** 72(3): 265-268.

Chiu, C., and Solarek, D. (2009). Chapter 17 - Modification of Starches. In **Starch (Third Edition)** (pp. 629-655). San Diego: Academic Press.

Colonna, J.T., and Mercier, C. (1989). Extrusion cooking of starch and starchy products. In C. Mercier and J.M. Harper (Eds.), **Extrusion Cooking** (pp. 247–320). St. Paul, MN: American Association of Cereal Chemists, Inc.

Dries, D.M., Gomand, S.V., Delcour, J.A., and Goderis, B. (2016). V-type crystal formation in starch by aqueous ethanol treatment: The effect of amylose degree of polymerization. **Food Hydrocolloids** 61: 649-661.

Dries, D.M., Gomand, S.V., Goderis, B., and Delcour, J.A. (2014). Structural and thermal transitions during the conversion from native to granular cold-water swelling maize starch. **Carbohydrate Polymers** 114: 196-205.

Dries, D.M., Gomand, S.V., Pycarelle, S.C., Smet, M., Goderis, B., and Delcour, J.A. (2017). Development of an infusion method for encapsulating ascorbyl palmitate in V-type granular cold-water swelling starch. **Carbohydrate Polymers** 165(Supplement C): 229-237.

Eastman, J.E., and Moore, C.O. (1984). Cold soluble water granular starch for gelled food compositions. **USPTO # 4.465.702**

French, A.D., and Murphy, V.G. (1977). Computer modeling in the study of starch. **Cereal Food World** 22(2): 61-70.

Grundschober, F., and Prey, V. (1963). Acetylation in aqueous solution. **Die Stärke** 15: 225-227.

Hatairat, P., Wolfgang, B., Sujin, S., and Saiyavit, V. (2003). Characterization and Utilization of Acid-modified Rice Starches for Use in Pharmaceutical Tablet Compression. **Starch - Stärke** 55(10): 464-475.

Hoover, R., and Manuel, H. (1996). The effect of heat-moisture treatment on the structure and physicochemical properties of normal maize, waxy maize, dull waxy maize and amylomaize V starches **Journal of Cereal Science** 23: 153-162.

Imberty, A., and Perez, S. (1988). A revisit to the three-dimensional structure of B-type starch. **Biopolymers** 27(8): 1205-1221.

Jacobs, H., Mischenko, N., Koch, M.H.J., Eerlingen, R.C., Delcour, J.A., and Reynaers, H. (1998). Evaluation of the impact of annealing on gelatinisation at intermediate water content of wheat and potato starches: A differential scanning calorimetry and small angle X-ray scattering study. **Carbohydrate Research** 306(1): 1-10.

Jane, J., Craig, S.A.S., Seib, P.A., and Hoseney, R.C. (1986a). Characterization of granular cold water-soluble starch. **Starch - Stärke** 38: 258-263.

Jane, J., Craig, S.A.S., Seib, P.A., and Hoseney, R.C. (1986b). A granular cold water-soluble starch gives a V-type X-ray diffraction pattern. **Carbohydrate Research** 150(1): c5-c6.

Jane, J., and Seib, P.A. (1991). Preparation of granular cold water swelling/soluble starches by alcoholic-alkali treatments. **USPTO # 5.057.157**

Jenkins, P.J., Cameron, R.E., and Donald, A.M. (1993). A universal feature in the structure of starch granules from different botanical sources. **Starch - Stärke** 45: 417-420.

Juszczak, L., Fortuna, T., and Wodnicka, K. (2002). Characteristics of cereal starch granules surface using nitrogen adsorption. **Journal of Food Engineering** 54(2): 103-110.

Karim, A.A., Sufha, E.H., and Zaidul, I.S.M. (2008). Dual Modification of Starch via Partial Enzymatic Hydrolysis in the Granular State and Subsequent Hydroxypropylation. **Journal of Agricultural and Food Chemistry** 56(22): 10901-10907.

Kaur, B., Ariffin, F., Bhat, R., and Karim, A.A. (2012). Progress in starch modification in the last decade. **Food Hydrocolloids** 26(2): 398-404.

Kaur, B., Fazilah, A., and Karim, A.A. (2011). Alcoholic-alkaline treatment of sago starch and its effect on physicochemical properties. **Food and Bioproducts Processing** 89(4): 463-471.

Kiseleva, V.I., Genkina, N.K., Tester, R., Wasserman, L.A., Popov, A.A., and Yuryev, V.P. (2004). Annealing of normal, low and high amylose starches extracted from barley cultivars grown under different environmental conditions. **Carbohydrate Polymers** 56(2): 157-168.

Lawal, M.V., Odeniyi, M.A., and Itiola, O.A. (2015). Effect of thermal and chemical modifications on the mechanical and release properties of paracetamol tablet formulations containing corn, cassava and sweet potato starches as filler-binders. **Asian Pacific Journal of Tropical Biomedicine** 5(7): 585-590.

Le Bail, P., Bizot, H., Pontoire, B., and Buleon, A. (1995). Polymorphic Transitions of Amylose-Ethanol Crystalline Complexes Induced by Moisture Exchanges. **Starch - Stärke** 47(6): 229-232.

Lemke, H., Burghammer, M., Flot, D., Rössle, M., and Riekel, C. (2004). Structural Processes during Starch Granule Hydration by Synchrotron Radiation Microdiffraction. **Biomacromolecules** 5(4): 1316-1324.

Light, J.M. (1990). Modified food starches: Why, where, and how. **Cereal Foods World** 35: 1081-1084.

Lowell, S., Shields, J.E., Thomas, M.A., and Thommes, M. (2010). **Characterization of porous solids and powders: surface area, pore size and density**: Kluwer Academic Publishers, Springer.

Majzoobi, M., Kaveh, Z., Blanchard, C.L., and Farahnaky, A. (2015). Physical properties of pregelatinized and granular cold water swelling maize starches in presence of acetic acid. **Food Hydrocolloids** 51: 375-382.

Odeniyi, M.A., and Ayorinde, J.O. (2014). Effects of modification and incorporation techniques on disintegrant properties of wheat (Triticum aestivum) starch in metronidazole tablet formulations. **Polimery w medycynie** 44(3): 147-155.

Oh, E.J., Choi, S.J., Lee, S.J., Kim, C.H., and Moon, T.W. (2008). Modification of granular corn starch with 4-alpha-glucanotransferase from Thermotoga maritima: effects on structural and physical properties. **Journal of Food Science** 73(3): C158-166.

Pachuau, L., Dutta, R.S., Devi, T.B., Deka, D., and Hauzel, L. (2018). Taro starch (Colocasia esculenta) and citric acid modified taro starch as tablet disintegrating agents. **International Journal of Biological Macromolecules** 118: 397-405.

Park, K.-H., Park, J.-H., Lee, S., Yoo, S.-H., and Kim, J.-W. (2008). Enzymatic Modification of Starch for Food Industry. In K.-H. Park (Ed.), **Carbohydrate-Active Enzymes** (pp. 157-183): Woodhead Publishing.

Pitchon, E., O'Rourke, J.D., and Joseph, T.H. (1981). Process for cooking or gelatinizing materials. **USPTO # 4.280.851**

Pratiwi, M., Faridah, D.N., and Lioe, H.N. (2018). Structural changes to starch after acid hydrolysis, debranching, autoclaving-cooling cycles, and heat moisture treatment (HMT): A review. **Starch - Stärke** 70(1-2): 1700028.

Rajagopalan, S., and Seib, P.A. (1991). Process for the preparation of granular cold water-soluble starch. **USPTO # 5.037.929**

Rajagopalan, S., and Seib, P.A. (1992a). Granular cold-water-soluble starches prepared at atmospheric pressure. **Journal of Cereal Science** 16(1): 13-28.

Rajagopalan, S., and Seib, P.A. (1992b). Properties of granular cold-water-soluble starches prepared at atmospheric pressure. **Journal of Cereal Science** 16(1): 29-40.

Rouquerol, F., Rouquerol, J., and Sing, K. (1999). CHAPTER 1 - Introduction. In **Adsorption by Powders and Porous Solids** (pp. 1-26). London: Academic Press.

Rutenberg, M.W., and Solarek, D. (1984). Starch derivatives: Production and uses. In R. Whistler, J.N. BeMiller and E.F. Paschall (Eds.), **Starch: Chemistry and Technology** (pp. 314-388). New York: Academic Press, Inc.

Sing, K.S.W., Everett, D.H., Haul, R.A.W., Moscou, L., Pierotti, R.A., Rouquerol, J., and Siemieniewska, T. (2008). Reporting Physisorption Data for Gas/Solid Systems. In **Handbook of Heterogeneous Catalysis**): Wiley-VCH Verlag GmbH & Co. KGaA.

Singh, J., and Singh, N. (2003). Studies on the morphological and rheological properties of granular cold water soluble corn and potato starches. **Food Hydrocolloids** 17(1): 63-72.

Stute, R. (1992). Hydrothermal modification of starches: the difference between annealing and heat moisture treatment. **Starch - Stärke** 6: 205-214.

Sujka, M., and Jamroz, J. (2007). Starch granule porosity and its changes by means of amylolysis. **International Agrophysics** 21.

Sujka, M., and Jamroz, J. (2009). α-Amylolysis of native potato and corn starches-SEM, AFM, nitrogen and iodine sorption investigations. **LWT - Food Science and Technology** 42(7): 1219-1224.

Sujka, M., and Jamroz, J. (2010). Characteristics of pores in native and hydrolyzed starch granules. **Starch - Stärke** 62(5): 229-235.

Suzuki, T., Chiba, A., and Yarno, T. (1997). Interpretation of small angle X-ray scattering from starch on the basis of fractals. **Carbohydrate Polymers** 34(4): 357-363.

Tharanathan, R.N. (2005). Starch-Value Addition by Modification. **Critical Reviews in Food Science and Nutrition** 45(5): 371-384.

Waduge, R.N., Hoover, R., Vasanthan, T., Gao, J., and Li, J.H. (2006). Effect of annealing on the structure and physicochemical properties of barley starches of varying amylose contents. **Food Research International** 39: 59-77.

Waigh, T.A., Gidley, M.J., Komanshek, B.U., and Donald, A.M. (2000). The phase transformations in starch during gelatinisation: a liquid crystalline approach. **Carbohydrate Research** 328(2): 165-176.

Wang, H., Lv, J., Jiang, S., Niu, B., Pang, M., and Jiang, S. (2016). Preparation and characterization of porous corn starch and its adsorption toward grape seed proanthocyanidins. **Starch - Stärke** 68(11-12): 1254-1263.

Wang, S., and Copeland, L. (2015). Effect of Acid Hydrolysis on Starch Structure and Functionality: A Review. **Critical Reviews in Food Science and Nutrition** 55(8): 1081-1097.

Wang, X., Yuan, Y., and Yue, T. (2015). The application of starch-based ingredients in flavor encapsulation. **Starch - Stärke** 67(3-4): 225-236.

Whittam, M.A., Orford, P.D., Ring, S.G., Clark, S.A., Parker, M.L., Cairns, P., and Miles, M.J. (1989). Aqueous dissolution of crystalline and amorphous amylose alcohol complexes. **International Journal of Biological Macromolecules** 11(6): 339-344.

Wise, D. (2000). **Handbook of Pharmaceutical Controlled Release Technology**. Boca Raton: CRC Press.

Wurzburg, O.B. (1986). Converted starches. In O.B. Wurzburg (Ed.), **Modified Starches: Properties and Uses** vol. 17-29). Boca Raton, FL: CRC Press.

Wynne-Jones, S., and Blanshard, J.M.V. (1986). Hydration studies of wheat starch, amylopectin, amylose gels and bread by proton magnetic resonance. **Carbohydrate Polymers** 6(4): 289-306.

Xie, S.X., Liu, Q., and Cui, S.W. (2005). Starch Modification and Applications. In S.W. Cui (Ed.), **Food Carbohydrates: Chemistry, Physical Properties, and Applications**). Boca Raton, Florida: CRC Press, Taylor & Francis Group.

Yu, J., Wang, N., and Ma, X. (2005). The effects of citric acid on the properties of thermoplastic starch plasticized by glycerol. **Starch - Stärke** 57: 494-504.

Zeller, B.L., Saleeb, F.Z., and Ludescher, R.D. (1998). Trends in development of porous carbohydrate food ingredients for use in flavor encapsulation. **Trends in Food Science & Technology** 9(11): 389-394.

Zhang, B., Cui, D., Liu, M., Gong, H., Huang, Y., and Han, F. (2012a). Corn porous starch: Preparation, characterization and adsorption property. **International Journal of Biological Macromolecules** 50(1): 250-256.

Zhang, B., Dhital, S., Haque, E., and Gidley, M.J. (2012b). Preparation and characterization of gelatinized granular starches from aqueous ethanol treatments. **Carbohydrate Polymers** 90(4): 1587-1594.

CHAPTER II

LITERATURE REVIEW

2.1   Introduction to starch

Starch is the second most used biopolymer in industry after cellulose since it is abundant, relatively cheap, and renewable (Rutenberg and Solarek, 1984).   The demand of starch for industries is projected to reach 182 million metric tons by 2022 (Inc, 2018) with portion of each starch sources as follows corn/maize (82.6%), wheat (8.8%), potato (6.3%), and others 2.3%   (Unit, 2011). The highest demand of starch comes from sweetener industry (Inc, 2018).   Also, trend shows that market of traditional starch sources such as maize, potato and wheat, moves to the other more economical starch sources, such as cassava, and sweet potato (Inc, 2018).

Understanding the starch market may lead to the development of starch derivative products; to produce starch products that satisfy consumer demands. For many years, native starches and starch-modified products have been widely used for ingredients of many different industrial sectors such as food and beverage, paper, textile, cosmetic, and pharmaceutical industries (Singh, Nath, and Anudwipa, 2010). The use of starch in food industry is boosted by the government policies that natural substances are preferable over the synthetic ones to be used in food products. For example, for low fat and low-calorie food, the fat can be replaced by starch derivative products   and   hydrocolloids.   Therefore,   a   comprehensive   view   of   starch

including starch origin, starch modifications, starch characteristics, and starch application, is necessary as a baseline of starch product development.

2.1.1   Native starch origin

Starch is a primary form of energy reservoir in various plants, produced in different organs of plants depending on the plant's types. For cereals, starch is produced in seeds of rice and wheat. For staple crops, starch can be found in roots and tubers of cassava and potato, respectively (Le Corre, Bras, and Dufresne, 2010). Even though starch may be produced in different plant organelle, most of starch researcher agrees that starch biosynthesis takes place in a specialized subcellular organelle called amyloplast which is blanked by a lipoprotein membrane (Buléon, Colonna, Planchot, and Ball, 1998; Buléon, Gallant, Bouchet, Mouille, D'Hulst, Kossmann, and Ball, 1997; Tetlow, 2011). Within this organelle, many enzymes catalyze the formation of the major starch components namely amylose and amylopectin. As the starch granule develops, the internal volume of the amyloplast is occupied by starch. Meanwhile, lipid and protein from the lipoprotein membrane integrate in the peripheral part of starch granule (Galliard and Bowler, 1987).

Traditionally, highly containing starch plants organelle such as seeds of rice, roots of tapioca, and tuber of potato is extracted with water to produce starch powder (Le Corre, et al., 2010). Modern technologies with sophisticated equipment have been implemented in starch industry to obtain a high yield of starch powder and to reduce the amount of water used during starch extraction. Therefore, different starches sources may employ different technology to produce starch (Figure 2.1) (Galliard, 1987). Principally, starch processing lines should also cover raw material handling and starch by-products processing.
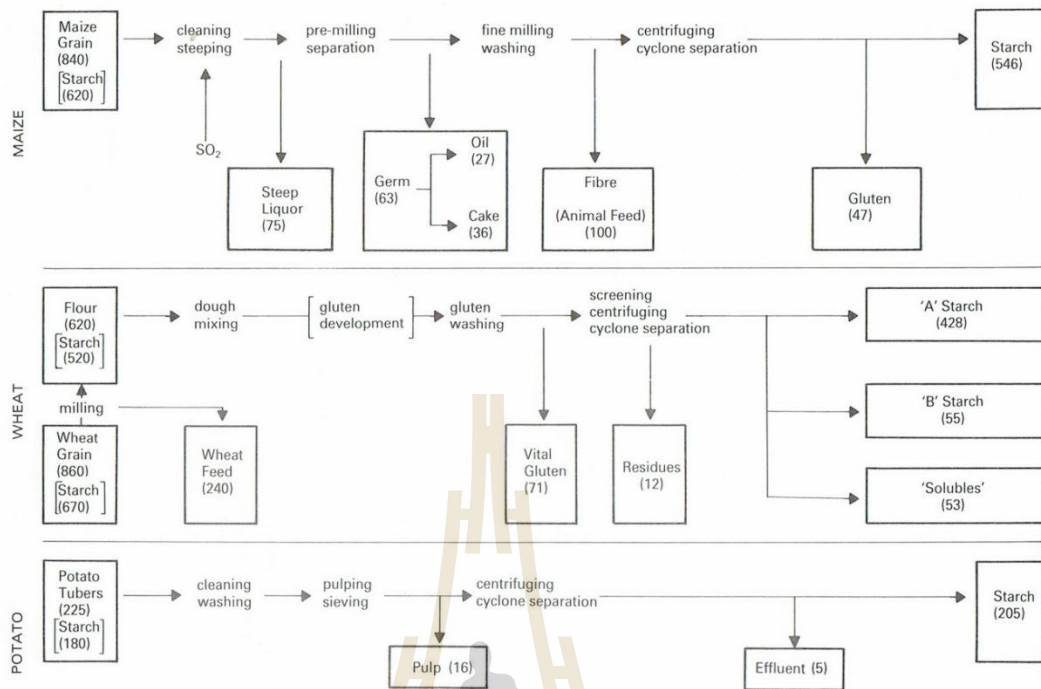
Figure 2.1   Simplified diagrams of starch production lines from maize, wheat, and

potato.

Source : Galliard (1987).

2.1.2   Granule of native starch: sizes and shapes

During starch development, starch granules grow by a radial extension from

the hilum (center) heading outside but not always in symmetrical direction

(Badenhuizen, 1969). For potato starch, the granule develops towards one end of the

proloid. For lenticular shape granules such as wheat, the granule development process

is more complicated since it involves a nucleus and planes formation (Evers, 1971;

Sandstedt, 1946).

Table 2.1 Size and shape of starch granules from different plants.

Plant sources	Size (µm)	Shape
potato	5-100	oval
maize	2-30	round and polyhedral
maize waxy	2-30	round and polyhedral
wheat	<10 & 10-35	discs
rice	2-10	polyhedral
tapioca	5-45	spherical / lenticular

Source : (Ayoub and Rizvi, 2009; Buléon, et al., 1998); Jane, Shen, Wang, and Maningat (1992); (Lindeboom, Chang, and Tyler, 2004; Tester, Karkalas, and Qi, 2004).

Starch granules develop in different sizes depending on the botanical origin, ranging from 2 (for wheat and rice) to 100 μm (for potato) (Buléon, et al., 1998). Size and shape of starch granule from different starch biological sources is shown in Table 2.1. The morphological properties of starch granule can be studied by using microscopy techniques including light and polarized normal microscopes and scanning electron microscopes. The starch granule shows different shapes under normal light microscope such as lenticular shape for tapioca starch granules and oval shape for potato starch granules, etc. Under the polarized light microscope, native starch shows a Maltese cross pattern which is the characteristic of native starches (Donald, Waigh, Jenkins, Gidley, Debet, and Smith, 1997). By using particle size analyzer, it can be revealed that maize starch granules exhibit monomodal distribution with size of 5-25 µm (Paterson, Hardacre, Li, and Rao, 2001). Meanwhile, wheat

starch granules show three modal distributions including lenticular A granules with size of 15 to 35 μm, small spherical or polyhedral B granules with size of 10-15 μm, and super small C granules with size less than 5 μm (Wilson, Bechtel, Todd, and Seib, 2006).

2.1.3 The structural arrangement of native starch

Chemically, starch is called biopolymer compound because it is composed of thousands of glucose as a monomer (Che, Li, Wang, Dong Chen, and Mao, 2007). Interestingly, there are only two basic starch structures, namely amylose and amylopectin, which exist with a very rare anomalous form (Figure 2.2). Amylose basically is constructed by a linear molecule of (1→4) linked α-D-glucopyranosyl units, but, today, it is known that slightly branched amylose molecules may be obtained from different starch sources (Le-Bail, Hesso, and Le-Bail, 2018). Amylopectin is highly branched polysaccharide composed of hundreds of short (1→4)-α-glucan chains, which are interlinked by (1→6)-α-linkages (Buléon, et al., 1998). For normal starch types, the relative weight percentages of amylose and amylopectin are ranging between 18-33% and 72-82%, respectively. However, a special species which is waxy starch contains less than 1% amylose (Buléon, et al., 1998). High amylose starch contains amylose up to 80% and it is commercially available in the market with the brand of Gelose and Hylon. Moreover, high amylose starch from maize is called amylomaize (Chen, Yu, Chen, and Li, 2006).
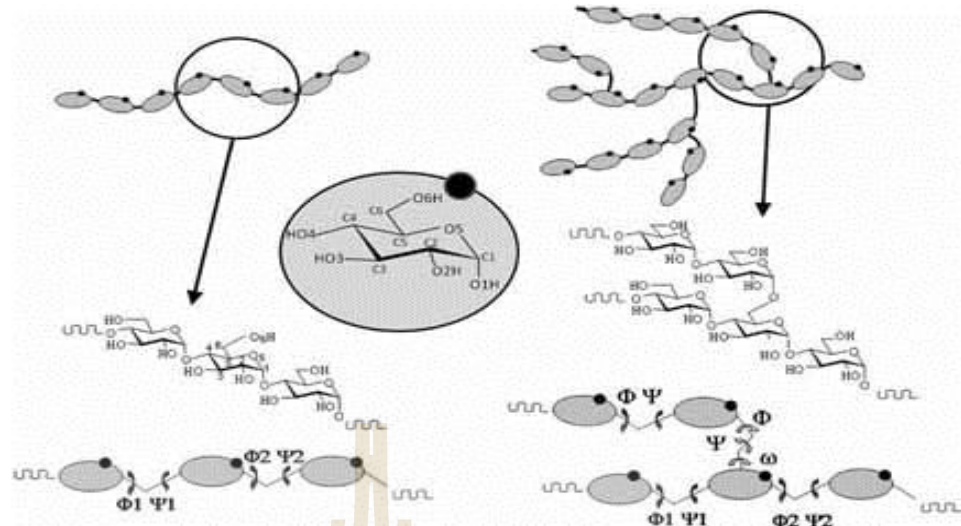
Figure 2.2 Basic structural motifs of amylose and amylopectin, along with the
labeling and torsion angles. Extension of the basic motifs to the
macromolecular structures.

Source : Pérez and Bertoft (2010).

Starch granule shows a unique structural organization when it is observed
from macroscopic to microscopic levels. Observation by transmission electron
microscope shows that the cross-section of starch granule appears like growth rings of
an onion-like structure with a diameter of about 100-400 nm. The growth ring is made
up of alternating of amorphous and semi-crystalline rings (Angellier, Putaux, Molina-
Boisseau, Dupeyre, and Dufresne, 2005; Pérez, et al., 2010). Illustration of the
structural organization of starch from the lowest to the highest observation levels is
shown in Figure 2.3 (Le Corre, et al., 2010). The figure illustrates the construction of
starch granule by its simplest components, amylose, and amylopectin. Amylopectin
constructs the double helix chains becoming an ordered structure known as crystalline

lamellae. Meanwhile, amylose chains lay at the amorphous lamellae which are the non-crystalline regions.
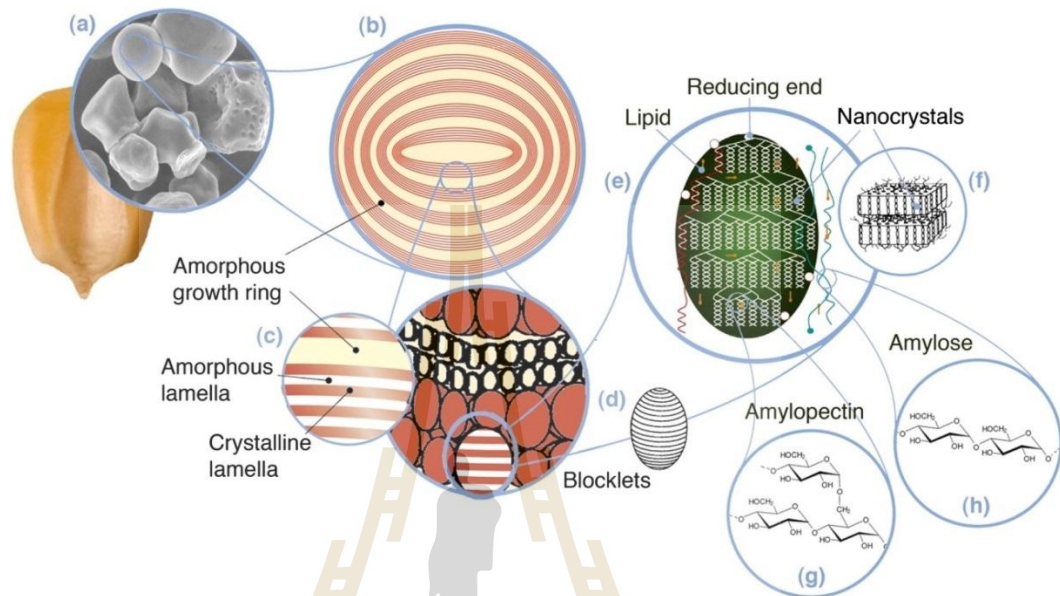
Figure 2.3   Starch multiscale structures: (a) starch granules from normal maize (30 μm), (b) amorphous and semi-crystalline growth rings (120-500 nm), (c) amorphous and crystalline lamellae (9 nm): magnified details of the semi-crystalline growth ring, (d) blocklet (20-50 nm) constituting unit of the growth rings, (e) amylopectin double helixes forming the crystalline lamellae of the blocklets, (f) nanocrystals: other representation of the crystalline lamellae called starch nanocrystals when separated by acid hydrolysis, (g) amylopectin's molecular structure, and (h) amylose's molecular structure (0.1-1 nm)

Source : Le Corre, et al. (2010).

X-ray diffraction or scattering techniques have been used extensively to study the crystalline structure of starch granules. Almost all X-ray diffraction patterns of major native starches have been identified and this information has been made available online (i.e. http://amidotheque.cermav.cnrs.fr). Essentially, the crystalline structure of starch granule is built by amylopectin chains entanglement which shows an ordered structure. Two basic diffractogram patterns, namely A and B-type, represent the crystalline type of native starches (Figure 2.4). Cereal starches, such as maize, exhibit an A-type crystalline pattern, while tuber and amylose-rich starches normally show a B-type crystalline pattern (Buléon, et al., 1998). The C-type crystalline pattern is shown when A and B-type crystalline patterns are coexisting on the diffractogram of starch.
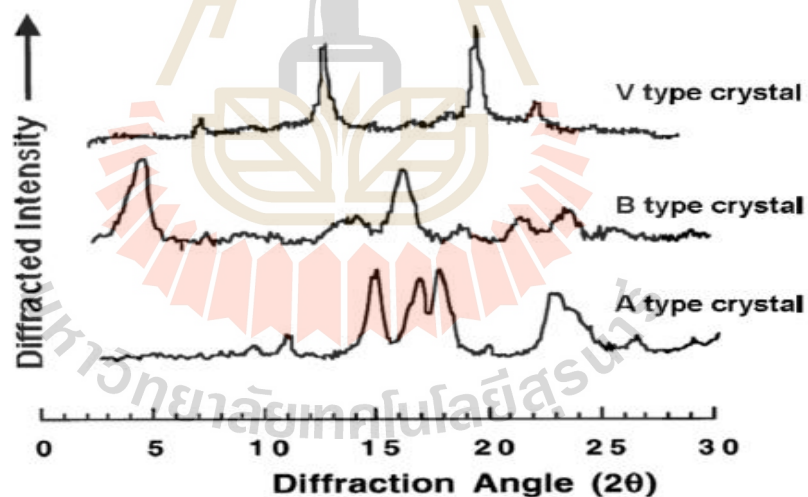
Figure 2.4 Typical X-ray diffractogram of native starch.

Source: Buléon, et al. (1998).

During the gelatinization of starch, the native crystalline of A or B melts; then, the V-type crystalline pattern appears (Figure 2.4) referring to a complex of amylose

with fatty acids and monoglycerides. In addition, retrograded amylose which is formed during the storage of starch paste exhibits a weak B-type crystalline pattern (Hizukuri, 1985).

Small angle X-ray scattering (SAXS) has been used to provide information about the lamellar structure of native and processed starches (Cameron and Donald, 1993; Donald, Kato, Perry, and Waigh, 2001; Waigh, Gidley, Komanshek, and Donald, 2000; Yuryev, Krivandin, Kiseleva, Wasserman, Genkina, Fornal, Blaszczak, and Schiraldi, 2004). Hydrated starch gives a good electron density contrast between the crystalline lamellae and the amorphous background, therefore allowing the SAXS to precisely distinguish the thickness of crystalline lamellae of native starch to be 4-5 nm (Blanche and Sun, 2004; Donald, et al., 1997; Putaux, Molina-Boisseau, Momaur, and Dufresne, 2003; Yuryev, et al., 2004). The crystalline lamellae may be disrupted during processing. The characteristic peak of the lamellar structure may disappear or decrease on its height, depending on the level of the disruption (Waigh, et al., 2000). In addition, long retrogradation process can bring back the SAXS peak at some extent (Waigh, et al., 2000).

2.2 Starch modifications

Native starch granules exhibit inherent property to insoluble in cold water. Starch gel produced from native starch tends to loss its viscosity and thickening power after cooking. Moreover, during storage, starch gel may undergo synersis in which the water leaches out of the gel matrix. Therefore, prior to application, native starch needs to be modified in order to improve the starch gel consistency during cooking and storage.

2.2.1 Overview of starch modification methods

Inherently, native starches are insoluble in cold water. However, starch can be cold water soluble after its native structure is altered through starch modification processes (Kaur, Ariffin, Bhat, and Karim, 2012; Tharanathan, 2005). There are three major methods to modify the starch structure, including physical, chemical and enzymatical approaches. Moreover, a combination of those treatments makes possible to tailor-made the modified starch to satisfy a certain starch specification.

Physical modification of starch involves treatments such as moisture, heat, shear, and radiation (Chiu and Solarek, 2009; Kaur, et al., 2012; Zia-ud-Din, Xiong, and Fei, 2017). Common examples of physical starch modification method are pre-gelatinization, annealing, heat-moisture treatment, and extrusion (Zia-ud-Din, et al., 2017). Currently, non-thermal treatments such as ultrasonication, pulsed electric field, high hydrostatic pressure, and microwave are developed to modify starch (Zia-ud-Din, et al., 2017). These methods are valuable to be implemented in a process particularly when the ingredients contain high-value components such as vitamins and flavors. These processes are also worth to preserve the product color and texture which cannot be done by traditional thermal processes (Li, Chen, Liu, and Chen, 2008; Marsellés-Fontanet and Martín-Belloso, 2007; Torregrosa, Esteve, Frígola, and Cortés, 2006).

Starch modifications by physical or thermal methods are considered to be the safest approach for starch modification. This because the modification doesn't involve chemical reagents, thus no chemical residue is left in the modified starch. However, some physical modification, such as cold water swelling starch, requires chemical

reagents (ethanol and sodium hydroxide) to act like catalyze. After the modification, the reagents can be removed from the product.

Starch is modified chemically by introducing functional groups such as carboxyl or carbonyl into the main structure of starch. Substitution reactions such as oxidation, esterification, and etherification are involved during chemical modification process. The properties of substituted starch such as molecular stability against mechanical shearing, acidic, and high-temperature hydrolysis can be enhanced after the chemical modification. Also, the gel viscosity becomes more stable during storage; the capability of starch to interact with ions increases, and the rate of retrogradation reduces (Xie, Liu, and Cui, 2005).

The second type of chemically modified starch product is cross-linked starch. The basic principle of starch modification by cross-linking reactions is that since starch contains two types of hydroxyl groups, primary (6-OH) and secondary (2-OH and 3-OH) groups, these hydroxyl groups can react with multifunctional reagents such as phosphoryl chloride, sodium trimetaphosphate, adipic acetic mixed anhydride, and mixtures of sodium trimetaphosphate and tripolyphosphates, resulting in cross-linked starches (Chiu, et al., 2009; Gao, Li, Bi, Mao, and Adhikari, 2014; Wongsagonsup, Shobsngob, Oonkhanond, and Varavinit, 2005). The main objectives of starch modification by cross-linking reactions are to restrict the swelling capability of starch granules during cooking and to prevent gelatinization of starch (Li, Wang, Li, Chiu, Zhang, Shi, Chen, and Mao, 2009).

The last method to alter the starch structure is enzymatical approaches. From many classes of enzyme, hydrolase is the most widely used in starch industry (Park, Park, Lee, Yoo, and Kim, 2008). Hydrolase is used to break the $(1\rightarrow4)$-α-linkages

and (1→6)-α-linkages of glucose chains. Some commercial hydrolase include α-amylase, β-amylase, glucoamylase, pullulanase, and isoamylase (Xie, et al., 2005). α-amylase is an endo-action hydrolase which can cleave the (1→4)-α-glucosidic bonds randomly within the glucose chains. This enzyme is used to convert a concentrated starch suspension becomes a low viscosity solution prior to saccharification process. β-amylase acts as an exo-acting hydrolase which cleaves glucose chains from a non-reducing ends. This enzyme converts amylose to maltose. Glucoamylase is an exo-acting enzyme that produces D-glucose from the non-reducing end of glucose chains during saccharification process. Pullulanase and isoamylase are called starch debranching enzymes because their capability to cleave the (1→6)-α-linkages of starch chains producing linear glucose chains (Hii, Tan, Ling, and Ariff, 2012; Kubo, Fujita, Harada, Matsuda, Satoh, and Nakamura, 1999).

2.3 Cold Water Swelling Starch (CWSS)

Native starches exhibit many poor properties, such as low cold water solubility, retrogradation during storage, etc. Therefore, their usage is limited for both food and non-food applications. Starch is more preferable to be treated by physical modification over chemical treatment because it doesn't produce chemical residue in the final product. Hence, modified starch produced by physical treatment is considered to be safer for human consumption (Kaur, et al., 2012).

One of the most popular starch modified product obtained by physical means is cold water swelling starch (CWSS). It was firstly developed in tandem with pre-gelatinized starch to overcome the low solubility of native starch (Eastman and Moore, 1984). These products were often called as instant starches. This is because of

their capability to adsorb cold water and swell promptly, giving appearance and texture of a cooked-like starch. Therefore, they commonly used for ready-to-be-consumed product (Eastman, et al., 1984). CWSS is superior compared to pre-gelatinized starch. This because CWSS exhibits greater solubility, smoother texture and more tolerance toward further processing (Light, 1990). However, most industry still prefers to use pre-gelatinized starch over CWSS which may be because the production cost of pre-gelatinized starch is lower than that of CWSS. The CWSS production requires high-price reactants such as ethanol and sodium hydroxide (Chen and Jane, 1994a; Dries, Gomand, Goderis, and Delcour, 2014; Jane, Craig, Seib, and Carl Hoseney, 1986a; Jane, Craig, Seib, and Hoseney, 1986b; Jane and Seib, 1991; Rajagopalan and Seib, 1992a, 1992b; Singh and Singh, 2003)

2.3.1 Methods to prepare cold water swelling starch

The effort for developing starch product that soluble in cold water has been started since mid of 1950. Knowledge on starch granule morphology and pasting behavior of native starch brought out the ideas to produce instantaneous soluble starch. Powell (1967) reported that pre-gelatinized starch could be prepared by drum drying, extrusion, and conventional cooking followed by spray drying processes. The pre-gelatinized starch product exhibits inferior properties such as graininess, less sheen and less flexible for further processing; thus the product has lower quality than the freshly cooked-up product. However, method of pre-gelatinized starch cooking is still implemented to prepare certain food products such as instant porridges.

Lindqvist (1979) was the first who revealed the ability of starch to gelatinize in cold water after treated with potassium iodide (KI) and potassium thiocyanate (KSCN). Pitchon, O'Rourke, and Joseph (1981) introduced a process to prepare

CWSS using a special spray drying technique. The starch slurry was atomized in an enclosed chamber from one nozzle, and then at the same time, the other nozzle injected a high-pressure steam to cook up the starch. The product showed indented spheres and swelled well upon rehydration. The major disadvantages of this technique were the high capital cost to construct the spray dryer and the high operation cost.

The first patent of CWSS preparation process was filled by Eastman, et al. (1984). In their method, normal starch was slurried in aqueous alcohol and then subjected to high temperature in a pressurized autoclave. The CWSS obtained by this method exhibited higher solubility than the normal starch. However, this method could not be applied for waxy starch because the starch is completely gelatinized during the conversion process. Eastman (1987) successfully polished up his previous method by converting the waxy starch became CWSS. The CWSS product obtained by this method was claimed to be chemically unmodified. The CWSS product can set become a sliceable gel without cooking or chilling when blended with aqueous sugar syrup. The CWSS product was also claimed to be useful for ingredient of many instantaneous food products such as pie fillings, jellies, demouldable desserts, and puddings.

Rajagopalan and Seib (1991) successfully patented another method to prepare CWSS. In their method, starch slurry of a mixture of starch, water and polyhydric alcohol was heated in atmospheric pressure. The successful keys of the method were mainly depending on the type of starch, type of polyhydric alcohol, temperature and the proportions of starch, water, and polyhydric alcohol. Aqueous propan-1,2-diol was the most preferable medium, although aqueous ethylene glycol, glycerol and any other four positional isomers of butandiol were also useful. Aqueous butandiol was

the most effective reagent to convert hydroxypropylated starch became CWSS, while aqueous glycerol was the most effective reagent when the starting material was potato starch. This finding was significant in terms of energy conservation for CWSS processing. They claimed that the method can be applied to produce CWSS from many starch sources such as cereal, tuber, root, and legume starches. They also reported that the CWSS products had cold water solubility ranged from 70 to 95%.

Another patent related to CWSS preparation method was released by Jane, et al. (1991). They claimed that the new method was capable for preparing CWSS from waxy rice or high amylose starches that could not be achieved by another previous method. In their method, they used a mixture of ethanol and alkali. The alkali (primarily NaOH) was functioned to swell the starch granules; meanwhile, the ethanol was used to prevent the starch granule from disintegration. The treated starch was then neutralized with HCl, washed and dried at 80°C. They found that the higher NaOH percentage resulted in the higher solubility of the product.

Simple CWSS preparation method was demonstrated by Zhang, Dhital, Haque, and Gidley (2012b). A mix of starch and aqueous alcohol was heated in a rotary evaporator in order to facilitate uniform mixing and at the same time to evaporate the reactant. The development was mainly intended to avoid the use of harsh chemical such as NaOH. Unfortunately, this method was not applicable to prepare CWSS from waxy starch which was due to rapid swelling and gelling upon conversion. Dries, et al. (2014) prepared CWSS by heating a mixture of water-ethanol in a leak-proof Schott bottle. The method is relatively simple to obtain CWSS in a lab scale. A new approach in CWSS preparation method was introduced by Wang, Zhai, and Zheng (2011) in which they used polyethylene glycol to gelatinize the starch. In

this method, polyethylene glycol acts as a grafting agent to create micro pits on the starch granule surface. Therefore, allowing water molecules to penetrate inward and swell the starch granule.

2.3.2 Starch structural changes during CWSS conversion

Jane, et al. (1986b) proposed a mechanism to explain the starch structural transition during CWSS conversion process. When starch slurry is heated, the native crystalline structure of starch melts, then, the presence of alcohol rapidly induces a single helical formation from amylopectin double helix, and eventually the V-type crystalline structure is formed with alcohol being located within the single helix cavities and possibly interstices. However, this mechanism cannot be applied to explain the CWSS conversion of waxy starch. Chen and Jane (1994b) reported that CWSS from waxy maize did not have V-type crystalline structure. Zhang, et al. (2012b) also reported that all CWSS displayed V-type crystalline except for partially converted waxy maize starch. Dries, et al. (2014) explored the structural transition of normal and waxy maize starches during CWSS conversion. For normal maize starch, conversion at 95°C allowed completely melting of A-type crystalline structure without losing their granular shape. Waxy maize starch which initially had A-type crystalline portion of 43%, after converted to CWSS conversion still retained its native crystallinity up to 30% and the V-type crystalline structure was formed with portion of 2% (Table 2.2). Under polarized light microscope, the granule of CWSS doesn't show the Maltese cross pattern but displays hazy birefringence on the granules periphery (Dries, Gomand, Delcour, and Goderis, 2016; Dries, et al., 2014; Jane, et al., 1986a; Rajagopalan, et al., 1992b; Zhang, et al., 2012b).

Jane, et al. (1986b) developed a model of CWSS conversion (Figure 2.5) to obtain a comprehensive understanding on the starch structural changes during CWSS conversion. The model was developed mainly based on the observation of starch structural changes of A-type starch during CWSS conversion. The model implies that the double helix of amylopectin clusters is converted to single helix structures. Based on this model, CWSS has a metastable structure that allows small molecule such as water to penetrate easily into the modified starch granules; hence hydration becomes faster even at low temperature. The model accommodates the finding of Dries, et al. (2014) in that amylose plays a role to preserve the starch granule integrity by the formation of stable V-type crystalline structure.

Table 2.2 Starch structural transition during CWSS conversion.

Samples	Percentage of		
	A-type crystalline	V-type crystalline	Amorphous
Native normal maize starch	27	2	71
Ethanol treated maize starch (68% v/v, 95°C)	28	2	70
Ethanol treated maize starch (58% v/v, 95°C)	21	12	67
Ethanol treated maize starch (53% v/v, 95°C)	4	17	79
Ethanol treated maize starch (48% v/v, 95°C)	0	18	82
Native waxy maize starch	43	0	57
Ethanol treated waxy starch (56% v/v, 95°C)	30	2	68

Source: modified from Dries, et al. (2014).
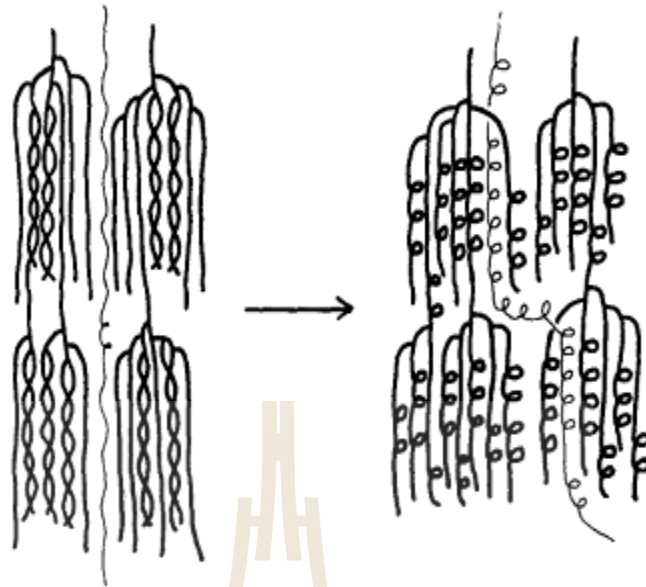
Figure 2.5 Proposed conversion of an A-type starch granule to a V-type granule (thin

line represents amylose, the thick line represents amylopectin)

Source : Jane, et al. (1986b).

2.3.3 Physical properties of cold water swelling starch

2.3.3.1 Cold water solubility and cold water adsorption of CWSS

Solubility in cold water is one of the most essential properties of CWSS. Pre-gelatinized starch and CWSS are both known as instantaneous soluble starch product; however, CWSS has lower solubility than pre-gelatinized starch. Majzoobi, Kaveh, Blanchard, and Farahnaky (2015) reported that the solubility of CWSS from maize starch was 6.24% while that of pre-gelatinized starch from maize starch was 8.45%. Decreasing or increasing pH of solution tends to increase the solubility of CWSS (Hedayati, Shahidi, Koocheki, Farahnaky, and Majzoobi, 2016). Moreover, increasing the solubilization temperature also increases the solubility of CWSS (Li, Cao, Fan, Ouyang, Luo, Zheng, and Zhang, 2014).

The water adsorption capacity of CWSS reflects the ability of CWSS to adsorb and hold water within its matrix. Pre-gelatinized starch shows higher cold water solubility than CWSS, but CWSS exhibits higher cold water adsorption capacity than pre-gelatinized starch. Jane, et al. (1986b) reported that CWSS from maize starch had water absorption capacity of 12.33 g/g while pre-gelatinized starch was 9.85 g/g. Hedayati, et al. (2016) also reported similar result in that the water adsorption capacity of CWSS from maize starch reached 13.35 g/g which was higher than that of pre-gelatinized starch (10.04 g/g). The water adsorption capacity of CWSS and pre-gelatinized starch increased at high pH and decreased at low pH (Hedayati, et al., 2016).

2.3.3.2 Thermal properties of CWSS

Rajagopalan, et al. (1992b) reported that all CWSS starches prepared by hot aqueous propan-1,2-diol did not show any melting endotherm peak. However, thermal investigation of CWSS was carried out from hydrated CWSS sample (Chen, et al., 1994b; Li, et al., 2014; Rajagopalan, et al., 1992b; Singh, et al., 2003). During CWSS conversion, water destroys the crystalline structure of native starch; at the same time amylose forms V-type crystalline structure of amylose-ethanol complex. The V-type crystalline structure is known to be soluble in water (French and Murphy, 1977). Thus, the V-type crystalline is a metastable crystal. Consequently, when water is mixed with CWSS, the water penetrates into the amorphous region, hydrates the V-type crystalline structure, and induces swelling process. Water also facilitates polymer chains mobility, hence, the internal structure of starch becomes disorder very quickly (Biliaderis, Maurice, and Vose, 1980).

In addition to the disappearance of the melting endotherm peak of CWSS, Kaur, Fazilah, and Karim (2011) reported that the glass transition temperature of CWSS was lower than that of their native counterparts. Water acts as a plasticizer which has ability to penetrate into amorphous and non-perfect crystalline regions, allowing the polymer chains to freely mobile. The presence of water in the polymer can be monitored by depressing the glass transition temperature and reducing the melting endotherm enthalpy (Krueger, Knutson, Inglett, and Walker, 1987). Li, et al. (2014) reported that the melting endotherm enthalpy of CWSS from buckwheat starch was lower (5.01 J/g) than that of its native counterpart (9.02 J/g). They also investigated that the melting endotherm enthalpy of pre-gelatinized starch was close to zero indicating the total loss of native crystalline structure and molecular order. The melting endotherm enthalpy is related to the disruption of amylopectin clusters (Miao, Zhang, and Jiang, 2009). Thus, the lower value of melting endotherm enthalpy of CWSS indicates the disruption of the double helices of CWSS during CWSS conversion.

2.3.4 Morphological properties of cold water swelling starch

The morphological properties of CWSS granules are totally different with that of native starch granules. The native starch granule shows relatively rigid bodies with distinct morphological characteristics. Native maize starch granules are round to polygonal in shapes with smooth surface (Chen, et al., 1994a; Dries, et al., 2014; Hedayati, et al., 2016; Majzoobi, et al., 2015; Zhang, et al., 2012b). Native potato granule has smooth surface with round to oval shape and broad size range from 5 to 100 μm (Dries, et al., 2016; Zhang, et al., 2012b). Processing of native starch to CWSS alters the granular morphology of starch drastically. Granules of CWSS from

maize starch enlarge, deform and loss integrity with no distinct shapes (Hedayati, et al., 2016). Also, it shows leathery texture on the granules surface (Rajagopalan, et al., 1992b) with indentation and wrinkling features (Chen, et al., 1994a; Rajagopalan, et al., 1992b; Zhang, et al., 2012b) and agglomerated fragments (Zhang, et al., 2012b). CWSS granules did not exhibit the Maltese cross characteristic of native starch but showed a weak discernable birefringence pattern at the granules periphery (Dries, et al., 2016; Jane, et al., 1986b).

For CWSS prepared by mixing starch with ethanol and NaOH (Chen, et al., 1994a), each reactant has different role in changing the morphology of CWSS granules. Jivan, Yarmand, and Madadlou (2014) reported that the higher sodium hydroxide ratio used during CWSS conversion, the deformation of CWSS granules became more pronounce. Moreover, the CWSS granules remained intact when higher ethanol proportion was used. This indicates that the presence of ethanol is effective to prevent starch granules from disintegration induced by NaOH (Chen, et al., 1994a). Moreover, deformation of the granular shape of CWSS was more pronounce when higher temperature is used during CWSS conversion (Dries, et al., 2014).

2.3.5 The V-type crystalline structure of amylose-ethanol complex

The V-type crystalline structure is formed when guest molecules resides in the cavity of amylose chain as observed by X-ray diffraction technique. This structure may present as an artifact of a complex between amylose and ethanol in CWSS. This because ethanol can be removed from the cavity of amylose by dehydration means (Dries, et al., 2014). Putseys, Lamberts, and Delcour (2010) classified three different methods to form the V-type crystalline structure of amylose inclusion complexes including (a) starting from starch and ligands, (b) starting from amylose and ligands

and (c) synthetizing amylose in the presence of the ligands. For some cases, the term of amylose inclusion complex may not proper. This is because some ligands such as menthone, fenchone, ethanol can be entrapped between the helices of the crystal (Helbert, 1994). Therefore, they can be removed by solvent extraction (Rondeau-Mouro, Bail, and Buléon, 2004) or drying (Dries, et al., 2014).

2.4 Pore characterization of starch

2.4.1 The importance of pore characterization study

Pore characterization is closely related to adsorption science. This is because pore characterization is one of many tools that can be used to study the adsorption phenomenon. Pore characterization covers the determination of pore sizes and shapes, pores behavior toward adsorptive and adsorbate, pore connectivity, specific surface area, and pore size distribution (Lowell, Shields, Thomas, and Thommes, 2010).

A natural phenomenon in which a solid surface contacts with fluids, gas and liquid, is called adsorption. Many examples of adsorption phenomenon can be found in our surroundings, for example dust attaches on the surface of solid, sponges adsorb soap water, etc. Scientists have studied this phenomenon since a long time ago and, today, adsorption is a well-established science in many disciplines such as chemistry, physics, agriculture, and material sciences.

The definition of adsorption was given by Rouquerol, Rouquerol, and Sing (1999b) that is the enrichment of material or an increase in the density of the fluid in the vicinity of an interface. Adsorption is differentiated from absorption in which adsorption is a surface phenomenon that refers to a higher concentration of liquid or gas on the surface of solid surface. Meanwhile, absorption occurs when molecules of

a substance are uniformly distributed in the bulk of the other. Famous examples of adsorption and absorption phenomena are immersion of plastic sheet and paper into a colored solution, respectively. However, in real situations, it is impossible or difficult to distinguish between adsorption and absorption. Therefore, sorption is used as general terminology which embraces both phenomena.

Science and technological aspects of adsorption are crucial for porous materials such as adsorbent, catalyst, encapsulating agent, and pigment (Lowell, et al., 2010). Gas-solid adsorption technique has been used to determine the sorption characteristic of porous materials. Gas-solid adsorption technique is also widely accepted by food scientists for pore characterization of a diverse range of food powders (Ray, Raychaudhuri, and Chakraborty, 2016), extruded products (Karathanos and Saravacos, 1993) and other food porous materials (Fannon, Hauber, and Bemiller, 1992; Juszczak, Fortuna, and Wodnicka, 2002; Mahmoudi Najafi, Baghaie, and Ashori, 2016; Sujka and Jamroz, 2010; Wang, Lv, Jiang, Niu, Pang, and Jiang, 2016).

2.4.2 Porosity

Porous materials are characterized by several parameters including porosity, pore size distribution, specific surface area and pore connectivity (Rigby, Fletcher, and Riley, 2003). The term of porosity is frequently used to give an illustration on how much space available for guest substances to stay within the internal matrix of the porous material (Hook, 2003). Generally, high porous materials can store a higher amount of guest substances than non-porous materials. This is because porous material contains higher porosity. Mathematically, porosity is expressed as the ratio of pore volume in the material over the total or bulk volume. Meanwhile, void space is the summation or combined volume of all pore spaces in a given material.

Rouquerol, et al. (1999b) illustrated several types of pores based on their interconnectivity (Figure 2.6). The first category of pores is called closed pores. These include those are totally isolated from their neighbors (a). These pores don't correlate with adsorption; however their presence influence macroscopic properties such as bulk density, mechanical strength, and thermal conductivity. Most of pores categorized as open pores have a continuous channel with the external surface of the body such as (b) (c) (d) (e) and (f). Some open pores may have opening only at one end such as (b) and (f); therefore, they are called as blind pores. Roughness (g) has a contribution in adsorption even at small portion. This is because particle with roughness shows higher surface area than the smooth one. Pores can also be classified based on their shape (Sing, Everett, Haul, Moscou, Pierotti, Rouquerol, and Siemieniewska, 2008). Pore may have different shapes such as cylinder, ink-bottle, funnel, and slit (Figure 2.7).
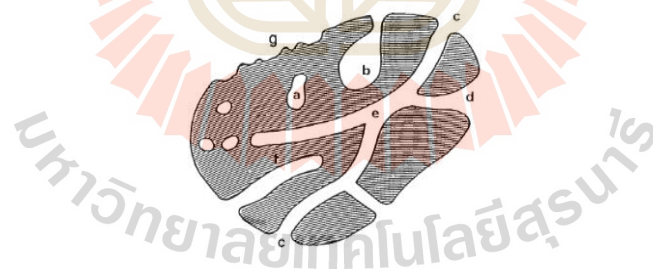
Figure 2.6 Schematic cross section of porous material.

Source: Rouquerol, et al. (1999b).
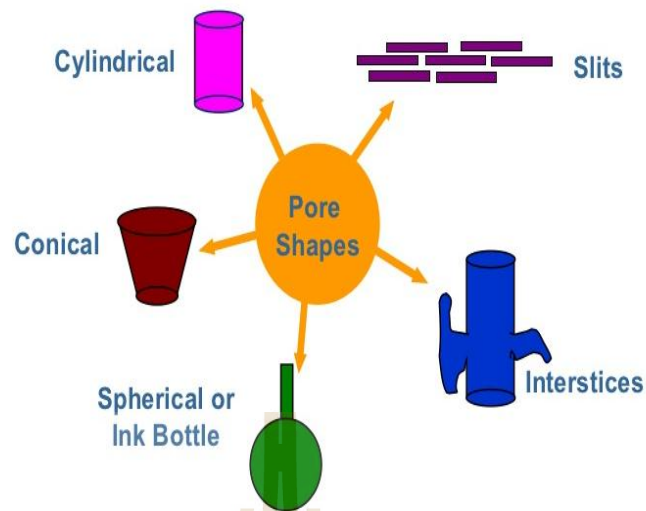
Figure 2.7 Pores classification according to their shapes.

Source: Rouquerol, Rouquerol, and Sing (1999c).

2.4.3 Methods to access pore characteristics

Methods to characterize pore are summarized in Figure 2.8. The method selection is based on the pore size of the porous material. Some techniques have been used to characterize pore of starch including: nitrogen sorption isotherm method (Juszczak, et al., 2002; Sujka and Jamroz, 2007; Sujka and Jamroz, 2009; Sujka, et al., 2010), water sorption isotherm (Hellman and Melvin, 1950), low and high pressure mercury porosimetry (Karathanos, et al., 1993; Sujka, et al., 2010), scanning electron microscope (Fannon, et al., 1992; Fannon, Shull, and Bemiller, 1993; Hall and Sayre, 1970), confocal laser scanning microscope (Huber and BeMiller, 1997; Huber and BeMiller, 2000; Kim and Huber, 2008), and transmission electron microscope (Sujka, et al., 2010).
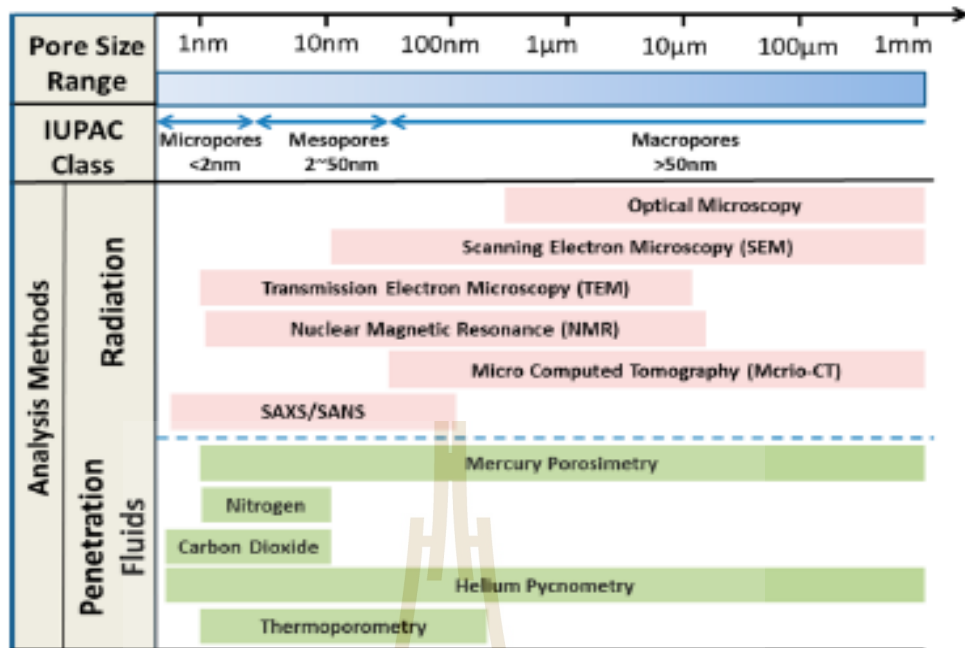
Figure 2.8 Methods for estimating porosity and pore size distribution of porous material.

Source: Zhao, Liu, Elsworth, Jiang, and Zhu (2014).

2.4.4 Pore characterization by gas adsorption method

Gas adsorption is one of the most widely accepted techniques for pore characterization, particularly to determine the specific surface area and pore size distribution. This technique allows assessment of pore in a vast range of sizes; therefore, it is recommended as a standard pore analysis method by IUPAC (Rouquerol, et al., 1999b).

Principally, in gas adsorption method, two materials at different state must be present and interact with each other in a system. The solid-state sample acts as adsorbent, and the adsorptive fluid is a substance that adsorbed by the adsorbent (Rouquerol, Rouquerol, and Sing, 1999a). Full sorption consisted of adsorption and

desorption branch. Adsorption branch constructed from low to high partial pressure which represents penetration of fluid into solid phase, meanwhile desorption represents removal adsorptive from adsorbent surface, and its direction starts from high to low partial pressure. Both adsorption and desorption occur at a constant temperature; therefore, it is known as sorption isotherm.

Based on the molecular interaction between adsorbent and adsorptive, it has been identified two types of sorption: the first is physisorption in which weak molecular interaction such as van der Waals interaction are involved. The second type of sorption involves chemical bonding between adsorbate molecules with an adsorbent called chemisorption (Lowell, et al., 2010).

According to the IUPAC, there are six basic types of sorption isotherms that most of porous material follows (Rouquerol, et al., 1999b). These sorption isotherms are determined based on physisorption principle and measured on a range of fluid-solid systems (Figure 2.9).
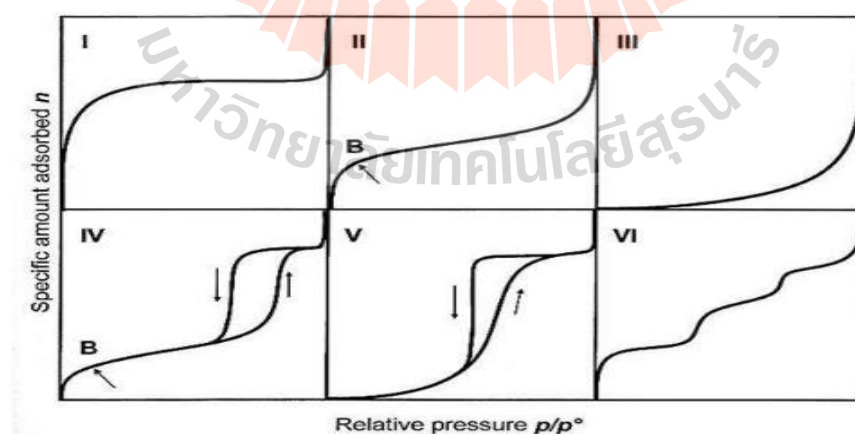
Figure 2.9 Six major types of sorption isotherms, according to the IUPAC classification.

Source: Rouquerol, et al. (1999b).

Briefly, type I isotherm indicates strong adsorbate-adsorbent interactions that usually occur in micropores which has pore width below 2 nm (Rouquerol, et al., 1999b). The type II isotherm is known as s-shape isotherm. This isotherm type is characterized by the presence of inflection point labeled as point B which is interpreted as a point where monolayer of adsorbate is completed or the onset of multilayer adsorption. This point was used by Brunauer, Emmett, and Teller (1938) to derive the BET equation. For non-porous and macroporous adsorbents, hysteresis phenomenon doesn't exist in type II isotherm. Type III isotherm is characteristic of weak adsorbent-adsorbate interactions (Rouquerol, et al., 1999a). Type IV isotherm is a characteristic of adsorbent that has a large number of mesopores. The main feature of this isotherm is its incomplete reversibility which is called hysteresis loop. Hysteresis loop of type IV isotherm is associated with capillary condensation which occurs during pore filling and emptying. IUPAC classified four types of hysteresis loops in type IV isotherm including H1, H2, H3 and H4 (Figure 2.10). Factors causing hysteresis are complicated, and some of them are still not well understood. Hysteresis can arise due to forces involved in the interaction between adsorptive and adsorbent that makes adsorptive delaying condensation. It can also happen due to pore network within the adsorbent matrix (Lowell, et al., 2010; Rouquerol, et al., 1999a; Seaton, 1991). Type V isotherm is similar to Type III and is also interpreted due to weak absorbent-adsorbate interactions. The Type V isotherm also exhibits a hysteresis loop which is due to the mechanism of pore filling and emptying by capillary condensation. The last type of IUPAC isotherm is type VI isotherm which is the characteristic of porous material that has uniform pore size or uniform surface

properties when accessed with spherically nonpolar adsorptives such as argon and krypton.
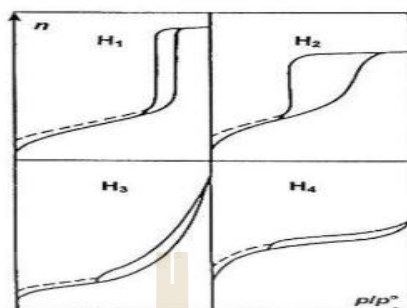
Figure 2.10 Hysteresis types of type IV isotherms

Source : Rouquerol, et al. (1999b).

Dubinin (1960) classified pores based on their width different: micropores, transitional pores (also now known as mesopores), and macropores. Then, IUPAC adopted this classification, hence defines three pore categories (Table 2.3).

Table 2.3 Classification of pores according to IUPAC based on their pore width.

Classification	Pore width
Micropores	Less than 2 nm
Mesopores	Between 2 – 50 nm
Macropores	More than 50 nm

Source: Rouquerol, et al. (1999b).

Adsorption science began to find its advancement after the BET equation was developed by Brunauer, et al. (1938) to predict the surface area of porous solids. The application of this science was more pronounce after Barrett, Joyner, and Halenda (1951) developed BJH method to determine pore size distribution.

2.4.5   Determining surface area

Porous material usually exhibits wide surface area. Porous material with wide surface area provides space for fluid molecules to lay on its surface (Lowell, et al., 2010). Therefore, the value of surface area of a porous material obtained from accurate measurement can represent the adsorption capability of the material.

The principle of surface area determination by adsorption technique is to measure the limit of a close-packed monolayer covering pores of material. The size of molecule used for surface area determination should be known; hence it will give a straightforward calculation to the specific surface area. Apart from the difficulties of its applicability, the chemisorption method gives a more accurate result for surface area determination compared to physisorption since physisorption generally involves multilayer adsorption. The difficulties in determining the monolayer capacity of multilayer adsorption are the molecular layering occurs at pressure well below that required for completion of the monolayer. This brings consequences of uncertainties on how to extract the monolayer capacity from the sorption isotherm data. However, Brunauer, et al. (1938) solved this problem, by developing a simple model isotherm (BET), which accounted the multilayer adsorption and used it to extract the monolayer capacity data then to give the specific surface area of the tested materials. The BET method is the most widely used technique to determine specific surface area and it is officially adopted by the IUPAC (Sing, et al., 2008). Prior to conducting a BET analysis, some assumptions should be taken as follow (Lowell, et al., 2010):

1.   The molecule in the first mono layer can be used as "site" for second molecules to form subsequent layers.

2.   It is assumed that the energy of adsorption for the first mono layer is different than that for the second and all subsequent layers. This means that the energy of adsorption for the second layer and above have the same value as the liquefaction energy E of the adsorptive (i.e., $E_2 = E^i = E_L$).

3.   It assumed that a uniform array of surface sites is formed with no lateral interactions between the adsorbed molecules. This third assumption is very critical because somehow it may deviate from reality. This assumption is derived from the second assumption that E_i is not dependent on the surface of the ith layer.

4.   The layers will not undergo condensation such that the multi-layer has an infinite thickness at $\frac{p}{p^0} = 1$ (i = ∞).

According to Sing, et al. (2008) the range of linearity of the BET plot is generally restricted to $\frac{p}{p^0} \leq 0.4$ (usually within the $\frac{p}{p^0}$ range of 0.05-0.3). The linear transformed BET equation provides a basis to plot the experimental isotherm data for calculating the surface area. By using the slope of the fit, the BET surface area can be determined as the monolayer capacity by using this following equation.

$$A_s(BET) = n_m^a L a_m$$

Where L is Avogadro constant, $A_s(BET)$ is the total surface area, the a_m is molecular cross-sectional area of nitrogen used in the analysis at temperature 77 K which is 0.162 nm^2. Eventually, the specific surface area $a_s(BET)$ can be calculated by dividing the BET surface area by the mass of adsorbent, m (Brunauer, et al., 1938).

$$a_s(BET) = \frac{A_s(BET)}{m}$$

2.4.6 Assessment of pore size distribution in the range of mesopore

Most micropore adsorbent exhibits type I isotherm, meanwhile mesopore adsorbent may possess type II or IV isotherm. For both adsorbent types, the total pore volume, V, are often derived from the amount of vapor adsorbed at a relative pressure close to one by assuming that pores are filled with condensed adsorptive in normal liquid state. Despite interpretation of isotherm graph is relatively complicated, prediction on the pore size distribution can be made by analyzing the isotherm graph.

For porous material that doesn't have macropores, the isotherm remains nearly horizontal over a range of $\frac{p}{p^0}$ approaching unity (1) and the total pore volume is well-defined. In the other case if macropores presence in the sample then the sample isotherm rises rapidly near $\frac{p}{p^0} = 1$ and if the macropores are very wide then the isotherm may exhibit an essentially vertical at the end of $\frac{p}{p^0} \approx 1$. According to the IUPAC guideline, it is necessary to take some precaution before conducting pore size distribution analysis. For instance, it is necessary to make sure that there are no 'cold spots' in the apparatus which can lead to bulk condensation of the gas and gives a false measure of adsorption in the volumetric method (Rouquerol, et al., 1999a). Hereafter, the pore size distribution analysis can be derived by determining the mean hydraulic radius, r_h, of a group of mesopores which is defined as :

$$r_h = \left(\frac{V}{A_s}\right)_p$$

Where $\left(\frac{V}{A_s}\right)_p$ is the ratio of the volume to the area of walls of the group.

The analysis is easy to be done if the pores have a well-defined shape. Therefore the a simple relationship between the mean hydraulic radius, r_h and the

mean pore radius, r_p can be developed. Thus, in the case of pores with non-intersecting cylindrical capillaries shapes, the relationship is simply defined as:

$$r_p = 2r_h$$

For a parallel-sided slit-shaped pore, r_h is half the slit width.

There are some established methods available for the determination of pore size distribution of mesopores. The most well-known is Kelvin model which has been derived according to the case of mesopores such as the Barrett, Joyner, and Halenda (BJH) method (Barrett, et al., 1951). Horváth and Kawazoe (1983) derived the Kelvin equation for pore size analysis in micropores region by considering the fluid-solid interactions. However, the most widely accepted method to determine the pore size distribution of mesopores is BJH method. This mainly because of its genericity to analyze a wide range of mesopores (Rouquerol, Rouquerol, and Sing, 1999d). The derived Kelvin equation is:

$$\frac{p}{p^0} = exp\left[\frac{-2\gamma v_1}{R\,Tr_c}\right]$$

where,

$p^0 =$ Saturated vapour Pressure at given temperature T

$\gamma =$ Liquid vapour surface tension

$v_1 =$ Liquid molar volume

R = Universal Gas constant

$r_c =$ Radius of curvature

Most of mesopores assessment methods are based on the application of the Kelvin equation and the concept of capillary condensation. However, the computation of pore size distribution by this method involves several assumptions (pore shape,

mechanism of pore filling, the validity of Kelvin equation, etc.) (Lowell, et al., 2010). Specifically, for mesopores analysis by the BJH method, assumptions should be made to assure that the conditions of pores satisfy the equation, as follow:

1.   The pores must be rigid.

2.   The pores shape are well defined either regular cylinders or parallel sided slits.

These assumptions somehow might contradict with the real nature of adsorbent (Rouquerol, et al., 1999d). However, these assumptions should be taken since the underlying principles of mesopore filling are not fully understood. In case of slit shape pore, analysis by BJH can be done by assuming the meniscus is hemicylindrical (Rouquerol, et al., 1999d).

2.4.7   Pore characterization of native and modified starch

Study to reveal the existence of porosity in native starch granules had been initiated by Fannon, et al. (1992). They found that pores in native starch granules are normal, real, anatomical features and are not artifacts produced during sample isolation, preparation, or observation. Some starches have pores on their surface such as wheat, rye, barley (Hall, et al., 1970) but some other doesn't have surface pores such as rice, oat, potato, tapioca, arrowroot and canna (Fannon, et al., 1992). These pores were referred as microscopic pores which mean that the pores can be observed visually by using microscopy techniques.

By using the IUPAC standard method, nitrogen adsorption isotherm, Sujka, et al. (2010) found that almost all native starches have pores with diameter of about 2-3 nm with an exception for corn and rice which have a diameter ranging from 100-200 nm. For native starch, rice starch has the highest surface area, and potato starch

exhibits the lowest one with BET surface area of 1.27 and 0.14 m^2/gram, respectively (Sujka, et al., 2010). However, surface area of native starch can be influenced by the sample preparation method. For instance, drying sample for long period may increase the surface area of sample (Juszczak, et al., 2002; Sujka, et al., 2009, 2010).

2.5   Hydration of starch

2.5.1   Introduction to hydration

Hydration by definition is a process of causing something to absorb water. In a broader chemical sense, hydration is combining a substance with water molecules to form a hydrated compound (Braun, Koztecki, McMahon, Price, and Reutzel-Edens, 2015; Laage, Elsaesser, and Hynes, 2017). The mechanisms of water to connect with a molecule include physisorption or binding water to a solid surface by hydrogen bonding, physical entrapment to form liquid inclusion, and absorption in localized disordered regions. Water adsorbed by these mechanism are mostly can be removed by heating methods. The other type of water-molecule interaction is chemically bonded water which is formed by chemical addition and hydrate formation (Braun, et al., 2015). This water type is difficult to be removed from the host molecule by heating means.

A molecule may get hydrated by two possible ways; first, water is added intentionally into the molecule for a certain purpose. A molecule contacts with water during processing steps, such as crystallization, lyophilization, wet granulation, aqueous film-coating, or spray-drying. The second way is a molecule may be exposed to water during storage in a high humidity environment. Unintended hydration may also occur when a dry molecule contacts another molecule that contains water. Water

may be adsorbed onto the surface of dry molecule and may be absorbed in the bulk structure of the molecule (Khankari and Grant, 1995).

Based on the interaction between water and host molecule, there are two states of water which are stoichiometric and non-stoichiometric hydrates (Brittain, 2009). For crystal structure, water in stoichiometric hydrates becomes an integral part of the crystal. Also, the water is essential to maintain the molecular network of the crystal. For nonstoichiometric hydrates, water is located in structural voids which act as a space filler.

Impact of water removal on crystal structure depends on the water location in the crystal structure. Removal of stoichiometric hydrate water gives a different crystal structure resulting in a disordered or amorphous state. Meanwhile, removal of non-stoichiometric hydrate water doesn't influence on the structure of the parental hydrate (Griesser, 2006). Stoichiometric hydrates influence the properties of crystal structure through several mechanisms including modifying the internal energy (entropy and enthalpy) of crystal, changing the shape and symmetry of unit crystal cell, and changing the thermodynamic activity of crystal (Khankari, et al., 1995). Hydration of crystal lattice produces a new unit crystal cell that different from the anhydrate crystal. Consequently, the physical properties of the hydrated crystal such as solubility, dissolution rate, and physical stability also different from the anhydrate crystal (Khankari, et al., 1995).

Hydrated molecules can be characterized by either classical analytical chemistry methods or modern instruments. The amount of physically entrapped water in a crystal structure can be quantitatively determined by using gravimetry or titrimetry methods (Williams, 1963). Many modern instruments are capable to

characterize the hydrated crystal structure such as X-ray powder diffractometry (Morris and Rodriguez-Hornedo, 1993), differential scanning calorimetry (Dollimore, 1996), thermogravimetric analysis (Dollimore, 1996), infrared spectroscopy (Carstensen, 1984), single crystal X-ray analysis (Carstensen, 1984), solid-state NMR, Raman spectroscopy, and isothermal microcalorimetry (Khankari, et al., 1995).

2.5.2 Hydration in starch processing

Water plays a critical role during starch processing. All starch processing and modifications process always involve hydration and dehydration steps. For example, starch powder is extracted from starch sources by using water as the solvent. After extraction, the water is then removed from the starch slurry by dehydrating means including filtration or centrifugation and drying process to obtain dry starch powder (Galliard, 1987; Thomas and Atwell, 1999). Starch gelatinization process requires water in excess to accomplish a fully gelatinized starch. Starch modification processes either physical or chemical modifications also involve water during the modification process. Starch modification by annealing and heat-moisture treatment exploits thermal energy and water content to alter the structure of starch (Stute, 1992). In starch modification by using chemical methods, water acts as a solvent of chemical reagents and medium for the chemical reaction to occur (Tomasik and Schilling, 2004; Zia-ud-Din, et al., 2017). Starch modification by enzymatical method requires water to facilitate the enzyme activity and to dilute the substrate (Park, et al., 2008).

Water facilitates movements of molecules in a chemical system. This is possible because water molecule in liquid state behaves as if it has two positive and two negative regions of charge in tetrahedral conformation (Khankari, et al., 1995). Water molecule interacts with its neighbors by a coordinate covalent (dative) bond or

by accepting a hydrogen bond at the negatively charged region. At the same time, the positively charged region of water molecule interacts with its neighbors via a donated hydrogen bond. Thus water molecule connects its neighbors via electron acceptor groups (or proton donors) and electron donor groups (or proton acceptors) mechanism. The water molecules interact with the other neighbor water molecules via hydrogen bond formation. The water molecule may also interact with other molecules with various types of van der Waals' interaction (dipole-dipole, dipole-induced dipole and dispersion forces). When various kinds of water molecule occur in a crystal structure, finite or infinite hydrogen-bonded three-dimensional water networks may be formed (Falk and Knop, 1973).

During starch processing or modification, water plays a role as a lubricating agent for the movement of starch components. At crystalline structural level, hydration induces movement of double helixes of amylopectin clusters toward the most stable conformation (Vermeylen, Derycke, Delcour, Goderis, Reynaers, and Koch, 2006; Waigh, et al., 2000). Hydration of starch under ambient conditions could enhance the B-polymorphic features for both A-type and B-type starches (Qiao, Zhang, Huang, Xie, Wang, Jiang, Zhao, and Zhu, 2017). The B-type crystalline structure of potato starch reaches its lowest steric hindrance conformation when it is hydrated with water in excess (Buleon, Le Bail, Colonna, and Bizot, 1998). During annealing, the dual effects of water and temperature reorient the crystallite toward the most stable conformation without changing the crystalline type (Waduge, Hoover, Vasanthan, Gao, and Li, 2006). Meanwhile, heat-moisture treatment alters the B-type of potato and yam starches to A- (or C-) type, and the C-type crystalline structure of arrowroot and cassava starches to A-type. Meanwhile, heat moisture treatment did not

change the A-type pattern of cereal starches but increase the intensity of its characteristic peaks (Hoover and Manuel, 1996; Hoover and Vasanthan, 1994). This indicates that combination of water and heat in heat-moisture treatment of starch moves some double helices into a more perfect position in the crystalline phase (Hoover, et al., 1996; Hoover, et al., 1994)

2.5.3 Retrogradation of starch gel during storage

Based on structural point of view, starch processing can be considered as an irreversible order-disorder transition from the semi-crystalline structure of native starch to amorphous structure (Jenkins and Donald, 1998). The loss of crystalline starch structure during heating can be brought back partially during cooling. During long time storage, water in starch gel or paste leaches out of the gel and a white precipitate eventually is formed. The phenomenon where water leaches out of the gel matrix is termed syneresis and the precipitation of starch is called retrogradation in which both are non-reversible processes (Imberty, Buléon, Tran, and Péerez, 1991).

During retrogradation, hydrated glucan chains loosen its binding with water and tend to form double helices among them. The rate of retrogradation is affected by many factors, such as starch concentration, molecular weight, and degree of hydration, temperature, pH and salt concentration. In starch gel system, retrogradation is observed as precipitated starch, while in low moisture content food, the occurrence of retrogradation process can be observed from texture hardening (Jonhed, 2006). Kainuma, Matsunaga, and Itagawa (1981) identified several changes during retrogradation process in starchy food such as increasing resistance to digestive enzymes, low ability to bind iodine, increasing the gel firmness and new crystalline

structure formation. Figure 2.11 is a representation of starch gelatinization during heating and starch retrogradation during long time storage.

Retrogradation of starch may involve individual or interaction of both starch components (i.e. amylose and amylopectin) with different rate and mechanism (Tako, Tamaki, Teruya, and Takeda, 2014). The long chain amylose molecules are known unstable in solution in which it tends to shrink as a result of low kinetic energy and Brownian motion of the amylose chains and water molecules. A consequence of this shrinkage is a new formation of intra and intermolecular bonding between both the hemiacetal oxygen atom and the adjacent OH-6 of the D-glucopyranosyl residues and the O-6 and OH-2 of glucopyranosyl residues on different molecules. This event leads to the precipitation of amylose in the aqueous system (Tako, et al., 2014; Tamaki, Konishi, and Tako, 2011). Interaction between amylose and amylopectin during retrogradation process is initiated by a similar mechanism as amylose retrogradation process (Tako, et al., 2014). This restriction induces hydrogen-bonding side by side between the O-3 and the OH-3 of glucose residues of amylose and amylopectin chains. Retrogradation caused by the interaction between amylopectin molecules occurs at a slower rate due to the interaction between short side chains has high kinetic energy (Tako, et al., 2014).
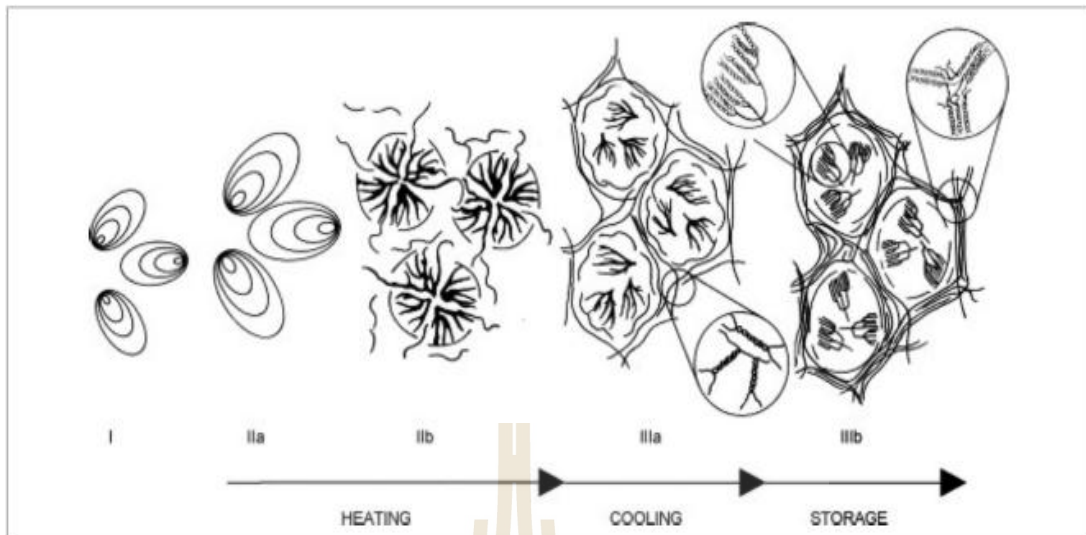
Figure 2.11 Process representing the changes that occur during heating, cooling, and
storage of a starch-water mixture. (I) Granules of native starch; (II)
gelatinization process which subsequent process including swelling [a]
and amylose out of granule structure due to partial granule disruption
[b], resulting in the formation of a starch paste; (III) retrogradation of
amylose network during cooling of the starch paste [a] and formation of
ordered structure of amylopectin (amylopectin retrogradation) during
storage [b].

Source: Goesaert, Brijs, Veraverbeke, Courtin, Gebruers, and Delcour
(2005).

In addition, the rate of retrogradation process is determined by starch
component interactions and also storage conditions (i.e. solvent, time and
temperature). The rule of thumb in retrogradation is that the longer storage time and
the lower temperature will result in the higher retrogradation rate. For gel from waxy
starch which doesn't have significant amount of amylose, retrogradation process

occurs at a slower rate than that occurs in gel of normal starch. Amylopectin retrogradation of waxy starch produces soft gel since no amylose re-association occurs in the system (Tang and Copeland, 2007). For gel of normal starch, retrogradation follows two ways, amylose chains re-association that occurs very rapidly at the beginning stage, and amylopectin chains re-association that happens at slower rate (Wang, Li, Copeland, Niu, and Wang, 2015). Amylose retrogradation is responsible for the initial hardness of starch gel and slower digestibility of processed foods.

2.5.4 Re-hydration of cold water swelling starch

After native starch was converted to CWSS, the native crystal structure of starch was destroyed, and the V-crystalline structure was formed (Chen, et al., 1994a; Jane, et al., 1986b). For CWSS prepared by ETS method, subsequent to the conversion process, the ethanol removal by drying means did not effect on the X-ray scattering pattern of the V crystalline structure (Dries, et al., 2014; Le Bail, Bizot, Pontoire, and Buleon, 1995; Whittam, Orford, Ring, Clark, Parker, Cairns, and Miles, 1989). Dries, et al. (2014) suggested that ethanol removal is not mandatory to obtain CWSS with high cold water swelling properties because ethanol is freely exchangeable with water.

Post processing, the V-type crystalline structure of CWSS can be altered by high humidity exposure during storage. Jane, et al. (1986b) reported that the V-type crystalline pattern of CWS disappeared after CWSS from corn starch was stored under 100% relative humidity for 13 days. They also reported that the A-type crystalline pattern reappeared and the modified starch became cold water-insoluble.

2.6 Encapsulation

2.6.1. Introduction to encapsulation

Encapsulation process can be defined as a process to entrap one substance (active agent) into another substance (wall material), producing encapsulated particles (Lakkis, 2007). Encapsulation process can be categorized based on the size of the encapsulated product such that nano-encapsulation, micro-encapsulation, encapsulation for the encapsulated product in nanometer, micrometer, and millimeter scale, respectively.

Generally, encapsulation process is carried out to protect high value-sensitive ingredients from any means that can destroy or reduce the functionality of the active ingredients. The goal of encapsulation can be specified as follow (Andres, 1977; Versic, 1988) :

1. To reduce the impact of environmental factors (e.g., light, oxygen, and water) that induces the degradation of active compounds.

2. To decrease the loss of active ingredient by leaching to the environment.

3. To ease the handling of the product such as to prevent from lumping, to improve the mixing homogeneity, and to convert the product from liquid to powder form.

4. To control the release of the active compounds i.e. delayed or sustained release

5. To camouflage the taste of the active compounds

6. To disperse the active ingredient homogenously in the encapsulating agent.

Encapsulation process follows three basic steps including identification and characterization of the active ingredient, selection of the encapsulating agent and selection of the encapsulation process (Fang and Bhandari, 2010; Wandrey, Bartkowiak, and Harding, 2009). The active ingredient is another term of encapsulated substance. Some articles also call it as an active agent, the core, the fill, the active, the internal, or payload phase. The encapsulated substance or active agent should be high value and sensitive ingredients such as colorants, flavors, vitamins, antioxidants, prebiotic and probiotic, and other sensitive ingredients (Shahidi and Han, 1993).

The substance to encapsulate active agent is called coating, wall, membrane, shell, capsule, carrier material, external phase, or matrix. The criteria of materials to be a good coating material are as follow (Desai and Park, 2005) :

1. Coating material should have good rheological properties at high concentration and easy workability during encapsulation.

2. If the product is an emulsion, the coating material should be able to disperse or emulsify the active material as a stable emulsion.

3. Coating material should pose low reactivity with the active ingredients during the encapsulation process and product storage.

4. Coating material should have the ability to seal and hold the active material within its structure during the encapsulation process or product storage.

5. Coating material should be able to release the active ingredient at the delivery target

6. Coating ingredient should able to protect the active ingredient from environmental effects (e.g., oxygen, heat, light, humidity).

7. Coating material should comply with the food grade solvents (e.g., water or ethanol) used in pharmaceutical or nutraceutical industries.

8. It is expected that coating material should less expensive than the active ingredients.

9. Coating material should be in food-grade status.

The reason for selecting encapsulating material depends on the active ingredient to be encapsulated and the encapsulation method. Some materials that can be selected for encapsulating agent are listed below (Shahidi, et al., 1993):

1. Native starch and its derivatives such as maltodextrins, corn syrup, dextran, sucrose, cyclodextrins.

2. Cellulose products: carboxymethyl cellulose, methyl cellulose, ethyl cellulose, nitrocellulose, acetyl cellulose, cellulose acetate phthalate, cellulose acetate-butylate-phthalate

3. Gum products: gum acacia, agar, sodium alginate, carrageenan

4. Lipid products: wax, paraffin, beeswax, tristearic acid, diglycerides, monoglycerides, oils, fats, hardened oils

5. Protein products: gluten, casein, gelatin, albumin, hemoglobin, peptides

Methods for encapsulation are summarized below (Shahidi, et al., 1993):

1. Physical methods: after the active ingredient is mixed with the coating materials, the mix is then dried to obtain the encapsulated product in the form of dry powder. Some drying method can be selected such as spray drying, spray chilling, spray cooling, fluid bed coating (spray coating in

fluidized bed), extrusion, multi-orifice centrifugal extrusion, co-crystallization, and freeze-drying (Ray, et al., 2016).

2. Two chemical methods can be selected for encapsulation including molecular inclusion (inclusion complexation) and interfacial polymerization.

3. The active ingredient and the coating material may interact by both physical and chemical interaction together in encapsulation by physicochemical methods such as coacervation, aqueous phase separation, organic phase separation, liposome entrapment.

Figure 2.12 Types of encapsulates.
Source : Zuidam and Nedovic (2010).

The active ingredient might be entrapped inside the encapsulating matrix with different system including reservoir, matrix and coated matrix (Figure 2.12) (Zuidam, et al., 2010). The reservoir encapsulation system is also known as capsule system in which a solid wall of capsule covers the core. Mixing the active ingredient with encapsulating material produces an encapsulated product which homogenously

distributed within the carrier, therefore, it called encapsulation by matrix system. Both approaches, reservoir and matrix systems, may be combined to obtain optimum encapsulation product. By this method, the active ingredient will obtain optimum protection from the environmental effects (Lakkis, 2007).

2.6.2. Encapsulation using starch derivatives as a matrix

Even though starch has only two major components (i.e., amylose and amylopectin), but it offers countless modification since hydroxyl groups on its backbone structure are readily to be modified. Therefore, starch derivatives are used as ingredients for many industrial applications including encapsulation technology. Starch products have been widely implemented for encapsulation matrix of functional foods such as octenyl succinic anhydride modified starch (OSA starch). It is widely utilized in microencapsulation of oil-soluble flavors, nutrients, fragrances, agri-chemicals, and pharmaceutical actives because it has an active surface of emulsifier to bind hydrophilic and hydrophobic compounds (Wandrey, et al., 2009). Other starch derivatives that have been explored for encapsulating agent including starch granule-stabilized pickering emulsion, native starch gel, porous starch granules, starch nanoparticles, substituted starches, cross-linked starch, oxidized and cross-linked starch hydrogel, hydrolyzed starch, and amylose inclusion complexes (Desai, et al., 2005; Fernandes, Borges, and Botrel, 2014; Jin, Li, and Malaki Nik, 2018; Li, 2014; Shahidi, et al., 1993; Zhu, 2017).

A starch derivative product that has also been explored for encapsulating matrix is porous starch. This is because porous starch shows high porosity, strong adsorption toward water and oil, excellent mechanical properties; stable its structural integrity when dispersed in solvents (Zhang, Cui, Liu, Gong, Huang, and Han, 2012a;

Zhao, Madson, and Whistler, 1996). WeiRong and HuiYuan (2002) investigated the capability of porous starch to be an adsorbent of water, oil, and ethanol (Table 2.4). Compared to native starch, the adsorption capacity of porous starch was higher with a range from 42-68%, depending on the type of fluids being adsorbed (WeiRong, et al., 2002).

Table 2.4 Adsorption capacity of native and porous starch towards some fluids.

Sample	Adsorptive capacity (gram fluid/ gram sample)		
	Water	Oil	Ethanol
Native rice starch	1.17	0.47	0.19
Porous rice starch	1.67	0.65	0.32

Source : WeiRong, et al. (2002)

2.6.3 Encapsulation using cold water swelling starch

There have been several attempts to use CWSS for encapsulating active ingredients (Chen and Jane, 1993; Dries, Gomand, Pycarelle, Smet, Goderis, and Delcour, 2017). Chen and Jane (1995) investigated CWSS for controlled release matrix of atrazine. A slurry of CWSS was mixed with atrazine by using mixing paddle to create a starch paste. They reported that no granular form of starch was observed. They also reported that atrazine was entrapped physically within the encapsulating matrix. The starch components of CWSS did not entrap atrazine within their structure as observed by XRD technique. Instead, they observed the B-type diffraction pattern of retrograded starch.

Dries, et al. (2017) encapsulated ascorbyl palmitate using a mixture of water-ethanol as the solubilization media and CWSS as the encapsulating matrix, and applied multiple encapsulation stages. They reported that water was required to induce complexation between amylose and ascorbyl palmitate to form V-crystalline structure. They suggested that CWSS is an ideal system for encapsulation heat stable component such as ascorbyl palmitate and also heat labile guest molecules such as unsaturated fatty acids or volatile flavor compounds.

2.6.4 Release properties of active compounds

The main goal to produce encapsulation product is to deliver active ingredient at a delivery target (Gibbs, Kermasha, Alli, and Mulligan, 1999; Madene, Jacquot, Scher, and Desobry, 2006; Nedovic, Kalusevic, Manojlovic, Levic, and Bugarski, 2011; Versic, 1988). Therefore, encapsulating material should be degraded at the release point. Generally, the release of active ingredients from encapsulating agent follows these below mechanisms (Shahidi, et al., 1993) :

1. Fracturations

The coating can be fractured by external forces (pressure, shearing, and gastric movement) or by internal forces (some microcapsules have a selective permeation coating). Coating made from hardened fats or waxes may release their contents at temperature above their melting point. Flavor in chewing gum is released during chewing in the mouth. The active ingredients may be released at a fast rate if the coating material undergoes fracture upon dissolution (Figure 2.13).
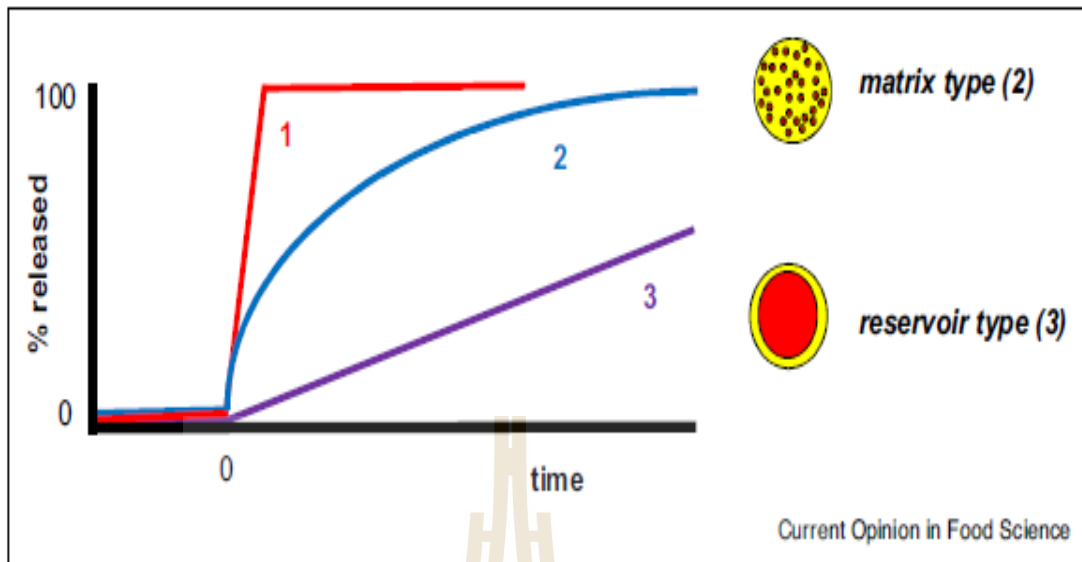
Figure 2.13 Ideal release profiles of active ingredients encapsulation by different

encapsulation system (1) burst release from soluble or broken delivery

systems, (2) first- or multiple order release from matrix types, or (3)

zero-order release from reservoir types.

Source Zuidam and Velikov (2018).

2. Diffusion

This release mechanism applies for encapsulation system that uses thin

layer microcapsule as semipermeable membrane. The diffusion of active ingredient is

driven by a concentration gradient inside the capsule and the surrounding medium,

passing through the semipermeable coating material (Mellenheim and Passy, 1985).

The release rate of active ingredient released by diffusion mechanism is usually

slower than that by other mechanisms (Figure 2.14).

3. Dissolution or melting

Coating agent can be destroyed by dissolution in an appropriate solvent or

by thermal means. For water-soluble coating, water is the medium to release the

active ingredient. Water-insoluble coatings also can be dissolved in an appropriate food grade solvent such as ethanol. Fat-based coating agent melts at a temperature above its melting temperature releasing the core ingredient, for example, chocolate products melt in the mouth.

4. Biodegradation

Enzymes are involved to release the encapsulated ingredient from the encapsulating matrix. For example, lipid coatings may be degraded by action of lipases (Yazawa, Arai, Kitajima, and Kondo, 1974).

The release mechanism of active ingredient from encapsulating matrix can be influenced by the form of encapsulated products, i.e. emulsion, soft capsules, tablet, etc. (Finch, 1994; Lakkis, 2007; Wise, 2000). Particularly for encapsulation product in form of a tablet, the active ingredient release is not only influenced by the encapsulating agent properties but also the characteristic of active ingredient.

For hydrophilic active ingredients, the release of active ingredients is influenced by diffusion/penetration of medium into the tablet (Bonferoni, Rossi, Ferrari, Bertoni, Sinistri, and Caramella, 1995; Tahara, Yamamoto, and Nishihata, 1996). After tablet is soaked in a dissolution buffer, water penetrates into tablet, leading to polymer swelling and drug dissolution. Water decreases the glassy rubbery temperature of polymer structure (e.g., for hydroxypropyl methylcellulose (HPMC) from 184°C to lower than 37°C (Gao and Meury, 1996a; Gao, Skoug, Nixon, Robert Ju, Stemm, and Sung, 1996b)) and rises the transformation of glassy polymer into a rubbery phase (gel layer). The hydration layer plays a vital role to control drug release of gel-forming matrix tablet. It acts as a diffusion barrier of active ingredients and

affects their dissolution rate (Yin, Li, Guo, Wu, Chen, de Matas, Shao, Xiao, York, He, and Zhang, 2013).

For tablet from starch containing paracrystalline structure of V-type crystalline and amorphous structures, when the tablet is hydrated, the starch components converts from amorphous arrangement to a B-type double helix structure as characterized by CP-MAS NMR spectroscopy (Shiftan, Ravenelle, Mateescu, and Marchessault, 2000). The double helical structure creates physical crosslinking points leading to the formation of 3D-networks which restrain the swelling of hydrated tablet.

For tablet containing poorly soluble active ingredients such as fatty acids and water-insoluble vitamins and pigments, tablet erosion is the rate-limiting factor for the release (Efentakis, Pagoni, Vlachou, and Avgoustakis, 2007; Gao, et al., 1996b). Upon soaking, a tablet containing hydrophobic compounds erodes gradually. The presence of hydrophobic compounds surrounding the polymer chains promotes disentanglement or disassociation of the chains (Arik Kibar, Gönenç, and Us, 2014). Other factors that influence the release behavior of poorly soluble active ingredients upon dissolution are particle size and crystalline structure of the polymer (Troy and Beringer, 2006).

2.7   References

Andres, C. (1977). Encapsulation ingredients: I. **Food Processing** 38(12): 44-56.

Angellier, H., Putaux, J.-L., Molina-Boisseau, S., Dupeyre, D., and Dufresne, A. (2005). Starch nanocrystal fillers in an acrylic polymer matrix **Macromolecular Symposia** 221(1): 95-104.

Arik Kibar, E.A., Gönenç, İ., and Us, F. (2014). Effects of Fatty Acid Addition on the Physicochemical Properties of Corn Starch. **International Journal of Food Properties** 17(1): 204-218.

Ayoub, A.S., and Rizvi, S.S.H. (2009). An overview on the technology of cross-linking of starch for nonfood applications. **Journal of Plastic Film and Sheeting** 25(1): 25-45.

Badenhuizen, N.P. (1969). **The biogenesis of starch granules in higher plants**. New York: Appleton-Century-Crofts.

Barrett, E.P., Joyner, L.G., and Halenda, P.P. (1951). The Determination of Pore Volume and Area Distributions in Porous Substances. I. Computations from Nitrogen Isotherms. **Journal of the American Chemical Society** 73(1): 373-380.

Biliaderis, C.G., Maurice, T.J., and Vose, J.R. (1980). Starch gelatinization phenomena studied by differential scanning calorimetry. **Journal of Food Science** 45(6): 1669-1674.

Blanche, S., and Sun, X. (2004). Physical characterization of starch extrudates as a function of melting transitions and extrusion conditions. **Advances in Polymer Technology** 23(4): 277-290.

Bonferoni, M.C., Rossi, S., Ferrari, F., Bertoni, M., Sinistri, R., and Caramella, C. (1995). Characterization of three hydroxypropyl methy cellulose substitution types: rheological properties and dissolution behavior. **European Journal of Pharmaceutics and Biopharmaceutics** 41: 242-246.

Braun, D.E., Koztecki, L.H., McMahon, J.A., Price, S.L., and Reutzel-Edens, S.M. (2015). Navigating the Waters of Unconventional Crystalline Hydrates. **Molecular pharmaceutics** 12(8): 3069-3088.

Brittain, H.G. (2009). **Polymorphism in Pharmaceutical Solids, second edition** (Vol. 192). London: Informar Healthcare.

Brunauer, S., Emmett, P.H., and Teller, E. (1938). Adsorption of Gases in Multimolecular Layers. **Journal of the American Chemical Society** 60(2): 309-319.

Buléon, A., Colonna, P., Planchot, V., and Ball, S. (1998). Starch granules: structure and biosynthesis. **International Journal of Biological Macromolecules** 23(2): 85-112.

Buléon, A., Gallant, D.J., Bouchet, B., Mouille, G., D'Hulst, C., Kossmann, J., and Ball, S. (1997). Starches from A to C: Chlamydomonas reinhardtii as a model microbial system to investigate the biosynthesis of the plant amylopectin crystal. **Plant Physiology** 115: 949-957.

Buleon, A., Le Bail, P., Colonna, P., and Bizot, H. (1998). Phase and polymorphic transitions of starches at low and intermediate water contents. In D.S. Reid (Ed.), **The Properties of Water in Foods ISOPOW 6** (pp. 160-178). Boston, MA: Springer US.

Cameron, R.E., and Donald, A.M. (1993). A small-angle x-ray scattering study of starch gelatinization in excess and limiting water. **Journal of Polymer Science Part B: Polymer Physics** 31(9): 1197-1203.

Carstensen, J.T. (1984). Solid-state chemistry of drugs. By Stephen R. Byrn. Academic Press, 111 Fifth Avenue, New York, NY 10003. 1982. 346 pp. 15 × 23 cm. Price $55.00. **Journal of Pharmaceutical Sciences** 73(4): 573-573.

Che, L.-M., Li, D., Wang, L.-J., Dong Chen, X., and Mao, Z.-H. (2007). Micronization and Hydrophobic Modification of Cassava Starch. **International Journal of Food Properties** 10(3): 527-536.

Chen, J., and Jane, J. (1993). Effectiveness of granular cold water soluble starch as a controlled release matrix. In Dissertation : Granular cold-water-soluble starch: preparation,characterization, and its use on controlled release of atrazine. **IOWA State University**.

Chen, J., and Jane, J. (1994a). Preparation of granular cold-water-soluble starches by alcoholic-alkaline treatment. **Cereal chemistry** 7(6): 618-622.

Chen, J., and Jane, J. (1994b). Properties of granular cold-water-soluble starches prepared by alcoholic-alkaline treatments. **Cereal chemistry** 71(6): 623-626.

Chen, J., and Jane, J. (1995). Effectiveness of granular cold-water-soluble starch as a controlled release matrix. **Cereal chemistry** 72(3): 265-268.

Chen, P., Yu, L., Chen, L., and Li, X. (2006). Morphology and Microstructure of Maize Starches with Different Amylose/Amylopectin Content. **Starch - Stärke** 58(12): 611-615.

Chiu, C., and Solarek, D. (2009). Chapter 17 - Modification of Starches. In **Starch (Third Edition)** (pp. 629-655). San Diego: Academic Press.

Desai, K.G.H., and Park, H.J. (2005). Recent developments in microencapsulation of food ingredients. **Drying Technology** 23: 1361-1394.

Dollimore, D. (1996). Thermal Analysis. **Analytical Chemistry** 68(12): 63-72.

Donald, A.M., Kato, K.L., Perry, P.A., and Waigh, T.A. (2001). Scattering Studies of the Internal Structure of Starch Granules. **Starch - Stärke** 53(10): 504-512.

Donald, A.M., Waigh, T.A., Jenkins, P.J., Gidley, M.J., Debet, M., and Smith, A. (1997). Internal structure of starch granules revealed by scattering studies. In P.J. Frazier, A.M. Donald and P. Richmond (Eds.), **Starch:Structure and Function** (pp. 172-179). Cambridge: The Royal Society of Chemistry.

Dries, D.M., Gomand, S.V., Delcour, J.A., and Goderis, B. (2016). V-type crystal formation in starch by aqueous ethanol treatment: The effect of amylose degree of polymerization. **Food Hydrocolloids** 61: 649-661.

Dries, D.M., Gomand, S.V., Goderis, B., and Delcour, J.A. (2014). Structural and thermal transitions during the conversion from native to granular cold-water swelling maize starch. **Carbohydrate Polymers** 114: 196-205.

Dries, D.M., Gomand, S.V., Pycarelle, S.C., Smet, M., Goderis, B., and Delcour, J.A. (2017). Development of an infusion method for encapsulating ascorbyl palmitate in V-type granular cold-water swelling starch. **Carbohydrate Polymers** 165(Supplement C): 229-237.

Dubinin, M.M. (1960). The Potential Theory of Adsorption of Gases and Vapors for Adsorbents with Energetically Nonuniform Surfaces. **Chemical Reviews** 60(2): 235-241.

Eastman, J.E. (1987). Cold water swelling starch composition. **USPTO # 4.634.596**

Eastman, J.E., and Moore, C.O. (1984). Cold soluble water granular starch for gelled food compositions. **USPTO # 4.465.702**

Efentakis, M., Pagoni, I., Vlachou, M., and Avgoustakis, K. (2007). Dimensional changes, gel layer evolution and drug release studies in hydrophilic matrices

loaded with drugs of different solubility. **International Journal of Pharmaceutics** 339: 66-75.

Evers, A.D. (1971). Scanning electron microscopy of wheat starch. III: Granule development in the endosperm. **Starch/Starke** 23: 157-162.

Falk, M., and Knop, O. (1973). **Water, a Comprehensive Treatise** (Vol. 2). New York: Plenum.

Fang, Z., and Bhandari, B. (2010). Encapsulation of polyphenols – a review. **Trends in Food Science & Technology** 21(10): 510-523.

Fannon, J.E., Hauber, R.J., and Bemiller, J.N. (1992). Surface pores of starch granules. **Cereal chemistry** 69: 284-288.

Fannon, J.E., Shull, J.M., and Bemiller, J.N. (1993). Interior channels of starch granules. **Cereal chemistry** 70(5): 611-613.

Fernandes, R.V.d.B., Borges, S.V., and Botrel, D.A. (2014). Gum arabic/starch/maltodextrin/inulin as wall materials on the microencapsulation of rosemary essential oil. **Carbohydrate Polymers** 101: 524-532.

Finch, C.A. (1994). Pharmaceutical technology: Controlled drug release, volume 2. Edited by J. I. Wells and M. H. Rubinstein. Simon & Schuster International Group, Hemel Hempstead, (Ellis Horwood Series), 1991. pp. 196, price £50.00. ISBN 0-13-662941-5. **Polymer International** 33(3): 341-341.

French, A.D., and Murphy, V.G. (1977). Computer modeling in the study of starch. **Cereal Food World** 22(2): 61-70.

Galliard, T. (1987). Starch availability and utilization. In T. Galliard (Ed.), **Starch: properties and potential (Critical reports on applied chemistry)** (pp. 1-15). Great Britain: John Wiley and Sons.

Galliard, T., and Bowler, P. (1987). Morphology and composition of starch. In T. Galliard (Ed.), **Starch: properties and potential (Critical reports on applied chemistry)** (pp. 55-78). Great Britain: John Wiley and Sons.

Gao, F., Li, D., Bi, C.-h., Mao, Z.-h., and Adhikari, B. (2014). Preparation and characterization of starch crosslinked with sodium trimetaphosphate and hydrolyzed by enzymes. **Carbohydrate Polymers** 103: 310-318.

Gao, P., and Meury, R.H. (1996a). Swelling of Hydroxypropyl Methylcellulose Matrix Tablets. 1. Characterization of Swelling Using a Novel Optical Imaging Method. **Journal of Pharmaceutical Sciences** 85(7): 725-731.

Gao, P., Skoug, J.W., Nixon, P.R., Robert Ju, T., Stemm, N.L., and Sung, K.-C. (1996b). Swelling of Hydroxypropyl Methylcellulose Matrix Tablets. 2. Mechanistic Study of the Influence of Formulation Variables on Matrix Performance and Drug Release. **Journal of Pharmaceutical Sciences** 85(7): 732-740.

Gibbs, B.F., Kermasha, S., Alli, I., and Mulligan, C.N. (1999). Encapsulation in the food industry: a review. **International Journal of Food Science and Nutrition** 50: 213-224.

Goesaert, H., Brijs, K., Veraverbeke, W.S., Courtin, C.M., Gebruers, K., and Delcour, J.A. (2005). Wheat flour constituents: how they impact bread quality, and how to impact their functionality. **Trends in Food Science & Technology** 16(1–3): 12-30.

Griesser, U.J. (2006). The Importance of Solvates. In R. Hilfiker (Ed.), **Polymorphism**).

Hall, D.M., and Sayre, J.G. (1970). A Scanning Electron-Microscope Study of Starches. **Textile Research Journal** 40(3): 256-266.

Hedayati, S., Shahidi, F., Koocheki, A., Farahnaky, A., and Majzoobi, M. (2016). Physical properties of pregelatinized and granular cold water swelling maize starches at different pH values. **International Journal of Biological Macromolecules** 91: 730-735.

Helbert, W. (1994). Donnees sur la structure du grain d'amidon et des produits de recristallisation de l'amylose., **University Joseph Fourier Genoble I**, France.

Hellman, N.N., and Melvin, E.H. (1950). Surface Area of Starch and its Role in Water Sorption. **Journal of the American Chemical Society** 72(11): 5186-5188.

Hii, S.L., Tan, J.S., Ling, T.C., and Ariff, A.B. (2012). Pullulanase: Role in Starch Hydrolysis and Potential Industrial Applications. **Enzyme Research** 2012: 14.

Hizukuri, S. (1985). Relationship between the distribution of the chain length of amylopectin and the crystalline structure of starch granules. **Carbohydrate Research** 141(2): 295-306.

Hook, J.R. (2003). An Introduction to Porosity. In vol. 44): Society of Petrophysicists and Well-Log Analysts.

Hoover, R., and Manuel, H. (1996). The effect of heat-moisture treatment on the structure and physicochemical properties of normal maize, waxy maize, dull waxy maize and amylomaize V starches **Journal of Cereal Science** 23: 153-162.

Hoover, R., and Vasanthan, T. (1994). Effect of heat-moisture treatment on the structure and physicochemical properties of cereal, legume, and tuber starches. **Carbohydrate Research** 252: 33-53.

Horváth, G., and Kawazoe, K. (1983). Method for calculation of effective pore size distribution in molecular sieve carbon. **Journal of Chemical Engineering of Japan** 16(6): 470-475.

Huber, K.C., and BeMiller, J.N. (1997). Visualization of Channels and Cavities of Corn and Sorghum Starch Granules. **Cereal Chemistry Journal** 74(5): 537-541.

Huber, K.C., and BeMiller, J.N. (2000). Channels of maize and sorghum starch granules. **Carbohydrate Polymers** 41(3): 269-276.

Imberty, A., Buléon, A., Tran, V., and Péerez, S. (1991). Recent advances in knowledge of starch structure. **Starch - Stärke** 43(10): 375-384.

Inc, G.I.A. (2018). Sustained Demand From Food and Nonfood End-Use Sectors to Drive Growth in the Global Starch Market. Global Industry Analysts Inc.

Jane, J., Craig, S.A.S., Seib, P.A., and Carl Hoseney, R. (1986a). A granular cold water-soluble starch gives a V-type X-ray diffraction pattern. **Carbohydrate Research** 150(1): c5-c6.

Jane, J., Craig, S.A.S., Seib, P.A., and Hoseney, R.C. (1986b). Characterization of granular cold water-soluble starch. **Starch - Stärke** 38: 258-263.

Jane, J., and Seib, P.A. (1991). Preparation of granular cold water swelling/soluble starches by alcoholic-alkali treatments. **USPTO # 5.057.157**

Jane, J., Shen, L., Wang, L., and Maningat, C.C. (1992). Preparation and Properties of Small-Particle Corn Starch. **Cereal chemistry** 69(3): 280-283.

Jenkins, P.J., and Donald, A.M. (1998). Gelatinisation of starch: a combined SAXS/WAXS/DSC and SANS study. **Carbohydrate Research** 308(1): 133-147.

Jin, Y., Li, J.Z., and Malaki Nik, A. (2018). Chapter 17 - Starch-Based Microencapsulation. In M. Sjöö and L. Nilsson (Eds.), **Starch in Food (Second Edition)** (pp. 661-690): Woodhead Publishing.

Jivan, M.J., Yarmand, M., and Madadlou, A. (2014). Preparation of cold water-soluble potato starch and its characterization. **Journal Food Science Technology** 51(3): 601-605.

Jonhed, A. (2006). Properties of modified starches and their use in the surface treatment of paper. **Karlstad University**, Sweden.

Juszczak, L., Fortuna, T., and Wodnicka, K. (2002). Characteristics of cereal starch granules surface using nitrogen adsorption. **Journal of Food Engineering** 54(2): 103-110.

Kainuma, K., Matsunaga, A., and Itagawa, M. (1981). New enzyme system - Beta-amylase-pullulanase - to determine the degree of gelatinization and rétrogradation of starch or starch products. **Journal of the Japanese Society of Starch Science** 28(4): 235-240.

Karathanos, V.T., and Saravacos, G.D. (1993). Porosity and pore size distribution of starch materials. **Journal of Food Engineering** 18(3): 259-280.

Kaur, B., Ariffin, F., Bhat, R., and Karim, A.A. (2012). Progress in starch modification in the last decade. **Food Hydrocolloids** 26: 398-404.

Kaur, B., Fazilah, A., and Karim, A.A. (2011). Alcoholic-alkaline treatment of sago starch and its effect on physicochemical properties. **Food and Bioproducts Processing** 89(4): 463-471.

Khankari, R.K., and Grant, D.J.W. (1995). Pharmaceutical hydrates. **Thermochimica Acta** 248: 61-79.

Kim, H.-S., and Huber, K.C. (2008). Channels within soft wheat starch A- and B-type granules. **Journal of Cereal Science** 48(1): 159-172.

Krueger, B.R., Knutson, C.A., Inglett, G.E., and Walker, C.E. (1987). A Differential Scanning Calorimetry Study on the Effect of Annealing on Gelatinization Behavior of Corn Starch. **Journal of Food Science** 52(3): 715-718.

Kubo, S., Fujita, T.C., Harada, K., Matsuda, Y., Satoh, T., and Nakamura, M. (1999). The starch-debranching enzymes isoamylase and pullulanase are both involved in amylopectin biosynthesis in rice endosperm. **Plant Physiology** 121 2: 399-410.

Laage, D., Elsaesser, T., and Hynes, J.T. (2017). Water Dynamics in the Hydration Shells of Biomolecules. **Chemical Reviews** 117(16): 10694-10725.

Lakkis, J.M. (2007). **Encapsulation and controlled release technologies in food systems**. Oxford, UK: Blackwell Publishing.

Le-Bail, P., Hesso, N., and Le-Bail, A. (2018). Chapter 15 - Starch in Baked Products. In M. Sjöö and L. Nilsson (Eds.), **Starch in Food (Second Edition)** (pp. 595-632): Woodhead Publishing.

Le Bail, P., Bizot, H., Pontoire, B., and Buleon, A. (1995). Polymorphic Transitions of Amylose-Ethanol Crystalline Complexes Induced by Moisture Exchanges. **Starch - Stärke** 47(6): 229-232.

Le Corre, D., Bras, J., and Dufresne, A. (2010). Starch Nanoparticles: A Review. **Biomacromolecules** 11(5): 1139-1153.

Li, B.Z., Wang, L.J., Li, D., Chiu, Y.L., Zhang, Z.J., Shi, J., Chen, X.D., and Mao, Z.H. (2009). Physical properties and loading capacity of starch-based

microparticles crosslinked with trisodium trimetaphosphate. **Journal of Food Engineering** 92(3): 255-260.

Li, J.Z. (2014). Chapter 18 - The Use of Starch-Based Materials for Microencapsulation. In A.G. Gaonkar, N. Vasisht, A.R. Khare and R. Sobel (Eds.), **Microencapsulation in the Food Industry** (pp. 195-210). San Diego: Academic Press.

Li, W., Cao, F., Fan, J., Ouyang, S., Luo, Q., Zheng, J., and Zhang, G. (2014). Physically modified common buckwheat starch and their physicochemical and structural properties. **Food Hydrocolloids** 40: 237-244.

Li, Y.-Q., Chen, Q., Liu, X.-H., and Chen, Z.-X. (2008). Inactivation of soybean lipoxygenase in soymilk by pulsed electric fields. **Food Chemistry** 109(2): 408-414.

Light, J.M. (1990). Modified food starches: Why, where, and how. **Cereal Foods World** 35: 1081-1084.

Lindeboom, N., Chang, P.R., and Tyler, R.T. (2004). Analytical, biochemical and physicochemical aspects of starch granule size, with emphasis on small granule starches: A review. **Starch - Stärke** 56(3-4): 89-99.

Lindqvist, I. (1979). Cold gelatinization of starch. **Starch - Stärke** 31: 195-200.

Lowell, S., Shields, J.E., Thomas, M.A., and Thommes, M. (2010). **Characterization of porous solids and powders: surface area, pore size and density**: Kluwer Academic Publishers, Springer.

Madene, A., Jacquot, M., Scher, J., and Desobry, S. (2006). Flavour encapsulation and controlled release – a review. **International Journal of Food Science & Technology** 41(1): 1-21.

Mahmoudi Najafi, S.H., Baghaie, M., and Ashori, A. (2016). Preparation and characterization of acetylated starch nanoparticles as drug carrier: Ciprofloxacin as a model. **International Journal of Biological Macromolecules** 87: 48-54.

Majzoobi, M., Kaveh, Z., Blanchard, C.L., and Farahnaky, A. (2015). Physical properties of pregelatinized and granular cold water swelling maize starches in presence of acetic acid. **Food Hydrocolloids** 51: 375-382.

Marsellés-Fontanet, Á.R., and Martín-Belloso, O. (2007). Optimization and validation of PEF processing conditions to inactivate oxidative enzymes of grape juice. **Journal of Food Engineering** 83(3): 452-462.

Mellenheim, C., and Passy, N. (1985). Choice of packages for foods with specific considerations of water activity. In D. Simatos and J.L. Multon (Eds.), **Properties of Water in Foods** (pp. 375). Dordrecht, The Netherlands: Martinus Nijhoff.

Miao, M., Zhang, T., and Jiang, B. (2009). Characterisations of kabuli and desi chickpea starches cultivated in China. **Food Chemistry** 113(4): 1025-1032.

Morris, K.R., and Rodriguez-Hornedo, N. (1993). **Encyclopedia of Pharmaceutical Technology** (Vol. 7). New York: Marcel Dekker.

Nedovic, V., Kalusevic, A., Manojlovic, V., Levic, S., and Bugarski, B. (2011). An overview of encapsulation technologies for food applications. **Procedia Food Science** 1: 1806-1815.

Park, K.-H., Park, J.-H., Lee, S., Yoo, S.-H., and Kim, J.-W. (2008). Enzymatic Modification of Starch for Food Industry. In K.-H. Park (Ed.), **Carbohydrate-Active Enzymes** (pp. 157-183): Woodhead Publishing.

Paterson, J.L., Hardacre, A., Li, P., and Rao, M.A. (2001). Rheology and granule size distributions of corn starch dispersions from two genotypes and grown in four regions. **Food Hydrocolloids** 15(4): 453-459.

Pérez, S., and Bertoft, E. (2010). The molecular structures of starch components and their contribution to the architecture of starch granules: A comprehensive review. **Starch - Stärke** 62(8): 389-420.

Pitchon, E., O'Rourke, J.D., and Joseph, T.H. (1981). Process for cooking or gelatinizing materials. **U.S.P.T.O #** U.S. Patent **4.280.851**

Powell, E.L. (1967). Production and use of pregelatinized starch. In R.L. Whistler and E.F. Paschall (Eds.), **Starch: Chemistry and Technology** vol. II). New York: Academic Press.

Putaux, J.-L., Molina-Boisseau, S., Momaur, T., and Dufresne, A. (2003). Platelet nanocrystals resulting from the disruption of waxy maize starch granules by acid hydrolysis. **Biomacromolecules** 4(5): 1198-1202.

Putseys, J.A., Lamberts, L., and Delcour, J.A. (2010). Amylose-inclusion complexes: Formation, identity and physico-chemical properties. **Journal of Cereal Science** 51(3): 238-247.

Qiao, D., Zhang, B., Huang, J., Xie, F., Wang, D.K., Jiang, F., Zhao, S., and Zhu, J. (2017). Hydration-induced crystalline transformation of starch polymer under ambient conditions. **International Journal of Biological Macromolecules** 103: 152-157.

Rajagopalan, S., and Seib, P.A. (1991). Process for the preparation of granular cold water-soluble starch. **USPTO #**

Rajagopalan, S., and Seib, P.A. (1992a). Granular cold-water-soluble starches prepared at atmospheric pressure. **Journal of Cereal Science** 16(1): 13-28.

Rajagopalan, S., and Seib, P.A. (1992b). Properties of granular cold-water-soluble starches prepared at atmospheric pressure. **Journal of Cereal Science** 16(1): 29-40.

Ray, S., Raychaudhuri, U., and Chakraborty, R. (2016). An overview of encapsulation of active compounds used in food products by drying technology. **Food Bioscience** 13: 76-83.

Rigby, S.P., Fletcher, R.S., and Riley, S.N. (2003). Determination of the cause of mercury entrapment during porosimetry experiments on sol–gel silica catalyst supports. **Applied Catalysis A: General** 247: 27-39.

Rondeau-Mouro, C., Bail, P.L., and Buléon, A. (2004). Structural investigation of amylose complexes with small ligands: inter- or intra-helical associations? **International Journal of Biological Macromolecules** 34(5): 251-257.

Rouquerol, F., Rouquerol, J., and Sing, K. (1999a). Adsorption by Powders and Porous Solids. In **Adsorption by Powders and Porous Solids** (pp. 1-26). London: Academic Press.

Rouquerol, F., Rouquerol, J., and Sing, K. (1999b). CHAPTER 1 - Introduction. In **Adsorption by Powders and Porous Solids** (pp. 1-26). London: Academic Press.

Rouquerol, F., Rouquerol, J., and Sing, K. (1999c). CHAPTER 2 - Thermodynamics of Adsorption at the Gas–Solid Interface. In **Adsorption by Powders and Porous Solids** (pp. 27-50). London: Academic Press.

Rouquerol, F., Rouquerol, J., and Sing, K. (1999d). CHAPTER 7 - Assessment of Mesoporosity. In **Adsorption by Powders and Porous Solids** (pp. 191-217). London: Academic Press.

Rutenberg, M.W., and Solarek, D. (1984). Starch derivatives: Production and uses. In R. Whistler, J.N. BeMiller and E.F. Paschall (Eds.), **Starch: Chemistry and Technology** (pp. 314–388). New York: Academic Press, Inc.

Sandstedt, R.M. (1946). Photomicrographic studies of wheat starch. 1. Development of the starch granules. **Cereal chemistry** 23: 337-359.

Seaton, N.A. (1991). Determination of the connectivity of porous solids from nitrogen sorption measurements. **Chemical Engineering Science** 46(8): 1895-1909.

Shahidi, F., and Han, X.Q. (1993). Encapsulation of food ingredients. **Critical Reviews in Food Science and Nutrition** 33(6): 501-547.

Shiftan, D., Ravenelle, F., Mateescu, M.A., and Marchessault, R.H. (2000). Change in the V/B Polymorph Ratio and T1 Relaxation of Epichlorohydrin Crosslinked High Amylose Starch Excipient. **Starch - Stärke** 52(6-7): 186-195.

Sing, K.S.W., Everett, D.H., Haul, R.A.W., Moscou, L., Pierotti, R.A., Rouquerol, J., and Siemieniewska, T. (2008). Reporting Physisorption Data for Gas/Solid Systems. In **Handbook of Heterogeneous Catalysis**): Wiley-VCH Verlag GmbH & Co. KGaA.

Singh, A.V., Nath, L.K., and Anudwipa, S.A. (2010). Pharmaceutical, food and non-food applications of modified starches: a critical review. **Electronic Journal of Environmental, Agricultural and Food Chemistry** 9: 1214-1221.

Singh, J., and Singh, N. (2003). Studies on the morphological and rheological properties of granular cold water soluble corn and potato starches. **Food Hydrocolloids** 17(1): 63-72.

Stute, R. (1992). Hydrothermal modification of starches: the difference between annealing and heat moisture treatment. **Starch - Stärke** 6: 205–214.

Sujka, M., and Jamroz, J. (2007). Starch granule porosity and its changes by means of amylolysis. v. 21.

Sujka, M., and Jamroz, J. (2009). α-Amylolysis of native potato and corn starches – SEM, AFM, nitrogen and iodine sorption investigations. **LWT - Food Science and Technology** 42(7): 1219-1224.

Sujka, M., and Jamroz, J. (2010). Characteristics of pores in native and hydrolyzed starch granules. **Starch - Stärke** 62(5): 229-235.

Tahara, K., Yamamoto, K., and Nishihata, T. (1996). Application of modelindependent and model analysis for the investigation of effect of drug solubility on its release rate from hydroxypropyl methy cellulose sustained release tablets. **International Journal of Pharmaceutics** 133: 17-27.

Tako, M., Tamaki, Y., Teruya, T., and Takeda, Y. (2014). The Principles of Starch Gelatinization and Retrogradation. **Food and Nutrition Sciences** Vol.05No.03: 12.

Tamaki, Y., Konishi, T., and Tako, M. (2011). Gelation and Retrogradation Mechanism of Wheat Amylose. **Materials** 4(10): 1763-1775.

Tang, M.C., and Copeland, L. (2007). Investigation of starch retrogradation using atomic force microscopy. **Carbohydrate Polymers** 70(1): 1-7.

Tester, R.F., Karkalas, J., and Qi, X. (2004). Starch-composition, fine structure and architecture. **Journal of Cereal Science** 39(2): 151-165.

Tetlow, I.J. (2011). Starch biosynthesis in developing seeds. **Seed Science Research** 21: 5-32.

Tharanathan, R.N. (2005). Starch — Value Addition by Modification. **Critical Reviews in Food Science and Nutrition** 45(5): 371-384.

Thomas, D.J., and Atwell, W.A. (1999). **Starches**. St. Paul: Eagen Press.

Tomasik, P., and Schilling, H. (2004). Chemical modification of starch. **Advances in Carbohydrate Chemistry & Biochemistry** 59: 175-403.

Torregrosa, F., Esteve, M.J., Frígola, A., and Cortés, C. (2006). Ascorbic acid stability during refrigerated storage of orange–carrot juice treated by high pulsed electric field and comparison with pasteurized juice. **Journal of Food Engineering** 73(4): 339-345.

Troy, D.B., and Beringer, P. (2006). **Remington: the science and practice of pharmacy 21st edition**. Philadelphia: Lippincott Williams and Wilkins.

Unit. (2011). Cassava Starch-Exploring a New Economic Frontier. In **The BSJ/UWI 2011 Starch Conference**). The Mona Visitors' Lodge and Conference Centre.

Vermeylen, R., Derycke, V., Delcour, J.A., Goderis, B., Reynaers, H., and Koch, M.H.J. (2006). Structural Transformations during Gelatinization of Starches in Limited Water: Combined Wide- and Small-Angle X-ray Scattering Study. **Biomacromolecules** 7(4): 1231-1238.

Versic, R.J. (1988). Flavor Encapsulation. In **Flavor Encapsulation** vol. 370 (pp. 1-6): American Chemical Society.

Waduge, R.N., Hoover, R., Vasanthan, T., Gao, J., and Li, J. (2006). Effect of annealing on the structure and physicochemical properties of barley starches of varying amylose content. **Food Research International** 39(1): 59-77.

Waigh, T.A., Gidley, M.J., Komanshek, B.U., and Donald, A.M. (2000). The phase transformations in starch during gelatinisation: a liquid crystalline approach. **Carbohydrate Research** 328(2): 165-176.

Wandrey, C., Bartkowiak, A., and Harding, S.E. (2009). Materials for encapsulation. In Z.N. J. and V.A. Nedovic (Eds.), **Encapsulation technologies for food active ingredients and food processing** (pp. 31-100). Dordrecht, The Netherlands: Springer.

Wang, H., Lv, J., Jiang, S., Niu, B., Pang, M., and Jiang, S. (2016). Preparation and characterization of porous corn starch and its adsorption toward grape seed proanthocyanidins. **Starch - Stärke** 68(11-12): 1254-1263.

Wang, J., Zhai, W., and Zheng, W. (2011). Preparation of granular cold-water-soluble corn starch by surface modification with poly(ethylene glycol). **Starch - Stärke** 63(10): 625-631.

Wang, S., Li, C., Copeland, L., Niu, Q., and Wang, S. (2015). Starch Retrogradation: A Comprehensive Review. **Comprehensive Reviews in Food Science and Food Safety** 14(5): 568-585.

WeiRong, Y., and HuiYuan, Y. (2002). Adsorbent Characteristics of Porous Starch. **Starch - Stärke** 54(6): 260-263.

Whittam, M.A., Orford, P.D., Ring, S.G., Clark, S.A., Parker, M.L., Cairns, P., and Miles, M.J. (1989). Aqueous dissolution of crystalline and amorphous

amylose alcohol complexes. **International Journal of Biological Macromolecules** 11(6): 339-344.

Williams, T.R. (1963). Handbook of analytical chemistry (Meites, Louis). **Journal of Chemical Education** 40(10): 560.

Wilson, J.D., Bechtel, D.B., Todd, T.C., and Seib, P.A. (2006). Measurement of Wheat Starch Granule Size Distribution Using Image Analysis and Laser Diffraction Technology. **Cereal chemistry** 83(3): 259-268.

Wise, D. (2000). **Handbook of Pharmaceutical Controlled Release Technology**. Boca Raton: CRC Press.

Wongsagonsup, R., Shobsngob, S., Oonkhanond, B., and Varavinit, S. (2005). Zeta Potential (ζ) and Pasting Properties of Phosphorylated or Crosslinked Rice Starches. **Starch - Stärke** 57(1): 32-37.

Xie, S.X., Liu, Q., and Cui, S.W. (2005). Starch Modification and Applications. In S.W. Cui (Ed.), **Food Carbohydrates: Chemistry, Physical Properties, and Applications**). Boca Raton, Florida: CRC Press, Taylor & Francis Group.

Yazawa, K., Arai, R., Kitajima, M., and Kondo, A. (1974). Method of Producing Oil and Fat Encapsulated Amino Acids. **USPTO # 3,804,776**

Yin, X., Li, H., Guo, Z., Wu, L., Chen, F., de Matas, M., Shao, Q., Xiao, T., York, P., He, Y., and Zhang, J. (2013). Quantification of swelling and erosion in the controlled release of a poorly water-soluble drug using synchrotron X-ray computed microtomography. **The AAPS journal** 15(4): 1025-1034.

Yuryev, V.P., Krivandin, A.V., Kiseleva, V.I., Wasserman, L.A., Genkina, N.K., Fornal, J., Blaszczak, W., and Schiraldi, A. (2004). Structural parameters of

amylopectin clusters and semicrystalline growth rings in wheat starches with different amylose content. **Carbohydrate Research** 339(16): 2683-2691.

Zhang, B., Cui, D., Liu, M., Gong, H., Huang, Y., and Han, F. (2012a). Corn porous starch: Preparation, characterization and adsorption property. **International Journal of Biological Macromolecules** 50(1): 250-256.

Zhang, B., Dhital, S., Haque, E., and Gidley, M.J. (2012b). Preparation and characterization of gelatinized granular starches from aqueous ethanol treatments. **Carbohydrate Polymers** 90(4): 1587-1594.

Zhao, J., Madson, M.A., and Whistler, R.L. (1996). Cavities in Porous Corn Starch Provide a Large Storage Space. **Cereal Chem.** 73(3): 379-380.

Zhao, Y., Liu, S., Elsworth, D., Jiang, Y., and Zhu, J. (2014). Pore Structure Characterization of Coal by Synchrotron Small-Angle X-ray Scattering and Transmission Electron Microscopy. **Energy & Fuels** 28(6): 3704-3711.

Zhu, F. (2017). Encapsulation and delivery of food ingredients using starch based systems. **Food Chemistry** 229: 542-552.

Zia-ud-Din, Xiong, H., and Fei, P. (2017). Physical and chemical modification of starches: A review. **Critical Reviews in Food Science and Nutrition** 57(12): 2691-2705.

Zuidam, N.J., and Nedovic, V.A. (2010). **Encapsulation technologies for active food ingredients and food processing**. USA: Springer.

Zuidam, N.J., and Velikov, K.P. (2018). Choosing the right delivery systems for functional ingredients in foods: an industrial perspective. **Current Opinion in Food Science** 21: 15-25.

CHAPTER III

STRUCTURAL TRANSFORMATIONS AT DIFFERENT ORGANIZATIONAL LEVELS OF ETHANOL-TREATED STARCH DURING HEATING

3.1   Abstract

Heating ethanol-treated starch (ETS) is the simplest method to produce granular cold-water swelling starch. Structural transformations of ethanol-treated maize and potato starch (ETMS and ETPS) at the crystalline, lamellae and granular structural levels during heating were investigated through in situ wide- and small-angle X-ray scattering (WAXS and SAXS) combined with light microscopy (LM). The result of in situ WAXS indicated that the native crystalline structure was slowly disrupted up to 82 and 60°C for ETMS and ETPS, respectively. The initial temperature for the formation of a V-type crystalline structure of ETMS was observed to be 86°C. The result of paracrystalline analysis suggested that the crystalline lamellae of ETS realigned toward a more ordered register when heated to 80°C and 70°C for ETMS and ETPS, respectively. The granular forms of ETMS and ETPS were still preserved at 100°C, although the characteristic of Maltese cross was not observed. A model was proposed to elucidate transformations of ETS at the three structural levels of starch during heating.

Keywords: structural transformations, crystalline structure, lamellae and granular levels, ethanol-treated starch.

3.2   Introduction

A stacked ring structure of alternating amorphous and crystalline layers, which are called clusters, comprises the architecture of native starch granules. The thickness of each amylopectin cluster is commonly 9-10 nm with a crystalline lamellae thickness of approximately 5-6 nm (Donald, Kato, Perry, and Waigh, 2001; Pikus, 2005). By light microscopy under a polarization mode, the specific radial arrangement of the growth ring gives rise to a Maltese cross pattern, which is a characteristic of native starches. Hydrated native starches show a peak in the SAXS pattern at a scattering vector value, q, of 0.062-0.066 Å^{-1} (Donald, et al., 2001; Jenkins and Donald, 1995; Pikus, 2005). This peak is believed to arise from the alternating crystalline and amorphous regions of amylopectin.

At the crystalline structural level, the double helices of amylopectin have different packing arrangements that lead to the characteristics of A-, B- or C-type crystalline structures observed by the wide angle X-ray scattering (WAXS) technique (Imberty, Chanzy, Pérez, Bulèon, and Tran, 1988). The WAXS pattern of V-type crystals is observed when amylose forms a complex with suitable ligands such as iodine, fatty acids and alcohols (Putseys, Lamberts, and Delcour, 2010).

Granular cold-water swelling starch (GCWSS) was first developed in tandem with pregelatinized starch to overcome the low solubility of native starch (Eastman and Moore, 1984). These products are often called 'instant starches' because of their ability to absorb cold water and swell promptly, giving the appearance and texture of

cooked starch. Therefore, they are used as raw materials for ready-to-be-consumed products. GCWSS is superior to pregelatinized starch in terms of its textural properties and appearance (Light, 1990).

There are three methods for preparing GCWSS, including: (a) a process that involves the annihilation of internal starch granules by a specially designed nozzle spray dryer (Pitchon, O'Rourke, and Joseph, 1981); (b) methods that heat starch with chemicals such as ethanol (Dries, Gomand, Goderis, and Delcour, 2014; Eastman, et al., 1984; Zhang, Dhital, Haque, and Gidley, 2012) or polyhydric alcohols (Rajagopalan and Seib, 1991), which act as anti-swelling agents; and (c) mixing a starch slurry with two different chemicals in which one is acting as a gelatinization inducer, for instance, sodium hydroxide, and the other is an anti-swelling agent such as ethanol (Jane and Seib, 1991). Each process has its own advantages and disadvantages in terms of processing greenness, cost and simplicity. Heating ethanol-treated starch (ETS) can be considered the simplest green process for preparing GCWSS because it only requires ethanol, which can be removed from the product by dehydration (Dries, et al., 2014; Zhang, et al., 2012).

Understanding the structure of GCWSS is necessary to explain its ability to absorb cold water and then swell immediately. Jane, Craig, Seib, and Hoseney (1986b) noticed that the Maltese cross characteristic disappeared for GCWSS, indicating that the semicrystalline structure has been destroyed. However, it was reported that GCWSS contains a V-type crystalline structure (Dries, et al., 2014; Jane, et al., 1986b; Zhang, et al., 2012), and the V-type crystalline structure of the amylose-ethanol complex is known to be soluble in cold water (French and Murphy, 1977).

A model of structural transformations from native starch (A-type) to GCWSS has been proposed by Jane, Craig, Seib, and Hoseney (1986a). Nonetheless, this model was oversimplified since it described the transformations as a single step process at the crystalline structural level, while related phenomena at higher structural levels were not considered. A model that includes the transformations of starch at different structural levels during GCWSS conversion is not yet available.

Dries, et al. (2014) attempted to observe the exothermic transition of V-type crystal formation by differential scanning calorimetry (DSC), but was not successful. Dries, Gomand, Delcour, and Goderis (2016) reported that the formation of a V-type crystalline structure was initiated by the native crystal melting at 95 °C for ETS containing amylose with a low degree of polymerization (DP), such as maize and rice. Furthermore, for starch containing amylose with a high DP (potato), the V-type crystalline structure was formed during holding at 95 °C and progressed during subsequent cooling. However, since they did not monitor the actual sample temperature throughout the conversion process, these conclusions needed further verification. The investigation of parameters during ETS heating, i.e., time and temperature, for the V-type crystalline formation would provide essential information for the design of a highly efficient process.

The present study provides a comprehensive investigation of structural transformations of starch during heating with ethanol. Alterations at three organizational levels of starch, including crystalline, lamellae, and granular structural levels, were investigated using in situ WAXS and SAXS techniques, combined with LM. Normal maize and potato starches were chosen to represent other polymorphs, i.e., A- and B-type crystalline structures, respectively.

3.3 Materials and methods

3.3.1 Materials

Normal maize and potato starches were received from National Starch and Chemicals Co. Ltd., Thailand. Analytical grade ethanol was purchased from Carlo Erba, France.

3.3.2 In situ WAXS and SAXS

3.3.2.1 In situ WAXS and SAXS experimental setup

In situ WAXS and SAXS experiments were carried out at the BL1.3W SAXS/WAXS station, Synchrotron Light Research Institute (SLRI), Nakhon Ratchasima, Thailand. The instrumental setup followed the method of Soontaranon and Rugmai (2012) with slight modifications. The sample to detector distances were set at 194.2 mm calibrated by a 4-bromo benzoic acid standard for WAXS, and 1705.9 mm calibrated by a silver behenate standard for SAXS. The X-ray energy was 9 keV. The WAXS and SAXS profiles were recorded by a MAR-CCD (SX165) detector.

The starch powder was dispersed in an ethanol solution (50% v/v) to prepare a 50% (w/v) starch slurry. The sample was sandwiched between two Kapton sheets inside a windowed copper cell. A thermocouple was inserted through a pinhole in the copper cell to monitor the sample temperature. A specially designed hot stage was heated to a set temperature (either 90 or 100°C). After reaching the set temperature, the sample cell was introduced into the slot of the hot stage, and then all experimental parameters were collected immediately. The WAXS and SAXS data were collected with 20 seconds of X-ray exposure time. The recording started from the first minute after introducing the sample into the hot stage until it reached the set temperature and

was then continuously recorded for 30 min. Each of the in situ WAXS and SAXS experiments was conducted as an independent experiment. A schematic diagram of the experimental setup is displayed in Figure 3.1.
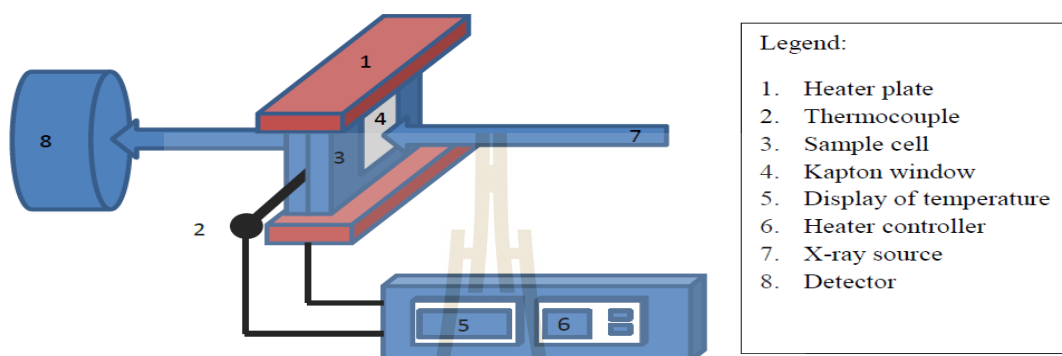
Figure 3.1 Schematic diagram of the experimental setup of in situ WAXS and SAXS studies.

3.3.2.2 General processing of in situ WAXS and SAXS data

An in-house program called SAXSIT (https://www.slri.or.th/en/bl13w-saxs.html) was employed to process the WAXS/SAXS pattern images to obtain the scattering profiles. After background correction, intensity normalization and circular averaging of the patterns, the WAXS data were presented as a plot of scattering angles (2θ) against scattering intensities. The WAXS data were reported in the 2θ range of 4 to 30°C. The SAXS data were presented as one-dimensional curves of intensity as a function of the scattering vector, q, in the range 0.25 to 2 nm^{-1}, where q is defined as

$$\mathbf{q} = \frac{4\pi \sin\theta}{\lambda} \qquad (1)$$

3.3.2.3 WAXS data analysis

As described in section 3.3.2.1, the WAXS samples were measured under an excess of solvent. Note that this caused baseline shifting on the resulting WAXS patterns, which brought about incomparable data for the percentage of crystallinity. Therefore, the amplitudes of the normalized crystal peaks were used instead to represent the structural transformations of starch during heating. Pseudo-Voigt peak functions were employed for peak fitting of the WAXS results, in which the fitting was carried out using the chi-squared minimization procedure.

3.3.2.4 SAXS data analysis

The paracrystalline model with infinite layers (Vainshtein, 1966) was employed to analyze the SAXS data by using SAXSIT software (Rugmai, Soontaranon, Chirawatkul, and Kaewhan, 2014). From this model, the average crystalline lamellae thickness (L_{crl}) can be determined assuming a constant density contrast between the crystalline and amorphous layers and a Gaussian variation in the crystalline and amorphous layer thickness (Yuryev, Krivandin, Kiseleva, Wasserman, Genkina, Fornal, Blaszczak, and Schiraldi, 2004). The intensity of the modeled SAXS data is then given by the sum of the paracrystalline terms and background functions, which include a constant and a power law term,

$$I(q) = I_0 \exp\left(-\sigma_{in}^2 q^2\right) \overline{|F(q, L_{crl})|^2} \ S(q) + I_{BG} \qquad (2)$$

where I_0 is an arbitrary scaling factor. The exponential term, $\exp(-\sigma_{in}^2 q^2)$, comes from the smoothing of the crystalline-amorphous interface. The average crystalline form factor, $\overline{|F(q, L_{crl})|^2}$, is calculated from

$$\overline{|F(q, L_{crl})|^2} = \frac{1}{\sqrt{2\pi\sigma_L}} \int_{-\infty}^{\infty} |F(q, x)|^2 \exp\left(-\frac{(x-L_{crl})^2}{2\sigma_L^2}\right) dy, \tag{3}$$

where the lamella form factor for a single crystalline lamella of thickness x, $F(q, x)$ is expressed as

$$F(q, x) = \frac{2 \sin\left(\frac{q x}{2}\right)}{q x}. \tag{4}$$

The structure factor $S(q)$ is given by

$$S(q) = \frac{1 - |G(q)|^2}{1 - 2|G(q)| \cos(q\alpha) + |G(q)|^2} \tag{5}$$

where $G(q)$ is a Fourier transform of the Gaussian period size distributions, $H(y)$:

$$G(q) = F[H(y)] \tag{6}$$

where

$$H(y) = \frac{1}{\sqrt{2\pi\sigma_\alpha}} \exp\left(-\frac{(y-\bar{\alpha})^2}{2\sigma_\alpha^2}\right) \tag{7}$$

An example of paracrystalline fit for native maize starch SAXS pattern is shown in Figure 3.2 The paracrystalline structure parameters, including the crystalline lamella thickness, L_{crl}, and the average repeat distance, $\bar{\alpha}$, were reported.
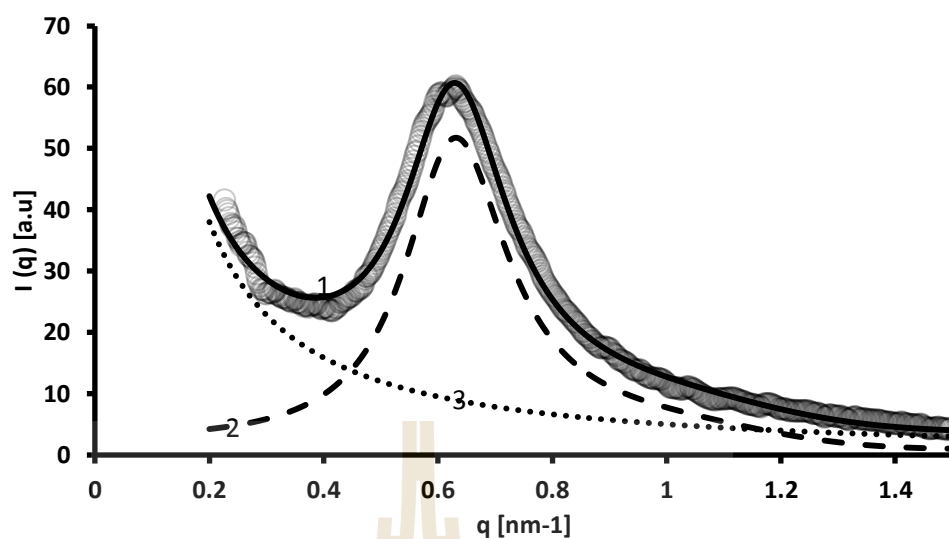
Figure 3.2 SAXS pattern of native maize starch at room temperature (1, open circles) and its fitting result by the paracrystalline model (1, solid line) by the sum of paracrystalline terms (2, dashed line) and background functions (3, dotted line).

Fractal analysis was applied to describe the structural transformations of the crystalline lamellae during heating of ETS following a procedure described by Suzuki, Chiba, and Yarno (1997) and Doutch and Gilbert (2013). The slope of the double log plot of SAXS data at the q region of the SAXS peak (0.5-0.8 nm^{-1}) was determined. The correlation coefficient (R^2) was used as an indicator of fitting linearity.

3.3.3 Morphology of starch granules

3.3.3.1 Sample preparation for the morphological study

Samples were prepared according to the method of Eastman (1987) and Dries, et al. (2014) with some modifications. Starch powder (15 g) was poured into a pressure-leak-proof bottle (Schott bottle) and dispersed with 135 ml of ethanol (50%

v/v). The samples were heated at different temperatures (80, 90 and 100 °C) using a water bath for 30 min. Then, the samples were placed at room temperature for 2 hours. The sediments were separated from the solvent by filtration and then washed with absolute ethanol and filtered three times to remove the excess water. The wet powders were dried using a vacuum oven at three subsequent temperatures of 35, 45, and 55 °C for 12 hours at each temperature. Samples were ground and sieved with a 150 µm sieve and subsequently dried in a vacuum oven at 65 °C for 24 hours. Samples were stored in a box containing silica gel prior to morphological studies.

3.3.3.2 Morphological observation

A light microscope (Zeiss Axio Scope A1, Jena, Germany) was employed to observe the granule morphologies and birefringence characteristics using normal and polarized modes, respectively.

3.4   Results and discussion

3.4.1   Transformations of ethanol-treated starch (ETS) at the crystalline structural level during heating

The transformations of crystalline structures for ethanol-treated maize starch (ETMS) and ethanol-treated potato starch (ETPS) during heating are displayed in Figure 3.3 and 3.4. Between heating temperatures of 40 and 82°C, the A-type crystalline structure of ETMS slightly changed, as seen from the normalized amplitude profile of the major peaks of A-type starch at 2θ of 15°, 17°, 18.1° and 23.3° (Figure 3.3A). The intensity of A-type crystal peaks decreased drastically as the temperature progressed from 82 to 88°C, and then it decreased more slowly at the subsequent temperatures. Surprisingly, some of the major A-type crystal peaks could

still be observed until the end of experiment (Figure 3.3A). This might be due to the high heat resistance of the amylopectin clusters of maize starch. Native maize starch contains amylose chains and amylose-lipid complexes that surround the amylopectin clusters and play significant roles in preserving the amylopectin clusters from disruptions (Saibene and Seetharaman, 2010; Tester, 1997). Amylose behaves similar to a rope that bonds starch components tightly and allows the starch granule to remain intact during physical or thermal treatments (Waduge, Hoover, Vasanthan, Gao, and Li, 2006). In addition, some of the solvent probably evaporated from the sample cell during heating, resulting in a lack of free water that is required to plasticize the native crystal. The temperature required to melt crystals of native starch at low or intermediate moisture contents is higher than that for starch in excess water (Svensson and Eliasson, 1995). Therefore, the entire native crystalline structure of starch was not completely destroyed during the heat treatment.

The limit of alteration of the B-type crystalline structure of ETPS was observed during heating from 40 to 60°C (Figure 3.4C). Above 60°C, the intensity of major B-type crystal peaks drastically decreased, and then the peaks disappeared after 88°C. It was noted that the temperature required to disrupt the B-type crystalline structure of ETPS was lower (60°C) than the A-type crystalline structure of ETMS (82°C). It is well-known that amylopectin clusters of potato starch are easier to disrupt because the B-type crystal contains higher water content within its structure, which accelerates the plasticization of double helices during heating. In addition, potato starch contains phosphate groups that assist with hydration of the double

Figure 3.3 In situ WAXS patterns of ethanol-treated maize starch (ETMS) (A) and
ethanol-treated potato starch (ETPS) (B) during heating.

Figure 3.4 Normalized amplitude profile of major peaks of A-type crystal of maize

starch (A), V-type crystal of ethanol-treated maize starch (ETMS) (B) and

B-type crystal of potato starch (C) during heating in in situ WAXS

experiments.

helices. The gelatinization temperature of native potato starch is in the range 52.5–72.0 °C (Shiotsubo, 1984) while that of native maize starch is 71.5–73.8 °C (Sandhu and Singh, 2007), depending on the botanical variety.

The development of the V-type crystalline formation of amylose complexes during heating ETMS was observed from an increase in the normalized amplitude of peaks at 2θ of 7.5°, 12.9° and 19.8° (Figure 3.4B) (Buleon, Le Bail, Colonna, and Bizot, 1998; Godet, Bizot, and Buleon, 1995; Le Bail, Bizot, Pontoire, and Buléon, 1995). In this experiment, the peak of V-type crystal of an amylose-lipid complex of native maize starch appeared at 2θ of 19.8° (Le Bail, Bizot, Ollivon, Keller, Bourgaux, and Buleon, 1999). The intensity of this peak was relatively unchanged from 40 °C to 84 °C. At 86 °C, the characteristic peaks for V-type crystals of the amylose-ethanol complex emerged at 2θ of 7.5° and 12.9° (Figure 3.4B). Then, all V-type crystal peaks grew as the temperature progressed from 86 °C to 90 °C. Therefore, 86 °C was the critical temperature to initiate the V-type crystalline formation of the amylose-ethanol complex. According to Biliaderis and Galloway (1989), a sufficient amount of energy is required to initiate the complexation of amylose. It is needed to unwind the amylose helix and insert the guest molecules. However, this complex may exist in an unordered state, which is known as a type I complex. The type I complex has a random distribution of its basic structural elements (i.e., helical segments), and it does not have a crystallographic register (Biliaderis, et al., 1989). To form a crystal of an amylose-inclusion complex, the energy of the system should be enough to melt its structural elements to form a nucleus. Then, the nuclei grew to form the crystalline structure (Biliaderis, et al., 1989). However, note that the temperature for V-type crystal formation found in this experiment is only

applicable under the specified experimental conditions, i.e., normal maize starch, 50% (w/v) starch concentration, and 50% (v/v) ethanol concentration.

No V-type crystal peak was observed in the X-ray scattering profiles of ETPS (Figure 3.3B). This might be because potato starch contains amylose with a higher DP compared to maize starch. The DP of potato amylose ranges from 840 to 22,000 glucose units, while that of maize starch is approximately 400–15,000 glucose units (McDonagh, 2012). Dries, et al. (2016) states that the DP of amylose is an important factor for determining the rate of V-type crystal formation. For low DP amylose starch (maize), V-type crystallization is completed at 95 °C, while for long DP amylose starch (potato), V-type crystal formation is initiated during an isothermal holding at 95 °C (Dries, et al., 2016). In addition, additional energy is required to melt the cocrystallized amylose-amylopectin cluster of B-type crystal in potato starch (Saibene, et al., 2010) to liberate and induce mobility of the cocrystallized amylose to form V-type crystal (Dries, et al., 2016). Therefore, for GCWSS prepared by heating starch with ethanol, the required energy for V-type crystal formation can be supplied by either heating for a longer time and/or at a higher temperature. Unfortunately, the V-type crystal formation for ETPS was not successful in the current experiment since a nonhermetic heating cell was used. Overall, it is suggested that the energy to initiate V-type crystal formation is higher for ETPS than for ETMS.

3.4.2 Structural transformations of ETS during heating at the lamellae level

The structural transformations of ETMS and ETPS at the lamellae level during heating are presented in Figure 3.5. At 40°C, SAXS peaks were observed at q values of 0.64 and 0.69 nm^{-1} for ETMS and ETPS, respectively, corresponding to D_{Bragg}
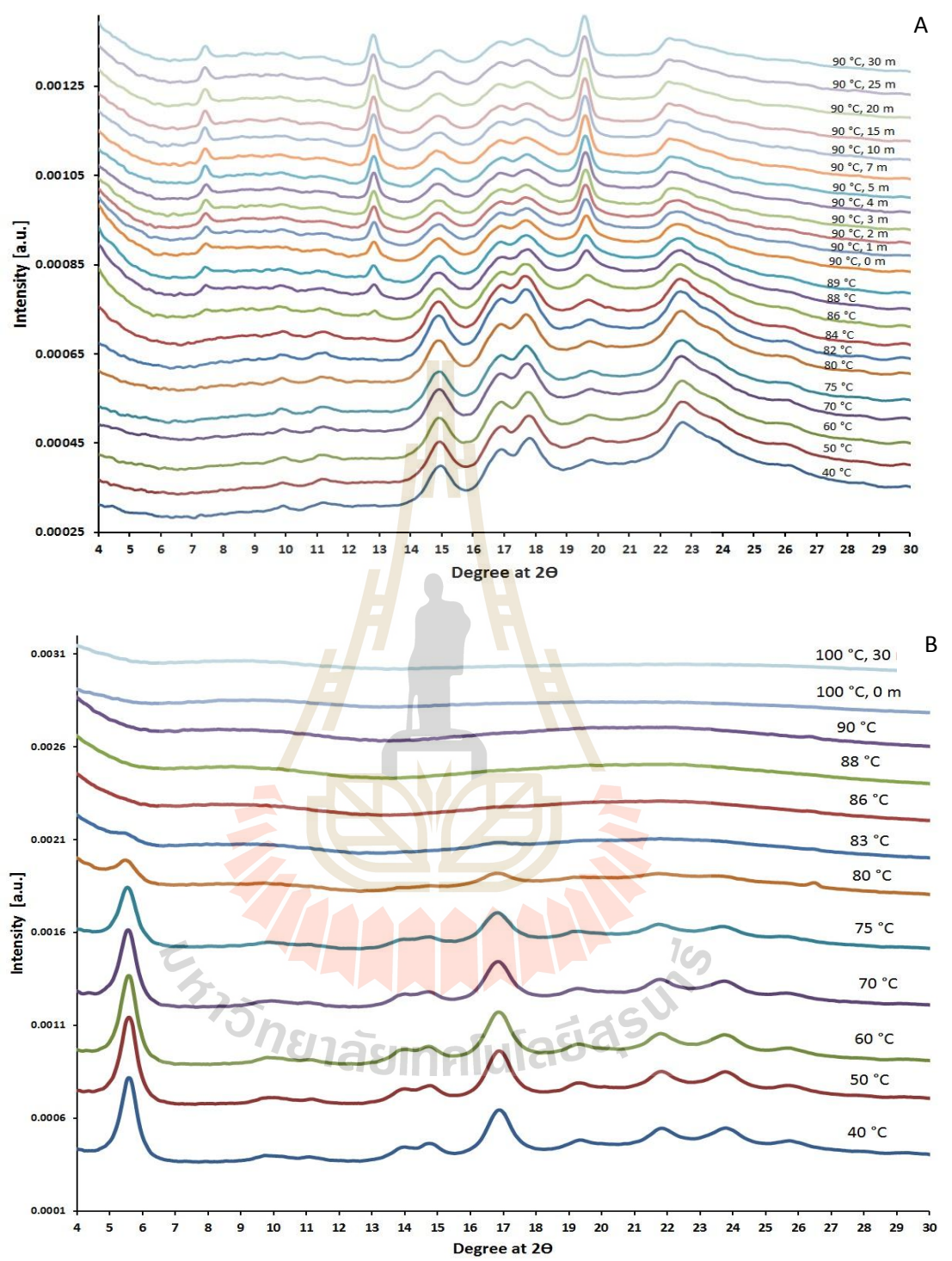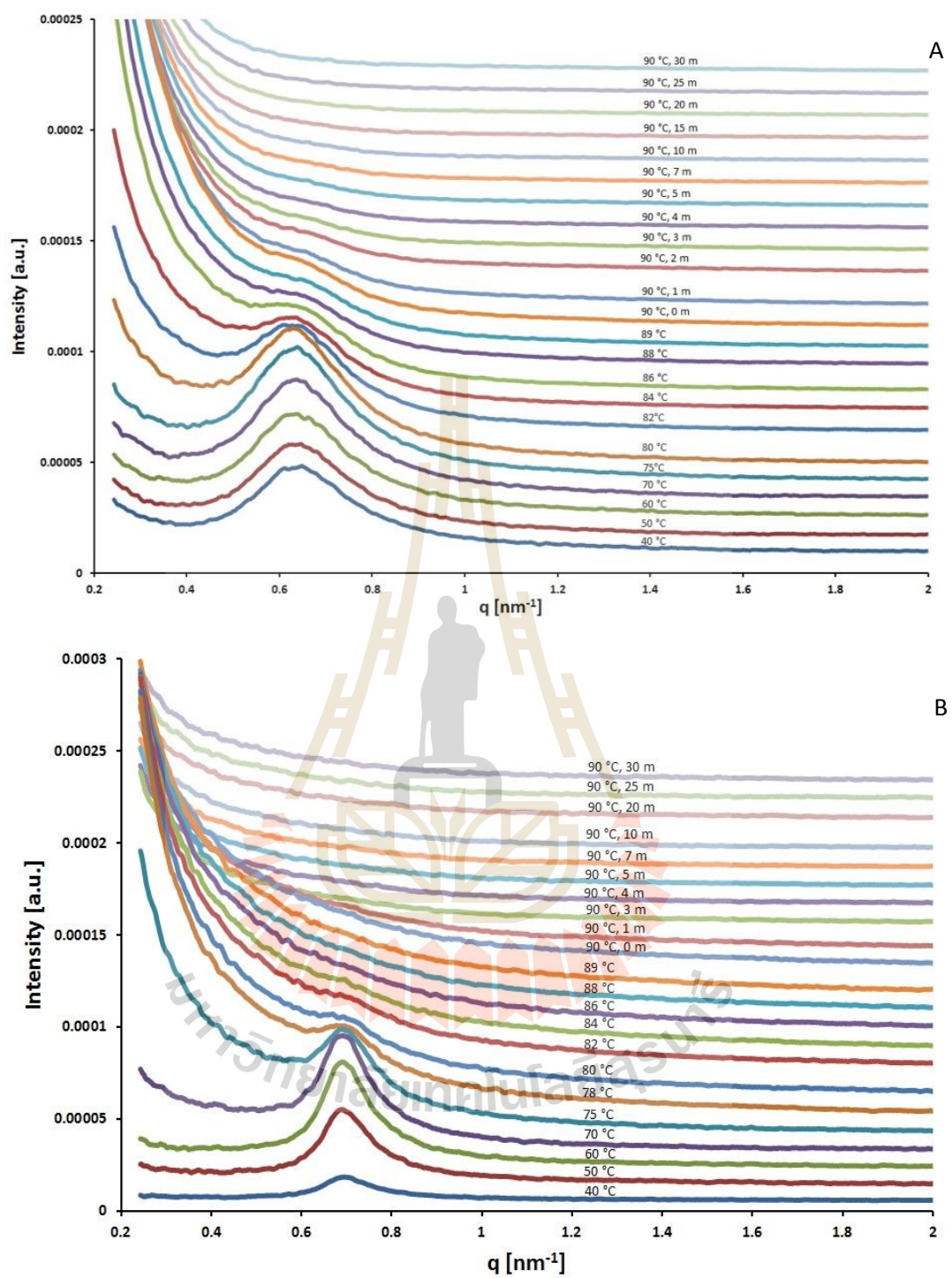
Figure 3.5 In situ SAXS patterns of ethanol-treated maize starch (ETMS) (A) and
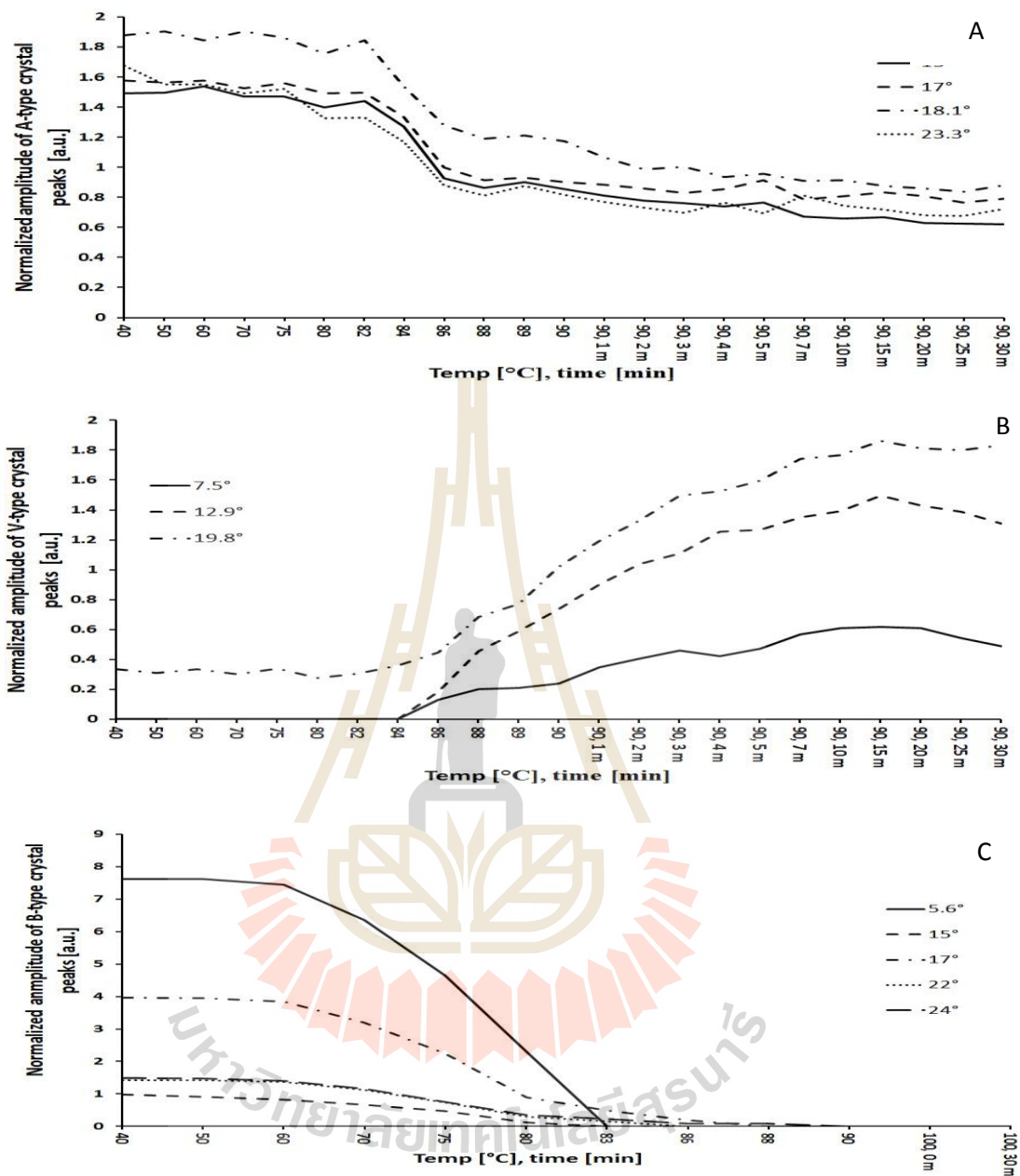
ethanol-treated potato starch (ETPS) (B) during heating.

Table 3.1 Lamellae structural parameters of ethanol-treated maize starch (ETMS) and ethanol-treated potato starch (ETPS) during heating.

Sample	Temperature [°C]	Lamellae structural parameters by paracrystalline model*			
		L_{crl} [nm]	σ_L [nm]	$\bar{\alpha}$ [nm]	σ_α [nm]
ETMS	40	3.9	0.8	9.1	2.5
	50	4.1	0.8	9.1	2.4
	60	4.3	0.7	9.2	2.4
	70	4.3	0.8	9.2	2.4
	75	4.7	0.4	9.2	2.4
	80	5.1	0	9.1	2.4
	82	4.9	0	9	2.4
	84	3.2	3	9.4	2.3
ETPS	40	3.9	0	8.8	1.6
	50	4	0	8.8	1.6
	60	4.3	0	8.9	1.6
	70	4.9	0	8.8	1.6
	75	2.7	0.1	8.7	1.5

*the paracrystalline model parameters are crystalline lamellae thickness (L_{crl}), average repeat distance ($\bar{\alpha}$) and mean square deviation of L (σ_L) and $\bar{\alpha}$ (σ_α).

spacing of native maize and potato starch of 9.8 and 9.1 nm, respectively (Donald, et al., 2001; Pikus, 2005). Surprisingly, as the temperature increased up to 75°C and 70 °C for ETMS and ETPS, respectively, their SAXS peaks became taller and sharpened (Figure 3.5). The results of paracrystalline fitting indicated that the crystalline lamellae thickness (L_{crl}) increased from 3.9 to 5.1 nm and 3.9 to 4.9 nm for ETMS and ETPS, respectively (Table 3.1). This result suggested that the double helices of

crystalline lamellae realigned toward a more ordered register (Vermeylen, Derycke, Delcour, Goderis, Reynaers, and Koch, 2006) and were probably followed by crystalline lamella expansion (Perry and Donald, 2000; Zhang, Chen, Xie, Li, Truss, Halley, Shamshina, Rogers, and McNally, 2015). Dispersion of starch in low-water-content solvent (50% ethanol) provides a smaller amount of free water to hydrate the mesogen of amylopectin. Then, when it is heated, the plasticizing effect of water is limited, and the thermal energy induces limited mobilization of the double helices. As a result, the double helices of amylopectin tend to realign and reorient themselves toward a more stable conformation, as indicated by the increase in crystalline lamella thickness (Perry, et al., 2000; Vermeylen, et al., 2006). At temperatures of 80 and 70 °C, the crystalline lamellae thicknesses of ETMS and ETPS reached their highest values of 5.1 and 4.9 nm, respectively (Table 3.1), indicating that the crystalline lamellae were at the most perfect register.

Above temperatures of 80 and 70°C, the SAXS peaks became gradually smaller and eventually disappeared at temperatures of 86 and 80°C for ETMS and ETPS, respectively (Figure 3.5). This can be attributed to the disruption of crystalline lamellae (Gallant, Bouchet, and Baldwin, 1997; Zhang, Li, Liu, Xie, and Chen, 2013; Zhang, Zhao, Li, Li, Xie, and Chen, 2014). This was also confirmed by the paracrystalline fitting results, for which the crystalline lamellae thickness (L_{crl}) decreased to 3.2 nm at 84°C and 2.7 nm at 75°C for ETMS and ETPS, respectively. High temperatures induce a higher molecular mobility of the unwinding mesogen and transform it into isotropic states (Waigh, Gidley, Komanshek, and Donald, 2000).

Regarding the fractal analysis results, the slopes of double log plots of SAXS data were -1.3 and -0.7 for ETMS and ETPS, respectively, at the final temperature.

This result suggested a drastic transformation at the lamellae level, in which the three-dimensional structure of crystalline lamellae (Jenkins and Donald, 1996) was converted to a fine structure. According to Beaucage (2012), the structure is likely to have a rod-like shape as the slope approaches -1. This structure correlates with the high water adsorption capability of ETS because the amylopectin chains are not compact in the double helix conformations but exist in a state of interconnected chains, which allows the hydroxyl groups of the amylopectin backbone to be readily exposed to water.

3.4.3 Morphological and structural transformations of ETS granules at the granular level

The morphological transformations of ETMS and ETPS at the granular level are shown in Figure 3.6. The native maize granules were round to polygonal in shape while the granules of native potato had oval shapes. Both starches showed distinct Maltese cross. When the starches were converted to ETS, their morphologies were transformed. At 80°C, the characteristic of Maltese crosses of native starches were slightly distorted, particularly at the center of the cross (Figure 3.6 B2 and F2). At 90 °C, most of the ETMS granules did not exhibit Maltese crosses, but the ETPS granules still showed some indiscernible patterns at their peripheries, as indicated by the arrows in Figure 3.6 C2 and G2. The presence of amylose-lipid complexes and integrated proteins at the periphery of maize starch granules prevents these areas from disruptions, i.e., from heat treatment or degrading enzymes (Dhital, Warren, Zhang, and Gidley, 2014; Tester, 1997; Tester, Karkalas, and Qi, 2004). Meanwhile, the periphery of potato starch contains a high amount of cocrystallized amylose with amylopectin clusters, which can also protect the granule periphery from
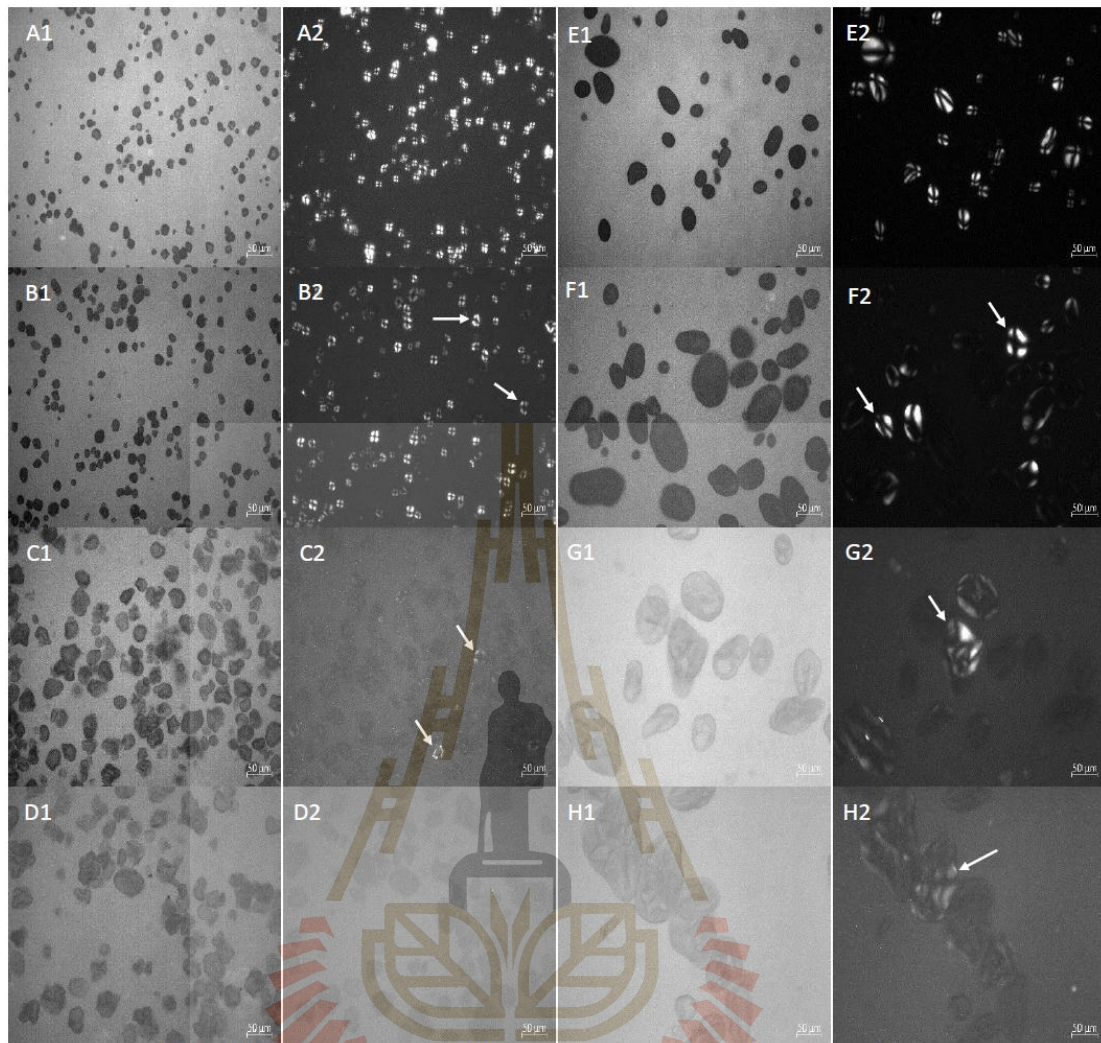
Figure 3.6 Bright field (1) and polarized light (2) micrographs of native maize (A)
and potato starches (E) and the corresponding ETS morphologies from 80
(B and F), 90 (C and G) and 100°C (D and H), respectively.

disruptions (Jenkins, et al., 1995; Kuakpetoon and Wang, 2007; Saibene, et al., 2010).
At 100°C, the ETMS granules did not exhibit the birefringence (Figure 3.6 D2), while
the ETPS granules still showed weak birefringence patterns (Figure 3.6 H2). This
result suggested that the resistance level of crystalline lamellae toward disruption is
dependent on the starch origin. It also implied that the crystalline lamellae of potato
starch were more resistance toward heat treatment at the periphery than at the hilum.

Even without perfect birefringence patterns, both ETS granules still preserved their granular form. Therefore, the preservation of the granule integrity of ETS was likely due to the role of amylose chains and amylose-ethanol complexes (Dries, et al., 2014). It was noted that the hazy birefringence characteristics of ETPS at 100°C were not detectable by SAXS, as evidenced by the fact that no peak was observed above 78°C (Figure 3.5B). This might be because the quantity of ETPS granules containing distorted lamellae was lower than the detection limit of SAXS.

3.4.4 A model of structural transformations of ETS during heating

A model of structural transformations of ETS during heating, shown in Figure 3.7, illustrates the transformations at three organizational levels: crystalline, lamellae and granular structures. Stage 0 illustrates the structural arrangement of dry native starch, in which the starch tends to have a less-organized lamellar structure (Vermeylen, et al., 2006). Addition of excess solvent leads to limited movement of double helices in the amylopectin clusters toward a better alignment (Waigh, et al., 2000), as illustrated in stage I. The excess solvent also causes different electron densities between the crystalline and amorphous lamellae; therefore, the characteristic peak of SAXS can be observed (Waigh, et al., 2000). Stage II illustrates the phenomenon at the initial heating temperatures ($> 40°C$), in which the thermal energy of the system starts to rise and is sufficient to mobilize the mesogen toward a more stable conformation, as indicated by the increase in crystalline lamellae thickness (Table 3.1). At this stage, distortion of the crystalline structure also occurs, as noticed from the decrease in major peaks of both A- and B-type crystals (Figure 3.4). The ability of crystalline lamellae to realign into the most perfect register is illustrated by
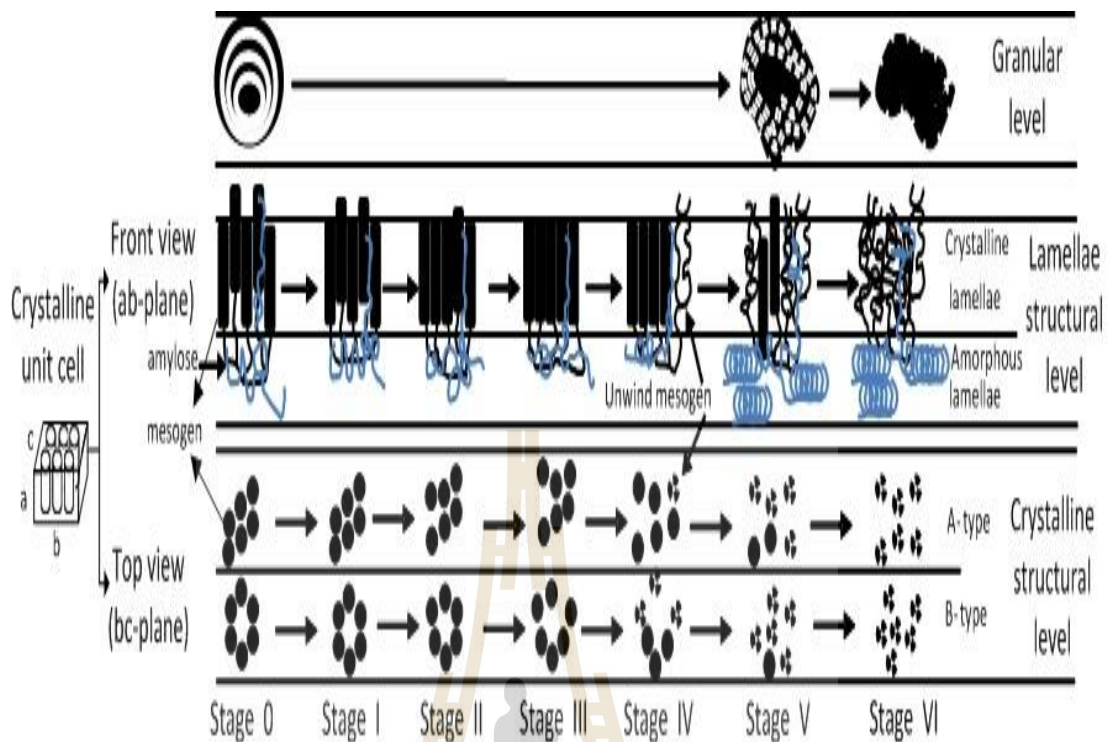
Figure 3.7 The proposed model of gradual structural transformations of ethanol-treated starch (ETS) during heating.

stage III. At this stage, the thicknesses of crystalline lamellae reached their highest values at 80 and 70°C for ETMS and ETPS, respectively (Table 3.1). Above this temperature, the crystalline lamella starts to be disrupted, as indicated by the decrease in crystalline lamellae thickness (Gallant, et al., 1997; Zhang, et al., 2013; Zhang, et al., 2014) (Table 3.1), which is illustrated by stage IV. Stage V depicts the realignment of amylose-ethanol complexes to facilitate the nucleation of a V-type crystalline structure, which was observed at 86°C for ETMS (Figure 3.4B). Note that stage V may overlap with stage IV, since the formation of V-type crystals occurred within the temperature range of crystalline lamellae disruption. Stage V illustrates that the disruption of crystalline lamellae extensively occurs at the amylopectin clusters

near the hilum rather than at the granule periphery. This was evidenced by the presence of hazy birefringence at the periphery of the ETS granules when they were observed under a polarized light microscope (Figure 3.6 C2 and G2). Stage VI illustrates the loss of birefringence of the ETS granules heated at high temperature (100°C), but they were still in granular form. This might be attributed to the role of amylose chains and amylose-ethanol complexes to preserve the integrity of the ETS granules.

3.5   Conclusions

In situ WAXS/SAXS combined with LM allowed assessment of structural transformations of ETS at its crystalline, lamellae and granular levels during heating. For ETMS, V-type crystalline structure formation was initiated at 86 °C. During ETS heating, the crystalline lamellae realigned toward a more perfect register before they were disrupted. The result of fractal analysis implied a transformation of ETS from a three-dimensional structure to a rod-like structure at the lamellae structural level. The granular structure of ETS was still preserved upon the loss of birefringence due to the role of amylose chains and amylose-ethanol complexes in maintaining its granular shape.

3.6   Acknowledgments

3.7   References

Beaucage, G. (2012). Combined Small-Angle Scattering for Characterization of Hierarchically Structured Polymer Systems over Nano-to-Micron Meter: Part II Theory. In K. Matyjaszewski and M. Möller (Eds.), **Polymer Science: A Comprehensive Reference** vol. 2 (pp. 399-409). Amsterdam: Elsevier BV.

Biliaderis, C.G., and Galloway, G. (1989). Crystallization behavior of amylose-V complexes: Structure-property relationships. **Carbohydrate Research** 189: 31-48.

Buleon, A., Le Bail, P., Colonna, P., and Bizot, H. (1998). Phase and polymorphic transitions of starches at low and intermediate water contents. In D.S. Reid (Ed.), **The Properties of Water in Foods ISOPOW 6** (pp. 160-178). Boston, MA: Springer US.

Dhital, S., Warren, F.J., Zhang, B., and Gidley, M.J. (2014). Amylase binding to starch granules under hydrolysing and non-hydrolysing conditions. **Carbohydrate Polymer** 113: 97-107.

Donald, A.M., Kato, K.L., Perry, P.A., and Waigh, T.A. (2001). Scattering Studies of the Internal Structure of Starch Granules. **Starch/Starke** 53(10): 504-512.

Doutch, J., and Gilbert, E.P. (2013). Characterisation of large scale structures in starch granules via small-angle neutron and X-ray scattering. **Carbohydrate Polymer** 91(1): 444-451.

Dries, D.M., Gomand, S.V., Delcour, J.A., and Goderis, B. (2016). V-type crystal formation in starch by aqueous ethanol treatment: The effect of amylose degree of polymerization. **Food Hydrocolloids** 61: 649-661.

Dries, D.M., Gomand, S.V., Goderis, B., and Delcour, J.A. (2014). Structural and thermal transitions during the conversion from native to granular cold-water swelling maize starch. **Carbohydrate Polymer** 114: 196-205.

Eastman, J.E. (1987). Cold water swelling starch composition. **USPTO # 4.634.596**

Eastman, J.E., and Moore, C.O. (1984). Cold soluble water granular starch for gelled food compositions. **USPTO # 4.465.702**

French, A.D., and Murphy, V.G. (1977). Computer modeling in the study of starch. **Cereal Food World** 22(2): 61-70.

Gallant, D.J., Bouchet, B., and Baldwin, P.M. (1997). Microscopy of starch: evidence of a new level of granule organization. **Carbohydrate Polymers** 32(3): 177-191.

Godet, M.C., Bizot, H., and Buleon, A. (1995). Crystallization of amylose-fatty acid complexes prepared with different amylose chain lengths. **Carbohydrate Polymers** 27(1): 47-52.

Imberty, A., Chanzy, H., Pérez, S., Bulèon, A., and Tran, V. (1988). The double-helical nature of the crystalline part of A-starch. **Journal of Molecular Biology** 201(2): 365-378.

Jane, J., Craig, S.A.S., Seib, P.A., and Hoseney, R.C. (1986a). Characterization of granular cold water-soluble starch. **Starch/Starke** 38: 258-263.

Jane, J., Craig, S.A.S., Seib, P.A., and Hoseney, R.C. (1986b). A granular cold water-soluble starch gives a V-type X-ray diffraction pattern. **Carbohydrate Research** 150(1): c5-c6.

Jane, J., and Seib, P.A. (1991). Preparation of granular cold water swelling/soluble starches by alcoholic-alkali treatments. **USPTO # 5.057.157**

Jenkins, P.J., and Donald, A.M. (1995). The influence of amylose on starch granule structure. **International Journal of Biological Macromolecule** 17: 315-321.

Jenkins, P.J., and Donald, A.M. (1996). Application of small-angle neutron scattering to the study of the structure of starch granules. **Polymer** 37(25): 5559-5568.

Kuakpetoon, D., and Wang, Y.-J. (2007). Internal structure and physicochemical properties of corn starches as revealed by chemical surface gelatinization. **Carbohydrate Research** 342(15): 2253-2263.

Le Bail, P., Bizot, H., Ollivon, M., Keller, G., Bourgaux, C., and Buleon, A. (1999). Monitoring the crystallization of amylose–lipid complexes during maize starch melting by synchrotron x-ray diffraction. **Biopolymer** 50(1): 99-110.

Le Bail, P., Bizot, H., Pontoire, B., and Buléon, A. (1995). Polymorphic transitions of amylose-ethanol crystalline complexes induced by moisture exchanges. **Starch/Starke** 47(6): 229-232.

Light, J.M. (1990). Modified food starches: why, what, where, and how. **Cereal Foods World** 35: 1081-1084.

McDonagh, P. (2012). 7 - Native, modified and clean label starches in foods and beverages. In **Natural Food Additives, Ingredients and Flavourings** (pp. 162-174): Woodhead Publishing

Perry, P.A., and Donald, A.M. (2000). The Role of Plasticization in Starch Granule Assembly. **Biomacromolecules** 1(3): 424-432.

Pikus, S. (2005). Small-angle x-ray scattering (SAXS) studies of the structure of starch and starch products. **Fibres and Textiles in Eastern Europe** 13(5 (53)): 82-86.

Pitchon, E., O'Rourke, J.D., and Joseph, T.H. (1981). Process for cooking or gelatinizing materials. **USPTO # 4.280.851**

Putseys, J.A., Lamberts, L., and Delcour, J.A. (2010). Amylose-inclusion complexes: Formation, identity and physico-chemical properties. **Journal of Cereal Science** 51(3): 238-247.

Rajagopalan, S., and Seib, P.A. (1991). Process for the preparation of granular cold water-soluble starch. **USPTO # 5.037.929**

Rugmai, S., Soontaranon, S., Chirawatkul, P., and Kaewhan, C. (2014). Small/Wide Angle X-ray Scattering (SAXS/WAXS) Station Manual: **Synchrotron Light Research Institute (Public Organization)**.

Saibene, D., and Seetharaman, K. (2010). Amylose involvement in the amylopectin clusters of potato starch granules. **Carbohydrate Polymers** 82(2): 376-383.

Sandhu, K.S., and Singh, N. (2007). Some properties of corn starches II: Physicochemical, gelatinization, retrogradation, pasting and gel textural properties. **Food Chemistry** 101: 1516–1524.

Shiotsubo, T. (1984). Gelatinization temperature of potato starch at the equilibrium state. **Agricultural and Biological Chemistry** 48(1): 1-7.

Soontaranon, S., and Rugmai, S. (2012). Small Angle X-ray Scattering at Siam Photon Laboratory. **Chinese Journal of Physics** 50(2): 204-210.

Suzuki, T., Chiba, A., and Yarno, T. (1997). Interpretation of small angle X-ray scattering from starch on the basis of fractals. **Carbohydrate Polymers** 34(4): 357-363.

Svensson, E., and Eliasson, A.-C. (1995). Crystalline changes in native wheat and potato starches at intermediate water levels during gelatinization. **Carbohydrate Polymers** 26(3): 171-176.

Tester, R.F. (1997). Starch: The polysaccharide fraction. In P.J. Frazier, P. Richmond and A.M. Donald (Eds.), **Starch: Structure and functionality.** (pp. 163-171). Cambridge: The Royal Society of Chemistry.

Tester, R.F., Karkalas, J., and Qi, X. (2004). Starch-composition, fine structure and architecture. **Journal of Cereal Science** 39(2): 151-165.

Vainshtein, B.K. (1966). Diffraction of X-Rays by Chain Molecules. Amsterdam: **Elsevier BV**.

Vermeylen, R., Derycke, V., Delcour, J.A., Goderis, B., Reynaers, H., and Koch, M.H.J. (2006). Structural Transformations during Gelatinization of Starches in Limited Water: Combined Wide- and Small-Angle X-ray Scattering Study. **Biomacromolecules** 7(4): 1231-1238.

Waduge, R.N., Hoover, R., Vasanthan, T., Gao, J., and Li, J.H. (2006). Effect of annealing on the structure and physicochemical properties of barley starches of varying amylose contents. **Food Research International** 39: 59-77.

Waigh, T.A., Gidley, M.J., Komanshek, B.U., and Donald, A.M. (2000). The phase transformations in starch during gelatinisation: a liquid crystalline approach. **Carbohydrate Research** 328(2): 165-176.

Yuryev, V.P., Krivandin, A.V., Kiseleva, V.I., Wasserman, L.A., Genkina, N.K., Fornal, J., Blaszczak, W., and Schiraldi, A. (2004). Structural parameters of amylopectin clusters and semicrystalline growth rings in wheat starches with different amylose content. **Carbohydrate Research** 339(16): 2683-2691.

Zhang, B., Chen, L., Xie, F., Li, X., Truss, R.W., Halley, P.J., Shamshina, J.L., Rogers, R.D., and McNally, T. (2015). Understanding the structural disorganization of starch in water-ionic liquid solutions. **Physical Chemistry Chemical Physics** 17(21): 13860-13871.

Zhang, B., Dhital, S., Haque, E., and Gidley, M.J. (2012). Preparation and characterization of gelatinized granular starches from aqueous ethanol treatments. **Carbohydrate Polymers** 90(4): 1587-1594.

Zhang, B., Li, X., Liu, J., Xie, F., and Chen, L. (2013). Supramolecular structure of A- and B-type granules of wheat starch. **Food Hydrocolloids** 31(1): 68-73.

Zhang, B., Zhao, Y., Li, X., Li, L., Xie, F., and Chen, L. (2014). Supramolecular structural changes of waxy and high-amylose cornstarches heated in abundant water. **Food Hydrocolloids** 35: 700-709.
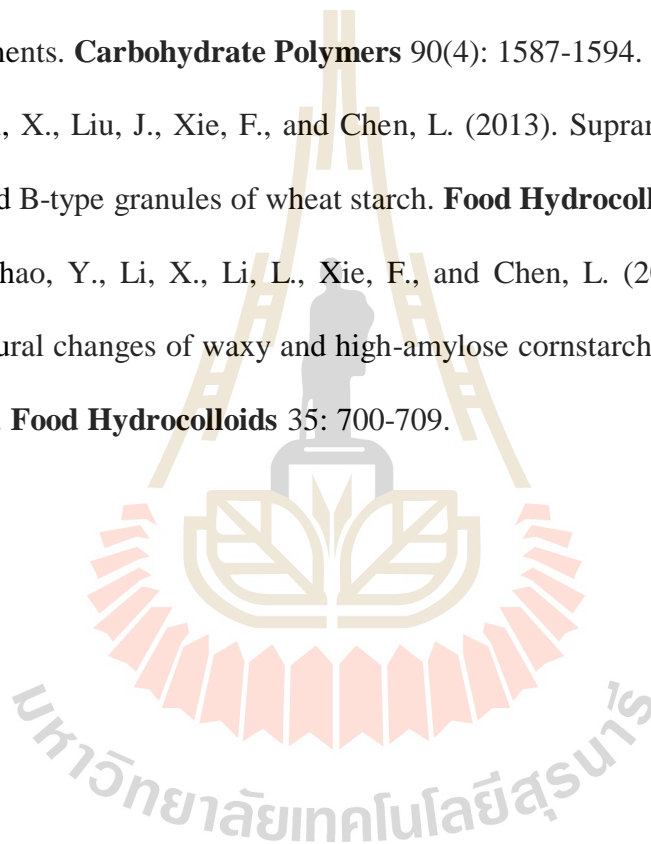
CHAPTER IV

THE INFLUENCE OF PORE CHARACTERISTICS AND STRUCTURAL PROPERTIES OF ETHANOL-TREATED STARCH ON ITS WATER ABSORPTION CAPACITY

4.1 Abstract

Ethanol-treated starch (ETS) is known to absorb a high amount of water at room temperature. The influence of pore characteristics and structural properties of ETS prepared from 4 different starch sources (maize, potato, cassava, and rice starches) at three conversion temperatures (80, 90 and 100°C) on the cold water absorption capacity (WAC) were investigated. The results indicate that ETS from maize and potato starches contains pores with the characteristic of non-rigid and slit-shaped pores. For granular ETS from maize and potato starches, water penetrates the granule through fissures, hydrates the amorphous regions, melts the V-type crystalline structure, and is held within the ETS granules upon water absorption. For non-granular ETS from cassava and rice starches, water hydrates the amorphous and V-type crystalline structures, and it is entrapped within the three-dimensional network of starch components entanglement upon contact with water.

Keywords: ethanol-treated starch, water absorption capacity, pore characteristics, V-type crystalline, and amorphous structures.

4.2   Introduction

Developing porous foods have become one of the most interesting research topics nowadays. New porous foods for specific applications, such as extruded products (Karathanos and Saravacos, 1993), encapsulating agents for flavor compounds (Weirong and Huiyuan, 2002), drug carriers (Najafi, Baghaie, and Ashori, 2016) and nutraceutical carriers (Wang, Lv, Jiang, Niu, Pang, and Jiang, 2016) are on increasing demand.

Porous food is differentiated from nonporous food based on the number of pores within their structure and also the other pore parameters including pore size distribution, specific surface area and pore connectivity (Rigby, Fletcher, and Riley, 2003). Porous foods contain higher porosity; therefore, it can store a higher amount of guest substances within its structure than non-porous foods.

Native starch granule is known to have low porosity. Nevertheless, it contains some sources of porosity within the granule. Hall and Sayre (1970) reported that wheat, rye, and barley starches exhibit surface pores. Moreover, Fannon, Hauber, and Bemiller (1992) stated that rice, oat, potato, tapioca, arrowroot, and canna starches did not have surface pores. However, the latest investigation by Sujka and Jamroz (2010) suggested that all native starch granules contain pores with different sizes when the nitrogen sorption isotherm method is used to probe the porosity of starch granule. The second source of porosity in native starch granule is the internal channels. Huber and BeMiller (1997) reported that they appeared as serpentine, which connects between internal cavities or channels and their opening on the granule surface. Karathanos, et al. (1993) observed that the length of the internal channel of waxy maize granules ranged from 0.07-0.10 μm. Most of the native starch granules also exhibit large voids

which are located at the hilum of granule (Fannon, Shull, and Bemiller, 1993; Hall and Sayre, 1973; Huber and BeMiller, 2000; Kim and Huber, 2008). During the dehydration process, the cavities within the starch granule may enlarge; therefore the size of cavities may contain the treatment history of the starch granule (Baldwin, Adler, Davies, and Melia, 1994). The pore size of native starch granule has been characterized (Juszczak, Fortuna, and Wodnicka, 2002; Sujka, et al., 2010); however, the other pore characteristics of native starch granule such as pore rigidity properties have not yet been reported.

Water absorption capacity is one method that can be used to evaluate the porosity of starch granule (Wang, et al., 2016). Water molecules penetrate the inner region of starch granule pass through the granule surface pores upon hydration. Then, water goes into the amorphous region and preferentially hydrate this part over the crystalline structure (Gallay and Puddington, 1943; Tako, Tamaki, Teruya, and Takeda, 2014; Zobel, Young, and Rocca, 1988). The water absorption capacity of starch is dependent on the number of pores, channels, and cavities within the starch granule (Wang, et al., 2016; Weirong, et al., 2002).

Porous starch is a modified starch product which is prepared to enhance the porosity of native starch, thus increasing its water absorption capacity (WAC) (Wang, et al., 2016; Weirong, et al., 2002). Another type of starch that exhibits high WAC is cold water swelling starch (CWSS). Many studies have reported the capability of CWSS to absorb water at low temperatures (Dries, Gomand, Goderis, and Delcour, 2014; Rajagopalan and Seib, 1992). CWSS can adsorb water up to 12 times more than its weight (Majzoobi, Kaveh, Blanchard, and Farahnaky, 2015). Meanwhile, porous starch can only maximally absorb water up to 3 times more than its weight (Wang, et

al., 2016). Thus, it is advantageous to use CWSS over porous starch in terms of its water absorption capacity.

Among methods to prepare CWSS, heating starch with ethanol, which is commonly termed as ethanol-treated starch (ETS), is considered to be the simplest method to produce CWSS. It only requires ethanol as the converting reactant which can be removed from the product by dehydration, thus leaving less or no residue of this reagent in the final product (Dries, et al., 2014; Zhang, Dhital, Haque, and Gidley, 2012).

Pore characteristics are a fundamental property of porous materials that influence their macroscopic properties, such as bulk density, mechanical strength, and thermal conductivity (Sing, Everett, Haul, Moscou, Pierotti, Rouquerol, and Siemieniewska, 1985). Moreover, it is essential to choose suitable porous materials for specific applications, such as for adsorbents, catalysts, encapsulating agents, and pigment carriers (Lowell, Shields, Thomas, and Thommes, 2010). Materials with high porosity mostly possess a high surface area and pore diameter size within the micropore range (i.e., less than 2 nm) (Lowell, et al., 2010; Sing, et al., 1985).

Porous starch contains pores in the macropore range since its pore diameter is predominantly about 1 μm (Sujka and Jamroz, 2009; Sujka, et al., 2010). Moreover, porous rice starch has the highest surface area (1.66 m^2/g) meanwhile porous potato starch has the lowest area (0.4 m^2/g) (Juszczak, et al., 2002; Sujka, et al., 2010). Therefore, porous rice starch possesses a high potential for use as a carrying agent (Sujka, et al., 2010). However, since pore characterizations of ETS have not yet been conducted, the main objective of the present study was to investigate the pore characteristics of ETS. The influence of this property on the WAC was studied.

Moreover, the influence of the structural properties of ETS on the WAC was included to gain a comprehensive view of factors influencing this property.

4.3 Materials and methods

4.3.1 Materials

Normal maize and potato starches were supplied by National Starch and Chemicals Ltd. (Bangkok, Thailand). Rice and cassava starches were provided by General Food Product Co. Ltd. and Sanguan Wongse Industries Co. Ltd. (Nakhon Ratchasima, Thailand), respectively. Analytical grade ethanol was purchased from Carlo Erba Ltd. (Val de Reuil, France).

4.3.2 Sample preparation

ETS was prepared by the method of Eastman and Moore (1984) and (Dries, et al., 2014) with some modifications. Starch (15 g) from different sources (maize (M0), potato (P0), cassava (C0), and rice (R0)) was dispersed with 135 ml of ethanol (50 %v/v) in Schott bottles. It was then heated at different temperatures of 80, 90 and 100 °C (M80, M90, M100, P80, P90, P100, C80, C90, C100, R80, R90, and R100) for 30 min and then cooled at room temperature for 3 h. The sediment was separated from the supernatant by vacuum filtration, washed with absolute ethanol three times and finally dried with a vacuum oven at 55°C for 12 h. The dried sample was ground and sieved (150 μm). Then, the samples were kept in a desiccator containing silica gel and stored at ambient temperature prior to analysis. All treatments were carried out in triplicate.

4.3.3 Cold water absorption capacity

A method described by Wang, et al. (2016) was modified to determine the cold water absorption capacity (WAC) of samples. Prior to the analysis, all samples were vacuum dried at a temperature of 70 °C for 24 h. A sample suspension of 0.5 g (5%(w/v)) was centrifuged (CR22GIII, Hitachi, Japan) at 1,500 rpm for 10 min at ambient temperature. The sediment was carefully separated from the supernatant. The WAC was determined according to the following equation:

$$\text{WAC } [\%] = \frac{\text{the weight of sediment [g]} - \text{the initial weight of sample [g]}}{\text{the initial weight of sample [g]}} \text{ x 100 \%} \quad (1)$$

4.3.4 Morphological properties

The morphological properties of the samples were observed by a Field Emission-Scanning Electron Microscope (Auriga[Tm]-Carl Zeiss, Jena, Germany). The sample was mounted on a metal stub which was previously covered with double-sided adhesive tape. The excess sample was removed by spraying it with nitrogen gas. Then, it was coated with gold, and an accelerating voltage of 2 kV was used during observation.

4.3.5 Pore characterization by nitrogen sorption isotherm

The pore characteristics of ETS were determined by the N_2 gas adsorption method using BELSORP mini-II sorption isotherm apparatus (MicrotracBel Corp., Osaka, Japan). High-purity nitrogen (99.99%) at a temperature of 77 K was used to measure the sorption isotherm of the samples. Prior to the analysis, all samples were vacuum dried at a temperature of 100°C for 24 h. A sample (0.1 g) was poured into a glass tube and degassed with a high vacuum unit at 100°C for 24 h. The specific surface area (BET surface area) and pore size distribution (BJH pore size distribution)

were determined according to the IUPAC standard method (Sing, et al., 1985). All measurements were performed in duplicate.

4.3.6 The crystalline structure of ETS

The crystalline structure of ETS was assessed by the wide-angle X-ray scattering (WAXS) technique. It was conducted at the beamline of 1.3 WAXS station, Synchrotron Light Research Institute (SLRI), Nakhon Ratchasima, Thailand. The beamline set up was adopted from that reported by Soontaranon and Rugmai (2012) with some modifications. The sample to detector distance was set at 188.9 mm and X-ray energy of 9 keV was used. The WAXS measurement was recorded by a MAR-CCD (SX165) detector with a detecting radius of 82.5 mm. Prior to the measurement, the sample moisture content was equilibrated in a closed chamber filled with saturated LiCl solution for 7 days. After the data acquisition, the WAXS data from the scattering angle at 2θ of 5 to 28° was normalized. A program called SAXSIT, which was developed in-house using MATLAB, was employed to fit the crystalline peaks by the pseudo-Voigt fitting method. Lastly, the relative crystallinity of samples was determined by the following equation:

$$\text{Relative Crystallinity } [\%] = \frac{\text{area of crystalline peaks}}{\text{total area of diffractogram}} \times 100\% \tag{2}$$

4.3.7 Statistical analysis

The experiments were carried out in three replications. Statistical analysis was performed using SPSS version 17.0 in which the ANOVA procedure was employed. Duncan's post-hoc test was used to verify the significant differences between the mean values (P<0.05).

4.4   Results and discussion

4.4.1   The cold water absorption capacity of ETS

Figure 4.1 displays the WAC profiles of native starches and their corresponding ETS. As the conversion temperature increased, the WAC values of all ETS samples increased proportionally independent to the origin of the native starch (Figure 4.1). The WAC values of ETS from maize, potato, cassava, and rice starches at the highest conversion temperature   ($100°C$) reached 796, 869, 645, and 854%, respectively. This result implies that a higher heating temperature is required to obtain ETS with higher WAC. For porous starch, the highest WAC is about 300% (Wang, et al., 2016). The presence of physical pore has been reported to be the most influencing factor for the high water absorption capability of porous starch (Wang, et al., 2016; Weirong, et al., 2002). For ETS, the water absorption capability might be influenced by the presence of V-crystalline structure (Dries, et al., 2014) since the V-type crystalline structure of the amylose-ethanol complex is soluble in cold water (French and Murphy, 1977).
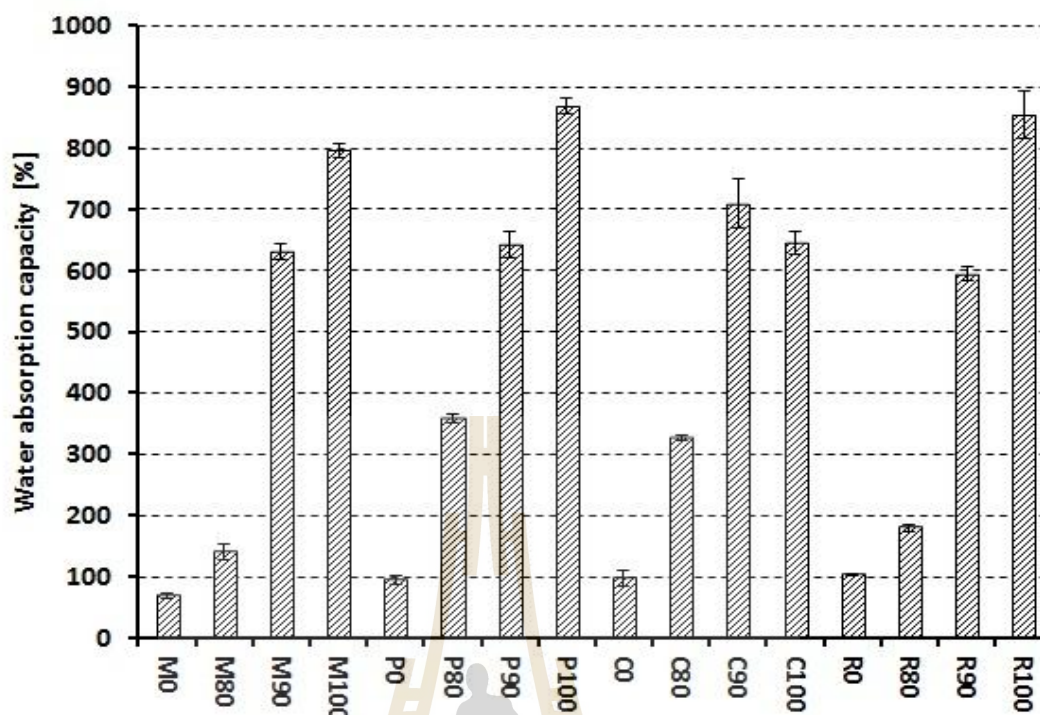
Figure 4.1 Water absorption capacity of native maize (M0), potato (P0), cassava (C0), rice (R0) and their corresponding ETS from the heating temperature of 80°C (M80/P80/C80/R80), 90°C (M90/P90/C90/R90) and 100°C (M100/P100/C100/R100), respectively. * Same letters indicate that samples are not statistically different (p>0.05).

4.4.2 Morphological properties of ETS

The morphological properties of native maize, potato, cassava, and rice starches and their corresponding ETS are presented in Figure 4.2. The native maize starch granules exhibited polyhydric to round shapes, and some granules showed pores on their surface. The native potato starch granules showed oval shapes with a smooth surface. The native cassava starch granules displayed round shapes with some truncated and smoothed surface granules. The native rice starch granules showed
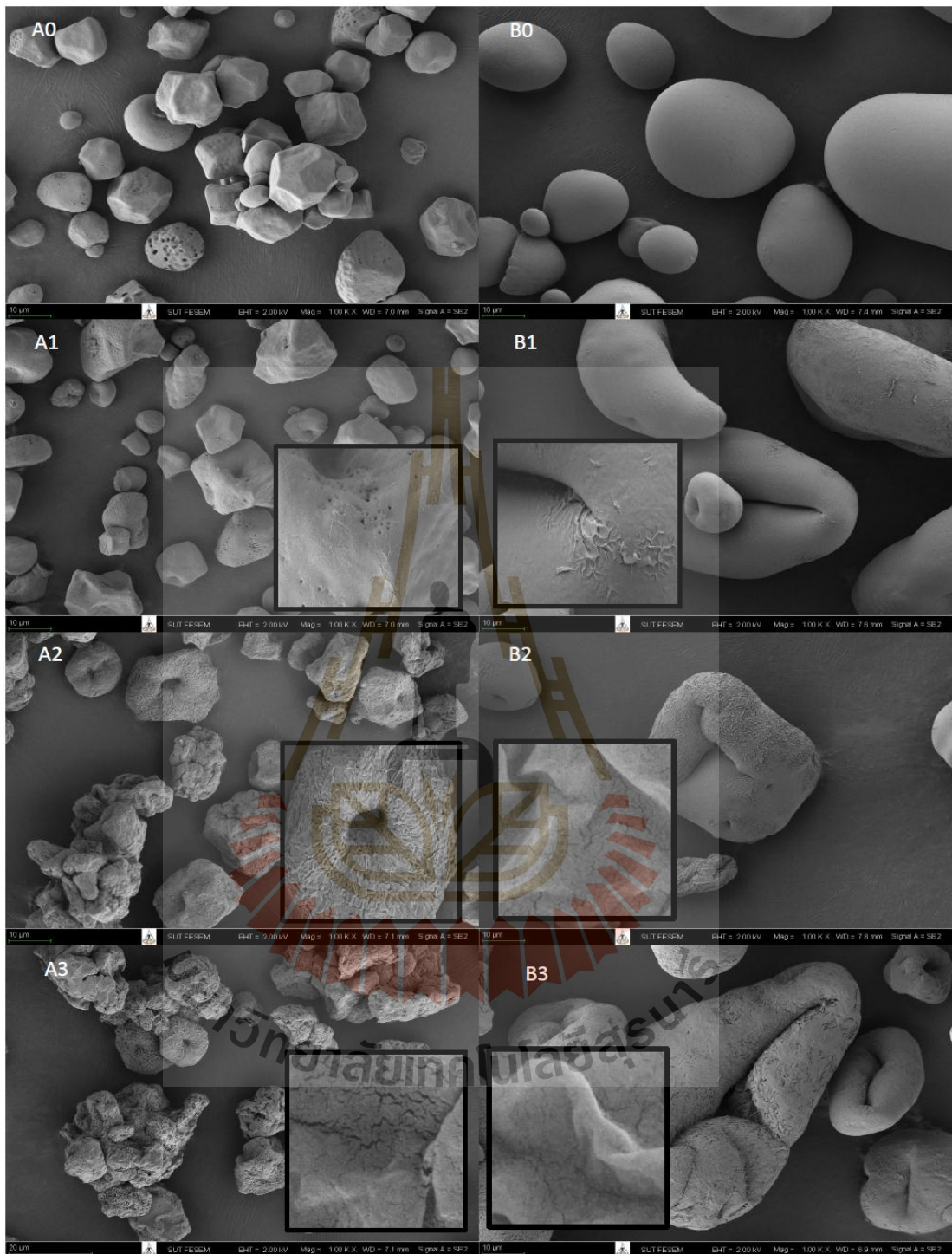
Figure 4.2.

Figure 4.2 Scanning electron micrograph of native maize (A0), potato (B0), cassava (C0), rice (D0) and their corresponding ETS from the heating temperatures of 80°C (A1/B1/C1/D1), 90°C (A2/B2/C2/D2) and 100°C (A3/B3/C3/D3), respectively.

polyhedral shapes and tended to aggregate (Chen, Yu, Chen, and Li, 2006; Jivan, Yarmand, and Madadlou, 2014; Juszczak, Fortuna, and Krok, 2003).

Among ETS from 80 °C, the granules of P80 showed the most obvious alteration in that most granules exhibited indentation and were donut shaped with wrinkles on their surface (Figure 4.2 B1). Some granules of C80 melted and became aggregated particles with a wrinkled surface (inset of Figure 4.2 C1). Also, some R80 granules were indented on their polyhedral sides (inset of Figure 4.2 D1). Drastic morphological alterations were observed on the surfaces of the ETS granules from the conversion temperature of 90 and 100 °C (Figure 4.2 A2, A3, B2, B3, C2, C3, D2, and D3). The M90, M100, P90 and P100 granules showed wrinkles and fissures on the granule surfaces (insets of Figure 4.2 A2, A3, B2, and B3), and some of them melted and stuck to each other. Moreover, M90 and M100 granules still exhibited granular forms (Figure 4.2 A2 and A3). The granular structure of P90 and P100 was also still preserved (Figure 4.2 B2 and B3). The capability of maize and potato starches to maintain their granular form during ETS conversion might be because they contain amylose with a high degree of polymerization (DP) (McDonagh, 2012) and amylose tie-chains (Saibene and Seetharaman, 2010). Amylose and amylose tie-chains hold their granular form tightly preventing them from excessive disruption during heating (Cheetham and Tao, 1998; Saibene, et al., 2010). In addition, ETS contains a V-type crystalline structure which also prevents the ETS granules from collapse (Dries, Gomand, Delcour, and Goderis, 2016; Dries, et al., 2014; Zhang, et al., 2012). It is suggested that these factors work collaboratively to prevent pore collapse and preserve the ETS granule integrity (Dries, et al., 2016; Dries, et al., 2014; Sarifudin, Soontaranon, Rugmai, and Tongta, 2019).

Granules of C90, C100, R90, and R100 underwent extreme morphological transformations in which the granules destroyed, melted and formed agglomerates (Figure 4 C2, C3, D2, and D3). The granular shapes of C100 and R100 also did not survive; instead, debris shaped-like particles were observed. Rice and cassava starch granules are known to be easier disrupted because the role of amylose in maintaining the granules integrity is limited due to the amylose of rice starch has low DP (Dries, et al., 2016) and cassava starch lacks amylose-tie chains (Rolland-Sabaté, Sánchez, Buléon, Colonna, Jaillais, Ceballos, and Dufour, 2012).

During water absorption, water may enter the ETS granule via fissures (insets of Figure 4.2 A2, A3, B2, and B3) on the granule surface of ETS from maize and potato starches. Then, water hydrates the inside granule regions preferentially the amorphous region (Gallay, et al., 1943; Tako, et al., 2014; Zobel, et al., 1988). Meanwhile, for non-granular ETS from cassava and rice starches, water immediately hydrates the outer surface of the particle once it contacts with water.

4.4.3 Pore characteristics of ethanol-treated starch.

The nitrogen sorption isotherms of native starches and their corresponding ETS are shown in Figure 4.3. The sorption isotherms of all native starches and their corresponding ETS showed an S-shape feature, which is a type II isotherm according to the IUPAC classification (Sing, et al., 1985). Moreover, the presence of hysteresis over the range of low partial pressure ($p/p_o < 0.6$) (downside insets of Figure 4.3) indicates that the pore of native starches and their corresponding ETS have a characteristic of non-rigid pores (Lowell, et al., 2010).
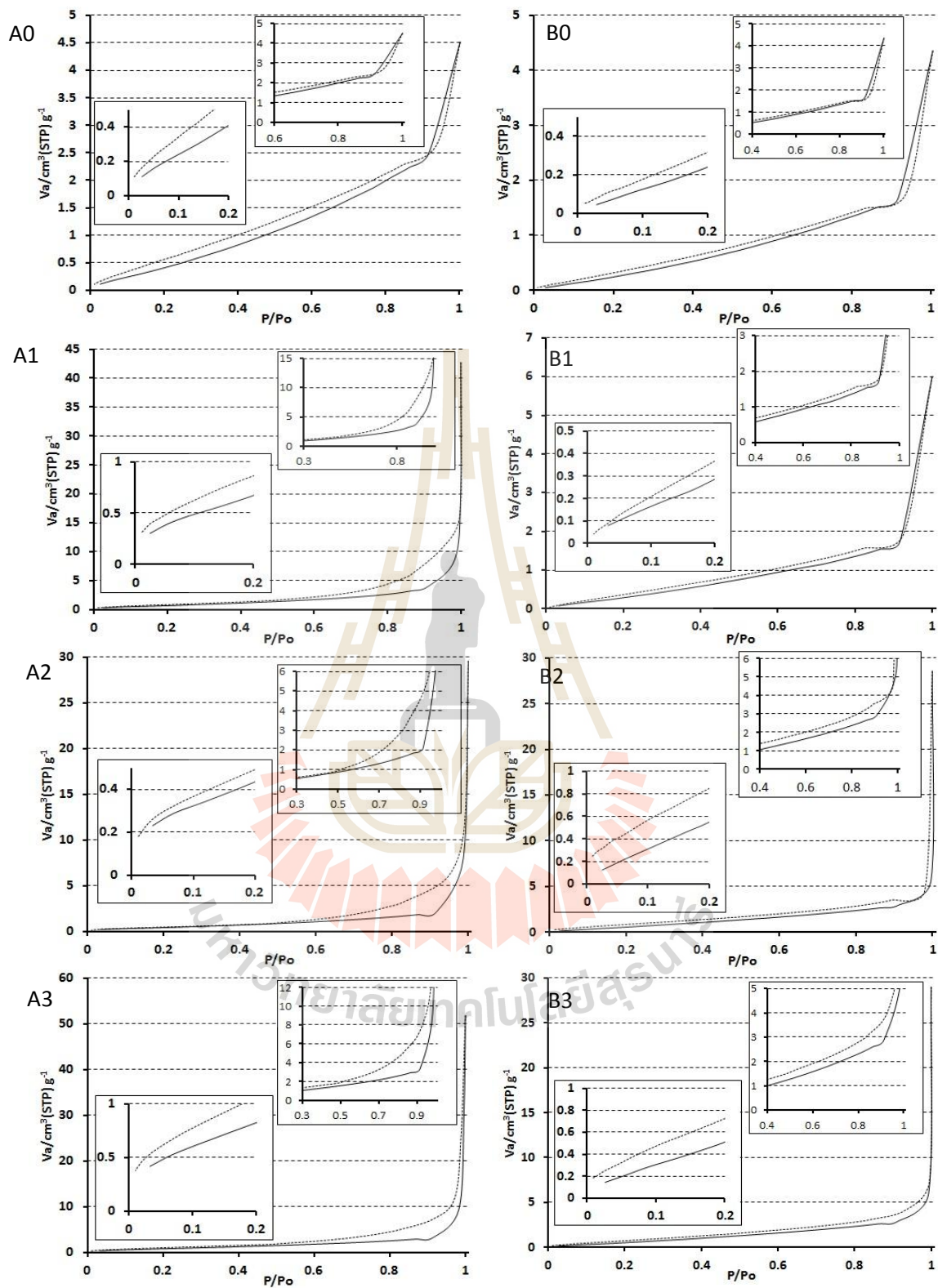
Figure 4.3

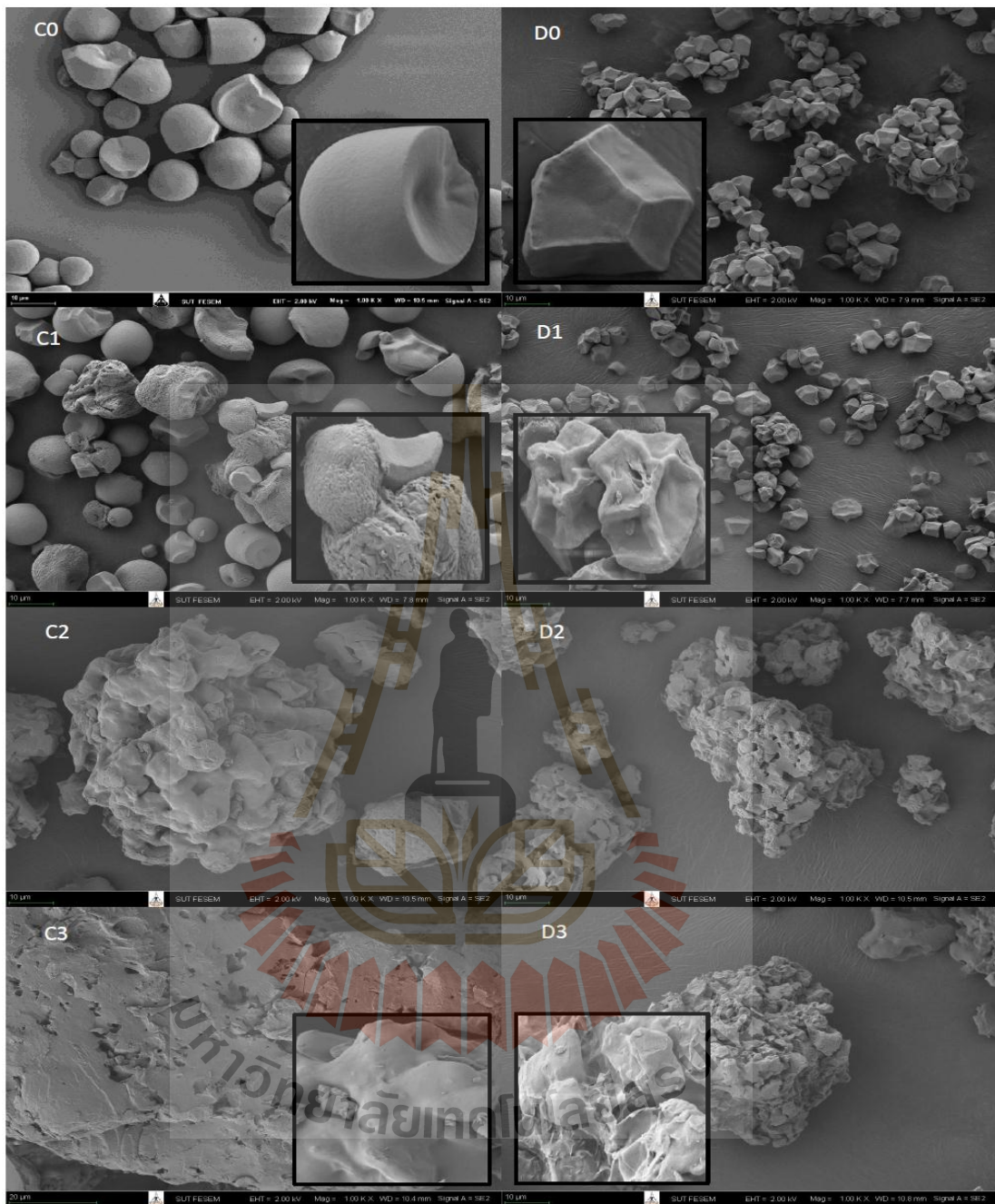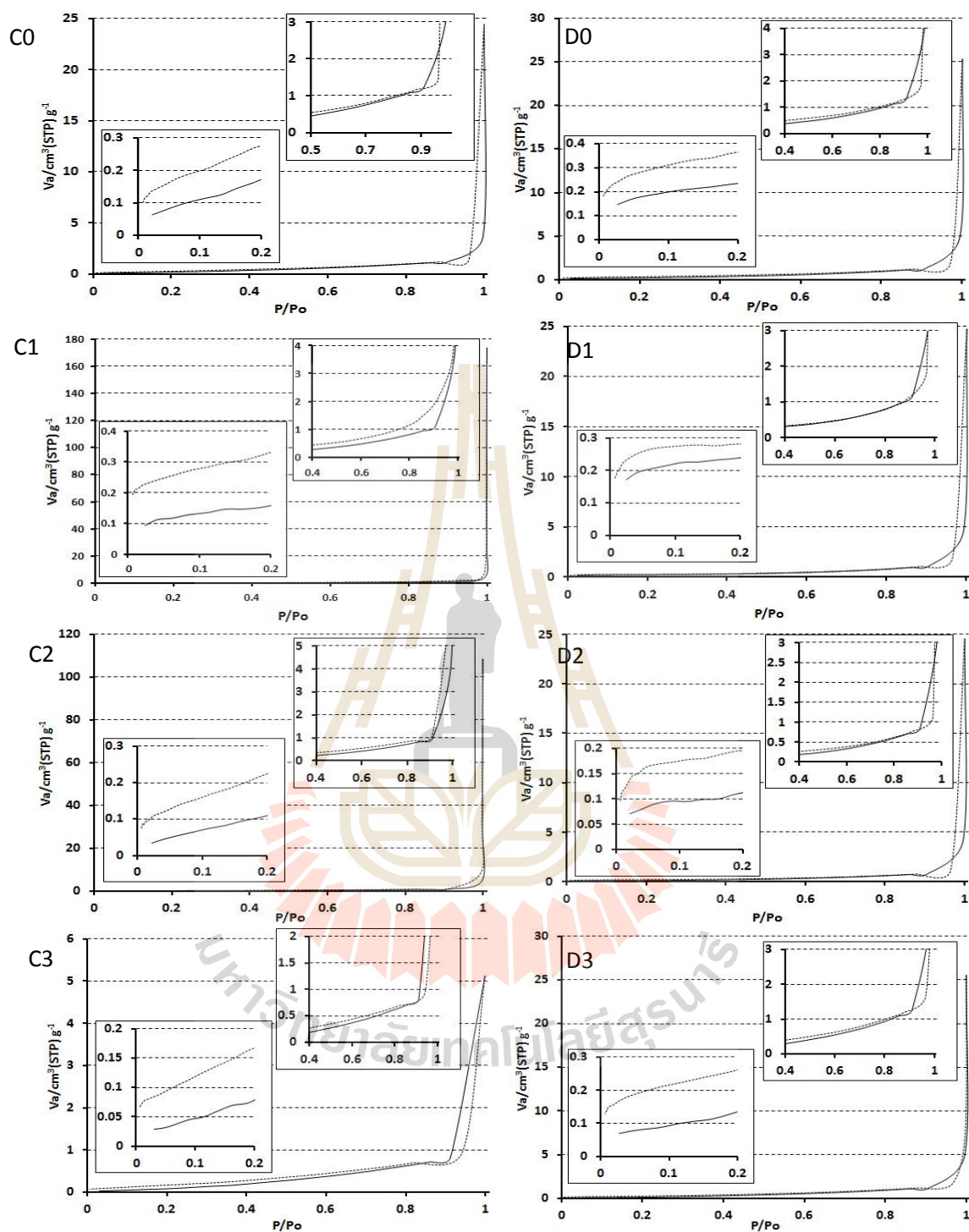**Figure 4.3** Nitrogen adsorption (solid line) / desorption (dashed line) isotherms of native maize (A0), potato (B0), cassava (C0), rice (D0) and their corresponding ETS from the heating temperatures of 80°C (A1/B1/C1/D1), 90°C (A2/B2/C2/D2) and 100°C (A3/B3/C3/D3), respectively.

Pores with the non-rigid feature are more susceptible toward environmental condition changes, i.e., pressure and temperature (Lowell, et al., 2010). Upon soaking starch in water, the water molecules penetrate the starch granule passthrough the surface pores of the granule. Then, the osmotic pressure of water gives pressure to the non-rigid pores. As a result, the starch granule swell at certain extent. Moreover, the hydration effect on the amorphous region (Gallay, et al., 1943; Tako, et al., 2014; Zobel, et al., 1988) might work collaboratively with the osmotic pressure effect to swell the starch granule.

At the high partial pressure (p/p_o 0.6-0.99), the hysteresis gaps of M80, M90, M100, P90, P100 and C80 isotherms (Figure 4.3 A1, A2, A3, B2, B3, and C1, respectively) became wider. These hysteresis shapes are almost similar to the type H3 of the IUPAC hysteresis shapes (Lowell, et al., 2010; Seaton, 1991); therefore, the pore of ETS probably has slit-shaped form as indicated by the slit-shaped fissures on the ETS granule surface (insets of Figure 4.2 A2, A3, B2, and B3). On the other hand, the hysteresis gaps of C90, C100, R80, R90 and R100 isotherms (Figure 4.3 C2, C3, D1, D2, and D3, respectively) at the high partial pressure does not develop which may indicate that the pore network of ETS from cassava and rice starches was destroyed at high temperature (90 and 100°C) as observed by the morphological data (Figure 4.2).

The profiles of the BET surface areas of native starches and their corresponding ETS are displayed in Figure 4.4 Among the native starches, rice starch exhibited the highest value (1.07 m^2/g), followed by maize starch (0.83 m^2/g), cassava starch (0.69 m^2/g) , and the lowest value was potato starch (0.35 m^2/g). The BET surface areas of native starches obtained in this experiment were slightly different from the previous reports (Sujka and Jamroz, 2007; Sujka, et al., 2009, 2010) which

may be due to the different sample preparation method used prior to the analysis, i.e., drying time and temperature (Fortuna, Januszewska, Juszczak, Kielski, and Pałasiński, 2000). The cavities within the starch granule may enlarge during drying starch process (Baldwin, et al., 1994); therefore, it may impact on the surface area of native starch. The BET surface areas of ETS from maize and potato starches increased as the temperature increased. In contrast, the BET surface areas of ETS
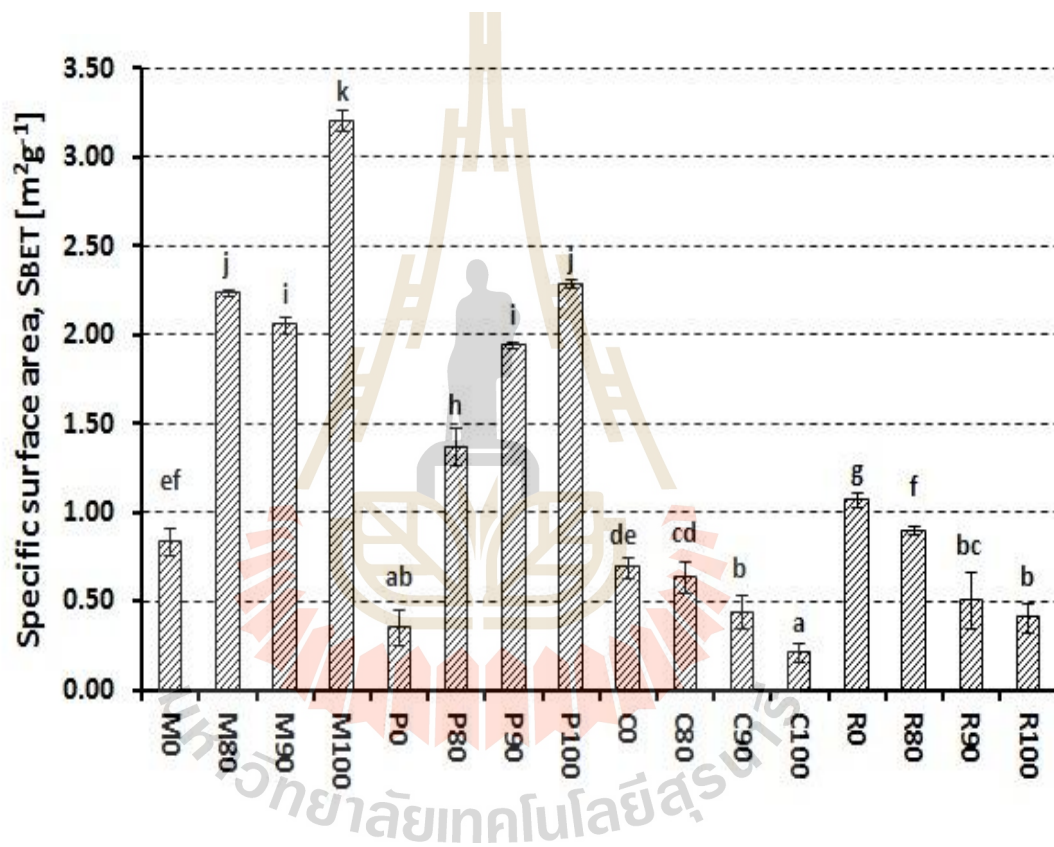
Figure 4.4 Specific surface area of native maize (M0), potato (P0), cassava (C0) and rice (R0) and their corresponding ETS from the heating temperatures of 80°C (M80/P80/C80/R80), 90°C (M90/P90/C90/R90) and 100°C (M100/P100/C100/R100), respectively. * Same letters represent that samples are not statistically different (p>0.05).

Figure 4.5 Pore size distribution of native maize (M0)(A), potato (P0)(B), cassava (C0)(C), rice (R0)(D) and their corresponding ETS from the heating temperatures of 80°C (M80/P80/C80/R80), 90°C (M90/P90/C90/R90) and 100°C (M100/P100/C100/R100), respectively.

Table 4.1 Total pore volume of native maize, potato, cassava and rice starches and their corresponding ETS.

Sample	Total pore volume [cm^3g^{-1}]
M0	3.45E-03±1.08E-03*
M80	24.1E-03±2.95E-03
M90	21.0E-03±2.65E-03
M100	31.5E-03±1.69E-03
P0	3.19E-03±0.926E-03
P80	9.11E-03±0.112E-03
P90	9.28E-03±0.108E-03
P100	10.3E-03±0.340E-03
C0	3.19E-03±1.44E-03
C80	70.3E-03±43.5E-03
C90	82.9E-03±40.0E-03
C100	1.91E-03±0.101E-03
R0	23.2E-03±22.2E-03
R80	41.7E-03±2.64E-03
R90	45.9E-03±0.446E-03
R100	53.6E-03±9.01E-03

*average±standard deviation

from cassava and rice starches decreased as the temperature increased (Figure 4.4). The BET surface areas of ETS from the highest temperature (100°C) of M100 and P100 reached 3.2 and 2.3 m²/g, respectively, while those of C100 and R100 were 0.2 and 0.4 m²/g, respectively. According to the adsorption theory, an adsorbent with a

high surface area contains a higher amount of pores as compared to a low surface area adsorbent (Lowell, et al., 2010). Therefore, the result suggests that for ETS from maize and potato starches, new pores are formed during ETS conversion, increasing the starch surface areas. At the high conversion temperatures (90 and 100°C), the ETS from maize and potato starches still showed granular forms (Figure 4.2). This result implies that the pores of ETS from maize and potato starches are located within the ETS granules. Moreover, it also suggests that for ETS from maize and potato starches, water fills the pores within the ETS granules during water absorption. Meanwhile, the granules of ETS from cassava and rice starches were destroyed (Figure 4.2); therefore, it indicates that pores which exist in native rice and cassava starches are annihilated during ETS conversion, resulting in the decrease of the granule surface areas (Figure 4.4).

The profiles of the pore size distribution of native starches and their corresponding ETS are shown in Figure 4.5. Meanwhile, the profile of total pore volume of all samples is tabulated in Table 4.1. Different starch sources possess different pore size distribution profiles. The native maize starch shows a broad pore size distribution in the mesopore range (2-50 nm) with major pores of 3.8 nm in size. The native potato also exhibits a bimodal pore size distribution profile in which the major pores are 3.3 and 4.8 nm. The native cassava and rice starches show a narrower pore size distribution with major pores of 3.7 and 16 nm respectively. Results of total pore volume of ETS samples indicate that the total pore of ETS are quite small compare to common adsorbent materials. This can be because the pores of ETS are mostly located near to the granule surface.

The result of pore size distribution analysis suggests that for ETS from maize starch, the new pores formed during ETS conversion has pore size distribution within the mesopore and macropore ranges (Figure 4.5 A). Meanwhile, for ETS from potato starch, the new pores have pore size distribution in mesopore ranges (Figure 4.5 B). The broad pore size distribution profile suggests that for ETS from maize and potato starches, the new pore formation and development occurs in a random manner resulting in broader pore size range. The new pores formed during ETS conversion may be originated from granules cracking as indicated by fissures on the ETS granules surface (insets of Figure 4.2 A2, A3, B2, and B3). During water absorption, the pores of granular ETS from maize and potato starches allow water penetration into the ETS granule. The pores of ETS from cassava and rice starches have a smaller size than those of their native starches (Figure 4.5 C and D) which could be due to pore collapse as confirmed by the low surface areas (Figure 4.4) and morphological data of both starches after converted to be ETS (Figure 4.2).

4.3.6 The crystalline structure of ETS

The WAXS patterns of native starches and their corresponding ETS are shown in Figure 4.6, and their crystallinity profiles are displayed in Figure 4.7. The major peaks of A-crystalline structure at 2θ of 9.9°, 11.2°, 15°, 17°, 18.1° and 23.3° (Buléon, Gallant, Bouchet, Mouille, D'Hulst, Kossmann, and Ball, 1997) were observed on the diffractogram of native maize, cassava, and rice starches. The peak associated with the amylose-lipid complex was observed on the diffractogram of native maize (M0)
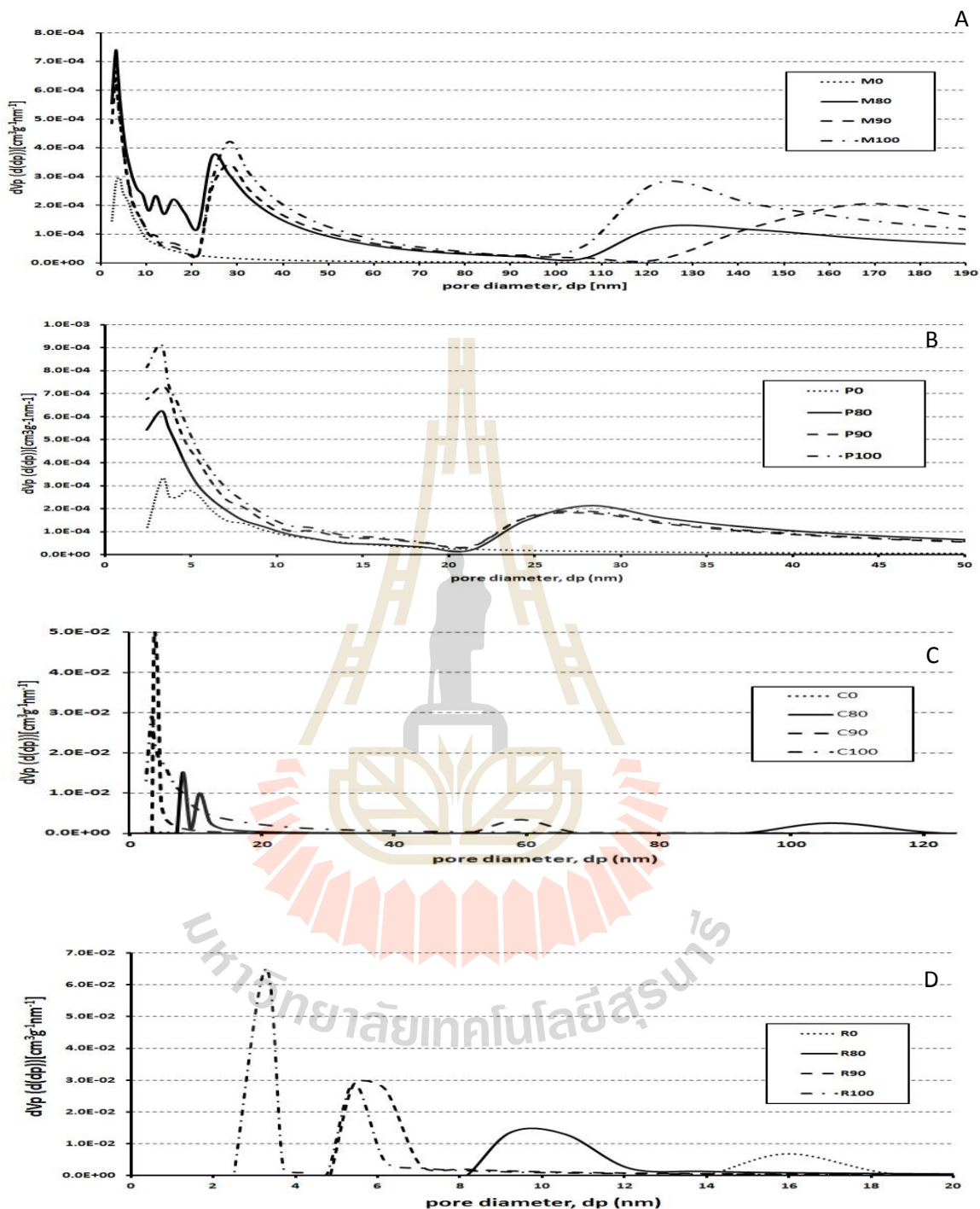
Figure 4.6 Diffractogram of native maize (M0) (A), potato (P0)(B), cassava (C0)(C) and rice (R0) (D) and their corresponding ETS from the heating temperatures of 80°C (M80/P80/C80/R80), 90°C (M90/P90/C90/R90) and 100°C (M100/P100/C100/R100), respectively

and rice (R0) at 2θ of 19.8° (Godet, Bizot, and Buléon, 1995) (Figure 4.6 A and D). Particularly for native potato starch (P0), the main identity peaks of B-crystalline structure appeared with relatively low intensity which because the sample was equilibrated at low humidity (equilibrium relative humidity of saturated LiCl solution is 11%) (Le Bail, Bizot, Pontoire, and Buleon, 1995) (Figure 4.6 B). The peaks of V-type crystalline structure of all ETS samples, which were identified at 2θ of 7.8 °, 13.6°, and 20.9° (Le Bail, et al., 1995) emerged at 90°C. However, the V-type

crystalline structure of ETS from cassava starch appeared at a lower temperature (80 °C) (Figure 4.6) which might be because the amylose of cassava starch are in free form (Rolland-Sabaté, et al., 2012) ; therefore it is easier to form a V-type crystalline structure at a low temperature (80°C). M90 and M100 showed doublet peaks at 2θ of 19.8° and 20.9° which were probably the result of a mixture of two V-type crystalline structures, namely Vh and Va, respectively (Le Bail, et al., 1995). While porous starch still bears a high proportion of the native crystalline structure (Wang, et al., 2016), ETS contains a high proportion of V-type crystalline structure of the amylose-ethanol complex (Zhang, et al., 2012) which is known to be water soluble (French, et al., 1977).

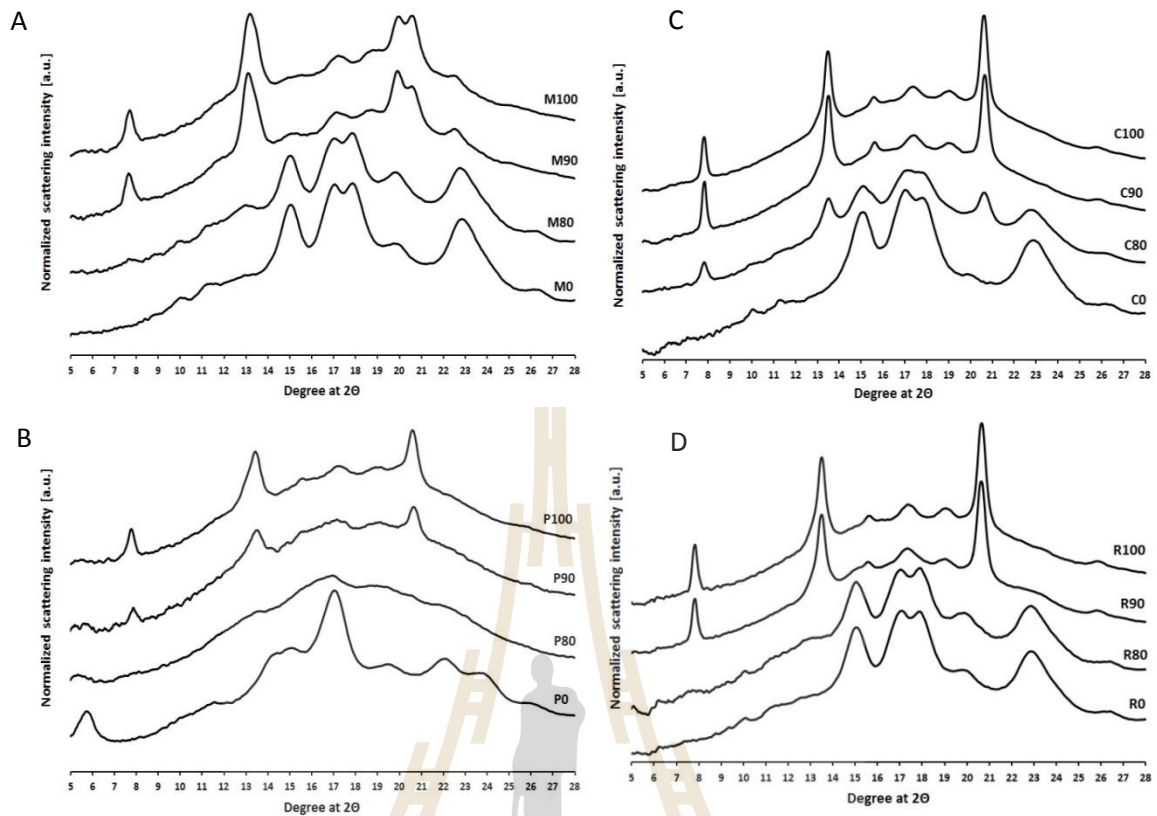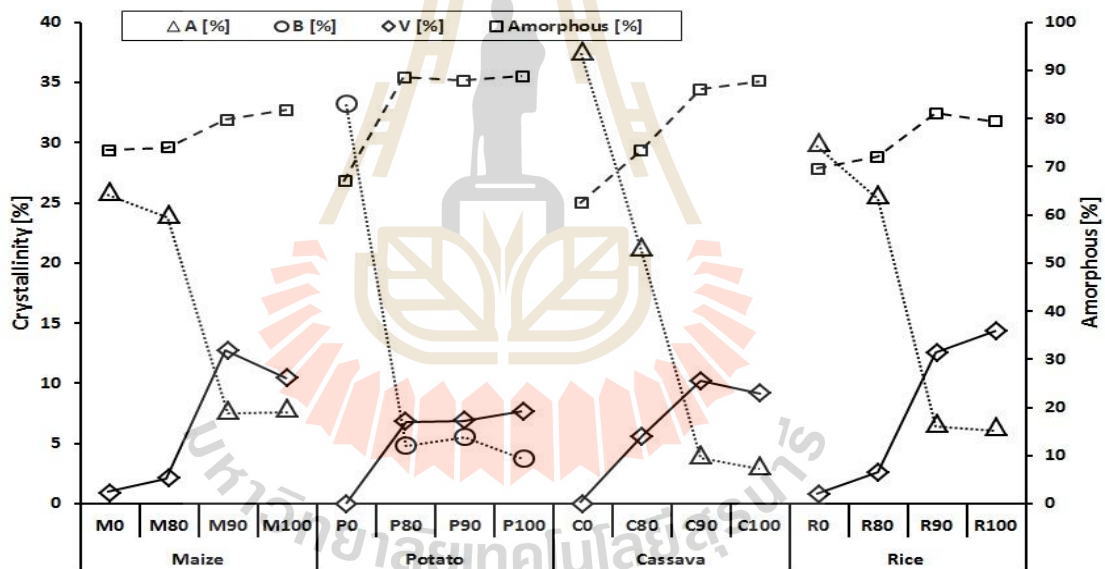**Figure 4.7** Crystallinity profile of native maize (M0) , potato (P0), cassava (C0) and rice (R0) and their corresponding ETS from the heating temperatures of 80°C (M80/P80/C80/R80), 90°C (M90/P90/C90/R90) and 100°C (M100/P100/C100/R100) including A-type crystalline (Δ), B-type crystalline (o) and V-type crystalline (◊), and amorphous (□) structures, respectively.

When the ETS conversion temperature increased, the native crystallinity decreased drastically, and the V-type crystallinity increased proportionally (Figure 4.7). During ETS conversion, the crystalline region was destroyed, consequently increased the amorphous proportion (Figure 4.7). The amorphous structure is known to have more voids within its structure (Jenkins and Donald, 1998); therefore water is easier to penetrate and hydrate the amorphous structure over the crystalline structure (Gallay, et al., 1943; Tako, et al., 2014; Zobel, et al., 1988).

Finally, two mechanisms during water absorption of ETS are proposed. For granular ETS from maize and potato starches, when the ETS granules contact with water, water penetrates the ETS granule via fissures on the surface of ETS granules (Figure 4.2). Then, water passes through the new pores which are formed during the ETS conversion (Figure 4.5). The pores of granular ETS from maize and potato starches with mesopore and macropore sizes allow water penetration into the ETS granule. Since ETS granules contain non-rigid pores (Figure 4.3) (Lowell, et al., 2010; Sing, et al., 1985), thus the osmotic pressure developed during water absorption might give a radial pressure expanding the ETS granules. Water preferentially penetrates and hydrates the amorphous structure (Gallay, et al., 1943; Tako, et al., 2014; Zobel, et al., 1988) also melts the V-type crystalline structure (French, et al., 1977). Finally, water is held within the granule of ETS from maize and potato starches (Figure 4.2).

Meanwhile, upon hydration the non-granular ETS from cassava and rice starches, water directly contacts with the amorphous regions at the outer surface of ETS particles (Figure 4.2). Then, the starch components in amorphous structure move slightly and entangle with the neighboring starch components forming a three-

dimensional network of a typical amylose-amylopectin-water gel structure which is commonly found in a gel system of fully gelatinized starch (Kawabata, Akuzawa, Ishii, Yazaki, and Otsubo, 1996). Therefore, for non-granular ETS from cassava and rice starches, water is entrapped within the three-dimensional structure of starch components entanglement during water absorption.

4.5   Conclusions

The pore characteristics and structural properties influence the water absorption capacity of ETS. Pores of ETS have characteristic of non-rigid and slit-shaped pores. During ETS conversion, the new pores are formed for ETS from maize and potato starches; meanwhile, the pores were annihilated for ETS from cassava and rice starches. ETS produced at higher conversion temperatures contains a higher percentage of V-type crystalline and amorphous structures. Upon water absorption, water penetrates the ETS granules via fissures on the surface of ETS granules; then, it passes through the new pores inside the ETS granules to hydrate the amorphous region and melt the V-type crystalline structure. For granular ETS from maize and potato starches, water is kept within the ETS granules upon water absorption. For non-granular ETS from cassava and rice starches, water hydrates the amorphous structure of the ETS particles and melts the V-type crystalline structure. Then, the water is entrapped within the three-dimensional structure of starch components entanglement upon hydration.

4.6 Acknowledgments

4.7 References

Baldwin, P.M., Adler, J., Davies, M.C., and Melia, C.D. (1994). Holes in Starch Granules: Confocal, SEM and Light Microscopy Studies of Starch Granule Structure. **Starch - Stärke** 46(9): 341-346.

Buléon, A., Gallant, D.J., Bouchet, B., Mouille, G., D'Hulst, C., Kossmann, J., and Ball, S. (1997). Starches from A to C: Chlamydomonas reinhardtii as a model microbial system to investigate the biosynthesis of the plant amylopectin crystal. **Plant Physiology** 115: 949-957.

Cheetham, N.W.H., and Tao, L. (1998). Variation in crystalline type with amylose content in maize starch granules: an X-ray powder diffraction study. **Carbohydrate Polymers** 36(4): 277-284.

Chen, P., Yu, L., Chen, L., and Li, X. (2006). Morphology and Microstructure of Maize Starches with Different Amylose/Amylopectin Content. **Starch - Stärke** 58(12): 611-615.

Dries, D.M., Gomand, S.V., Delcour, J.A., and Goderis, B. (2016). V-type crystal formation in starch by aqueous ethanol treatment: The effect of amylose degree of polymerization. **Food Hydrocolloids** 61: 649-661.

Dries, D.M., Gomand, S.V., Goderis, B., and Delcour, J.A. (2014). Structural and thermal transitions during the conversion from native to granular cold-water swelling maize starch. **Carbohydrate Polymers** 114: 196-205.

Eastman, J.E., and Moore, C.O. (1984). Cold soluble water granular starch for gelled food compositions. **USPTO # 4.465.702**

Fannon, J.E., Hauber, R.J., and Bemiller, J.N. (1992). Surface pores of starch granules. **Cereal chemistry** 69: 284-288.

Fannon, J.E., Shull, J.M., and Bemiller, J.N. (1993). Interior channels of starch granules. **Cereal chemistry** 70(5): 611-613.

Fortuna, T., Januszewska, R., Juszczak, L., Kielski, A., and Pałasiński, M. (2000). The influence of starch pore characteristics on pasting behavior. **International Journal of Food Science and Technology** 35(3): 285-291.

French, A.D., and Murphy, V.G. (1977). Computer modeling in the study of starch. **Cereal Food World** 22(2): 61-70.

Gallay, W., and Puddington, I.E. (1943). The hydration of starch below the gelatinization temperature. **Canadian Journal of Research** 21b(9): 179-185.

Godet, M.C., Bizot, H., and Buléon, A. (1995). Crystallization of amylose-fatty acid complexes prepared with different amylose chain lengths. **Carbohydrate Polymers** 27(1): 47-52.

Hall, D.M., and Sayre, J.G. (1970). A Scanning Electron-Microscope Study of Starches. **Textile Research Journal** 40(3): 256-266.

Hall, D.M., and Sayre, J.G. (1973). A Comparision of Starch Granules as Seen by Both Scanning Electron and Ordinary Light Microscopy. **Starch - Stärke** 25(4): 119-123.

Huber, K.C., and BeMiller, J.N. (1997). Visualization of Channels and Cavities of Corn and Sorghum Starch Granules. **Cereal Chemistry Journal** 74(5): 537-541.

Huber, K.C., and BeMiller, J.N. (2000). Channels of maize and sorghum starch granules. **Carbohydrate Polymers** 41(3): 269-276.

Jenkins, P.J., and Donald, A.M. (1998). Gelatinisation of starch: a combined SAXS/WAXS/DSC and SANS study. **Carbohydrate Research** 308(1): 133-147.

Jivan, M.J., Yarmand, M., and Madadlou, A. (2014). Preparation of cold water-soluble potato starch and its characterization. **Journal of Food Science and Technology** 51(3): 601-605.

Juszczak, L., Fortuna, T., and Krok, F. (2003). Non-contact atomic force microscopy of starch granules surface. Part I. Potato and tapioca starches. **Starch - Stärke** 55: 1-7.

Juszczak, L., Fortuna, T., and Wodnicka, K. (2002). Characteristics of cereal starch granules surface using nitrogen adsorption. **Journal of Food Engineering** 54(2): 103-110.

Karathanos, V.T., and Saravacos, G.D. (1993). Porosity and pore size distribution of starch materials. **Journal of Food Engineering** 18(3): 259-280.

Kawabata, A., Akuzawa, S., Ishii, Y., Yazaki, T., and Otsubo, Y. (1996). Sol-Gel Transition and Elasticity of Starch. **Bioscience Biotechnology and Biochemistry** 60(4): 567-570.

Kim, H., and Huber, K.C. (2008). Channels within soft wheat starch A- and B-type granules. **Journal of Cereal Science** 48(1): 159-172.

Le Bail, P., Bizot, H., Pontoire, B., and Buleon, A. (1995). Polymorphic Transitions of Amylose-Ethanol Crystalline Complexes Induced by Moisture Exchanges. **Starch - Stärke** 47(6): 229-232.

Lowell, S., Shields, J.E., Thomas, M.A., and Thommes, M. (2010). Characterization of porous solids and powders: surface area, pore size and density: **Kluwer Academic Publishers, Springer**.

Majzoobi, M., Kaveh, Z., Blanchard, C.L., and Farahnaky, A. (2015). Physical properties of pregelatinized and granular cold water swelling maize starches in presence of acetic acid. **Food Hydrocolloids** 51: 375-382.

McDonagh, P. (2012). 7 - Native, modified and clean label starches in foods and beverages. In Natural Food Additives, Ingredients and Flavourings (pp. 162-174): **Woodhead Publishing**

Najafi, S.H.M., Baghaie, M., and Ashori, A. (2016). Preparation and characterization of acetylated starch nanoparticles as drug carrier: Ciprofloxacin as a model. **International Journal of Biological Macromolecules** 87: 48-54.

Rajagopalan, S., and Seib, P.A. (1992). Properties of granular cold-water-soluble starches prepared at atmospheric pressure. **Journal of Cereal Science** 16(1): 29-40.

Rigby, S.P., Fletcher, R.S., and Riley, S.N. (2003). Determination of the cause of mercury entrapment during porosimetry experiments on sol–gel silica catalyst supports. **Applied Catalysis A: General** 247: 27-39.

Rolland-Sabaté, A., Sánchez, T., Buléon, A., Colonna, P., Jaillais, B., Ceballos, H., and Dufour, D. (2012). Structural characterization of novel cassava starches with low and high-amylose contents in comparison with other commercial sources. **Food Hydrocolloids** 27(1): 161-174.

Saibene, D., and Seetharaman, K. (2010). Amylose involvement in the amylopectin clusters of potato starch granules. **Carbohydrate Polymers** 82(2): 376-383.

Sarifudin, A., Soontaranon, S., Rugmai, S., and Tongta, S. (2019). Structural transformations at different organizational levels of ethanol-treated starch during heating. **International Journal of Biological Macromolecules** 132: 1131-1139.

Seaton, N.A. (1991). Determination of the connectivity of porous solids from nitrogen sorption measurements. **Chemical Engineering Science** 46(8): 1895-1909.

Sing, K.S.W., Everett, D.H., Haul, R.A.W., Moscou, L., Pierotti, R.A., Rouquerol, J., and Siemieniewska, T. (1985). Reporting physisorption data for gas/solid systems with special reference to the determination of surface area and porosity (Recommendations 1984). **Pure and Applied Chemistry** 57(4): 603-619.

Soontaranon, S., and Rugmai, S. (2012). Small Angle X-ray Scattering at Siam Photon Laboratory. **Chinese Journal of Physics** 50(2): 204-210.

Sujka, M., and Jamroz, J. (2007). Starch granule porosity and its changes by means of amylolysis. **International Agrophysics** 21.

Sujka, M., and Jamroz, J. (2009). α-Amylolysis of native potato and corn starches – SEM, AFM, nitrogen and iodine sorption investigations. **LWT Food Science and Technology** 42(7): 1219-1224.

Sujka, M., and Jamroz, J. (2010). Characteristics of pores in native and hydrolyzed starch granules. **Starch - Stärke** 62(5): 229-235.

Tako, M., Tamaki, Y., Teruya, T., and Takeda, Y. (2014). The Principles of Starch Gelatinization and Retrogradation. **Food and Nutrition Sciences** Vol.05No.03: 12.

Wang, H., Lv, J., Jiang, S., Niu, B., Pang, M., and Jiang, S. (2016). Preparation and characterization of porous corn starch and its adsorption toward grape seed proanthocyanidins. **Starch - Stärke** 68(11-12): 1254-1263.

Weirong, Y., and Huiyuan, Y. (2002). Adsorbent Characteristics of Porous Starch. **Starch - Stärke** 54(6): 260-263.

Zhang, B., Dhital, S., Haque, E., and Gidley, M.J. (2012). Preparation and characterization of gelatinized granular starches from aqueous ethanol treatments. **Carbohydrate Polymers** 90(4): 1587-1594.

Zobel, H.F., Young, S.N., and Rocca, L.A. (1988). Starch gelatinization: an X-ray diffraction study. **Cereal chemistry** 65(6): 443-446.
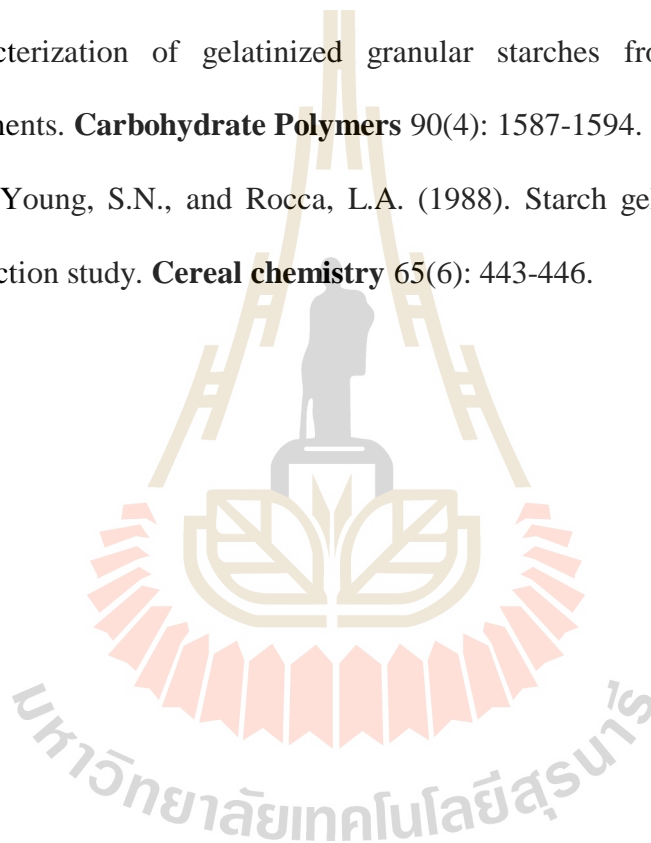
CHAPTER V

EFFECT OF STORAGE HUMIDITY ON THE STRUCTURAL, MORPHOLOGICAL PROPERTIES AND WATER ADSORPTION CAPACITY OF ETHANOL-TREATED STARCH

5.1 Abstract

Storage condition affects the properties of a product. The effects of storage humidity on the structural, morphological properties and water adsorption capacity (WAC) of maize and potato ETS were investigated. Results indicated that at a low storage humidity of 11%, the structural, morphological and WAC of ETS can be preserved. Increasing the storage humidity induced the water plasticization effect which changed the structural and morphological properties of the ETS and also decreased its WAC.

Keywords: storage humidity, ethanol-treated starch, structural, morphological, water adsorption capacity.

5.2 Introduction

Ethanol-treated starch (ETS) is a modified starch which has the capability to swell in cold water; therefore, it is also known as cold water swelling starch (CWSS). Even though its processing involves ethanol but it is considered as physically-treated

starch because after the conversion process the ethanol is removed by filtration and its residue can be evaporated easily from the product by dehydration means; thus, less or no residue of this reagent is found in the final product (Dries, Gomand, Goderis, and Delcour, 2014). Thus, processing native starch to ETS processing can be considered as a green process.

The most important property of ETS is its great capability for adsorbing water at low temperature (Chen and Jane, 1994a; Dries, et al., 2014; Jane, Craig, Seib, and Hoseney, 1986a, 1986b; Jane and Seib, 1991; Rajagopalan and Seib, 1991, 1992a, 1992b; Singh and Singh, 2003; Zhang, Dhital, Haque, and Gidley, 2012). It can adsorb water up to 12 times more than its weight (Majzoobi, Kaveh, Blanchard, and Farahnaky, 2015). It is much higher than porous starch which can maximally adsorb water up to 3 times more than its weight (Wang, Lv, Jiang, Niu, Pang, and Jiang, 2016). Therefore, in the early finding of this starch, it is mostly used as raw material for ready to consume products such as instant porridges and puddings (Eastman and Moore, 1984).

The capability of ETS in adsorbing water is because it contains the V-crystal as backbone of its structure (Chen and Jane, 1994b; Hedayati, Shahidi, Koocheki, Farahnaky, and Majzoobi, 2016; Jivan, Yarmand, and Madadlou, 2014; Kaur, Fazilah, and Karim, 2011; Majzoobi, et al., 2015; Meng and Rao, 2005; Rajagopalan, et al., 1992b; Zhang, et al., 2012). During the conversion process, the native crystal of starch is destroyed and the V-crystalline is formed. Then, the ethanol is removed by drying means without giving effect on the X-ray scattering pattern of the V crystalline structure (Dries, et al., 2014; Le Bail, Bizot, Pontoire, and Buleon, 1995; Whittam, Orford, Ring, Clark, Parker, Cairns, and Miles, 1989). In addition, Dries, et al. (2014)

suggested that ethanol removal is not mandatory to obtain CWSS with high cold water swelling properties because when CWSS is soaked in water the ethanol is freely exchangeable with the water.

Jane, et al. (1986a) investigated the effect of storage the CWS corn starch under 100% relative humidity exposures for 13 days. They reported that the V-pattern disappeared and the A-type pattern re-appeared also the modified starch became cold water-insoluble. However, the investigation of CWS from different starting materials and storage humidity has not yet been conducted.

The present study investigated the effect of storage humidity (11%, 57%, and 100%) on the properties of maize and potato ETS including structural, morphological properties and also water adsorption capacity.

5.3   Materials and method

5.3.1   Materials

Normal maize starch was purchased from a local store and potato starch was obtained from National Starch and Chemicals Ltd-Thailand. Ethanol solution 50% (v/v) was prepared by mixing absolute analytical grade ethanol (Carlo Erba-France) with de-ionized water.

5.3.2   ETS preparation

The ETS was prepared according to the method of Eastman, et al. (1984) and Dries, et al. (2014) with some modifications. One portion of starch powder from two different sources (maize and potato) were weighted, poured into the pressure leak proof bottle (Schott bottle) and dispersed with 9 portions of ethanol (50 %v/v). The samples were then heated in a water bath for 30 min at a temperature of 90. Then the

samples were cooled for about 2 hours at room temperature. The sediments were separated from the solvent by filtration and then washed with absolute ethanol and filtered, respectively, at least three times to remove the excess of water. Finally, the wet powders were dried using vacuum oven at three subsequent temperature levels (35, 45, and 55°C) for 12 hours for each temperature level. Samples were ground and sieved with 150 µm sieve and subsequently were dried with vacuum oven at 65°C for 24 hours. Samples were stored in desiccators containing silica gel and stored at ambient temperature prior to its analysis. All treatments were carried out at least in duplicate.

5.3.3   Humidity exposure experiment

The samples were stored in a closed chamber containing saturated salts solutions and water correspond to its equilibrium relative humidity including LiCl, NaBr, and water for relative humidity of 11%, 57 % and 100 %, respectively, for 6 days at constant temperature (25°C).

5.3.4   Wide angle X-ray scattering (WAXS) analysis

The WAXS analysis was conducted on the subsequent day after the humidity exposure treatment at the beamline of 1.3 WAXS station, Synchrotron Light Research Institute (SLRI), Nakhon Ratchasima, Thailand. The beamline was set according to Soontaranon and Rugmai (2012) with some modifications. The sample to detector distance was 188.897 mm and the X-ray energy was 9 keV. The WAXS spectrum was recorded by MAR-CCD (SX165) detector with its detecting radius was 82.5 mm. The WAXS data was collected from 60 seconds of X-ray exposure time. A program called SAXSIT which was developed in house (https://www.slri.or.th/en/bl13w-saxs.html) was used for data analysis. The pseudo-Voigt fitting method was employed to process

the WAXS data. The total crystallinity of samples then was calculated by the equation 1. The crystallinity contributed by the V-crystalline type peaks was etermined from the three position of V-crystal identity peaks including at the position 2θ of 7.45°, 12.93°, and 19.84° (Buleon, Le Bail, Colonna, and Bizot, 1998).

$$\% \text{ Total Crystallinity} = \frac{\text{Area of crystalline peaks}}{\text{Area of amorphous peak} + \text{Area of crystalline peaks}} \text{ x } 100 \quad (1)$$

5.3.5 Morphological properties after storage

The morphological properties of samples after humidity exposure treatment were observed by using Field Emission-Scanning Electron Microscope (Auriga FEG SEM, Carl Zeiss, Germany). Prior to the analysis, the samples were dehumidified with vacuum oven at three subsequent temperature levels (35, 45, and 55°C) for about 12 hrs. The dried sample was mounted on a metal plated with double-sided adhesive tape, sprayed with nitrogen gas to remove the excess sample, then it was coated with a thin film of gold and examined at 3 kV of accelerating voltage and 3000-30,000 x magnifications.

5.3.6 Morphological properties during humidity exposure

The morphological behavior of samples during humidity exposure was observed by using environmental scanning electron microscope (E-SEM, X-max, Quanta 450). A drop of 0.2% starch solution sample was mounted on a metal plated, dehumidified for about 2 hrs, and observed by ESEM mode at 20 kV of accelerating voltage and 750-850 kPa chamber pressure. Images of the sample were captured at different relative humidity from 80 to 97% at magnification of 2100x and 600x for maize and potato, respectively.

5.3.7   Water adsorption capacity (WAC)

A method described by Wang, et al. (2016) was modified and used to determine the cold water adsorption capacity of the samples. Prior to the analysis, all samples were vacuum dried at 70°C for 24 hours. Sample suspension (5%(w/v)) was centrifuged (CR22GIII, Hitachi, Japan) at 1500 rpm for 10 min at ambient temperature. The sediment was carefully separated from the supernatant. The cold water absorption capacity was determined according to the following equation:

$$\text{Cold water absorption capacity} \left(\frac{g}{g}\right) = \frac{\text{weight of sediment}}{\text{the initial weight of the sample}} \times 100 \quad (2)$$

5.4   Results and discussion

5.4.1   Influence of storage humidity on the structure of ETS

The structural transformation of ETS influenced by the storage humidity can be seen in the evolution of the wide angle X-ray (WAXS) patterns of ETS as displayed in Figure 5.1. Maize ETS at humidity 11% exhibited the characteristic peaks of Vh crystal at position 2θ of 7.5°, 12.9°, and 19.8° which is the hydrous state of the V-type crystal (Buleon, et al., 1998). At this humidity, one characteristic peak of anhydrous state of V crystal or Va also appeared at the position 2θ of 20.9° together with the peak position of 2θ of 19.8° as dublet peaks. This indicated that at this humidity level, the amylose inclusion complex existed together in the form of mixture of both hydrous and anhydrous states. At this humidity level, the total
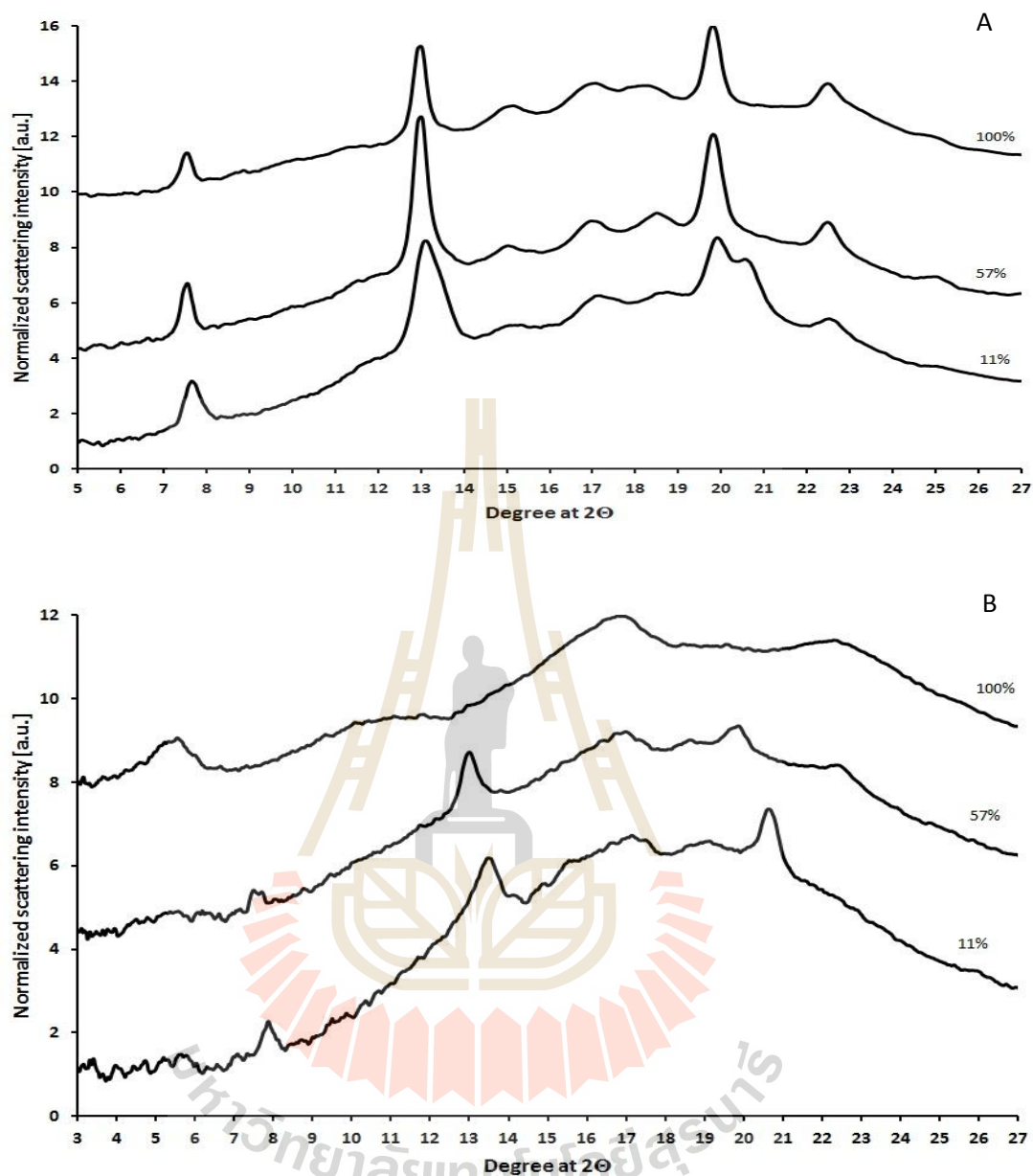
Figure 5.1 WAXS patterns of maize (A) and potato (B) ETS after storage at humidity

11%, 57% , and 100%.

crystallinity was 20% in which about 12.7% was contributed by the V-crystalline (Table 5.1). This was possible because the humidity of 11% is quite low if compared to normal environment humidity. Therefore, it is capable to remove partly the moisture from the amylose complex structure. At the humidity level of 57%, the characteristic peak of Va at 2θ of 20.9° disappeared but only the three characteristic

160

peaks of Vh crystal appeared. This suggested that at this humidity level, no remaining Va structure existed due to the moisture hydration of the Va crystal structure. This was also marked by the slight increase of the contribution of crystallinity from the V-crystalline structure up to 13.1% (Table 5.1). At the highest humidity exposure level, the three characteristic peaks of Vh crystal were still existed but their intensity lowered as indicated by the decrease of the total crystallinity down to 18.2% in which this drastic decrease was contributed by the crystallinity from the V-crystalline structure (9.9%). This results emphasized that humidity exposure partly destroy the V-crystalline structure. More excessive V-crystal disruption can be occurred at higher water hydration level, i.e. water solubilization. The V-crystal of amylose-ethanol complex is known to be water soluble (French and Murphy, 1977).

Table 5.1 The crystallinity of maize and potato ETS at different storage humidity.

Sample	ERH [%]	Total crystallinity [%]	Crystallinity contributed by V type crystalline peaks [%]
Maize ETS	11	20.4±0.2*	12.7±0.3
	57	20.1±0.4	13.1±0.3
	100	18.2±0.2	9.9±0.2
Potato ETS	11	12.5±0.9	6.9±0.5
	57	8.9±0.2	5.1±0.2
	100	16.1±0.5	3.2±0.2

*average ± standard deviation

As the V-crystal of ETS in contact with water then it lost its crystalline structure; instead, the amorphous structure is observed (Dries, Gomand, Pycarelle, Smet, Goderis, and Delcour, 2017). Due to the loss of the V-crystalline structure, the characteristic peaks of the native crystal of maize slightly increased particularly at the position 2θ of 15, 17, 18.1 and 23.3° as also reported by Jane, et al. (1986a).

At the humidity level of 11%, the potato ETS exhibited the all three characteristic peaks of Va crystalline structure at the position 2θ of 7.9°, 13.6°, and 20.9°. Some characteristic peaks of native B-type crystal at the position 2θ of 17.6 and 19.7° were also observed as broad rumpled peaks. The total crystallinity was 12.5% in which 6.9% was contributed by the V-type crystalline structure (Table 5.1). At the humidity level of 57%, the effect of moisture hydration on the Va-crystalline structure was observed, resulting in the transformation from Va to Vh crystalline structure. This was indicated by the shifting of the peak positions toward lower angle from the 2θ of 13.6° to 12.9° and 20.9° to 19.8°. It was also observed that the peak at 2θ of 22.5° appeared which is one of the characteristic peaks of B-type crystalline structure (Buléon, Gallant, Bouchet, Mouille, D'Hulst, Kossmann, and Ball, 1997). At the highest humidity exposure level, all characteristic of the V-crystalline peaks disappeared but the characteristic peaks of the B-type crystalline structure of the retrograded starch were observed as broad peaks at 2θ of 5.6, 17 and 22°. This implied that for potato ETS the high humidity level can facilitate the re-association of the chains of amylopectin clusters. This retrogradation was not observed during humidity exposure of maize ETS which may be due to the shorter chains of amylopectin cluster of maize as reported by Jane, et al. (1986a).

5.4.2 Morphological properties of ETS after storage at different humidity level

The effect of humidity exposure on the morphological properties of ETS granules is shown in Figure 5.2. At low humidity level of 11%, both maize and potato ETS granules surface exhibited donuts shapes with indentations, rough and full of
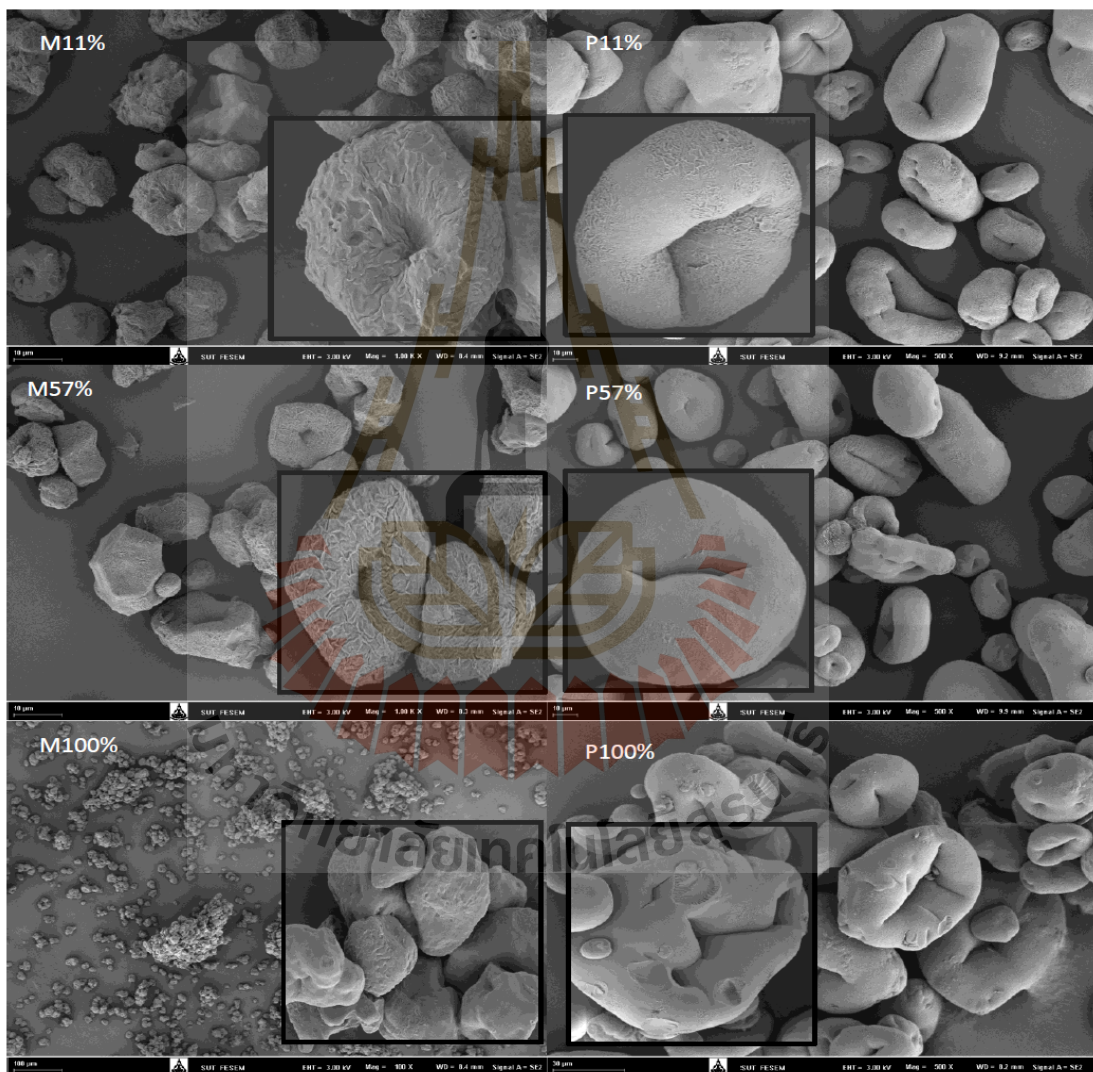
Figure 5.2 Morphology of maize (M) and potato (P) ETS after storage at humidity 11% , 57%, and 100%.

wrinkles which also have been reported elsewhere (Jane, et al., 1991; Majzoobi, et al., 2015; Rajagopalan, et al., 1992a). At the humidity of 57%, both maize and potato ETS granules surface were looked smoother compared to that of humidity of 11% in which the smooth surface of potato ETS granules were more obvious. Moreover, they were smoother at the highest humidity level. These results implied the higher humidity resulted in the higher plasticization effect of the ETS granule, thus the ETS granules surface became smoother. The smoothing effect was more obvious for potato ETS than that of maize ETS. This can be due to retrogradation of short chains of amylopectin clusters of potato ETS occurred more intensive.

5.4.3 Morphological properties of ETS during humidity exposure

The morphological properties of ETS granules during humidity exposure are displayed in Figure 5.3. At the lowest humidity level, the morphological features of ETS such as wrinkles and indentations were observed. As the humidity increased, some moisture was adsorbed by the granule surface. At high equilibrium relative humidity the moisture begun condensing and it was able to plasticize the granule surface. As a result, the granule surface became smoother and the granules expanded to bigger sizes. However, at the highest humidity level the condensed water obscured the observation due to the electron beam is highly diffracted by the condensed water resulting in black spots on the SEM images.

5.4.4 Effect of storage humidity on the water adsorption capacity of ETS

The effect of storage humidity on the WAC of ETS is presented in Figure 5.4. At the humidity level of 11%, the WAC of maize ETS was 345% while that of potato ETS was 457%. Then, as the storage humidity increased, the WAC of ETS decreased
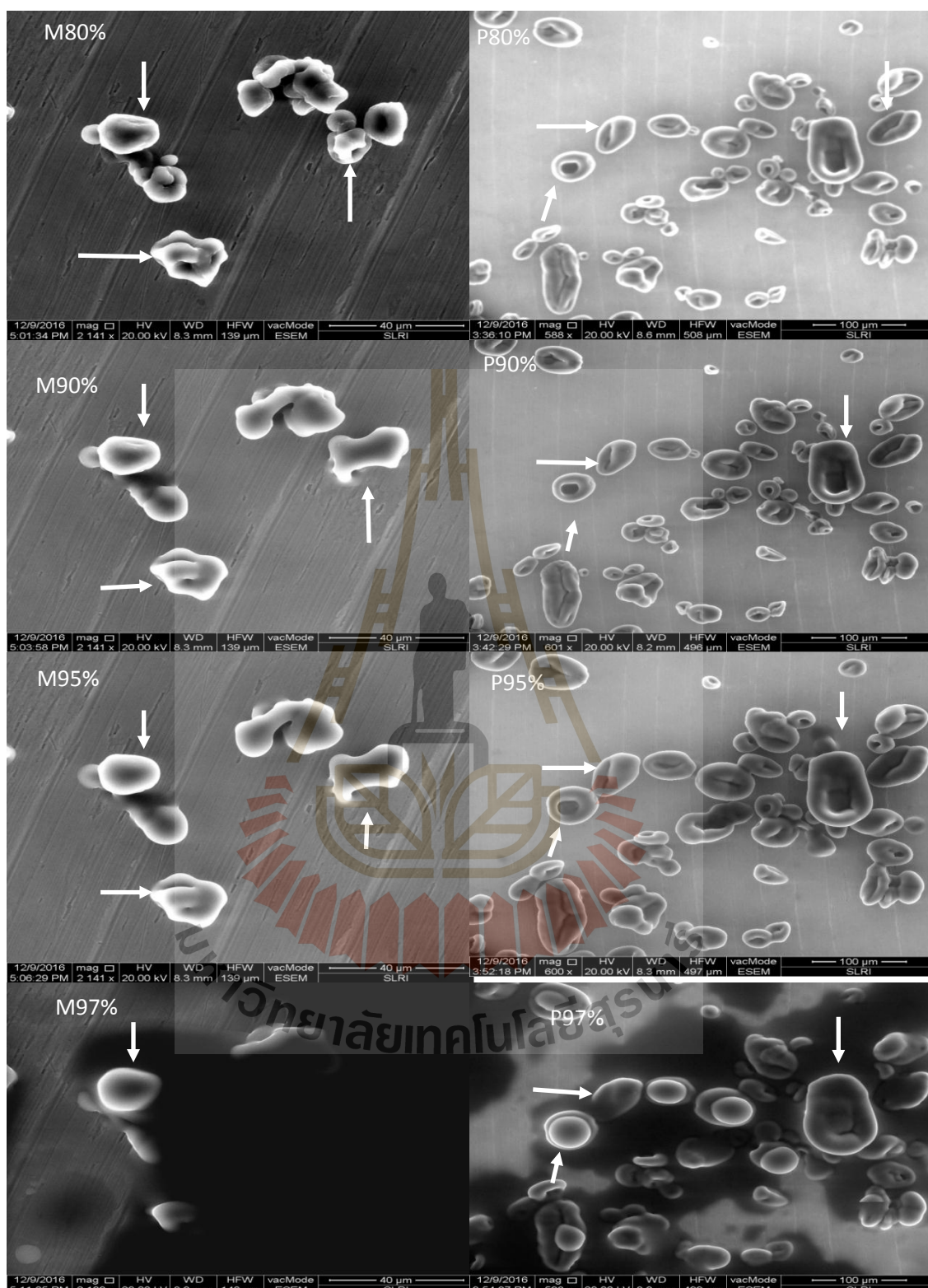
Figure 5.3 Morphology of maize (M) and potato (P) ETS during humidity exposure at

equilibrium relative humidity of 80%, 90%, 95% and 97%.

in which the decrease of potato ETS was more pronounced. The WAC of ETS is closely related to the presence of the V-crystalline structure in the modified starch (Dries, et al., 2014; Hedayati, et al., 2016; Kaur, et al., 2011). These is because the V-crystal is known water-soluble (French, et al., 1977) while the native crystal of starch is insoluble. In addition, the morphological features of ETS granules surface such as wrinkles, fissures and indentations (Majzoobi, et al., 2015; Rajagopalan, et al., 1992b; Zhang, et al., 2012) might increase the ETS granule surface area. This means more hydroxyl groups are exposed to the water, resulting in high WAC since high adsorption commonly requires high surface area (Lowell, Shields, Thomas, and Thommes, 2010).
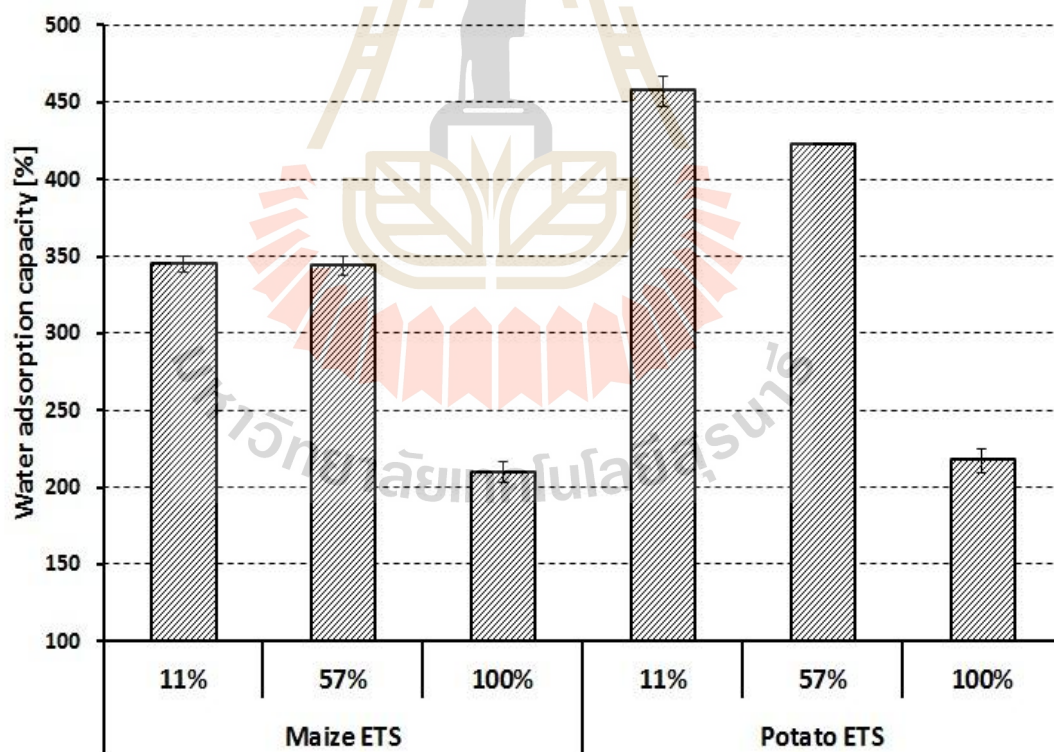
Figure 5.4 Water adsorption capacity of maize (A) and potato (B) ETS after storage at humidity 11% , 57%, and 100%.

5.5 Conclusions

Storage in different humidity level affects the structural, morphological properties and also water adsorption capacity of ETS. At the humidity level of 11%, the existence of V-type crystal structures, and the morphological features of ETS including wrinkles, fissures, and indentations on the ETS granule can be preserved. As the storage humidity increased, the crystallinity contributed by V-crystal structure reduced, the ETS granules surface became smoother and its WAC values decreased. The lower storage humidity is more preferable to store the ETS since it less affects to its properties, mainly to the WAC of ETS.

5.6 Acknowledgments

5.7 References

Buléon, A., Gallant, D.J., Bouchet, B., Mouille, G., D'Hulst, C., Kossmann, J., and Ball, S. (1997). Starches from A to C: Chlamydomonas reinhardtii as a model microbial system to investigate the biosynthesis of the plant amylopectin crystal. **Plant Physiology** 115: 949-957.

Buleon, A., Le Bail, P., Colonna, P., and Bizot, H. (1998). Phase and polymorphic transitions of starches at low and intermediate water contents. In D.S. Reid (Ed.), The Properties of Water in Foods ISOPOW 6 (pp. 160-178). Boston, MA: **Springer US**.

Chen, J., and Jane, J. (1994a). Preparation of granular cold-water-soluble starches by alcoholic-alkaline treatment. **Cereal chemistry** 7(6): 618-622.

Chen, J., and Jane, J. (1994b). Properties of granular cold-water-soluble starches prepared by alcoholic-alkaline treatments. **Cereal chemistry** 71(6): 623-626.

Dries, D.M., Gomand, S.V., Goderis, B., and Delcour, J.A. (2014). Structural and thermal transitions during the conversion from native to granular cold-water swelling maize starch. **Carbohydrate Polymers** 114: 196-205.

Dries, D.M., Gomand, S.V., Pycarelle, S.C., Smet, M., Goderis, B., and Delcour, J.A. (2017). Development of an infusion method for encapsulating ascorbyl palmitate in V-type granular cold-water swelling starch. **Carbohydrate Polymers** 165(Supplement C): 229-237.

Eastman, J.E., and Moore, C.O. (1984). Cold soluble water granular starch for gelled food compositions. **USPTO # 4.465.702**

French, A.D., and Murphy, V.G. (1977). Computer modeling in the study of starch. **Cereal Food World** 22(2): 61-70.

Hedayati, S., Shahidi, F., Koocheki, A., Farahnaky, A., and Majzoobi, M. (2016). Physical properties of pregelatinized and granular cold water swelling maize starches at different pH values. **International Journal of Biological Macromolecules** 91: 730-735.

Jane, J., Craig, S.A.S., Seib, P.A., and Hoseney, R.C. (1986a). Characterization of granular cold water-soluble starch. **Starch - Stärke** 38: 258-263.

Jane, J., Craig, S.A.S., Seib, P.A., and Hoseney, R.C. (1986b). A granular cold water-soluble starch gives a V-type X-ray diffraction pattern. **Carbohydrate Research** 150(1): c5-c6.

Jane, J., and Seib, P.A. (1991). Preparation of granular cold water swelling/soluble starches by alcoholic-alkali treatments. **USPTO # 5.057.157**

Jivan, M.J., Yarmand, M., and Madadlou, A. (2014). Preparation of cold water-soluble potato starch and its characterization. **Journal Food Science Technology** 51(3): 601-605.

Kaur, B., Fazilah, A., and Karim, A.A. (2011). Alcoholic-alkaline treatment of sago starch and its effect on physicochemical properties. **Food and Bioproducts Processing** 89(4): 463-471.

Le Bail, P., Bizot, H., Pontoire, B., and Buleon, A. (1995). Polymorphic Transitions of Amylose-Ethanol Crystalline Complexes Induced by Moisture Exchanges. **Starch - Stärke** 47(6): 229-232.

Lowell, S., Shields, J.E., Thomas, M.A., and Thommes, M. (2010). Characterization of porous solids and powders: surface area, pore size and density: **Kluwer Academic Publishers, Springer**.

Majzoobi, M., Kaveh, Z., Blanchard, C.L., and Farahnaky, A. (2015). Physical properties of pregelatinized and granular cold water swelling maize starches in presence of acetic acid. **Food Hydrocolloids** 51: 375-382.

Meng, Y., and Rao, M.A. (2005). Rheological and structural properties of cold-water-swelling and heated cross-linked waxy maize starch dispersions prepared in apple juice and water. **Carbohydrate Polymers** 60(3): 291-300.

Rajagopalan, S., and Seib, P.A. (1991). Process for the preparation of granular cold water-soluble starch. **USPTO # 5.037.929**

Rajagopalan, S., and Seib, P.A. (1992a). Granular cold-water-soluble starches prepared at atmospheric pressure. **Journal of Cereal Science** 16(1): 13-28.

Rajagopalan, S., and Seib, P.A. (1992b). Properties of granular cold-water-soluble starches prepared at atmospheric pressure. **Journal of Cereal Science** 16(1): 29-40.

Singh, J., and Singh, N. (2003). Studies on the morphological and rheological properties of granular cold water soluble corn and potato starches. **Food Hydrocolloids** 17(1): 63-72.

Soontaranon, S., and Rugmai, S. (2012). Small Angle X-ray Scattering at Siam Photon Laboratory. **Chinese Journal of Physics** 50(2): 204-210.

Wang, H., Lv, J., Jiang, S., Niu, B., Pang, M., and Jiang, S. (2016). Preparation and characterization of porous corn starch and its adsorption toward grape seed proanthocyanidins. **Starch - Stärke** 68(11-12): 1254-1263.

Whittam, M.A., Orford, P.D., Ring, S.G., Clark, S.A., Parker, M.L., Cairns, P., and Miles, M.J. (1989). Aqueous dissolution of crystalline and amorphous amylose alcohol complexes. **International Journal of Biological Macromolecules** 11(6): 339-344.

Zhang, B., Dhital, S., Haque, E., and Gidley, M.J. (2012). Preparation and characterization of gelatinized granular starches from aqueous ethanol treatments. **Carbohydrate Polymers** 90(4): 1587-1594.

CHAPTER VI

ALTERATIONS ON THE STRUCTURAL AND MORPHOLOGICAL PROPERTIES OF ETHANOL-TREATED STARCH BEFORE AND AFTER HYDRATION

6.1   Abstract

Ethanol-treated starch (ETS) swells immediately upon contact with water. The alterations on the structural and morphological properties of ETS prepared from maize and potato starches at three temperatures (80, 90 and 100°C) before and after hydration were investigated. The results showed that upon hydration the V-crystal structure of ETS was destroyed resulting amorphous structure. At the lamellae level, hydrated ETS formed a sheet-like structure. No granular form was observed after ETS from 90 and 100°C were hydrated.

Keywords: ethanol-treated starch, crystalline and lamellae structure, morphology, hydration.

6.2   Introduction

Cold water swelling starch (CWSS) has been known for more than a decade for its capability to easily swell in cold water. Taking advantages of this property, this modified starch has been used for the ingredient of many ready to consume products such as instant porridges, pie fillings, jellies, demouldable desserts and puddings

(Eastman and Moore, 1984). Moreover, this starch gives superior texture and appearance properties on the products compared to the pre-gelatinized starch (Light, 1990).

One method to prepare CWSS is heating starch with the presence of ethanol; therefore, the CWSS prepared by this method is often called as ethanol-treated starch (ETS). Moreover, this method can also be considered as the green process since it only requires ethanol as the only reagent which is reusable. The ETS method is also considered the simplest one compared to the other CWSS preparation methods because it doesn't need additional step to remove the ethanol residue since it can be removed during drying the product (Dries, Gomand, Goderis, and Delcour, 2014).

The most important property of ETS is its capability for adsorbing water at low temperature (Chen and Jane, 1994a; Dries, et al., 2014; Jane, Craig, Seib, and Hoseney, 1986a, 1986b; Jane and Seib, 1991; Rajagopalan and Seib, 1991, 1992a, 1992b; Singh and Singh, 2003). Majzoobi, Kaveh, Blanchard, and Farahnaky (2015) reported that ETS can adsorb water up to 12 times more than its weight. It is believed that this capability is because it contains the V-crystalline structure. During the conversion process, the native crystal of starch is destroyed and the V-crystalline is formed (Chen and Jane, 1994b; Hedayati, Shahidi, Koocheki, Farahnaky, and Majzoobi, 2016; Jivan, Yarmand, and Madadlou, 2014; Kaur, Fazilah, and Karim, 2011; Majzoobi, et al., 2015; Meng and Rao, 2005; Rajagopalan, et al., 1992b; Zhang, Dhital, Haque, and Gidley, 2012).

Jane, et al. (1986a) reported that the V-crystal pattern was lost when CWSS from corn starch was exposed with saturated air for 13 days, but, the A-type pattern reappeared and the CWSS became cold water-insoluble. Even though CWSS is well-

known for its capability to immediately adsorb cold water. However, the investigation of structural and morphological properties of CWSS after contacting with water has not, yet, been fully conducted. Thus the present study is to fulfill this gap by investigating the alterations on the structural and morphological properties of ETS before and after hydration.

6.3   Materials and method

6.3.1   Materials

Normal maize and potato starches were supplied by the National Starch and Chemicals Ltd, Thailand. Analytical grade ethanol reagent was purchased from Carlo Erba, France.

6.3.2   ETS preparation

The ETS was prepared according to the method of Eastman, et al. (1984) and Dries, et al. (2014) with slight modifications. One portion of starch powder from two different sources (maize (M) and potato (P)) was weighted, poured into the pressure leak proof bottle (Schott bottle) and dispersed with 9 portions of ethanol (50 %v/v). The samples were then heated in a water bath for 30 min in three different temperatures (80, 90 or 100°C). After heating, the samples were then cooled for about 2 hours at room temperature. The sediments were separated from the solvent by filtration and then washed with absolute ethanol and filtered, respectively, at least three times to remove the excess of water. Finally, the wet powder was dried using a vacuum oven at 55°C for 12 hours. Samples were ground and sieved with 150 μm mesh sieve. Samples were kept in a silica gel contained box and stored at ambient temperature prior to analysis. All treatments were carried out at least in duplicate.

6.3.3   Wide and small angle X-ray scattering (WAXS and SAXS) analysis

For WAXS analysis, the hydrated sample was prepared by hydrating the dry ETS sample with water in excess. Then, the wet sample was freeze-dried using a freeze dryer (Lyovac GT2, GEA Lyophil GmbH, Hürth, Germany). The moisture content of all samples for WAXS analysis was equilibrated in a closed chamber filled with saturated LiCl solution for 7 days.

Two types of samples were prepared for SAXS analysis. The hydrated samples were prepared by hydrating the sample with an excess of water (50% weight fraction of dry matter) to form a starch slurry. The un-hydrated samples were stored in a desiccator containing silica gel prior to SAXS analysis.

The WAXS and SAXS analysis were performed at the beamline of 1.3 WAXS station, Synchrotron Light Research Institute (SLRI), Nakhon Ratchasima, Thailand. The beamline was set according to Soontaranon and Rugmai (2012) with some modifications. The sample to detector distance for WAXS and SAXS experiments were set to be 188.897 mm by 4-bromo benzoic acid standard, and 1705.9 mm by silver behenate ($AgC_{22}H_{43}O_2$) standard respectively. The X-ray energy was 9 keV. The WAXS and SAXS data were collected from 60 seconds of X-ray exposure time. The WAXS data was presented as an x-y plot of scattering intensity against scattering angle (2θ). The WAXS data was reported from the range at 2θ of 5 to 27°. The SAXS data were presented as a one-dimensional curve of intensity, $I(q) = F(q)$ where q is scattering vector and $I(q)$ is collected from the scattering vector range between 0.3 and 1.5 nm^{-1}.

6.3.4 Morphological properties

The morphological properties of samples before and after hydration were observed by Field Emission-Scanning Electron Microscope (Auriga FEG SEM, Carl Zeiss, Germany). Prior to the analysis, the samples were dehumidified with vacuum oven at 70°C for about 12 hrs. The dried sample was mounted on a metal stub with double-sided adhesive tape, sprayed with nitrogen gas to remove the excess sample, and then it was coated with a thin film of gold and examined at 5 kV of accelerating voltage.

6.4   Results and discussion

6.4.1   Effect of hydration on the crystal structure of ETS

The WAXS patterns of native maize and potato starches and their corresponding ETS are shown in Figure 6.1. There were very slight distortions on the WAXS patterns of native maize and potato starches before and after hydration which may be caused by freeze-drying during sample preparation. However, all identity peaks of native maize starch structure which is A-type crystalline were observed at 2θ of 9.9°, 11.2°, 15°, 17°, 18.1° and 23.3° (Buléon, Gallant, Bouchet, Mouille, D'Hulst, Kossmann, and Ball, 1997). Meanwhile, the identity peaks of native potato starch structure which is B-type crystalline were exhibited at 2θ of 6.6°, 15°, 17°, 22° and 24° (Buléon, et al., 1997).
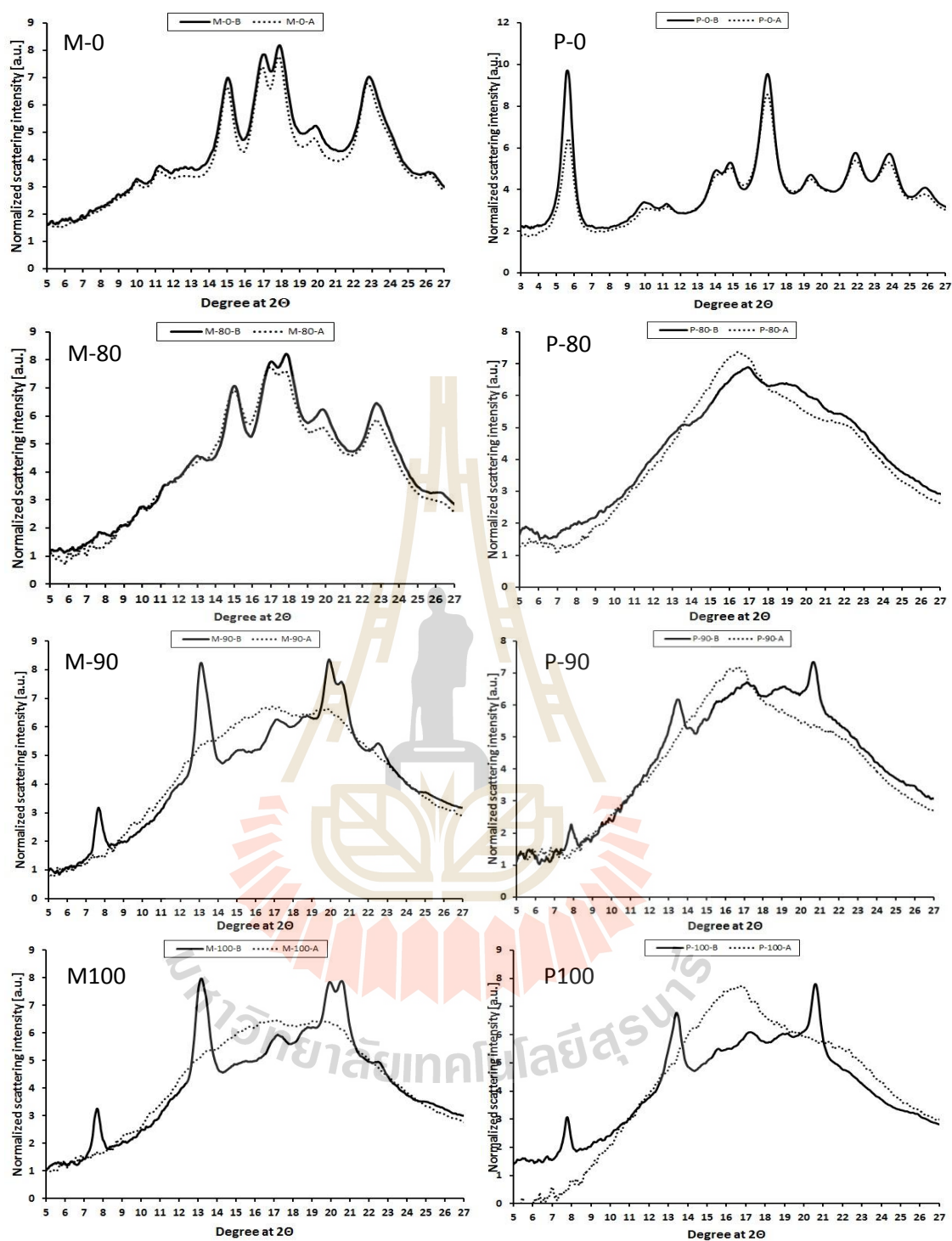
Figure 6.1 Wide angle X-ray scattering patterns of native maize (M-0) and potato (P-0) starches, and their corresponding ETS from different conversion temperature ((M/P-80) 80, (M/P-90) 90, (M/P-100) 100 °C) before (B) and after (A) water absorption.

The peaks of M-80 were relatively un-changed after hydration (Figure 6.1 M-80). This is because M-80 still holds the crystalline structure of native maize starch. The A-type crystal of native maize starch has a relatively compact structure which un-accessible by water during hydration (Buleon, Le Bail, Colonna, and Bizot, 1998; Le Bail, Bizot, Pontoire, and Buléon, 1995). Results showed that P-80 before hydration was no longer holding its parental crystal structure (Figure 6.1 P-80). The crystal structure of P-80 was destroyed during ETS processing resulting in amorphous structure. After hydration, therefore the amorphous structure of P-80 was relatively un-changed.

Before hydration, all ETS from temperature 90 and 100°C exhibited the V-crystalline structure (Figure 6.1 M-90, M-100, P-90 and P-100) which was identified from peaks at 2θ of 7.5°, 12.9°, and 19.8° (Buleon, et al., 1998; Le Bail, et al., 1995). M-90 and M-100 showed doublet peaks at 2θ of 19.8° and 20.9° which probably were contributed by the mixture of two V-crystalline structures namely Vh and Va respectively (Buleon, et al., 1998). After hydration, all identity peaks of V-crystal disappeared. This is because of the V-crystalline structure of amylose-ethanol complex melted upon contact with water since it is known to be soluble in cold water (French and Murphy, 1977).

6.4.2 Effect of hydration on the lamellae structure of ETS

The SAXS patterns of native maize and potato starches and their corresponding ETS before and after hydration are displayed in Figure 6.2. The hydrated native maize and potato starches exhibited a characteristic peak of SAXS pattern which was seen in reciprocal space, q, of 0.64 and 0.69 nm^{-1} which were correspond to the D_{Bragg} spacing of native maize and potato starches of 9.8 and 9.1

nm, respectively (Donald, Kato, Perry, and Waigh, 2001; Jenkins and Donald, 1995; Pikus, 2005).
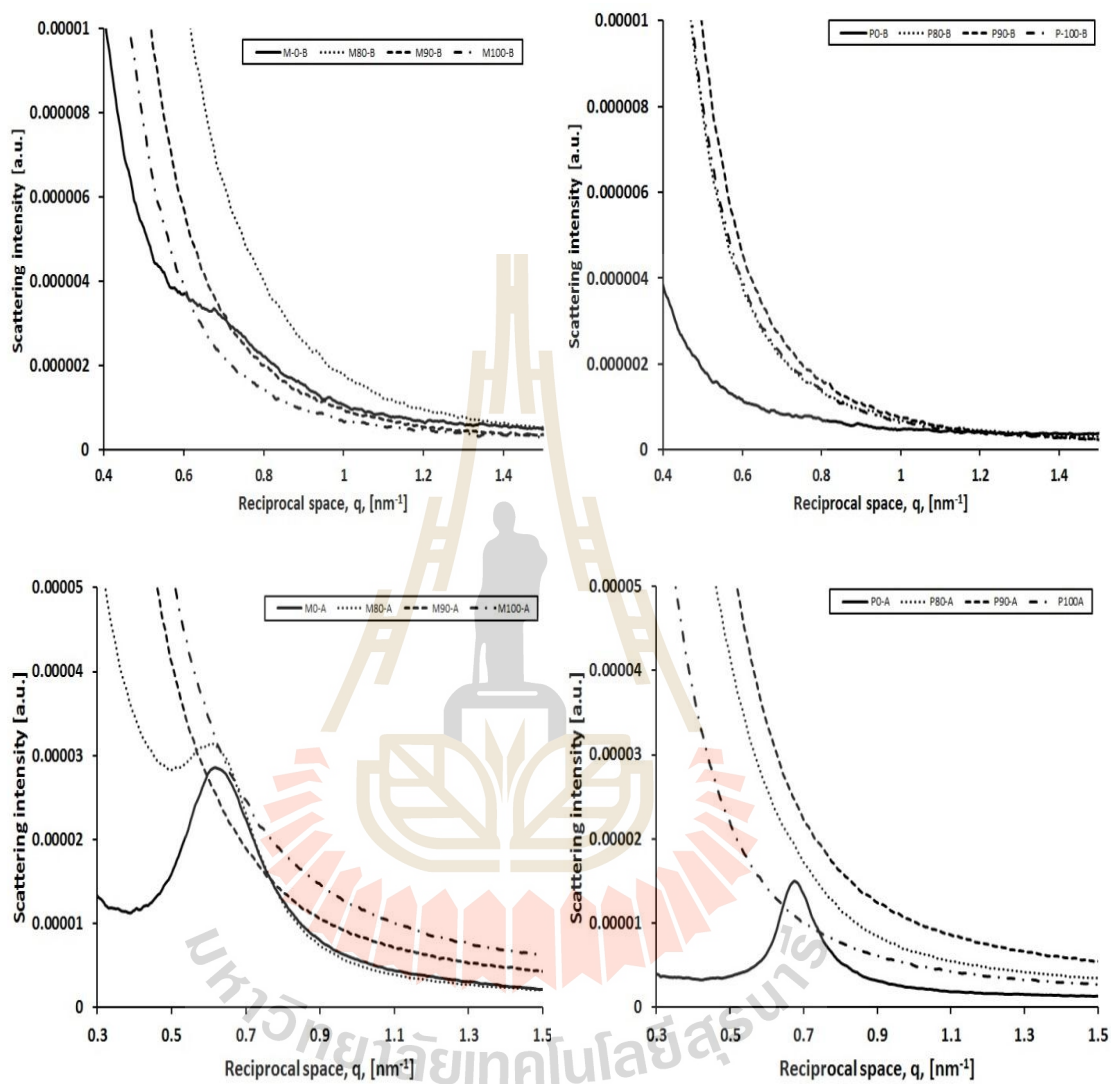

Figure 6.2 Small angle X-ray scattering patterns of native maize (M-0) and potato (P-0) starches, and their corresponding ETS from different conversion temperature ((M/P-80) 80, (M/P-90) 90, (M/P-100) 100°C) before (B) and after (A) hydration.

When starch is hydrated with excess water at ambient temperature, the double helixes of amylopectin of the crystalline lamella or known as mesogens are aligned toward more ordered structure or smectic state (Vermeylen, Derycke, Delcour, Goderis, Reynaers, and Koch, 2006). At this state, the stacked halos structure of alternating amorphous and crystalline lamellae of native starch was observed as a characteristic peak of SAXS pattern. Meanwhile, for non-hydrated starch, its lamellar organization is distorted; Therefore it was seen as a bump on the SAXS pattern of dry native maize starch (Figure 6.2 M-0-B), while no peak was detected on that of dry native potato starch (Figure 6.2 P-0-B).

All SAXS patterns of ETS before hydration did not exhibit peak. It is believed that for dry starches, the scattering may be detected as a surface fractal because the averaged density of the starch granules and the air will be more significant for scattering intensity than the density fluctuation in the starch granules (Suzuki, Chiba, and Yarno, 1997). Table 6.1 indicated that the slopes of the double log plot of SAXS of ETS before hydration showed values closed to -4, while their natives were about -2. According to the fractal theory, these values can be interpreted that the surface of ETS was rougher than their native (Beaucage, 2012; Suzuki, et al., 1997).

No peak was observed on the SAXS pattern of all hydrated ETS (Figure 6.2). The slopes of double log plot of SAXS of hydrated ETS showed values close to -2 (Table 6.1). When starch is hydrated, water fills the gaps between the starch granules and it is absorbed by the amorphous regions inside the starch granules. Consequently, the density difference between the amorphous and crystalline regions inside the starch granules becomes prominent rather than at the surface of the granules. Then, the scattering intensity is believed to arise from the mass inside the starch granules rather

than from the surface of starch granules. According to the fractal theory, SAXS pattern transformation from peak pattern to linear pattern with slope of double log plot of SAXS closed to -2 is an indication that there is transformation from three dimensional structure of crystalline lamellae to become surface-like or sheet-like arrangement (Beaucage, 2012; Suzuki, et al., 1997).

Table 6.1 Slope of double log plot of SAXS data of native maize (M-0) and potato (P-0) starches, and their corresponding ETS from different conversion temperature ((M/P-80) 80, (M/P-90) 90, (M/P-100) 100°C) before (B) and after (A) hydration at q range of 0.4-1.0 nm^{-1}.

Sample	B		A	
	Slope	R^2	Slope	R^2
M-0	-2.2	0.98	-1.0	0.28
M-80	-3.7	1.00	-2.2	0.80
M-90	-3.7	1.00	-2.3	1.00
M-100	-3.5	1.00	-2.2	1.00
P-0	-2.1	0.98	-0.2	0.01
P-80	-3.6	1.00	-2.7	1.00
P-90	-3.8	1.00	-2.5	1.00
P-100	-3.7	1.00	-2.2	1.00

6.4.3 Morphological properties of ETS before and after hydration

The morphological properties of native maize, and potato starches and their corresponding ETS are presented in Figure 6.3. There were no morphological differences
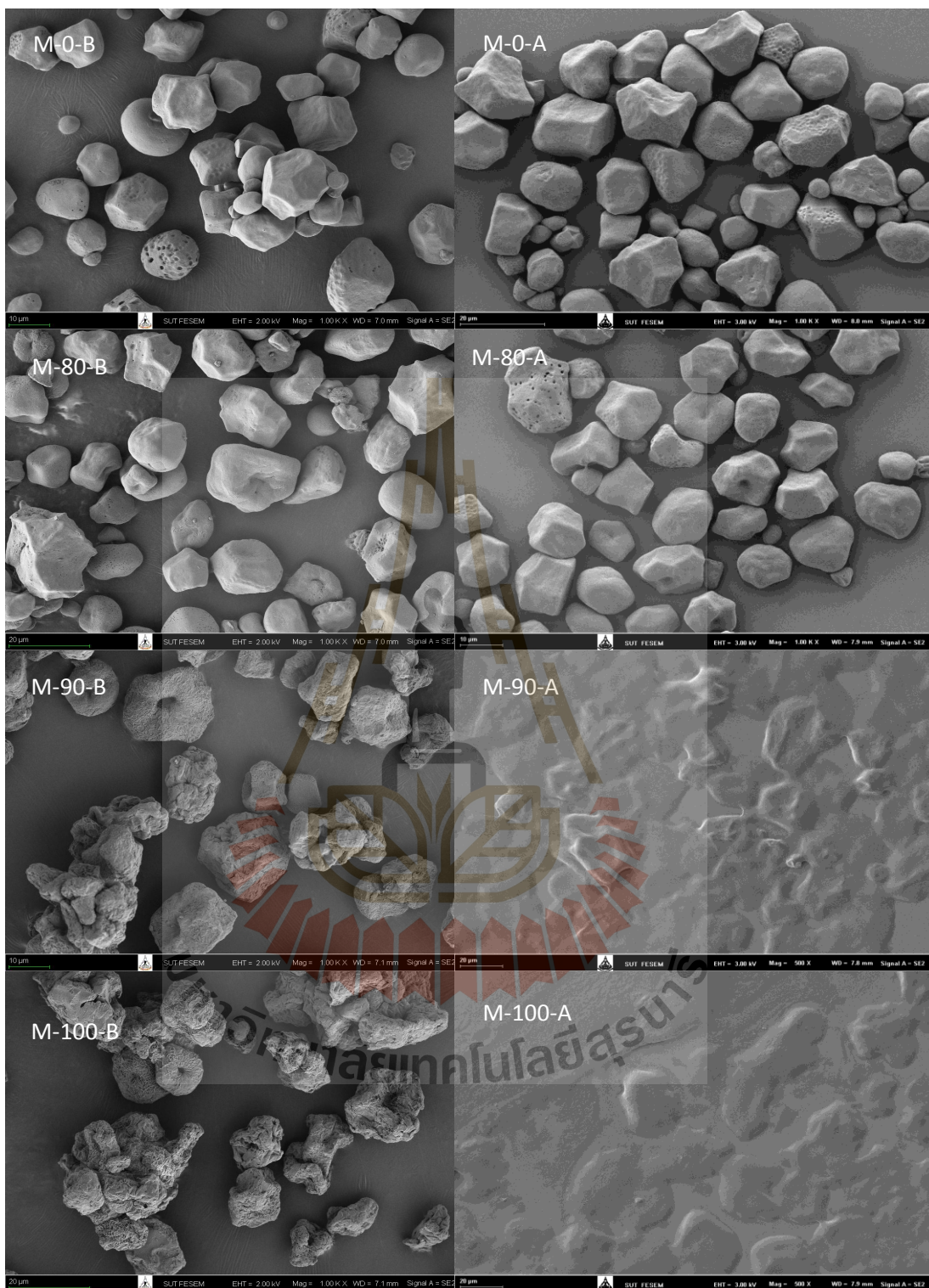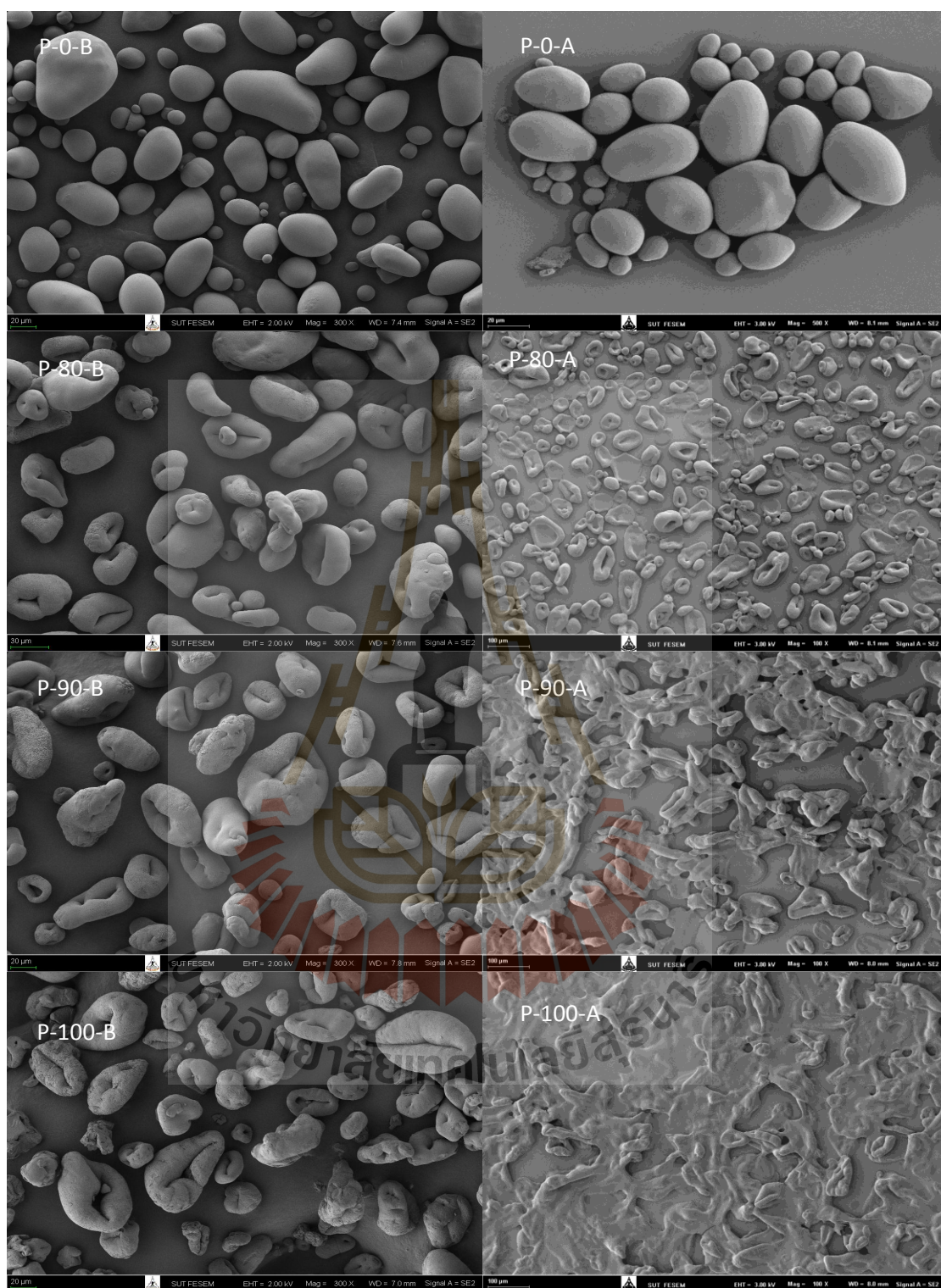
Figure 6.3

Figure 6.3 Morphology of native maize (M-0) and potato (P-0) starches, and their
corresponding ETS from different conversion temperature ((M/P-80) 80,
(M/P-90) 90, (M/P-100) 100°C) before (B) and after (A) hydration.

between the granules of native maize starch before and after hydration, and so do the granules of native potato starch. The native maize starch granules exhibited polyhydric to round shapes with some granules showing pores on their surface while the native potato starch granules showed oval shapes with a smooth surface (Chen, Yu, Chen, and Li, 2006; Jivan, et al., 2014; Juszczak, Fortuna, and Krok, 2003).

Overall, granules appearance of M-80 before hydration was looked similar to its native with some granules were indented (Figure 6.3 M-0 and M-80), meanwhile most P80 granules exhibited indentation and having donut shapes-like with wrinkles on their surface (Figure 6.3 P-80-B). The un-hydrated ETS granules from temperature of 90 and 100 °C mostly showed donut shapes with wrinkles on their surface and also some of them melted to each other. After hydration, the M-80 granules were still in granular form while those of P-80 mostly collapsed.

After hydration, all granules of M-90 and M-100 totally melted (Figure 6.3 M-90 and M-100). The P-90 and P-100 granules melted but the periphery between their granules still can be observed (Figure 6.3 P-90 and P-100). This indicated that granules of ETS from maize starch were more susceptible to hydration than that of ETS from potato starch. Potato starch contains amylose with a higher DP compared to maize starch in which the DP of potato amylose ranges from 840 to 22,000 glucose units, while that of maize starch is approximately 400–15,000 glucose units (McDonagh, 2012). Amylose behaves similarly to a rope that bonds starch components tightly (Waduge, Hoover, Vasanthan, Gao, and Li, 2006). Therefore, starch with longer amylose has higher resistance toward physical or thermal treatments. The periphery of potato starch also contains a high amount of cocrystallized amylose with amylopectin clusters, which protect its granule periphery

from disruptions (Jenkins, et al., 1995; Kuakpetoon and Wang, 2007; Saibene and Seetharaman, 2010).

6.5 Conclusions

After hydration, the V-crystalline structure of ETS disappeared due to crystal melting. Conversion from native starch to ETS brought drastic transformation at lamellae level in that three-dimensional structures of crystalline lamellae were converted to sheet-like structures. At the granular level, the morphology of ETS from potato starch showed higher resistance toward granule disruption during hydration compared to that of ETS from maize starch.

6.6 Acknowledgments

6.7 References

Beaucage, G. (2012). Combined Small-Angle Scattering for Characterization of Hierarchically Structured Polymer Systems over Nano-to-Micron Meter: Part II Theory. In K. Matyjaszewski and M. Möller (Eds.), Polymer Science: A Comprehensive Reference vol. 2 (pp. 399-409). Amsterdam: **Elsevier BV.**

Buléon, A., Gallant, D.J., Bouchet, B., Mouille, G., D'Hulst, C., Kossmann, J., and Ball, S. (1997). Starches from A to C: Chlamydomonas reinhardtii as a model microbial system to investigate the biosynthesis of the plant amylopectin crystal. **Plant Physiology** 115: 949-957.

Buleon, A., Le Bail, P., Colonna, P., and Bizot, H. (1998). Phase and polymorphic transitions of starches at low and intermediate water contents. In D.S. Reid (Ed.), The Properties of Water in Foods ISOPOW 6 (pp. 160-178). Boston, MA: **Springer US**.

Chen, J., and Jane, J. (1994a). Preparation of granular cold-water-soluble starches by alcoholic-alkaline treatment. **Cereal chemistry** 7(6): 618-622.

Chen, J., and Jane, J. (1994b). Properties of granular cold-water-soluble starches prepared by alcoholic-alkaline treatments. **Cereal chemistry** 71(6): 623-626.

Chen, P., Yu, L., Chen, L., and Li, X. (2006). Morphology and Microstructure of Maize Starches with Different Amylose/Amylopectin Content. **Starch - Stärke** 58(12): 611-615.

Donald, A.M., Kato, K.L., Perry, P.A., and Waigh, T.A. (2001). Scattering Studies of the Internal Structure of Starch Granules. **Starch - Stärke** 53(10): 504-512.

Dries, D.M., Gomand, S.V., Goderis, B., and Delcour, J.A. (2014). Structural and thermal transitions during the conversion from native to granular cold-water swelling maize starch. **Carbohydrate Polymers** 114: 196-205.

Eastman, J.E., and Moore, C.O. (1984). Cold soluble water granular starch for gelled food compositions. **USPTO # 4.465.702**

French, A.D., and Murphy, V.G. (1977). Computer modeling in the study of starch. **Cereal Food World** 22(2): 61-70.

Hedayati, S., Shahidi, F., Koocheki, A., Farahnaky, A., and Majzoobi, M. (2016). Physical properties of pregelatinized and granular cold water swelling maize starches at different pH values. **International Journal of Biological Macromolecules** 91: 730-735.

Jane, J., Craig, S.A.S., Seib, P.A., and Hoseney, R.C. (1986a). Characterization of granular cold water-soluble starch. **Starch - Stärke** 38: 258-263.

Jane, J., Craig, S.A.S., Seib, P.A., and Hoseney, R.C. (1986b). A granular cold water-soluble starch gives a V-type X-ray diffraction pattern. **Carbohydrate Research** 150(1): c5-c6.

Jane, J., and Seib, P.A. (1991). Preparation of granular cold water swelling/soluble starches by alcoholic-alkali treatments. **USPTO # 5.057.157**

Jenkins, P.J., and Donald, A.M. (1995). The influence of amylose on starch granule structure. **International Journal of Biological Macromolecules** 17: 315-321.

Jivan, M.J., Yarmand, M., and Madadlou, A. (2014). Preparation of cold water-soluble potato starch and its characterization. **Journal Food Science Technology** 51(3): 601-605.

Juszczak, L., Fortuna, T., and Krok, F. (2003). Non-contact atomic force microscopy of starch granules surface. Part I. Potato and tapioca starches. **Starch - Stärke** 55: 1-7.

Kaur, B., Fazilah, A., and Karim, A.A. (2011). Alcoholic-alkaline treatment of sago starch and its effect on physicochemical properties. **Food and Bioproducts Processing** 89(4): 463-471.

Kuakpetoon, D., and Wang, Y.-J. (2007). Internal structure and physicochemical properties of corn starches as revealed by chemical surface gelatinization. **Carbohydrate Research** 342(15): 2253-2263.

Le Bail, P., Bizot, H., Pontoire, B., and Buléon, A. (1995). Polymorphic Transitions of Amylose-Ethanol Crystalline Complexes Induced by Moisture Exchanges. **Starch - Stärke** 47(6): 229-232.

Light, J.M. (1990). Modified food starches: Why, where, and how. **Cereal Foods World** 35: 1081-1084.

Majzoobi, M., Kaveh, Z., Blanchard, C.L., and Farahnaky, A. (2015). Physical properties of pregelatinized and granular cold water swelling maize starches in presence of acetic acid. **Food Hydrocolloids** 51: 375-382.

McDonagh, P. (2012). 7 - Native, modified and clean label starches in foods and beverages. In Natural Food Additives, Ingredients and Flavourings (pp. 162-174): **Woodhead Publishing**.

Meng, Y., and Rao, M.A. (2005). Rheological and structural properties of cold-water-swelling and heated cross-linked waxy maize starch dispersions prepared in apple juice and water. **Carbohydrate Polymers** 60(3): 291-300.

Pikus, S. (2005). Small-angle x-ray scattering (SAXS) studies of the structure of starch and starch products. **Fibres and Textiles in Eastern Europe** 13(5 (53)): 82-86.

Rajagopalan, S., and Seib, P.A. (1991). Process for the preparation of granular cold water-soluble starch. **USPTO # 5.037.929**

Rajagopalan, S., and Seib, P.A. (1992a). Granular cold-water-soluble starches prepared at atmospheric pressure. **Journal of Cereal Science** 16(1): 13-28.

Rajagopalan, S., and Seib, P.A. (1992b). Properties of granular cold-water-soluble starches prepared at atmospheric pressure. **Journal of Cereal Science** 16(1): 29-40.

Saibene, D., and Seetharaman, K. (2010). Amylose involvement in the amylopectin clusters of potato starch granules. **Carbohydrate Polymers** 82(2): 376-383.

Singh, J., and Singh, N. (2003). Studies on the morphological and rheological properties of granular cold water soluble corn and potato starches. **Food Hydrocolloids** 17(1): 63-72.

Soontaranon, S., and Rugmai, S. (2012). Small Angle X-ray Scattering at Siam Photon Laboratory. **Chinese Journal of Physics** 50(2): 204-210.

Suzuki, T., Chiba, A., and Yarno, T. (1997). Interpretation of small angle X-ray scattering from starch on the basis of fractals. **Carbohydrate Polymers** 34(4): 357-363.

Vermeylen, R., Derycke, V., Delcour, J.A., Goderis, B., Reynaers, H., and Koch, M.H.J. (2006). Structural Transformations during Gelatinization of Starches in Limited Water: Combined Wide- and Small-Angle X-ray Scattering Study. **Biomacromolecules** 7(4): 1231-1238.

Waduge, R.N., Hoover, R., Vasanthan, T., Gao, J., and Li, J.H. (2006). Effect of annealing on the structure and physicochemical properties of barley starches of varying amylose contents. **Food Research International** 39: 59-77.

Zhang, B., Dhital, S., Haque, E., and Gidley, M.J. (2012). Preparation and characterization of gelatinized granular starches from aqueous ethanol treatments. **Carbohydrate Polymers** 90(4): 1587-1594.

CHAPTER VII

RELEASE RELATED PROPERTIES OF TABLET FROM ETHANOL-TREATED STARCH FOR AN ENCAPSULATION MATRIX OF LAURIC ACID AND ASCORBIC ACID

7.1 Abstract

Ethanol-treated starch (ETS) shows potentiality to be used for an encapsulation matrix. This research was aimed to evaluate the release related properties of lauric acid- and ascorbic acid-ETS tablets. ETS was prepared from cassava starch (C) at three temperatures: 80, 90 and 100°C (C-80, C-90, and C-100). The active compounds were encapsulated into ETS tablets by two methods including dry mixing and ethanol solubilization. Tablet parameters including structural, morphological, mechanical strength, hydration behavior, and release properties were investigated. The structural analysis result indicated no complexation between the active compounds and the ETS components. Morphological data showed that ETS of C-80 exhibited granular form, while that of C-90 and C-100 displayed non-granular structure. Tablet from non-granular ETS exhibited low friability and high crushing strength indexes. Upon soaking, tablets from C-80 dispersed immediately and released the encapsulated compounds rapidly. The results of hydration behavior and

release properties analysis suggested that tablets from non-granular ETS were suitable for sustained release system in which LA and AA were released by different mechanisms.

Keywords: ethanol-treated starch, matrix, encapsulation, lauric acid, ascorbic acid, mechanical strength, hydration behavior, and release properties.

7.2 Introduction

Research on encapsulation technology and delivery system of food ingredients and nutraceuticals is growing. It covers modification of functional food ingredients, development of innovative coating materials and improvement of encapsulation methods (Shahidi and Han, 1993; Zuidam and Velikov, 2018). Moreover, the selection of optimal encapsulating techniques and encapsulating materials is also one of the greatest challenges in encapsulation technology development.

There are several encapsulation methods that have been implemented in the food industry including spray drying, spray cooling or chilling, solvent evaporation, polymerization, fluidized-bed coating, extrusion, lyophilization, coacervation and liposome entrapment (Zuidam, et al., 2018). The fundamental reason for selecting encapsulation method is the physicochemical properties of the core and coating materials. However, the encapsulation process should also be considered particularly when sensitive ingredients are the encapsulated compounds. Encapsulation methods which involve heating or drying process at high temperature are not suitable for volatile compounds and heat labile ingredients such as flavor agents, vitamins, and antioxidant compounds (Madene, Jacquot, Scher, and Desobry, 2006; Sauvant, Cansell, Hadj Sassi, and Atgié, 2012; Shahidi, et al., 1993).

Starch products have been widely implemented to encapsulate functional foods. Many starch derivatives have been explored for this purpose, for example, starch granule-stabilized pickering emulsion, native starch gel, porous starch granules, starch nanoparticles, substituted starches, cross-linked starch, oxidized and cross-linked starch hydrogel, hydrolyzed starch, and amylose inclusion complexes (Zhu, 2017). For safety concerns, the use of physically and enzymatically-treated starches for encapsulation agent is highly recommended over the chemically-modified starches (Chen and Jane, 1994).

Compared to the other physically-treated starches, cold water swelling starch (CWSS) offers many advantages. It is cold water soluble and retains water as high as 12 times more than its weight (Majzoobi, Kaveh, Blanchard, and Farahnaky, 2015). Heating starch with ethanol or termed ethanol-treated starch (ETS) can be considered as the simplest method to prepare CWSS. This is because the process only requires ethanol as food grade reactant which can be removed from the final product by drying (Dries, Gomand, Goderis, and Delcour, 2014).

There are several attempts to encapsulate active ingredients by CWSS. The encapsulation product properties using CWSS as the encapsulating agent are influenced by the encapsulation process (Chen and Jane, 1995; Dries, Gomand, Pycarelle, Smet, Goderis, and Delcour, 2017; Zhang, Dhital, Haque, and Gidley, 2012). Chen, et al. (1995) encapsulated atrazine using water as the solvent and CWSS as the encapsulating matrix. They reported that no complexation between atrazine and starch components; instead, B-type diffraction of retrograded starch was observed. Dries, et al. (2017) encapsulated ascorbyl palmitate using a mixture of water-ethanol as the solubilization media and CWSS as the encapsulating matrix and applied

multiple encapsulation stages. They noticed that some portion of water in aqueous ethanol was required to induce complexation between ascorbyl palmitate and amylose for obtaining V-type crystalline structure. However, the use of multiple encapsulation stages is not practical for industrial implementation.

One form of the most popular presentations of encapsulation products is a tablet. Tablet is used to deliver pharmaceutical agents for medication purposes or nutraceutical ingredients for health-enhancing goals (Patel, Panchal, Patel, Brahmbhatt, and Suthar, 2011). Besides the active ingredients, the tablet may also contain suitable excipients such as diluents agents, binders or granulating agents, glidants (flow aids), lubricants, dis-integrants, sweeteners or flavor enhancer and pigments (Manish and Abhay, 2012). Modified starch has been implemented for tablet excipient for several decades (Hatairat, Wolfgang, Sujin, and Saiyavit, 2003; Lawal, Odeniyi, and Itiola, 2015; Odeniyi and Ayorinde, 2014; Pachuau, Dutta, Devi, Deka, and Hauzel, 2018). However, evaluation toward the release related properties of ETS tablet has never been conducted.

This study was mainly designed to evaluate the release related properties of tablet from ETS for encapsulating matrix of lauric acid and ascorbic acid. The active ingredients were encapsulated into ETS tablets by two methods, including dry mixing and ethanol solubilization. The structural, morphological, physical, mechanical strength, hydration behavior and release properties of the lauric acid- and ascorbic acid-ETS tablets were investigated.

7.3 Materials and method

7.3.1 Materials

Cassava starch was supplied by Sanguan Wongse Industries Co. Ltd. (Nakhon Ratchasima, Thailand). L (+) ascorbic acid and ethanol were of analytical grade and purchased from Carlo Erba Ltd. (Val de Reuil, France). Lauric acid with a purity of 99% was obtained from Acros Organics (New Jersey, USA).

7.3.2 Ethanol-treated starch preparation

A method described by Eastman and Moore (1984) and Dries, et al. (2014) was modified to prepare the ETS. Ethanol-treated cassava starch from the conversion temperatures of 80, 90 and 10 °C (coded as C-80, C-90, and C-100, respectively) was prepared by mixing cassava starch (15 g) with 135 ml of ethanol (50 %v/v). The slurry was heated in a Schott bottle at those temperatures for 30 min and then cooled at room temperature for 3 h. The sediment was filtered and washed with absolute ethanol three times, and finally, it was vacuum dried at 70°C for 24 h. The dried lump was ground by Waring blender™ and sieved (150 μm) (Retsch, Haan, Germany).

7.3.3 Methods to encapsulate the active compounds and tablet preparation

The active ingredients, AA and LA, were encapsulated with ETS by using two different methods. In dry mixing (D) method, 8 g of active ingredient was dry mixed with 42 g of ETS. In ethanol solubilization (S) method, 8 g of active ingredient was dissolved in ethanol (800 ml) in a beaker glass, and then the ETS was added gradually and stirred for 30 min. Then the slurry was air dried using fume hood for 48 h. The dried lump was ground by Waring blender™; then it was sieved with a 150 μm screen (Retsch, Haan, Germany). All treatments were performed in duplicate.

Tablet (0.5 g) was prepared by hydraulic hand press (www.mtixtl.com, MTI Corporation, California, USA). The compression pressure was 271.11 MNm^{-2}, and the duration of compression was 1 min. Tablets were kept in an airtight box containing silica gel prior to analysis.

7.3.4 Crystalline structure

Wide-angle X-ray scattering (WAXS) technique at the beamline of 1.3 WAXS station (Synchrotron Light Research Institute (SLRI), Nakhon Ratchasima, Thailand) was employed to determine the crystal structure of samples. A modified method of Soontaranon and Rugmai (2012) was used to set the beam line in which the sample to detector distance was 188.9 mm, and the X-ray energy was 9 keV. The WAXS spectrum was recorded by MAR-CCD (SX165) detector. Prior to analysis, the sample was kept in a closed chamber filled with saturated LiCl solution for 7 days to equilibrate the moisture content. The WAXS data was presented from the scattering angle at 2θ of 2 to 29°.

7.3.5 Morphological properties

The morphological properties of samples were observed by using Field Emission-Scanning Electron Microscope (Auriga FEG SEM, Carl Zeiss, Germany). The sample was mounted on a stub with double-sided adhesive tape; then it was sprayed with nitrogen gas to remove the excess sample. Prior observation, the sample was coated with a thin film of gold. The sample was examined using an accelerating voltage of 2 kV.

7.3.6 Mechanical strength properties of lauric acid- and ascorbic acid-ETS tablets

The friability index of the tablet was determined according to the method of Lawal, et al. (2015) with some modifications. A friability apparatus (Vankel Friability Tester Model 45-2000, North Carolina, USA) was operated at 25 rounds per min. The tablets were removed from the friabilator, dusted and reweighed. The friability index was calculated according to Equation 1.

$$\text{Friability } [\%] = \frac{\text{Initial weight (g)-Final weight (g)}}{\text{Initial weight (g)}} \text{ x } 100 \tag{1}$$

The crushing strength index of the tablet was determined by a tablet hardness tester (Vankel Model VK200, North Carolina, USA). The load was gradually increased by gently lowering the compression hand until the tablet fractured. The crushing strength value of tablet was recorded as the value of the load on the gauge at the fracture point (Commission, 2010).

7.3.7 Hydration behavior of lauric acid- and ascorbic acid-ETS tablets

Method of Gao and Meury (1996) was modified to observe the hydration behavior of lauric acid- and ascorbic acid-ETS tablets during soaking. The tablet was mounted on the bottom of 250 ml beaker glass using a squared double-sided tape of 2 mm x 2 mm. A bulb of 24 Watt with cool daylight luminance (63 lm/watt) (Phillips Inc., Eindhoven, Netherland) was used as the source of background light. The tablet image before and upon contact with water was captured by a digital camera (Canon PowerShot G11, New York, USA) at a certain capturing interval. The schematic diagram of the experimental set up is displayed in Figure 7.1.
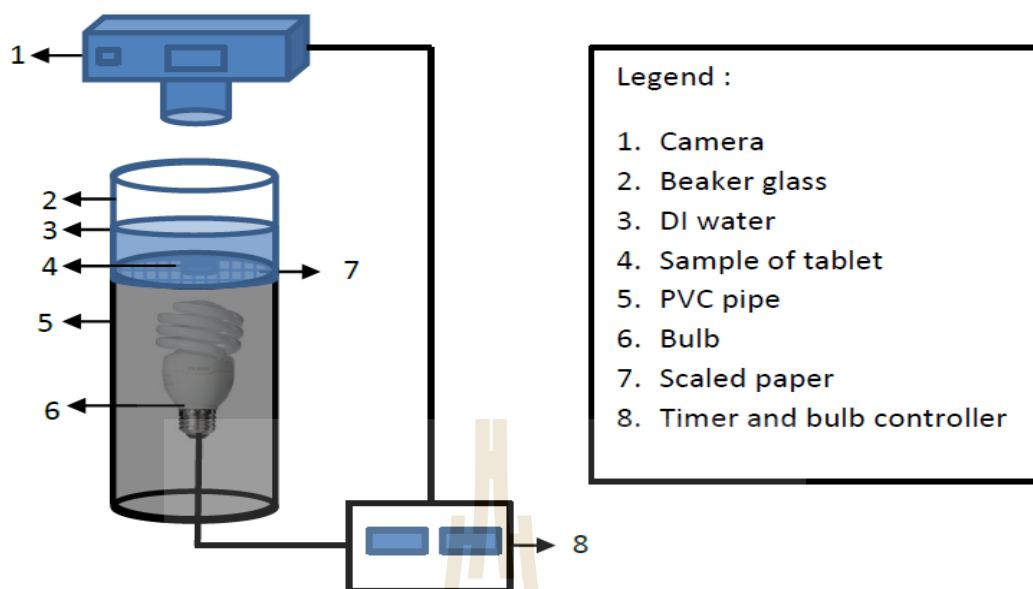
Figure 7.1 The schematic diagram of experimental set up to observe the hydration behavior of lauric acid and ascorbic acid-ETS (ethanol-treated starch) tablets.

The image analysis of tablet was performed by Image-J software following a method of Gao, et al. (1996) with some modifications. The illustration of the tablet image processing is presented in Figure 7.2. First, the area of interest was marked by using a rectangular frame (20.53 mm x 1.4 mm) which was created pass through the center of the image of the tablet. Then, the averaged gray level was obtained over the selected area (Figure 7.2 A). The dimensional scale was calibrated by using a square on the scaled paper in which 1 mm was equal to 41.5 pixels. The un-hydrated core diameter of sample (Figure 7.2 B) was determined by using the grey value of a dry tablet as the standard to level the un-hydrated core (Figure 7.2 C).
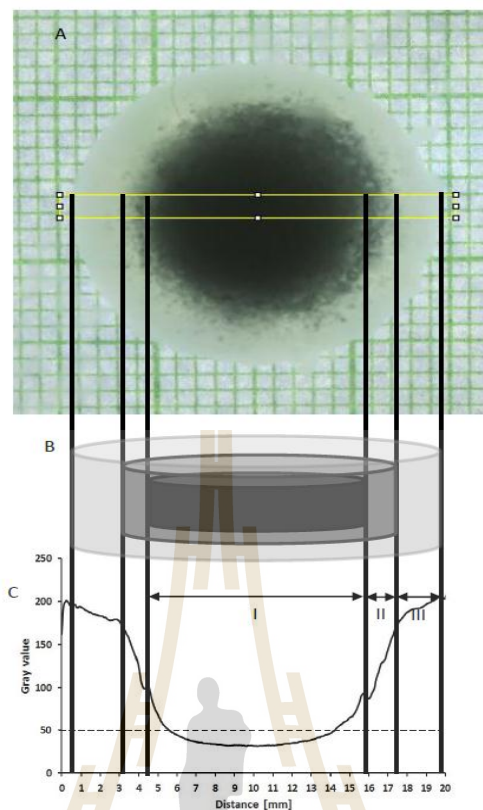
Figure 7.2 (A) optical image of C-100-AA-D tablet observed in situ in the radial direction after hydration for 240 minutes. (B) illustration of tablet swelling correspond to the obtained optical image, (C) gray level of the obtained image by applying a horizontal rectangular measuring frame (20.53 mm x 1.4 mm) through the center of tablet as shown in part A. zone I: Glassy (unhydrated) core, zone II: diffusion zone, zone III: swelling zone.

7.3.8 Release properties of lauric acid- and ascorbic acid-ETS tablets

A tablet was weighed and placed in a perforated tube. The tube was immersed in a 250 ml beaker glass containing deionized water (100 ml) then immediately the immersion time was counted. At a certain time interval, the tube was taken out of the

water, and then the water was stirred by a magnetic stirrer (1000 rpm) for 2 min.

Sample (500 µl) was withdrawn from the water; transferred into a bottle and then it

was diluted with a suitable solvent (1500 µl). The sample was filtered with 0.45 µm

nylon syringe filter and transferred into an amber glass-Agilent GC vial of 2 ml. Then,

it was sealed with SPTA-Agilent GC vial cup. Samples were stored in a refrigerator at

4°C prior to analysis. Methanol and buffer of 3 mM potassium dihydrogen phosphate

in 0.35%v/v ortho-phosphoric acid solution were used as the diluting solvent for LA

and AA, respectively.

The lauric acid release was assayed by a direct injection-gas-chromatography

method of Yang and Choong (2001) with some modifications. Sample (0.1 ml) was

directly injected into gas chromatography (GC Varian CP-3800, FID Detector, DB-

FFAP capillary column: length 30 m, diameter 0.20 mm, and film thickness 0.25µm)

operated with H_2 flow rate of 30 ml/min, air flow rate of 300 ml/min and helium as

the carrier gas at flow rate of 3 ml/min. The temperatures at the detector and injector

ports were 280 and 240°C, respectively. The oven temperature was programmed at 75

°C for 1 min, raised to 180°C at 6 °C/min, then increased to 230°C at 10 °C/min, and

finally held at 230°C for 5 min. Lauric acid solutions from concentration 2.5 to 500

ppm were prepared as the external standard. The lauric acid was detected at a

retention time of 24.22 min.

Ascorbic acid was determined by high-performance liquid chromatography

following a method of Lakshanasomya (1998) with slight modifications. Sample (20

µl) was injected into HPLC (HPLC Agilent, Model 1220 Infinity LC with Agilent

column, Model Zorbax Eclipse® XDB-C18: length 150 mm, diameter 4.6 mm and

film thickness 5 µm). The mobile phase was deionized water; it flows at rate 0.5

ml/min. Ascorbic acid was detected by a UV detector at 248 nm. Ascorbic acid solutions from concentration 2.5 to 500 ppm were prepared as the external standard. Ascorbic acid was detected at a retention time of 4.7 min. All analysis was performed in duplicate.

7.3.9   Statistical analysis

The experiments were carried out in duplicate. Analysis of variance (ANOVA) was carried out using SPSS software version 17.0. The mean of treatments was compared using Duncan's post hoc test.

7.4   Results and discussion

7.4.1   The crystalline structure

The WAXS patterns of lauric acid- and ascorbic acid-ETS tablets and their corresponding ETS are displayed in Figure 7.3. The characteristic peaks of A-type crystalline structure of native cassava starch at 2θ of 15°, 17°, 18.1° and 22.5° (Buléon, Gallant, Bouchet, Mouille, D'Hulst, Kossmann, and Ball, 1997) was observed on the diffractogram of C-80 (Figure 7.3A). For C-90 and C-100, the identity peaks of V-type crystalline structure appeared at 2θ of 7.8°, 13.6° and 20.9° (Buleon, Le Bail, Colonna, and Bizot, 1998).

The encapsulation methods influenced the diffractogram pattern of lauric acid-ETS tablet. For samples of lauric acid-ETS tablets prepared by dry mixing method, the identity peaks of lauric acid crystal appeared together with the peaks of native and V-type crystalline structures. The major peaks of LA crystal were observed at 2θ of 3.3°, 19.9°, 21.3°, and 23.6° and some minor peaks at 2θ of 6.5°, 9.7°, 18.3°, 18.9°,
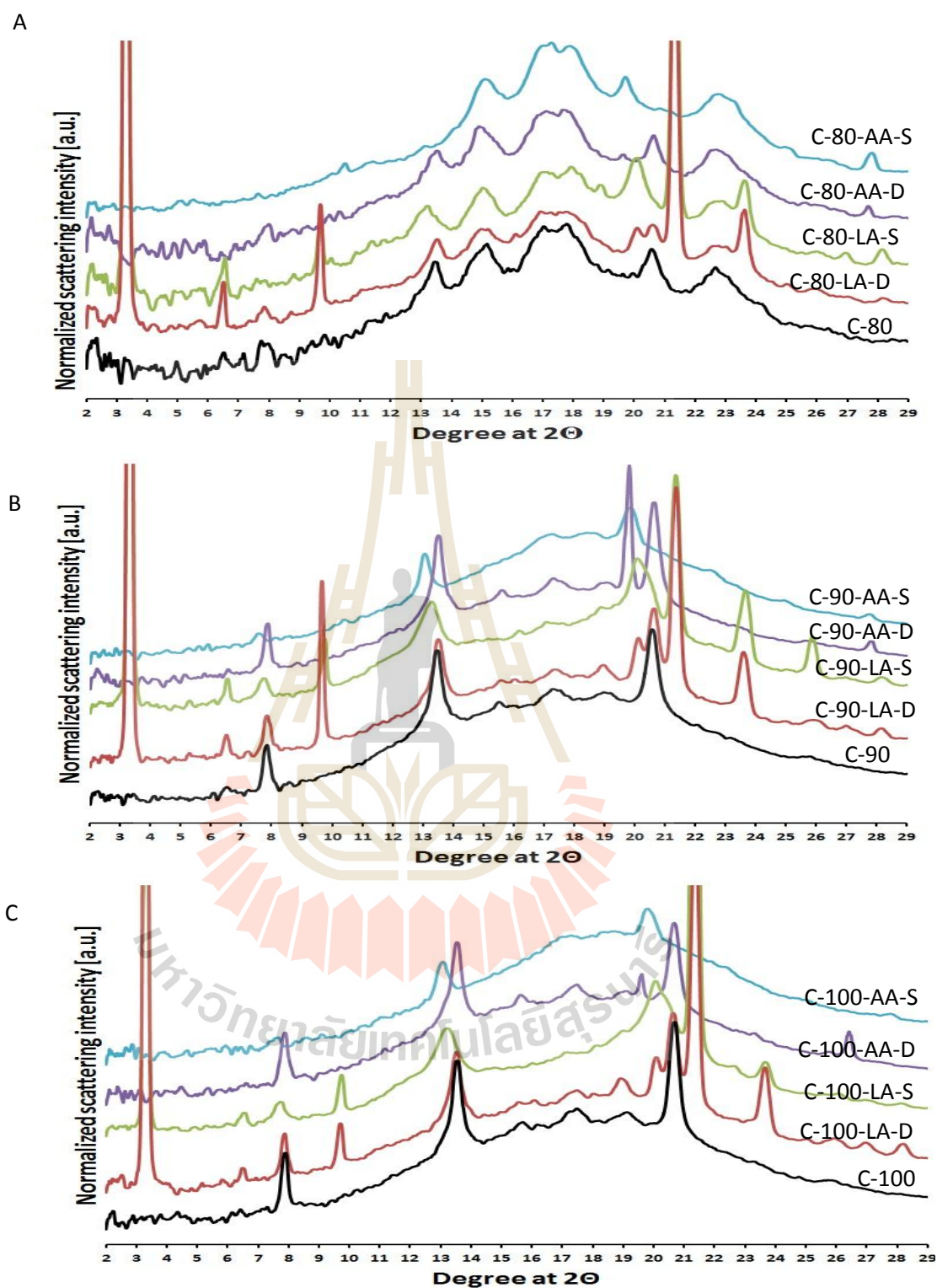
Figure 7.3 WAXS patterns of lauric acid (LA)- and ascorbic acid (AA)-ETS (ethanol-treated starch) tablets by dry mixing (D) and ethanol solubilization (S) methods and their corresponding ETS from temperatures of 80 (C-80) (A), 90 (C-90) (B), and 100 (C-100) (C)°C.

25.8°, 26.9° and 28.1° (Figure 7.3A, B, and C). This result suggested that complexation between lauric acid and ETS components did not occur in the lauric acid-ETS tablet prepared by dry mixing method. Position and intensity of peak on the diffratogram of lauric acid crystal may be altered since lauric acid crystal is known to exhibit polymorphism due to spontaneous structural transformation induced by environmental changing (Lomer, 1963; Vand, Morley, and Lomer, 1951).

The identity peaks of V-type crystalline structure of lauric acid-ETS tablet prepared by ethanol solubilization method slightly shifted to left from 7.9° to 7.5°, 13.6° to 12.9° and 20.6° to 19.8° and the peak intensity also reduced (Figure 7.3 A, B and C). The peak shifting of V-type crystalline structure may occur due to hydration of anhydrous V-type crystal (Va) to become hydrated V-type crystal (Vh) (Buleon, et al., 1998). This might be because the sample was exposed to humidity during ethanol solubilization process.

The identity peaks of ascorbic acid crystal were observed on the diffractogram of ascorbic acid-ETS tablet prepared by dry mixing method at 2θ of 19.8°, 26.4° and 27.6° (Figure 7.3A C-80-AA-D, Figure 7.3B C-90-AA-D, and Fig 7.3C C-100-AA-D). Meanwhile, no identity peak of ascorbic acid crystal was detected on the diffractogram of ascorbic acid-ETS tablet prepared by ethanol solubilization method. This might be because the ascorbic acid underwent oxidation during ethanol solubilization process. The identity peak of V-crystalline structure of ascorbic acid-ETS tablet by ethanol solubilization method also shifted to left and reduced their intensity. This confirmed that all samples prepared by ethanol solubilization method were exposed to humidity during ethanol solubilization process.

7.4.2 Morphological properties

Morphological properties of ETS granules and their corresponding lauric acid- and ascorbic acid-ETS granules are shown in Figure 7.4. Granules of C-80 were still in granular forms with some granules partially melted, indented, and wrinkled (Figure 7.4A C-80 inset). Meanwhile, C-90 and C-100 were no longer in granular forms (Figure 7.4B C-90 inset and Figure 7.4C C-100 inset). They melted and formed big aggregates or debris-like particles. Native cassava starch lacks amylose-tie chains; therefore, it is fragile and easy to be disrupted during heat treatments (Rolland-Sabaté, Sánchez, Buléon, Colonna, Jaillais, Ceballos, and Dufour, 2012). Thus, cassava starch lost its granular forms when it was converted to ETS at high temperatures (90 and 100 °C).

Lauric acid encapsulation by dry mixing (D) and ethanol solubilization (S) methods promoted granules aggregation (Figure 7.4A, B, and C). Lauric acid molecules might attach on the granule surface bridging the starch granules via hydrophobic interactions among the LA molecules (Holte, Kuran, Richmond, and Johnson, 2014). Therefore, it is speculated that the lauric acid molecules encapsulated by ethanol solubilization method might distribute more homogenous covering the ETS granules surface rather than those encapsulated by dry mixing method. As a result the ETS particles became easier to stick to each other forming aggregates (Figure 7.4A C-80-LA-S, Figure 7.4B C-90-LA-S, and Figure 7.4C C-100-LA-S).
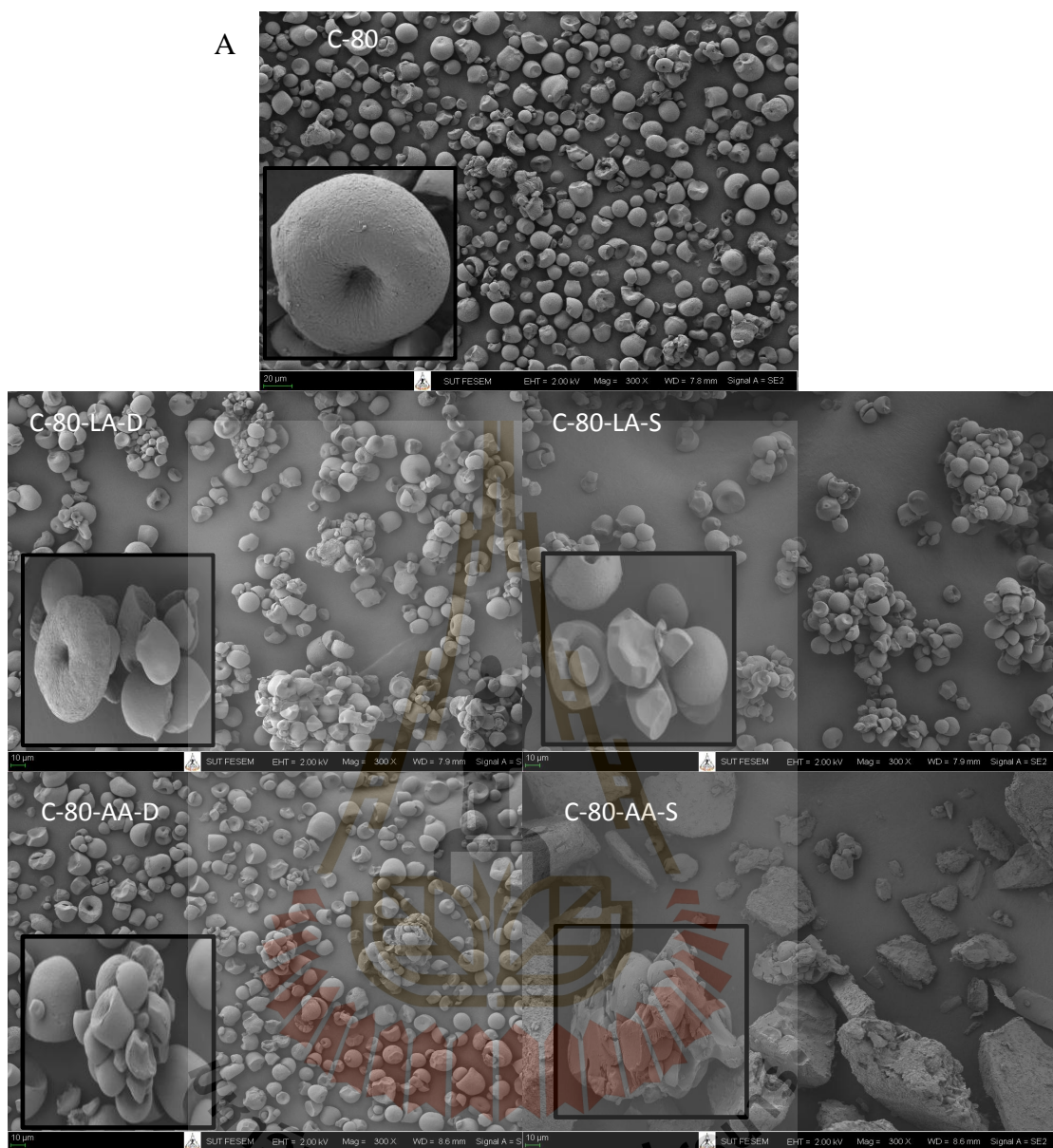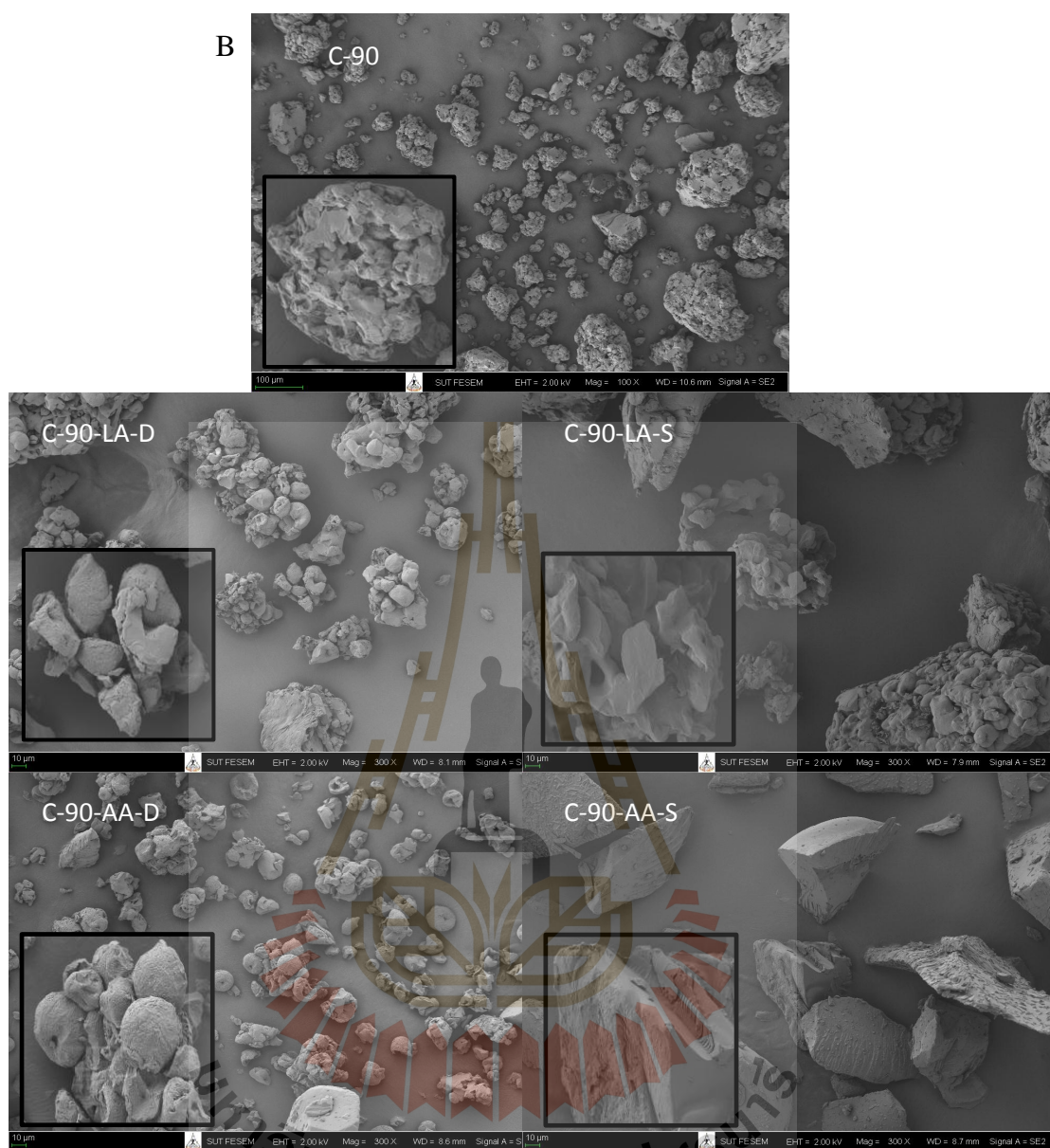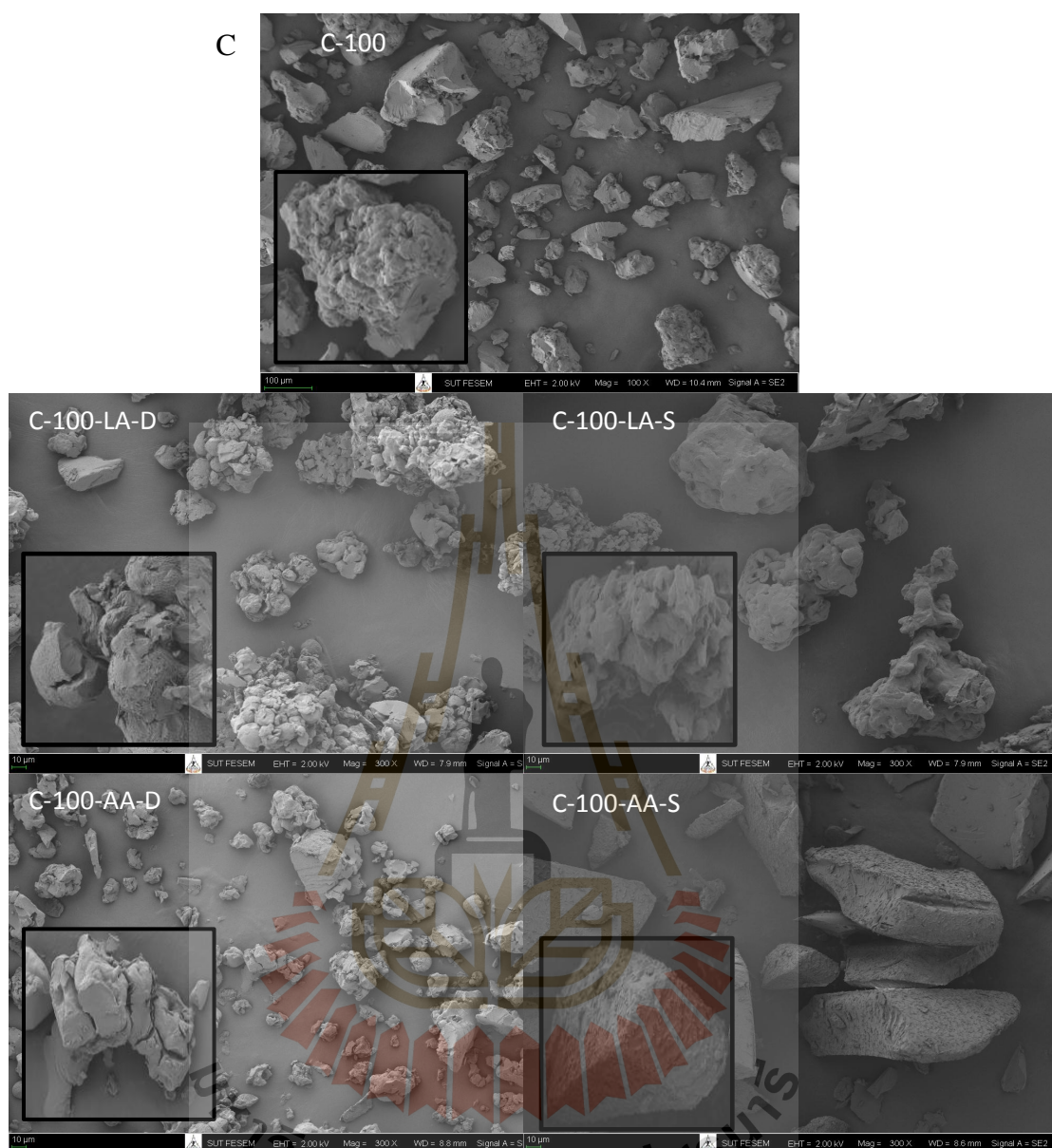
Figure 7.4

Figure 7.4

Figure 7.4 Morphology lauric acid (LA)- and ascorbic acid (AA)-ETS (ethanol-treated starch) tablets by dry mixing (D) and ethanol solubilization (S) methods and their corresponding ETS from temperatures of 80 (C-80) (A), 90 (C-90) (B), and 100 (C-100) (C)°C.

Ascorbic acid encapsulated by dry mixing method did not influence to the morphological properties of ETS granules (Figure 7.4A C-80-AA-D, Figure 7.4B C-90-AA-D, and Figure 7.4C C-100-AA-D). However, ascorbic acid encapsulated by ethanol solubilization method impacted to the ETS granules morphology. The C-80-AA-S, C-90-AA-S and C-100-AA-S samples were looked like aggregated particles or lumps, indicating that the granular form of ETS was destroyed during the ethanol solubilization process. Moreover, tablets of ascorbic acid encapsulated by ethanol solubilization method have color of brown. This might indicate that the ascorbic acid released hydrogen ions during ethanol solubilisation process. One mole of L-ascorbic acid molecule in solution releases two hydrogen ions ($2H^+$) (Ruiz, Aldaz, and Dominguez, 1977). These hydrogen ions may facilitate the hydrolysis of starch components resulting in the granule destruction (Figure 7.4.A C-80-AA-S, Figure 7.4.B C-90-AA-S and Figure 7.4.C C-100-AA-S).

7.4.3 Mechanical strength properties of lauric acid- and ascorbic acid-ETS tablets

The friability and crushing strength indexes of lauric acid- and ascorbic acid-ETS tablets are displayed in Figure 7.5 and Figure 7.6, respectively. Regardless of the active compounds, tablets of non-granular ETS (C-90 and C-100) showed lower friability and higher crushing strength indexes than those of granular ETS (C-80). This might be due to that the particles of non-granular ETS anchored each other when they were compressed into a tablet thus resulting in a non-fragile tablet. Tablet prepared from native starch showed a lower crushing strength index than that prepared from modified starches (Lawal, et al., 2015).

Figure 7.6 indicates that lauric acid- and ascorbic acid-ETS tablets prepared by ethanol solubilization method exhibited higher crushing strength than that prepared by dry mixing method. Samples prepared by ethanol solubilization method might get hydrated during ethanol solubilization process, resulting in the granules melting as confirmed by the crystal structure analysis (Figure 7.3) and morphological analysis (Figure 7.4). When they were compressed into a tablet, it is likely that there were entanglements among the particles producing a strong tablet as indicated by the high crushing strength index (Figure 7.6). The strong tablet is required to ensure that a tablet is robust enough to withstand with various post-compaction stress during handling and transportation (Okoye, Onyekweli, Kunle, and Arhewoh, 2010).
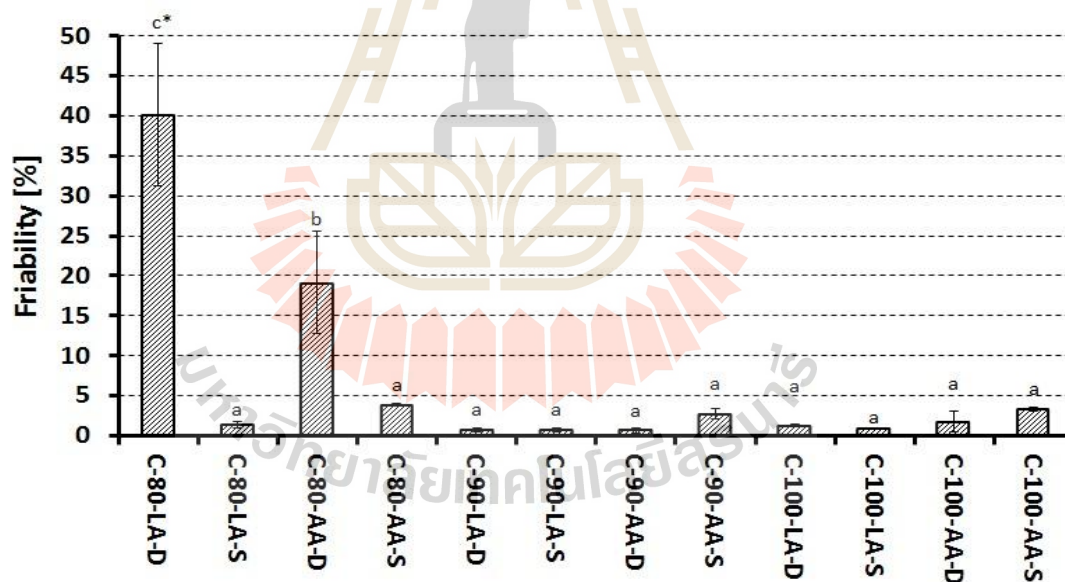

Figure 7.5 Friability properties of lauric acid (LA)- and ascorbic acid (AA)-ETS (ethanol-treated starch) tablets from temperatures of 80 (C-80), 90 (C-90) and 100 (C-100)°C by dry mixing (D) and ethanol solubilization (S) methods. Vertical error bars represent standard deviation. * Same letters indicate that samples are not statistically different (p>0.05).
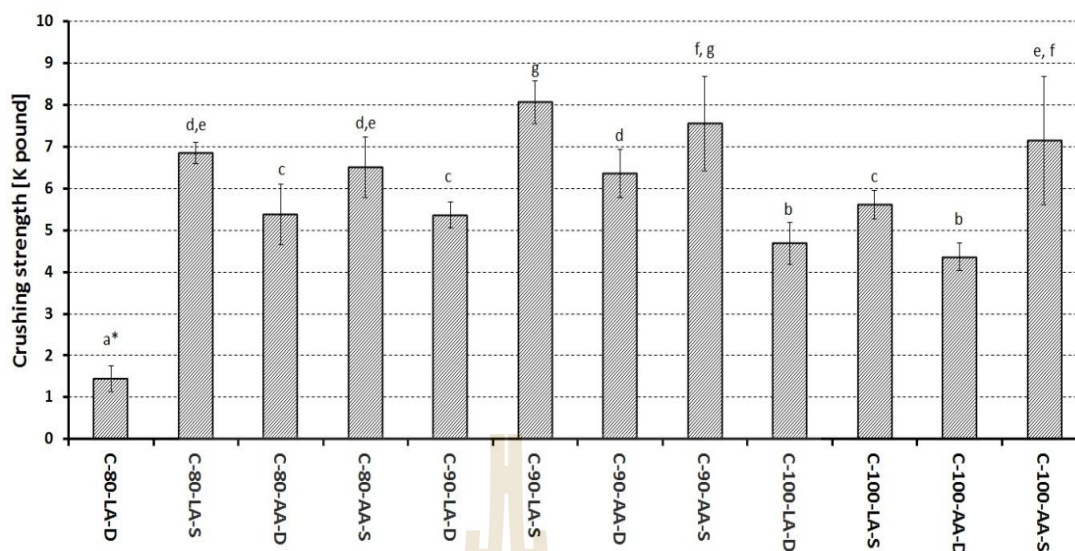
Figure 7.6   Crushing strength properties of lauric acid (LA)- and ascorbic acid (AA)-

ETS (ethanol-treated starch) tablets from temperatures of 80 (C-80), 90

(C-90) and 100 (C-100)°C by dry mixing (D) and ethanol solubilization

(S) methods. Vertical error bars represent standard deviation. * Same

letters represent that samples are not statistically different (p>0.05).

7.4.4   Hydration behavior of lauric acid- and ascorbic acid-ETS tablets

Hydration profiles of lauric acid- and ascorbic acid-ETS tablets are displayed

in Figure 7.7. It is presented as profiles of the unhydrated core of tablets which were

the result of image processing of the tablets hydration behavior (Figure 7.8). Upon

contact with water, tablets prepared from granular ETS (C-80) swollen immediately at

a time less than 1 min; then they were dispersed in the medium. However, tablet of C-

80-AA-S eroded gradually until it dispersed completely after 30 min (Figure 7.7A and

Figure 7.8A). This might be due to that the particles of C-80-AA-S were entangled

each other during soaking, preventing spontaneous dispersion. Particles entanglement

during soaking was probably easier to occur for melted-irregular shaped particles of
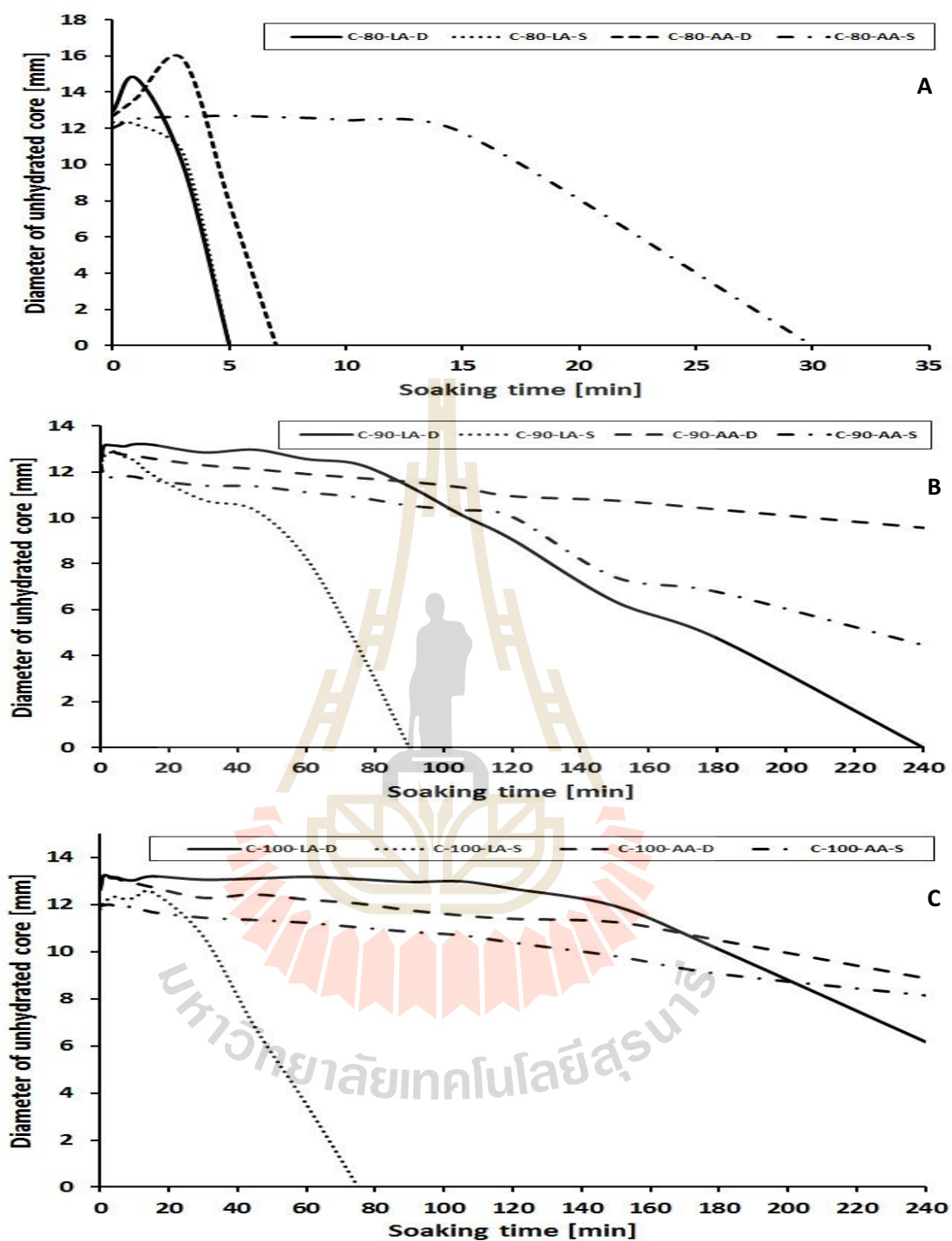
Figure 7.7 Hydration profile of lauric acid (LA)- and ascorbic acid (AA)-ETS (ethanol-treated starch) tablets from temperatures of 80 (C-80), 90 (C-90) and 100 (C-100)°C by dry mixing (D) and ethanol solubilization (S) methods.

C-80-AA-S (Figure 7.4A C-80-AA-S) rather than granular particles (Figure 7.4A C-80-LA-D, C-80-LA-S, and C-80-AA-D).

Upon soaking, the lauric acid-ETS tablets from non-granular ETS (C-90 and C-100) encapsulated by dry mixing method eroded gradually then dispersed completely after 240 min (Figure 7.7B and C and Figure 7.8B and C). For tablet containing poorly water-soluble compounds, such as LA, erosion of matrix is its rate-limiting factor (Efentakis, Pagoni, Vlachou, and Avgoustakis, 2007). The presence of lauric acid surrounding the starch components promotes disentanglement or disassociation among starch components (Arik Kibar, Gönenç, and Us, 2014).

The lauric acid-ETS tablets from non-granular ETS (C-90 and C-100) encapsulated by ethanol solubilization method eroded faster than those prepared by dry mixing method in which they dispersed completely at 90 and 75 min, respectively (Figure 7.7B and C). It was expected that the LA encapsulation by ethanol solubilization (S) method produced a tablet with more homogenous distributed LA. Therefore, the more distributed LA in the tablet, the faster the tablet disintegrated during soaking.
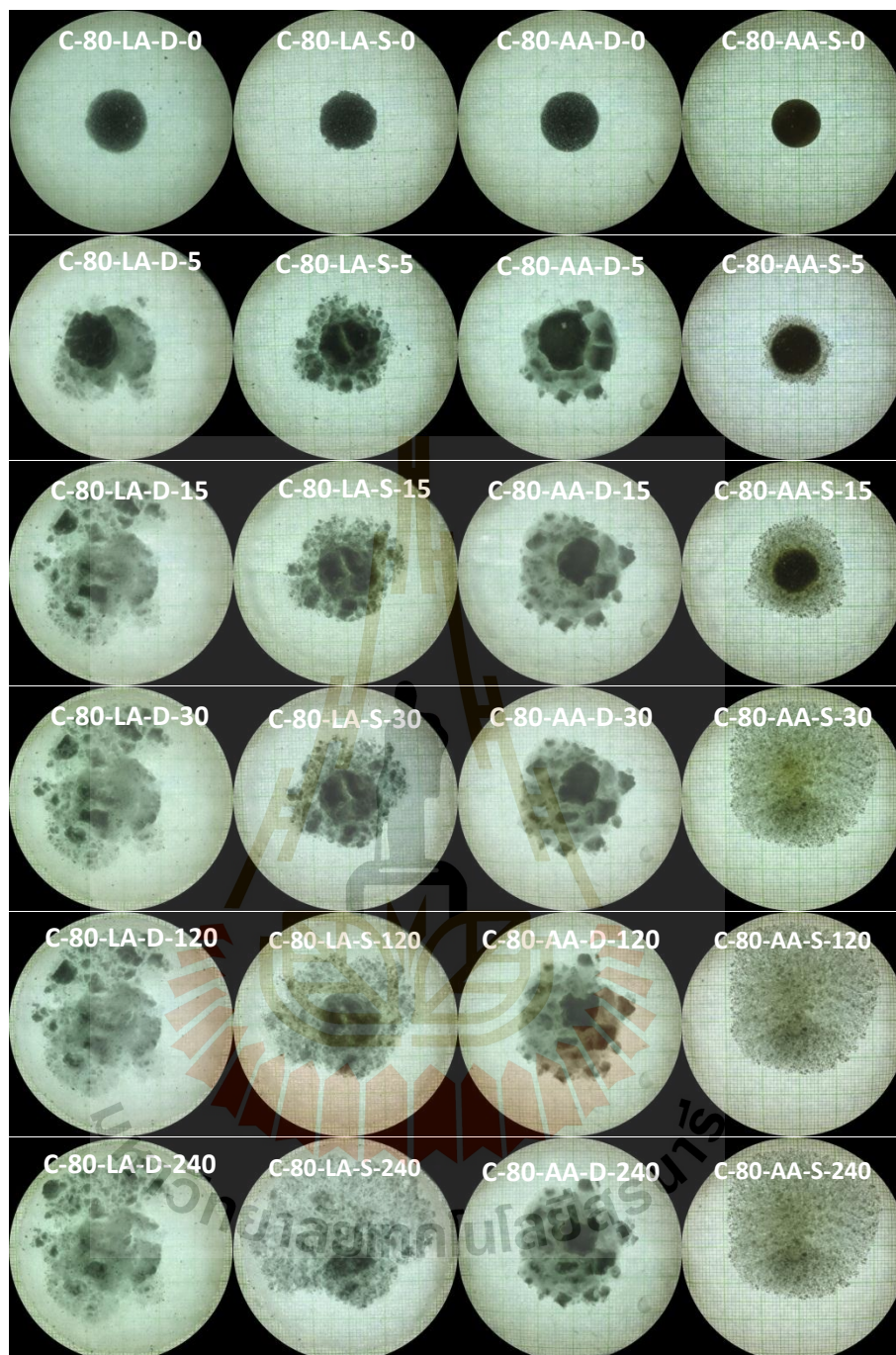
A

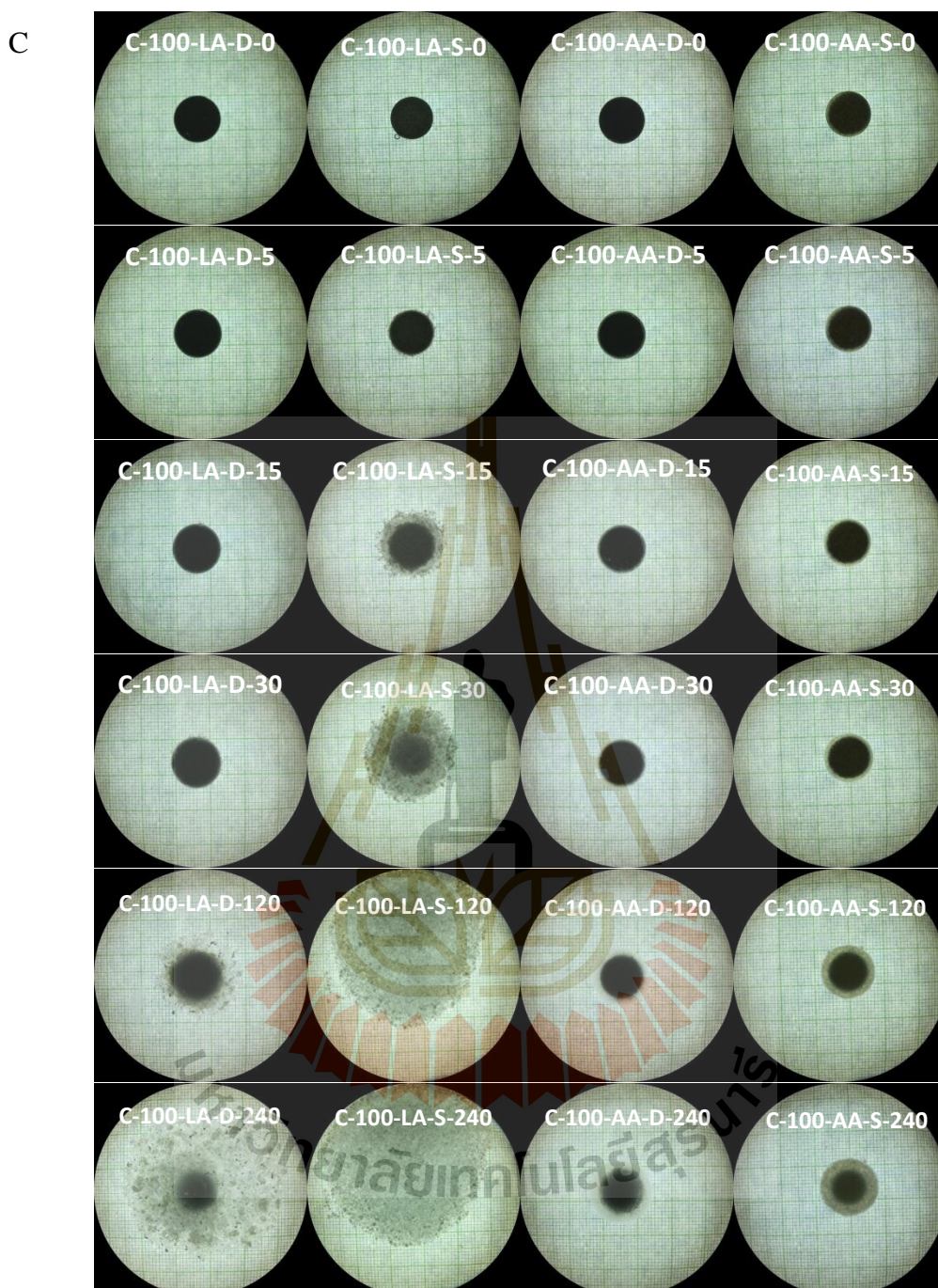**Figure 7.8**

B

Figure 7.8

Figure 7.8 Hydration behavior of lauric acid (LA)- and ascorbic acid (AA)-ETS (ethanol-treated starch) tablets from temperatures of 80 (C-80) (A), 90 (C-90) (B) and 100 (C-100) (C)°C by dry mixing (D) and ethanol solubilization (S) methods, soaked at certain time intervals (0, 5, 15, 30, 120, 240 min).

The ascorbic acid-ETS tablets from non-granular ETS (C-90 and C-100) prepared by dry mixing (D) and ethanol solubilization (S) methods adsorbed water slowly (Figure 7.7B and C), then swollen to a certain extent without degradation or erosion (Figure 7.8B and C). ETS contains paracrystalline structure which is mainly composed of V-type single helix and amorphous regions (Sarifudin, Soontaranon, Rugmai, and Tongta, 2019). During hydration, the amorphous structure converts to a B-type double helix (Shiftan, Ravenelle, Mateescu, and Marchessault, 2000). Then, the double helical structure forms physical crosslinking points with other starch components which lead to the formation of a 3D-network. The crosslinked structure inhibits water penetration and restrains the tablet swelling during soaking.

7.4.5 Release properties of lauric acid- and ascorbic acid-ETS tablets

The release properties of lauric acid- and ascorbic acid-ETS tablets are shown in Figure 7.9. More than 50% of lauric acid content in the granular ETS tablets (C-80-LA-D and C-80-LA-S) was released in the first minutes upon soaking before it reached stationary stage (Figure 7.9A1). Meanwhile, the lauric acid content in non-granular ETS tablets (C-90-LA-D, C-90-LA-S, C-100-LA-D, and C-100-LA-S) was released slower than those in granular ETS tablets. Moreover, the lauric acid content in the ETS tablet prepared by ethanol solubilization method was released faster than those prepared by dry mixing method (Figure 7.9A2 and A3). It suggests that the release profile of lauric acid-ETS tablets (Figure 7.9) followed its hydration behavior (Figure 7.7) in that the lauric acid-ETS tablets prepared by ethanol solubilization method eroded faster than those prepared by dry mixing method. This finding was in
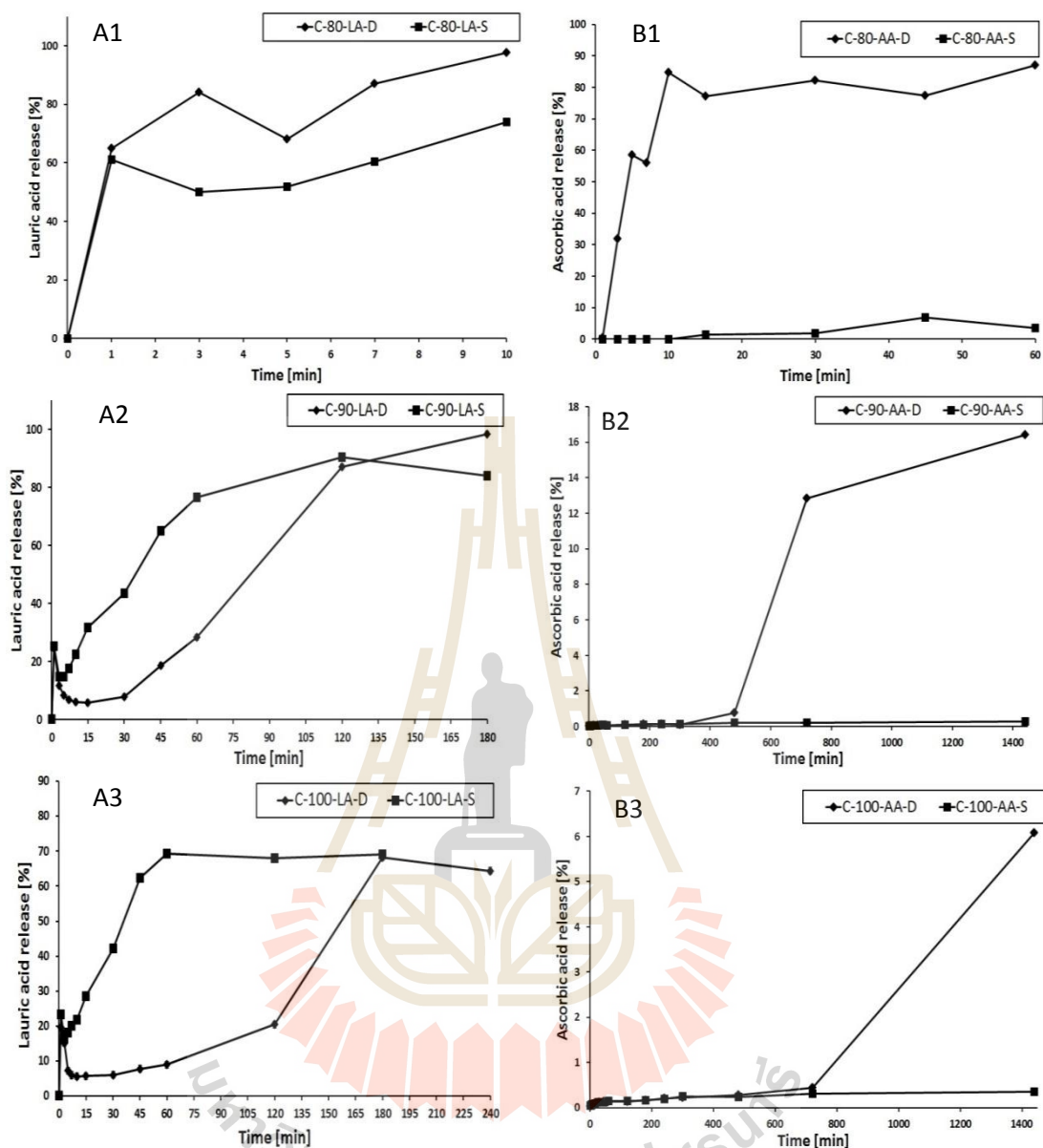
Figure 7.9 The release profile of lauric acid (LA)- and ascorbic acid (AA)-ETS (ethanol-treated starch) tablets from temperatures of 80 (C-80), 90 (C-90) and 100 (C-100)°C by dry mixing (D) and ethanol solubilization (S) methods.

accordance with the previous report (Yin, Li, Guo, Wu, Chen, de Matas, Shao, Xiao, York, He, and Zhang, 2013) in that the drug release system of poorly soluble compounds mostly influenced by the matrix erosion.

The result indicates that the lauric acid content in the ETS tablets was not fully released into the medium (Figure 7.9A2 and A3) which might be because they were entrapped inside the starch matrix. For encapsulation of poorly soluble compounds, the rate and amount of compound release from swellable matrices are not only dependent on the drug dissolution and diffusion but also on the compound translocation in the gel because of polymer swelling (Yin, et al., 2013).

Ascorbic acid in the granular ETS tablets prepared by dry mixing (D) method (C-80-AA-D) was released at about 10 minutes after soaking (Figure 7.9B1). Meanwhile, ascorbic acid in non-granular ETS tablets prepared by dry mixing (D) method (C-90-AA-D and C-100-AA-D) was released at a slower rate than those in granular ETS prepared by the same encapsulation method (C-80-AA-D) (Figure 7.9B2 and B3). Moreover, the maximum released amount of ascorbic acid of C-90-AA-D and C-100-AA-D tablets was only 15 and 6%, respectively, at the end of observation (1440 min). This might be because the ascorbic acid was entrapped in the inside of the swollen matrix since no agitation was carried out during soaking. For tablet containing highly soluble compound, such as ascorbic acid, the active compound release might be limited by water penetration (Tahara, Yamamoto, and Nishihata, 1996) or diffusion (Bonferoni, Rossi, Ferrari, Bertoni, Sinistri, and Caramella, 1995).

Unfortunately, our treatment to encapsulate ascorbic acid with ETS by ethanol solubilization method was not successful. The color of the samples became brown.

This was probably because the ascorbic acid underwent oxidation during the ethanol solubilization process. The ascorbic acid oxidation was also noticed from the diffractogram of these samples in that no peak of ascorbic acid crystal was observed (Figure 7.3B and C). Despite this negative result, it was evidenced that for non-granular ETS tablets, the ascorbic acid oxidation did not significantly influence the tablets hydration behavior (Figure 7.7B and C and Figure 7.8B and C). This finding might be beneficial for encapsulation other ethanol-soluble compounds, such as flavonoid compounds (i.e. rutin and quercetin), which may need to be sustained release (Lauro, Torre, Maggi, De Simone, Conte, and Aquino, 2002).

7.5   Conclusions

Complexation between the lauric acid and ascorbic acid and the starch components of ETS did not occur during the encapsulation process. The C-80 tablets showed granular form, while the C-90 and C-100 tablets exhibited a non-granular structure. Tablets prepared from non-granular ETS showed higher mechanical strength properties than that prepared from granular ETS. Upon soaking, the tablets of granular ETS dispersed and released the active compounds rapidly; thus it is suitable for a fast release system. Meanwhile, tablets from non-granular ETS adsorbed water, swollen or dispersed, then released the active compounds slowly, thus it is proper for sustained release system. The lauric acid and ascorbic acid in non-granular ETS tablets were released by erosion and diffusion mechanisms, respectively.

7.6   Acknowledgments

7.7 References

Arik Kibar, E.A., Gönenç, İ., and Us, F. (2014). Effects of Fatty Acid Addition on the Physicochemical Properties of Corn Starch. **International Journal of Food Properties** 17(1): 204-218.

Bonferoni, M.C., Rossi, S., Ferrari, F., Bertoni, M., Sinistri, R., and Caramella, C. (1995). Characterization of three hydroxypropyl methy cellulose substitution types: rheological properties and dissolution behavior. **European Journal of Pharmaceutics and Biopharmaceutics** 41: 242-246.

Buléon, A., Gallant, D.J., Bouchet, B., Mouille, G., D'Hulst, C., Kossmann, J., and Ball, S. (1997). Starches from A to C: Chlamydomonas reinhardtii as a model microbial system to investigate the biosynthesis of the plant amylopectin crystal. **Plant Physiology** 115: 949-957.

Buleon, A., Le Bail, P., Colonna, P., and Bizot, H. (1998). Phase and polymorphic transitions of starches at low and intermediate water contents. In D.S. Reid (Ed.), The Properties of Water in Foods ISOPOW 6 (pp. 160-178). Boston, MA: **Springer US**.

Chen, J., and Jane, J. (1994). Properties of granular cold-water-soluble starches prepared by alcoholic-alkaline treatments. **Cereal chemistry** 71(6): 623-626.

Chen, J., and Jane, J. (1995). Effectiveness of granular cold-water-soluble starch as a controlled release matrix. **Cereal chemistry** 72(3): 265-268.

Commission, B.P. (2010). British Pharmacopoeia. vol. II. London. British Pharmacopoeia Commission.

Dries, D.M., Gomand, S.V., Goderis, B., and Delcour, J.A. (2014). Structural and thermal transitions during the conversion from native to granular cold-water swelling maize starch. **Carbohydrate Polymers** 114: 196-205.

Dries, D.M., Gomand, S.V., Pycarelle, S.C., Smet, M., Goderis, B., and Delcour, J.A. (2017). Development of an infusion method for encapsulating ascorbyl palmitate in V-type granular cold-water swelling starch. **Carbohydrate Polymers** 165(Supplement C): 229-237.

Eastman, J.E., and Moore, C.O. (1984). Cold soluble water granular starch for gelled food compositions. **USPTO # 4.465.702**

Efentakis, M., Pagoni, I., Vlachou, M., and Avgoustakis, K. (2007). Dimensional changes, gel layer evolution and drug release studies in hydrophilic matrices loaded with drugs of different solubility. **International Journal of Pharmaceutics** 339: 66-75.

Gao, P., and Meury, R.H. (1996). Swelling of Hydroxypropyl Methylcellulose Matrix Tablets. 1. Characterization of Swelling Using a Novel Optical Imaging Method. **Journal of Pharmaceutical Sciences** 85(7): 725-731.

Hatairat, P., Wolfgang, B., Sujin, S., and Saiyavit, V. (2003). Characterization and Utilization of Acid-modified Rice Starches for Use in Pharmaceutical Tablet Compression. **Starch - Stärke** 55(10): 464-475.

Holte, L.K., Kuran, B.A., Richmond, L.G., and Johnson, K.E. (2014). Computational Modeling of Lauric Acid at the Organic−Water Interface. **The Journal of Physical Chemistry C** 118: 10024-10032.

Lakshanasomya, N. (1998). Determination on Vitamin C in Some Kinds of Food by HPLC. **Bulletin of Department Medical Science** 40(3): 347-357.

Lauro, M.R., Torre, M.L., Maggi, L., De Simone, F., Conte, U., and Aquino, R.P. (2002). Fast- and slow-release tablets for oral administration of flavonoids: rutin and quercetin. **Drug Development and Industrial Pharmacy** 28(4): 371-379.

Lawal, M.V., Odeniyi, M.A., and Itiola, O.A. (2015). Effect of thermal and chemical modifications on the mechanical and release properties of paracetamol tablet formulations containing corn, cassava and sweet potato starches as filler-binders. **Asian Pacific Journal of Tropical Biomedicine** 5(7): 585-590.

Lomer, T. (1963). The crystal and molecular structure of lauric acid (form A). **Acta Crystallographica** 16(10): 984-988.

Madene, A., Jacquot, M., Scher, J., and Desobry, S. (2006). Flavour encapsulation and controlled release – a review. **International Journal of Food Science & Technology** 41(1): 1-21.

Majzoobi, M., Kaveh, Z., Blanchard, C.L., and Farahnaky, A. (2015). Physical properties of pregelatinized and granular cold water swelling maize starches in presence of acetic acid. **Food Hydrocolloids** 51: 375-382.

Manish, J., and Abhay, K. (2012). Sustained release matrix type drug delivery system: A review. **Journal of Drug Delivery and Therapeutics** 2(6): 142-148.

Odeniyi, M.A., and Ayorinde, J.O. (2014). Effects of modification and incorporation techniques on disintegrant properties of wheat (Triticum aestivum) starch in metronidazole tablet formulations. **Polimery w Medycynie** 44(3): 147-155.

Okoye, E.I., Onyekweli, A.O., Kunle, O.O., and Arhewoh, M.I. (2010). Brittle fracture index (BFI) as a tool in the classification, grouping and ranking of

some binders used in tablet formulation: Lactose tablets. **Scientific Research and Essays** 5(5): 500-506.

Pachuau, L., Dutta, R.S., Devi, T.B., Deka, D., and Hauzel, L. (2018). Taro starch (Colocasia esculenta) and citric acid modified taro starch as tablet disintegrating agents. **International Journal of Biological Macromolecules** 118: 397-405.

Patel, H., Panchal, D.R., Patel, U., Brahmbhatt, T., and Suthar, M. (2011). Matrix Type Drug Delivery System: A Review. **Journal of Pharmaceutical Science and Bioscientific Research (JPSBR)** 1(3): 143-151.

Rolland-Sabaté, A., Sánchez, T., Buléon, A., Colonna, P., Jaillais, B., Ceballos, H., and Dufour, D. (2012). Structural characterization of novel cassava starches with low and high-amylose contents in comparison with other commercial sources. **Food Hydrocolloids** 27(1): 161-174.

Ruiz, J.J., Aldaz, A., and Dominguez, M. (1977). Mechanism of L-ascorbic acid oxidation and dehydro-L-ascorbic acid reduction on a mercury electrode. I. Acid medium. **Canadian Journal of Chemistry** 55(15): 2799-2806.

Sarifudin, A., Soontaranon, S., Rugmai, S., and Tongta, S. (2019). Structural transformations at different organizational levels of ethanol-treated starch during heating. **International Journal of Biological Macromolecules** 132: 1131-1139.

Sauvant, P., Cansell, M., Hadj Sassi, A., and Atgié, C. (2012). Vitamin A enrichment: Caution with encapsulation strategies used for food applications. **Food Research International** 46(2): 469-479.

Shahidi, F., and Han, X.Q. (1993). Encapsulation of food ingredients. **Critical Reviews in Food Science and Nutrition** 33(6): 501-547.

Shiftan, D, Ravenelle, F., Mateescu, M.A., and Marchessault, R.H. (2000). Change in the V/B Polymorph Ratio and T1 Relaxation of Epichlorohydrin Crosslinked High Amylose Starch Excipient. **Starch - Stärke** 52(6-7): 186-195.

Soontaranon, S., and Rugmai, S. (2012). Small Angle X-ray Scattering at Siam Photon Laboratory. **Chinese Journal of Physics** 50(2): 204-210.

Tahara, K., Yamamoto, K., and Nishihata, T. (1996). Application of modelindependent and model analysis for the investigation of effect of drug solubility on its release rate from hydroxypropyl methy cellulose sustained release tablets. **International Journal of Pharmaceutics** 133: 17-27.

Vand, V., Morley, W.M., and Lomer, T.R. (1951). The crystal sructure of lauric acid. **Acta Crystallographica** 4(4): 324-329.

Yang, M.-H., and Choong, Y.-M. (2001). A rapid gas chromatographic method for direct determination of short-chain (C2–C12) volatile organic acids in foods. **Food Chemistry** 75(1): 101-108.

Yin, X., Li, H., Guo, Z., Wu, L., Chen, F., de Matas, M., Shao, Q., Xiao, T., York, P., He, Y., and Zhang, J. (2013). Quantification of swelling and erosion in the controlled release of a poorly water-soluble drug using synchrotron X-ray computed microtomography. **The AAPS journal** 15(4): 1025-1034.

Zhang, B., Dhital, S., Haque, E., and Gidley, M.J. (2012). Preparation and characterization of gelatinized granular starches from aqueous ethanol treatments. **Carbohydrate Polymers** 90(4): 1587-1594.

Zhu, F. (2017). Encapsulation and delivery of food ingredients using starch based systems. **Food Chemistry** 229: 542-552.

Zuidam, N.J., and Velikov, K.P. (2018). Choosing the right delivery systems for functional ingredients in foods: an industrial perspective. **Current Opinion in Food Science** 21: 15-25.

CHAPTER VIII

SUMMARY

Structural transformation at the crystalline, lamellae and granular levels of ethanol-treated starch (ETS) during heating was studied by using combination of in situ wide and small angle X-ray scattering techniques (WAXS/SAXS) and light microscope (LM). Results indicated that the V-type crystalline structure formation of ethanol-treated maize starch was started at 86°C. Result of SAXS indicated that during ETS heating, the crystalline lamellae realigned toward a more perfect register before they were disrupted. From fractal analysis, it can be observed that there was transformation of ETS from a three-dimensional structure to a rod-like structure at the lamellae structural level. At granular level, morphological analysis indicated that ETS still preserved its granular form upon the loss of birefringence. This might be due to the role of amylose chains and amylose-ethanol complexes for maintaining the ETS granular shape during heating.

The pore of ETS exhibited characteristic of non-rigid and slit-shaped pores. After ETS conversion, most pores of ETS from maize starch were in the category of mesopore and macropore, while pores of ETS from potato starch were in the mesopore range. The pores of ETS from cassava and rice starches were destroyed during ETS conversion at high temperatures (90 and 100°C). Pores of ETS may be originated from fissures, wrinkles, and indentations shown on the granule surface of of ETS. For granular ETS from maize and potato starches, water penetrates the

granule through fissures, hydrates the amorphous regions, melts the V-type crystalline structure, and is held within the ETS granules upon water absorption. For non-granular ETS from cassava and rice starches, water hydrates the amorphous and V-type crystalline structures, and it is entrapped within the three-dimensional network of starch components entanglement upon contact with water.

Humidity exposure altered the structure, morphological and water adsorption capacity (WAC) properties of ETS. At the lowest humidity level (11%), ETS still showed its V-type crystalline structure and morphological features including wrinkles, fissures, and indentations. However, as the humidity level increased, the crystallinity contributed by V-crystal structure reduced, the ETS granules surface became smoother and its WAC values decreased. Therefore, low humidity environment is recommended for storing the ETS.

Upon hydration in excess, the V-crystalline structure of ETS disappeared. There were drastic structural transformations of ETS at lamellae level upon soaking in that three-dimensional structures of crystalline lamellae were converted to sheet-like structures. Results indicated that granule of ETS from potato starch showed higher resistance toward granule disruption during hydration compared to ETS from maize starch.

Results indicated that encapsulation of lauric acid (LA) and ascorbic acid (AA) by using ETS through dry mixing (D) and ethanol solubilization (S) methods did not initiate complexation between the LA or AA and starch components of ETS. Ethanol treated cassava starch prepared from 80°C showed granular form, while those from 90 and 100°C exhibited a non-granular structure. Tablets prepared from non-granular ETS exhibited higher mechanical strength properties than that prepared from granular

ETS. Upon soaking, the tablets of granular ETS were suitable for fast release system since they dispersed and released the encapsulated compounds rapidly. Meanwhile, the tablets from non-granular ETS were proper for sustained release system since they adsorbed water, swollen or dispersed and released the entrapped compounds slowly. The release mechanism of LA and AA in non-granular ETS tablets was erosion and diffusion, respectively.
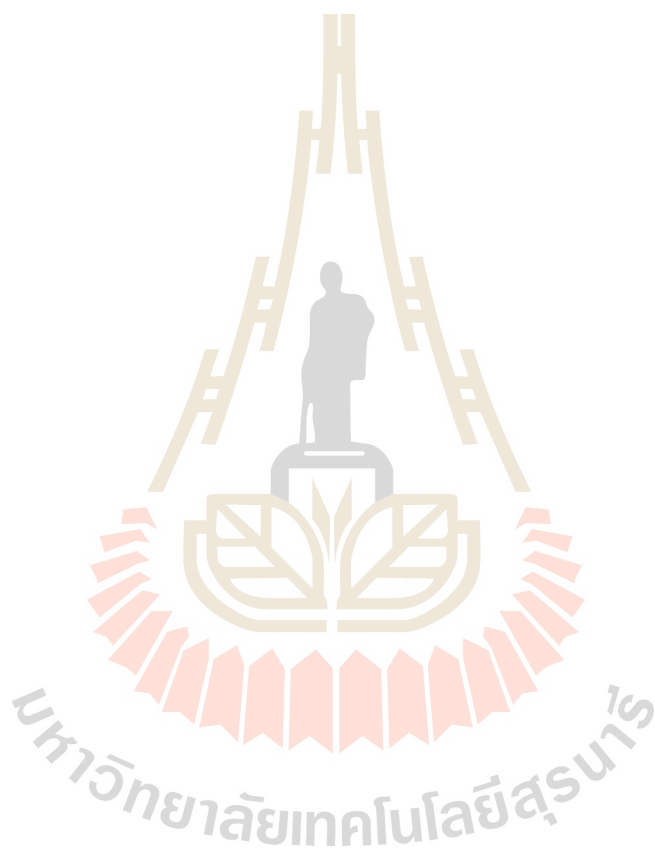
CURRICULUM VITAE

Achmat Sarifudin was born in September 17th, 1981, at the District of Klaten, Province of Central of Java, Indonesia. He studied his elementary school (1988-1993), junior high school (1993-1996) to senior high school (1996-1999) in the Distric of Klaten, Province of Central of Java. He moved to Bogor, Province of West of Java, Indonesia, to pursue his bachelor degree at Bogor Agricultural University in the major of food technology and human nutrition from 1999 to 2004. His research for bachelor degree thesis was entitled "Food additive exposure assessment based on the individual consumption data at Bogor regency, Province of West of Java". After graduated, he worked at the Directorate of Food Safety Surveillance and Extension, National Agency for Drug and Food Control (NADFC), Republic of Indonesia for about 1.5 years. Then he moved to work at PT. Central Pangan Pertiwi (Group of Charoen Pokphand Indonesia) as supervisor in the department of Quality Assurance until 2005. He moved to work as researcher at the Research Center for Appropriate Technology, Indonesian Institute of Sciences (P2TTG-LIPI) from 2005 until now. He obtained opportunity to continue his education in the master degree level at the Department Of Agriculture Engineering, College of Food and Agricultural Sciences, King Saud University, Kingdom of Saudi Arabia in the major of food process engineering from 2009 to 2012. His research for master degree level was entitled "Effect of Reactive Extrusion Process on Starch Hydrolysis for Production of Dextrin Nano Particles". Finally, in 2015, he pursued his doctoral degree at the School of Food Technology,

Institute of Agricultural Technology, Suranaree University of Technology (SUT), Kingdom of Thailand, funded by SUT scholarship for ASEAN countries.

During his career, he has published scientific reports published by local and international publishers; he has also attended local and international conferences. His professional career and publications including publications during his study in PhD program can be traced through the following channels:

1. Google scholar:

   https://scholar.google.co.id/citations?user=I-vewfkAAAAJ&hl=en ,

2. Research gate:

   https://www.researchgate.net/profile/Achmat_Sarifudin/publications ,

3. Indonesian researcher database :

   http://sinta2.ristekdikti.go.id/authors/detail?id=6244338&view=overview

4. Scopus:

   https://www.scopus.com/authid/detail.uri?authorId=36638369200

5. Orcid:

   https://orcid.org/0000-0002-9964-517X

6. Mendeley :

   https://www.mendeley.com/profiles/achmat-sarifudin2/publications/